College of Instrumentation & Electrical Engineering, Jilin University

Academic Practice "Six in One" Training Project

English Proceedings

2014 (First Half)

CONTENTS

Design of Locomotive Control Device

Tao Liu , Jing-shuai Miao

（Jilin university instrument science and engineering institute,changchun,130021）

***Abstract*—In order to improve the running of locomotives, reducing the impact of human factors on passenger locomotives, we through the application of automatic control theory to combine sensor technology and design with MSP430F149 chip as the core processor of locomotive running automatic control device. The device consists of a microprocessor module, color recognition module, obstacle detection module, voice-announce module and motor driver module. The modules by means of a coordinated operation can increase locomotive running safety and avoid accidents from occurring.**

I. INTRODUCTION

WITH the increasing vigorous development of China's national economy and people's living standards, the railway passenger and cargo traffic will become increasingly large [1]. Locomotive running through the manual control, automatic control plus manual operation mode and the way in which the latter is now widely used in a more safe and reliable operation runs. The development of locomotive has experienced manual control and automatic control plus manual operation mode, and the way in which the latter is a more widely used now safe and reliable operation runs. Using this semi-automatic operation mode control, which has the human disturbance factor, makes the security status of the locomotive run by a certain degree of threat. In railway transportation there is half of the accidents of subversion by the aggressive signal caused by the driver [2]. Reference [3] shows that to reduce accidents, reduce the incidence of railway accidents, and study unmanned train control system intelligent diagnosis and repair systems become one of the major challenges facing the Railway transportation of automation technology in current and future period of time. In this locomotive designed to run automatic control device which has applied sensor technology to determine locomotives and added he common emergency situations (obstacle detection) responses makes trains safer and more reliable during operation.

II .Procedure for Paper Submission

The design of the device which is combined with control theory and motor drive technology has the ability to identify common locomotive desired signal and make the appropriate maneuver experimental measures. In this design writer focuses on the ground system signal lights signal how to pickup, platform-stop voice prompts, obstacle detection and motor-driven aspects. Using modular research methods, the above problem into a microprocessor, ground system module, color recognition module, a voice module, obstacle detection module and the motor drive module of six modules. The microprocessor module which analysis and processing the signals from each module, corresponds stress measures to achieve full automation model locomotive running.

III. System Hardware Circuit Design

We designed the device consists of six components: ground system module, color recognition module, the microprocessor module, voice module, obstacle detection module, motor drive module. Ground system module is a necessary part of the locomotive ground signals required for the design mainly includes site information, lights set up, and voice prompts, etc; Color recognition module consists of a color TCS230 sensor is able to pick up the tricolor (red, yellow, green) signal lights color; Voice module provides passenger locomotives internal to remind passengers to get off the site and other essential message; Obstacle detection module can detect an obstacle in front of an obstacle whether has the greater risk and show that the system has the ability to burst dangerous matters stress response; Motor drive module is part of the power system; Also part of the LCD screen is used for the locomotive running status considerations and test parts. Its working principle: the design wakes in the morning at 5:30 by the lights, runs under the guidance of lights, processing and analysis the obstacles, achieve roundtrip operation and ends operations to pit overhaul at 9:30 pm. The hardware system block diagram has shown in Fig 1.

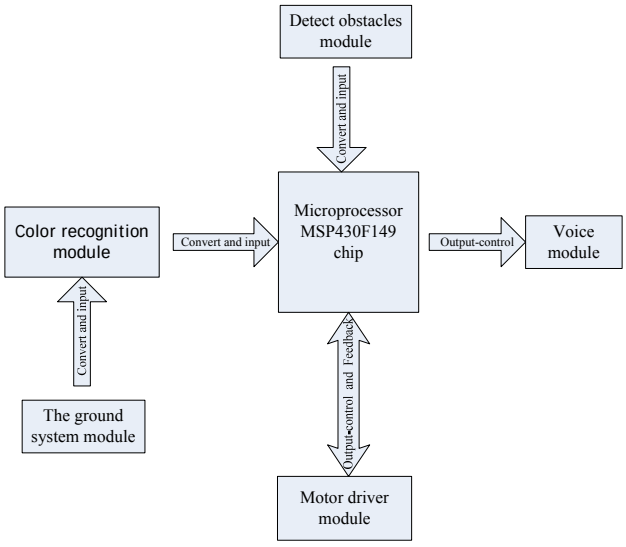

Fig.1.The hardware system block diagram.

Pursuant to hardware system block diagram and we study each module to select the desired components. Using this method we can get out of the available hardware circuit diagram shown in Fig 2.

A. Obstacle Detection Module

This module contains the HR-SR04 ultrasonic sensor integration module, which is to transmit the ultrasonic probe, ultrasonic receiver probe, CX20106A 74LS04 chip circuit and an amplifier circuit chip. The module's operating voltage and high stability at work.The quiescent current is less than 2mA.It ranges from 2cm-5m and the accuracy can reach 0.3cm, blind only 2cm.[4]. In actual operation within the range of 50cm stress triggers interrupt and the locomotive should stop and remove obstacles. On the position of the sensor arrangement uses inverted triangle on the lower modes. Using the stable shape and symmetry of the equilateral triangular design of the stand makes the existence of obstacles threatening judge more reliable. As shown in Fig 3, the bottom of which is a front view where the graph .

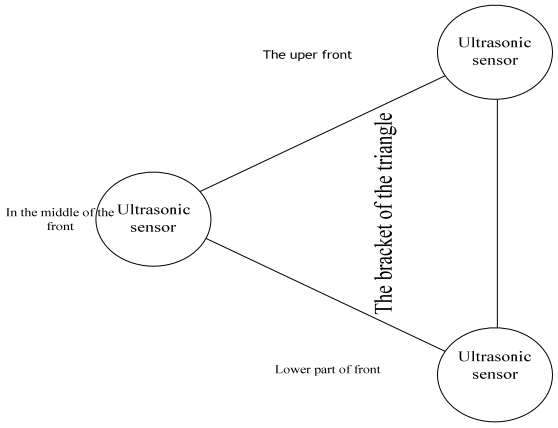

Fig.3. Location of obstacle detection sensor module.

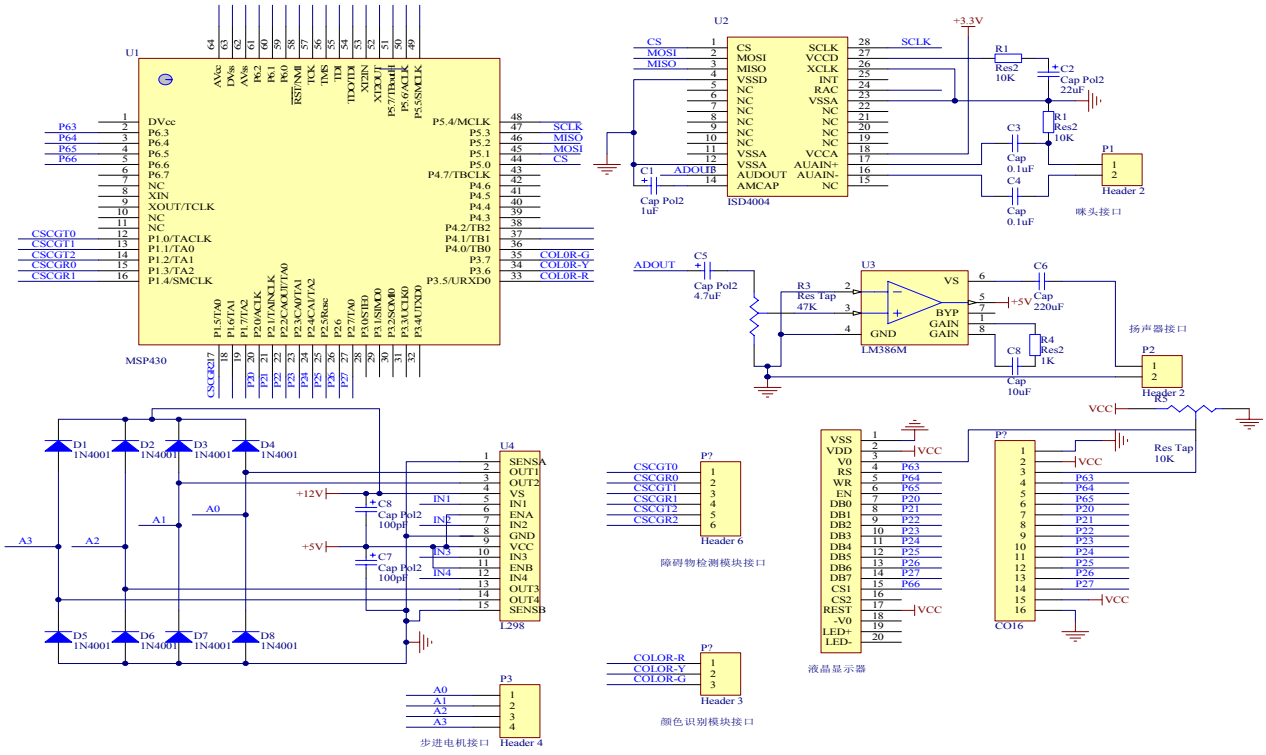

Fig.2 Hardware circuit diagram.

B. Color Recognition Module

The module uses TCS230 that is a programmable color light-to-frequency converter introduced by the American company TAOS (Texas Advanced Optoelectronic Solutions).The sensor has a high resolution, programmable color selection and output scaling, single power supply, etc; It can transform color information directly into a frequency signal and directly connected to the microcontroller. It can also be accurately measured color of an object, and not affected by ambient light. It has good noise immunity and measurement accuracy [5]-[7]. Since in the

acquisition sensor TCS230 tri-chromatic (RGB) values of the frequency of the red, blue, green sensitivity of the three primary color lights causes a different frequency measured RGB inaccuracies [8], and therefore the need for a white balance adjustment before the test .After adjusting that, it has accurate color recognition performance and good resistance in a sealed and natural light conditions [9]. By writing frequency identification red, yellow and green colors of the program can output the converted, then by comparing the red, yellow and green band frequency size can be determined why the input color signals. This method circuit is simple and practical program. Since TCS230 integrated sensor module used, it can be directly connected with the processor, the hardware circuit is very simple.

C. Ground System Module

This module is independent of the device design, the separate existence of auxiliary modules. This module provides signal lamp signal arrival time ,prompts the current time and suggests that the timing is on, shut down the system and other information, which is the normal operation of the locomotive to provide the necessary conditions. The module is designed in a long orbital model S = 5m. Module has a total of five sites, in addition to the originating station and terminal, and has three sites in the middle. The track has a curved arc of 4.8rad corners. Its arc length L = 0.24m, and its tilt angle corners 0.061rad, Then get the locomotive running through the calculations required speed limit here is v1 = 3cm / s. Then consider docking station is set to 20 seconds time, and the average speed to normal operating portion is v2 = 5cm / s.

D. Voice Module

Voice module is designed to train one of medium to communicate with the passengers, and the use of user-friendly voice prompts can effectively remind passengers to get off, and note compartment's hygiene. This module uses ISD4004 voice chip that is manufactured by the United States ISD. It has a long recording time, recording up to 10 million times repeated, with the advantages of high-quality, natural voice reduction technology and other. Before overall test needs to be a voice entry operations.

E. Motor Driving Module

Motor drive module as part of the overall power state directly affects the quality of their work running. The design requirements for stability is relatively high. There are two ways controlling the drive motor: closed-loop control and open-loop control. Open-loop control system to outside interference in the work process a greater impact, is not conducive to the stable operation of the locomotive, and closed-loop control system can effectively solve these problems. Selecting when using closed-loop control system operated incremental PID controller algorithm can effectively avoid the impact of outside interference [10]-[11]. The mathematical expression of incremental PID controller is:

$$\mathrm{D}u(k) = u(k) - u(k-1) = K_p + [e(k) - e(k-1)] +$$

$$K_p \frac{T}{T_i} e(k) + K_p \frac{T_d}{T}[e(k) - 2e(k-1) + e(k-2)]$$

$$= K_p[e(k) - e(k-1)] + K_i e(k) + K_d[e(k) - 2e(k-1) + e(k-2)]$$

$$= (K_p + K_i + K_d)e(k) - (K_p + 2K_d)e(k-1) + K_d e(k-2)$$

$$= me(k) + ne(k-1) + re(k).$$

Wherein

$m = (K_p + K_i + K_d)$, $n = (K_p + 2K_d)$, $r = K_p$,

$K_i = \frac{K_p T}{T_i}$ is called integral coefficient;

$K_d = \frac{K_p T_d}{T}$ is called the differential coefficient;

K_p is called a proportionality coefficient;

T_i is called integration time constant;

T_d is called differential time constant;.

Incremental PID controller algorithm has the advantage of improving the windup, manual and automatic switching of small shocks, small system overshoot and dynamic time is shortened and improved dynamic performance effectively. Using the above incremental PID controller algorithm programming, we can make a reasonable adjustment factor locomotive running smoothly. Closed-loop system can be designed schematic shown in Figure 3.

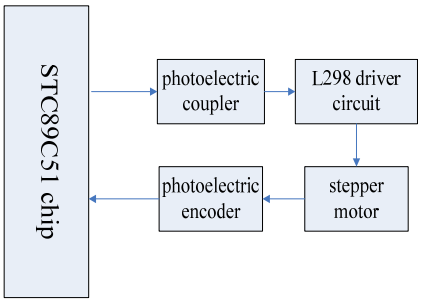

Fig.4. The closed loop system diagram..

From Fig4, we can get out that STC89C51 chip can

get through L298 driver circuit and photoelectric coupler to control the operation of the stepper motor. Optical encoder play a role in detecting the motor speed, and the resulting value is returned to the microcontroller for comparison, thus the microcontroller could combine with incremental PID algorithm to adjust the number of pulses by the difference to smooth the operation of the motor.

IV. Software Design

From half past nine at night to half past five in the morning the next day, the unit is in standby state, when early 5:30, locomotive begins operating in green signal under the action of awakening. The yellow light encountered in the process of operation, the locomotive speeds down, in case of a red signal, delay to slow down and stop, and broadcasting sites, after a certain time, the locomotive starts at a lower speed, in case of a green signal, and the running speed accelerate to normal operation. If large obstacles encountered in the operation process, we need to brake the locomotive to overcome the obstacles. Thus we can design program of microprocessor control process as shown in Fig 5.

V. Results and Analysis of Test Systems

After the completion of the design, we need a

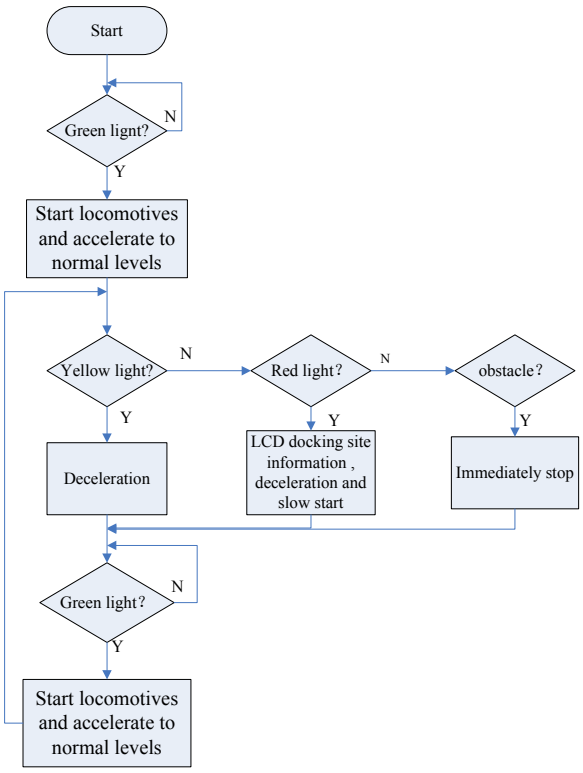

Fig.5 Software design of microprocessor control section.

functional test. The test method is: for the first time, set the ground module signal the open and shut down time (after only a design, no need to design), test the performance of the system module on the ground, and then put the locomotive model on the orbit, ground system reopened, observe the running state of locomotive model, mainly check and ratify color recognition module, motor operation, voice, liquid crystal display module whether or not working correctly. Also observe the continuity and automation of locomotive in the process of running, at the same time, using a stopwatch measure the locomotive round-trip time used at a time and the time through the corner, a total of three groups

TABLEI

TEST AND PREDICTED RESULTS

Serial number	Determination of the number			
	first	second	third	The average
Round-trip time(t/s)	270.5	255.8	260.9	262.4
Round-trip predict time(t/s)	263.2	263.2	263.2	263.2
Bend time(t/s)	7.5	8.2s	7.8	7.8
Bend predict time(t/s)	8	8	8	8

From the data in front of the formula we can get the locomotive round-trip time is: the total time t = (sites dock time) t1 + (bend time-consuming long) t2 + (work correctly time) t3, which in the process of back and forth there are eight dock sites, each of them uses the 20 s, bend arc length L = 0.24 m, the default rate is 3 cm/s, according to t2 = L/v1, obtained the curve time = 8 seconds . Works part time length according to t3 = (S - L)/v2, about 95.2 S. Therefore, a trip back and forth, model locomotive time-consuming t1 = 20 + 8 + 8 x 95.2 = 263.2 s, forward bend time-consuming t2 = 8 s. Combining with the measured data and the analysis, the comparison results can be obtained are shown in table I.

Through the test, basically, each module can be effective to finish the task, but the color sensor module identification efficiency is a little low, the voice module works slower, the main reason is that the strong light during the day affected the sensor for identifying the color light, causing the slowing , which we can plus shield method to make the interference intensity reduce to the range we can allow, at the same time , reduce the running speed of locomotive, give sensors more time for recognition . After modified the model locomotive running speed is about 5 cm/s, the

voice module is improved to avoid the problem that the locomotive arrived at the site but has not reported to the site. After modification , by table I we can see the test data is close to the predicted value, the average gap and predicted value has a slightly smaller difference , so we can predict the system running time of after debugging ,the locomotive operate 80 times back and forth in one day, under the condition of this , the error can be controlled in a minute or so, so the overall performance can get effective guarantee.

VI. Conclusions

In locomotive running control device design process focuses on the combination of automatic control theory, sensor technology and power electronics theory, based on the idea of modularization to overall design, model of locomotive can be implemented in the practical application of automatic control operation, meet the design requirements. It provides no one wanted by the operation of the train operation control system key technology, the model of locomotive are compared with actual locomotive in such aspects as technology there is a big gap, but still we can see it as a kind of model of unmanned train operation system to explore in the laboratory which has certain innovation exploring significance. In addition, this design has the clear and pure and fresh, simple structure, reasonable performance, the characteristics of low cost, suitable for children educational toys as product promotion, help children's development of thinking and cognition, have certain commercial value and market prospect.

References

[1] Y.-X. Liu, “Situation and Development of the locomotive brake”, No.1. vol. 28 Electric Locomotives & Mass transit Vehicles, 2005,pp.6-9.

[2] Б．Д．Никифоров & W.-J. Song, “Train braking and automatic control system of the Russian railways ”,J. Foreign ocomotive. 1995 ,pp.36-42.

[3] L.-M. Jia & X.-D. Zhang, Railway transportation automation-status-problems and challenges , A.The Proceedings of Chinese Control conference in 1994 ,C.1994 .

[4] Q.-P. Liu, “Microcontroller-based design of ultrasonic range finder”,No.3,vol.26,J.Journal of Jiangxi Vocational and Technical College of Electricity,2013,pp.40-42.

[5] F.-Z. Xie, H.-D. Zou & N.-X. Wu,“A color detection device based on the TCS230 and its application on the intelligent assembly robot for obstacle avoidance” ,No.1, vol.20,J. Chinese Journal of Engineering Design,2013,pp.60-61.

[6] J.-M. Hu, “Color sensor TCS230 and its color identification circuit”, No.1, J. Micro-controllers & Embedded System,2006.pp.40-41.

[7] A.-M. Wang , X.-C. Shang & L. Zhao, “Design of the measurement of oil-water based on TCS230 vol.9,J.Machinery Design & Manufacture , 2010,pp.21-22.

[8] Y.-F. Zhang & Y.-B. Hou, “Fuzzy identification algorithm of TCS230 color sensor”, No.4,vol.39,J.Optical Technigue, 2013, pp. 377-378.

[9] H.-H. Pan, L. Chen, B.-Q. Huang & J.-Y. Meng. “High-precision color recognition system based on TCS230 sensor”,No.6,vol,25,J. Sensors and Instrumentation,2009,pp.159-161.

[10] W.-P. Pan, G. Xu, & J.-S. Zhang, “Proteus-based close-loop control of stepper motor simulation”,No.2.vol.31,J. Coal Mine Machinery, 2010,pp.46-47.

[11] C.-M. Wang, X.-M. Liu & Y.-J. Ji,“Continuous and Discrete Control System”, BeiJing: Science Press,2008,pp.402-403.

Wireless Dynamic Electro-Cadio-Gram Mornitring System

Ling zhen-bao ; Jiao Ye-jun; Liu Jin-xin; Pei Li-ran

(College of instrumentation and electrical engineering,Jilin University,Changchun 130061,)

***Abstract*—Since the lead wires of the traditional ECG monitoring devices inter wine with each other,it will distort the ECG,lead to activity restriction of the patients.What's more,The ECG can't be saved in time after collecting it and so on.We put forward the idea that using ZigBee wireless transmission technology,with the core control device based on MSP430F149 processor system and TF card for data storage devices,to assemble a real-time collection and storage of human ECG signal portable lead wires electricity storage system prototype.With the function of data collection,wireless transmission and the file storage,and the characteristics of low power consumption,lead-free detection and remote monitoring,the prototype can provide with convenience for ECG signal acquisition and timely data storage.**

***Keyword*—Portable; No lead wire; Storage signal; Remote monitoring; Signal analysis**

I.INTRODUCTION

AT present,the heart head blood-vessel disease cause of death in the column of the first in our country,is the chief diseases affect human health today[1].Its morbidity,mortality,recurrence rate,morbidity are among the first,and become the top killer of harm to people's health[2].Ordinary ECG examination can only record a short ECG signal When the client is quiet,Cannot objectively reflect the malignant arrhythmia and myocardial ischemia,etc[3].at the same time,Its can't record sleep,sports,work tired or mood swings,and other specific condition of ECG waveform[4].The limitation of lead wire would make patient feel limited ,also makes the operation of the monitoring exists great inconvenience.Mostly used in detecting method is fixed ECG monitoring instrument,Always cable system,These complicated equipment and attachment bring to patients and doctors a lot of inconvenience and its expensive[5].Only a single monitor.So a timely manner or long-term ECG monitoring and storage is particularly important for patients.

The currently existing ECG monitoring system or ECG signal is stored by the PC,Or only a small amount of ECG signal by a microprocessor implementation of storage,has been difficult to meet the further development of ECG monitoring,ECG monitoring instrument has been toward the trend of a more portable,networking and no lead.there is a wireless radiation safety,seamless roaming and wireless network costs,and other issues in ECG monitoring system Based on the infrared,blue tooth,GPRS wireless transmission technologies,So the IEEE 802.15.4 / ZigBee wireless communication standard combined with TF portable storage technology has become the effective ways to solve ECG detection and storage.

To this end,the author designed Holter monitor prototype without lead wire based on ZigBee,through the method of modular ,choose CC2530 wireless module to construct wireless ECG sensor network,which realizes the ECG data wireless transmission,through the MSP430 SCM ECG signal acquisition and processing and the data deposited in the TF card,Then the PC analysis data of TF card and diagnosis .

II.THE SYSTEM DESIGN

The design of the hardware system structure diagram is shown in figure 1,The system hardware design with low power consumption,portable design concept,Mainly includes the acquisition module,ZigBee RF transceiver module and control for the center with MSP430 storage module,The acquisition module is composed of signal pickup circuit and control circuit,its mainly responsible for

ECG signal acquisition and front-end processing,RF transceiver module is responsible for acquisition module after the preliminary processing of ECG analog signal digital and sent to the receiver,Eventually msp430 main controller to deal with the data received,and stored in the TF card,The obtained data can be directly uploaded to the PC through the main controller,can also be done by the TF card uploaded to PC ECG signal analysis judgment.

III.ACQUISITION MODULE DESIGN

In view of the ECG signals are weak,low signal-to-noise ratio,low amplitude,etc,So weak in the process of acquisition of ECG signal to interference,especially the work of 50 hz frequency harmonic interference.In order to be able to accurately capture the ECG signal,the design use as shown in figure 2 a circuit for signal disposal.The low power consumption,low noise,low offset voltage,high precision instrument amplifier AD620 chip was used as the front-end amplifier circuit in Acquisition module,the pick up of ECG signal is amplified,and the gain formula:

$$G = \frac{49.9}{R_g} + 1 \qquad (1)$$

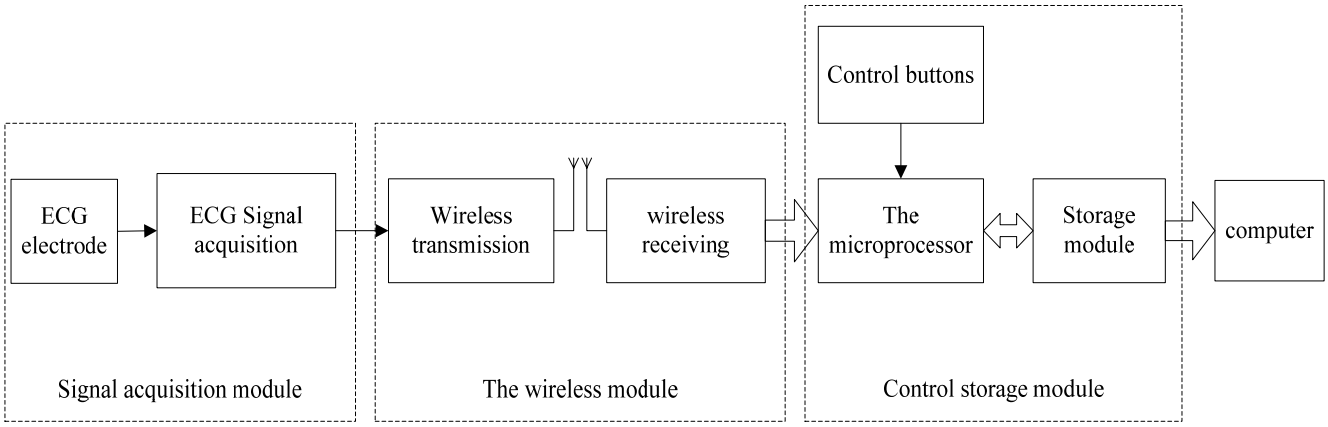

Fig.1 The whole structure block diagram

R_g Choose 10 kW ,the gain value is about six times ,With the right leg drive circuit for AD620 reference ground,High-pass filter cutoff frequency is 0.3 Hz,the cut-off frequency of 130 Hz low pass filter and the center frequency of 50 Hz trap constitute filter circuit， Secondary amplifying choose low noise,the chopper stabilizing zero op-amp chip OP07 enlarged signals 50 times.Finally,the signal disposal adder to 0-3.3 V range,in order to satisfy the requirement of ZigBee A/D conversion,

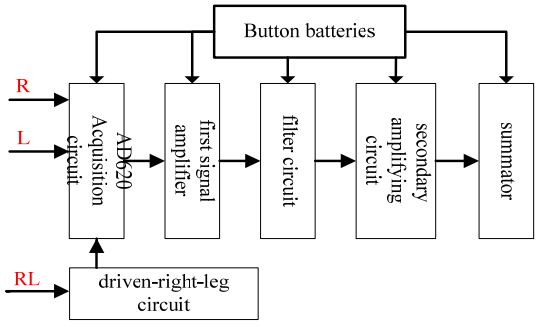

Fig.2 Acquisition module principle diagram

IV.ZIGBEE RF TRANSCEIVER MODULE

A.ZigBee technology introduction

ZigBee technology is a kind of information in small scale wireless transmission systems,strong anti-interference ability [10],it is a short distance,low cost,low power consumption,low rate of wireless network technology [12],As A new generation of SOC chip CC2530 on-chip system,ZigBee support IEEE802.15.4 standard,it is A combination of A fully integrated,high-performance RF transceiver and A 8051 microprocessor,also integrates 8 KB of RAM,128 KB of programmable flash and 14 ADC converter (A/D),etc.,to meet the requirements of the system of high integration,low power consumption.

B.ZigBee module

ZigBee wireless module is composed of the sender and the receiver,the main implementation of ECG signal D/A conversion,signal receiving and data processing,initial data through serial communication by the receiving end to MSP430 single chip microcomputer.

ZigBee module circuit structure as shown in figure 3,ZigBee delivery module first served as the data

conversion/task,so using ZigBee chip internal 14 A/D

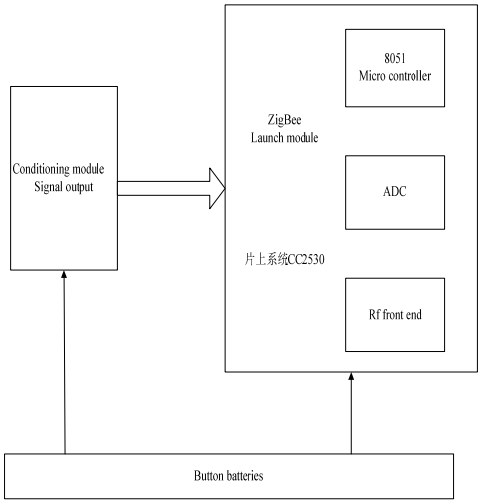

Fig.3 ZigBee Schematic Diagram

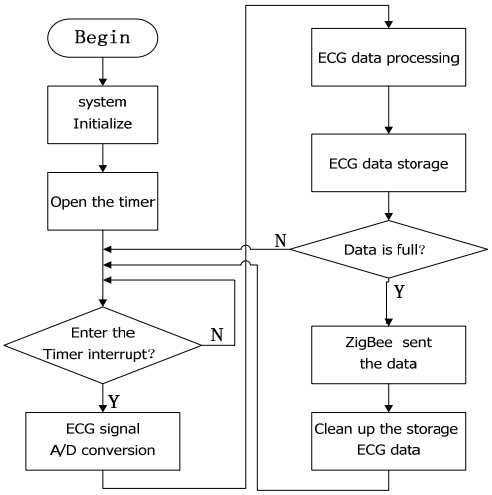

Fig.4 acquisition and send flow

module,P0.7 as electrical analog signal input port,set the reference voltage of 3.3 V,the clock frequency to DIV = 128 points,and adopts the 00 - FF reshipment counting mode interrupt automatically,set twice for an A/D sampling interrupt.Sampling period Ts:

$$Ts = 2 \cdot 256 \cdot DIV \cdot \frac{1}{f_{osc}} \qquad (2)$$

The DIV is the clock points frequency number,fosc is clock frequency of timer T3,sampling period calculated Ts = 2 ms,the sampling rate is 500 hz.Each time the conversion results are 14 bit,only 12 bit effectively.There are two bytes.Once every 15 conversion results package sent to the receiver via a wireless network,collect send program flow chart as shown in figure 4.

ZigBee is not immediately sent to the microprocessor after receive data from serial port,but after the data scale transformation,binary data is converted to electrical signal voltage value,and magnified 100 times sent to the microprocessor as integer.

Conversion formula:

$$ECGV = \mathrm{adc}, \frac{3.3}{2^{14}} \cdot 100 \qquad (3)$$

single-byte ECGV is converted in ECG signals,ADC is A/D conversion value,converted signal is sent to the microprocessor.

V.CONTROL STORAGE MODULE

A.Data reception and processing

Data received by the receiver of ZigBee,the main controller complete processing and data analysis in the TF card,because the data needs to be deposited in the PC to consult,analyze,so master controller need to produce Windows support FAT16 file system on the TF card.The flow chart of data receiving stored as shown in figure 5.

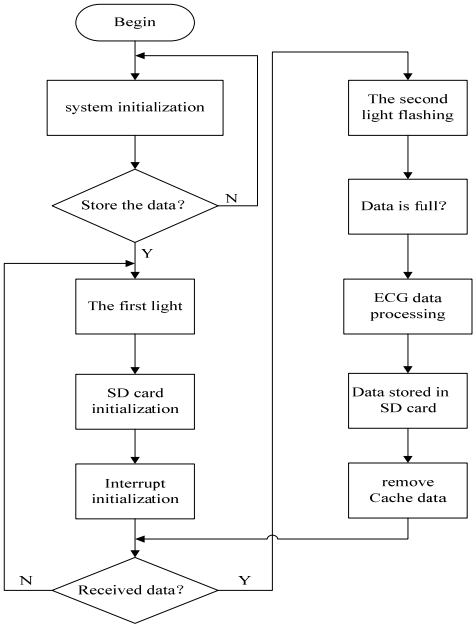

Fig5 receive and storage flow diagram

B.The data of dynamic storage

Signal acquisition part using the ZigBee internal A/D convert analog ECG signal into digital signal

with 500 Hz sampling rate,each sample point eight occupy the space of A byte,so for A day of continuous recording the space used for:

500(b/s)* 3600(s/h)*24(h)=42187.5(kb)=41.2(MB)

When we use the TF card produces Windows support FAT16 file system TXT document data,every 512 bytes of data file of the building space size is 2 KB.TF card used in the continuous recording of space for:

500(b/s)* 3600(s/h)*24(h)*2(kb)/512(b)=16875(kb)

=164.79(MB)

The design of the actual use 2G TF card as the storage medium,so this design can achieve up to 12 days of ECG data acquisition and playback.Overcomes the traditional shortcomings of the electrocardiogram machine records only a short time,the long time of ECG signal dynamic storage requirements.

C.The realization of real-time acquisition and storage

ZigBee wireless transmission speed is faster,so when the receiver and the main control issue of communication rate is greater than a part of the gathering,data loss will not occur.

So ZigBee is realized by using 9600 baud rate of the receiver and the main controller of the communication,due to the acquisition of signals for 4000bit/s,and the data transmission to the control system is 9600 bit/s,so the signal collected in the process of data transmission to the control system of no signal loss.

Single chip MSP430 through hardware USART communicate with ZigBee in 9600 baud rate,using interrupt way to receive ECG data.And then through the USART module in communicate with SD card SPI synchronous communication mode,make data save in the SD card.

VI.THE SOFTWARE DESIGN AND TEST RESULTS

A.PC software design

PC software is the core of the application of system,it was carried out on the patient's ECG data display,analysis and storage convenient staff analysis of patient's condition and rehabi- litation instruction[3],PC software written by matlab program to analyze the ECG data of TF card and display of ECG waveform,at the same time a certain automatic analysis of ECG waveform,display is shown in figure 6.

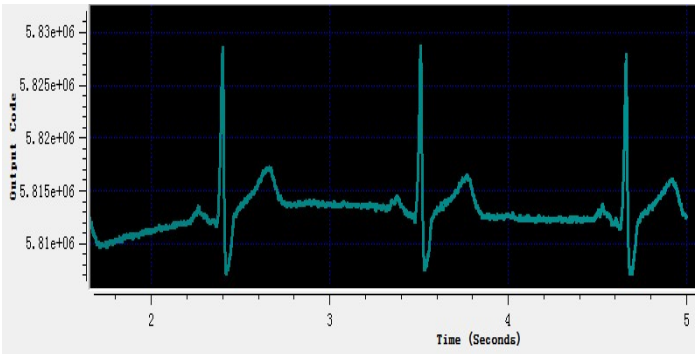

Fig.6 ECG signal display in principal computer

B.Transmission distance

Holter monitor without lead to reduce the patient's bondage,patients can move freely after wearing,so experiment test the prototype of the sender and the receiver in the condition of different transmission distance,test results are shown in table 1,the transmission distance outside obstructions in the table for sending and receiving the linear distance,indoor obstacles choice in a different room,maximum distance measurement can transfer.Transmission effects differ due to different obstacles,so the test result is at a maximum distance of transmission test under different kinds obstacles of average.

TABLE1

No lead Holter system transmission distance test

	The maximum transmission distance is an obstacle	the maximum transmission distance there is No obstacle
outdoor	50m	80m
indoor	30m	50m

Because the system is mainly used in hospital or family,so the system can meet the needs of users.

VII.CONCLUSION

The author designed without lead Holter monitoring system has the characteristics of low cost,module integration and convenient carrying,prototype is mainly through the signal conditioning module and ZigBee module to get the

digital ECG signal,and then sent to the master node,the data stored in the form of TXT file,stored data can be analyzed by PC software.Laid the foundation for product of Holter monitor.But the test results show that the prototype work time less than ideal state.So plan to improve the software program,in order to reduce power consumption.

References

[1] Su Qiong-hua，Wang Yu-hui，Hospital Pharmaceutical Care Viewed from Perspective of Rational Combinationof ChinesePatent Drugs With Western Medicine for Patients with Cardiovascular and Cerebrovascular Diseases[J]，China Pharmacy，2009，,19（5）：394-395.

[2] Zang Yi-ming，Fan Rong，Annihilation of the first health-killer(cardiovascular diseases) in cooperationwithmult-i branchesof science[J]，Chinese Heart Journal，2006，18(5)

[3] Wang Li，Zhang Yue，Zhang Long-fei，ECG Data Processing Mechanism of Remote Wireless ECG Monitor[J]，Computer Engineering，2010，36（15）：291-293.

[4] Wang Zhi-jie，Her Wei-xing，Lv Ji-dong，The research and implementation of portable wireless ECG acquisition device[J]，2010，36（11）：95-101.

[5] Wang Qing，Wu Xiao-pei，ECG Monitoring System Based on ZigBee Wireless Network[J]，Industrial control computer，2011，24(4)：18-20.

[6] Xu Ling-ling，Yang Jing-chang，Hao Ming-gang，Community ECG monitoring system based on ZigBee network[C]，2012，31（2）：16-21.

[7] Sun Xin，Application of ZigBee technology in 3PL intelligence warehouse[J]，2012，35（14）：8-10.

[8] Li Su-yi，Zhang Hong-jing，Lu xia，et al，Wireless Dynamic ECG Monitoring System Based on ZigBee Technology[J]，Journal of Jilin University，2012，30（5）：450-455.

[9] Analog Devices，op07 datasheet[Z]，2003.

[10]Jin Hai-long，Tang Li-zhi，Du Jun，ECG detecting system based on zigbee technology[C]，The Ninth Younth Conference of China Instrument and Control Society，2007：730-733.

[11]Gao Wei-lan，Zigbee：Review of a new generation of wireless networks[C]，Silicon valley，2010：18-21.

[12]Li Xiao-mei，Liu Shi-long，Liu Wei，Application Safety of Wireless Medical Equipment[J]，Industrial control computer，2011，26（1）：64-66.

Intelligent power socket of reducing the mounting current

Zhang Linhang; Xie Mingxue; Xiong Yuan; Liuyajiao

(College of Instrumentation and Electrical Engineering, Jilin University, Changchun 130022,China)

***Abstract*—in view of the standby power consumption of household appliances, this paper proposes an intelligent power socket based on MSP430F149 MCU for cutting off the mounting current. It samplings mounting current by a coil current transformer, compares with the preset value after analog-to-digital conversion to drives relay to cut off the power supply current. Severally tested on different appliances, it achieves the purpose of reducing power consumption.**

***Keywords*—mounting current intelligent power socket current transformer relay**

0 FOREWORD

WITH the development of Technology,Household appliances have entered the intelligent-age.Although these appliances have been closed,If not timely supply unplug the plug from the socket will cause power loss,The current generation of this state is Standby Current.Common electrical standby current and standby power consumption as shown in Table 1.According to information,Currently the average standby power consumption of urban households Equivalent these families the equivalent of a 15 ~ 30W incandescent lamp every day, Standby power consumption accounts for 3% to 13% of household consumption,National standby power consumption is equivalent to the total electricity generation of several large thermal power plants

For reducing standby power consumption in the literature [1], [2], [3] mentioned several solutions.Generally speaking there are two aspects, first, national regulations common electrical standby power standards, appliance manufacturers from improved internal circuitry, the second is to set the total household power control switch. But the crux of the problem lies in the standby state and people's consumption habits prevalent.This paper presents a new socket, it electricity from people's bad habit of starting, ultra-low power microcontroller detects electricity by the state, in the non-working state automatically cut off the electrical circuit.Greatly reduces the standby power consumption, fit today's low-carbon energy, green environmental protection requirements of the times.

Tab. 1 Standby current value of household appliances

Device Name	Standby current measurements/ mA	Standby current average /mA	Standby Power Consumption/W	24 hours standby power consumption
Laptop	11～87	43	10	0.24
Television	19～106	53	12	0.29
DVD player	10～34	27	6	0.14
Microwave	2～3	2.5	0.6	0.01
Air conditioning	10～23	16	4	0.10
Washing machine	7～15	10	2	0.05
Modem	52～81	61	13	0.31
Speakers	7.3～60	30	7	0.17

1 THE OVERALL SYSTEM ARCHITECTURE

The system set forth herein by a power module, MSP430F149 microcontroller, a current transformer, the relay drive circuit, short circuit protection components. The overall system structure shown in Fig 1.

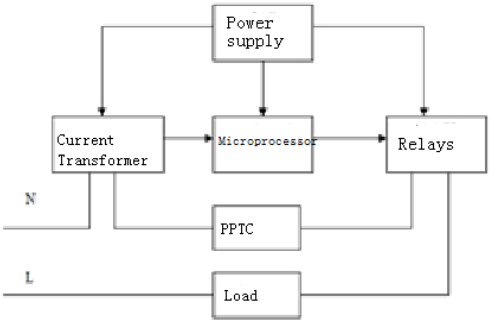

Fig.1 The principle diagram of the system

2 HARDWARE DESIGN

2.1 Host Controller Module

System using MSP430F149 microcontroller as controller. MSP430F149 is Texas Instruments has developed a class of single-chip 16-bit bus with the FLASH. It uses a 16-bit bus, unified addressing peripherals and memory addressing range of up to 64K, you can also expand the memory with a unified external interrupt management, has a wealth of on-chip peripheral modules. Due to FLASH type, you can online and download to the microcontroller for debugging, because the JTAG port and FET (FLASH EMULATION TOOL) is directly connected, without additional simulation tools, convenient and practical, and can work in ultra-low-power mode [4] . You can choose to run in the ultra-low-power mode, which is one of the biggest advantages of the single-chip, in addition, there is a single-chip peripheral A / D, simplifying the design of the circuit structure.

2.2 current detection circuit

Is the core module of the current detection circuit, which is the source of the measurement data obtained. This design uses two scenarios. A program using the current transformer, the circuit shown in Figure 2. The circuit structure is simple, low cost, efficient use of the electromagnetic 220V mains isolation separates the microcontroller to ensure safe performance. But the drawback is the low measurement accuracy, the specific relationship between the ratio of the number of turns and the tightness of circling about, there will be a strict ratio between the volume slightly, is not conducive to smaller footprint. Option II, the use of Hall current sensors. ACS712 current sensor is a linear Allegro launched, the device built-in precision linear Hall sensor circuit low bias, AC or DC current proportional to the energy output of the detected voltage. Low noise, fast response time (corresponding to step input current, output rise time is 5μs), 50 kHz bandwidth and maximum total output error is 4% higher output sensitivity (66mV / A ~ 185 mV / A), easy to use , cost-effective and high insulation voltage [5]. Measurement circuit shown in Fig 3.

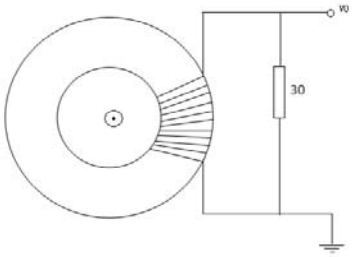

Fig.2 the measuring circuit of current transformer

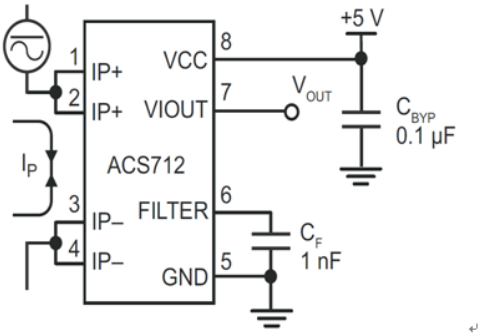

Fig.3 ACS712 measuring circuit

ACS712ELCTR-05B-T, the detection range is ± 5A, sensitivity of 185mV / A. The master controller module design uses MSP430F149 own 12 ADC, an internal reference voltage is set 1.5V, 1LBS = 0.366mV. The 1LBS corresponding current sensor input current I = (0.366/185) A = 1.978mA. Table 1 shows that can meet the standby current measurement accuracy can distinguish operating current and standby current.

Measurement accuracy because there is demand for the product is not very strict, just need to have a more rough comparison capabilities, determine with the current state of electrical work can be. From the point of view of product promotion need to reduce costs, reduce production difficult, so a final option.

2.3 the driver circuit of relay

The relay system is an execution unit, the choice is HK4100F. The driving circuit shown in Figure 4.

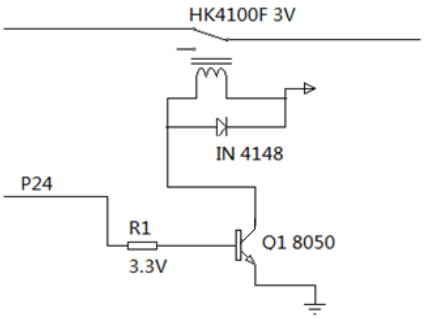

Fig.4 the driver circuit of relay

2.4 Overcurrent protection circuit

Overcurrent protection circuit for protection of the line, more important is the protection of certain electronic components in the system are not damaged.two methods can be considered: one, using a fuse. Thermal fuse can not be restored once burnout, so in this work try to use recoverable fuse, such as PPTC; the other is to lap fast protection circuitry:once short , in order to reduce the judging time, the voltage comparator generates a TTL signal, which controls relay disconnected, as shown in Figure 5.

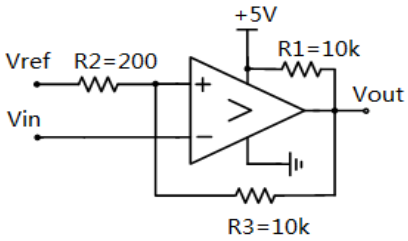

Fig.5 comparator with Hysteresis

2.5 level conversion circuit

In order to reduce the volume and weight of power socket , the system uses a battery-powered. But MSP430F149 MCU support 3.3V power supply, so a level conversion is required, level conversion circuit shown in Figure 6.

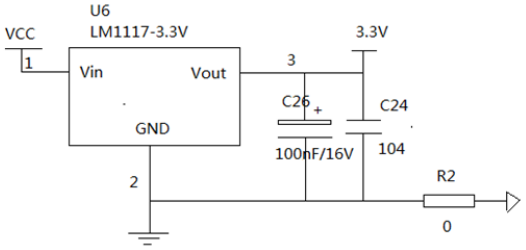

Fig.6 circuit of Level conversion

3 SOFTWARE DESIGN

By comparing the real-time current and a preset current, judges the state of the appliances to control the relay . Fig.7 shows a flowchart of the program:

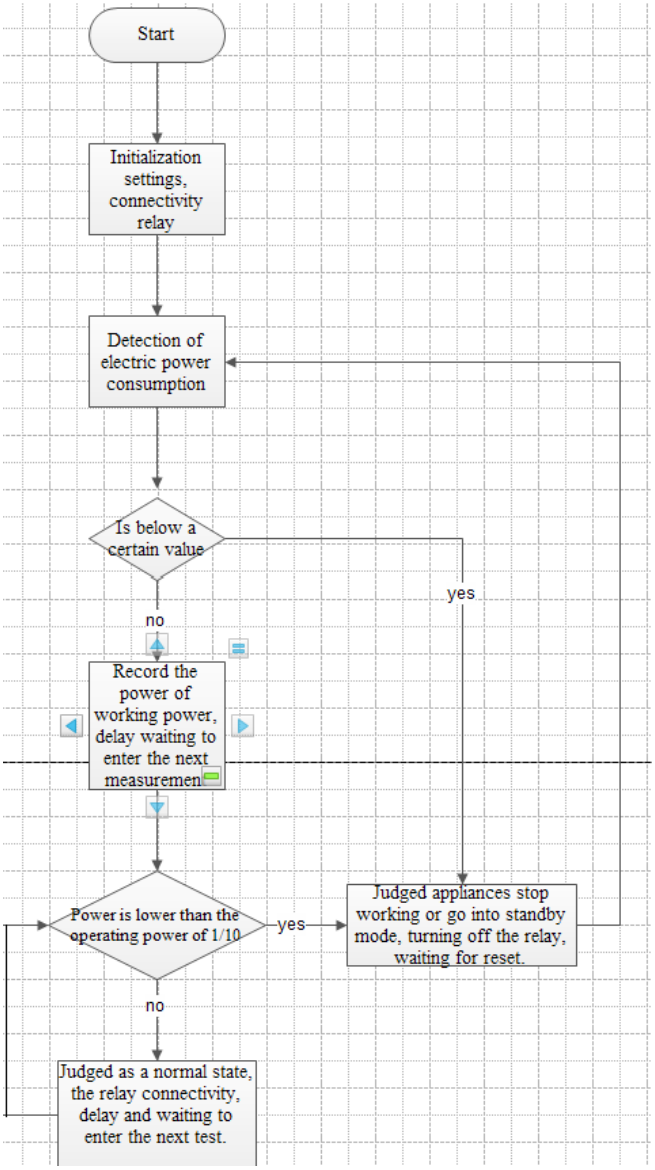

Fig.7 program flow char

4 SYSTEM TESTING AND RESULTS ANALYSIS

Physical model shown in Figure 8. Phone, electric iron, monitors, drinking fountains and other appliances were tested, the specific method is: let the appliances in working condition, and then press the reset switch, observe the power socket wether timely break the circuit channel or not when the appliances in standby mode. After several tests, the power socket can identify with the electrical work status,with fast power-down features.

5 CONCLUSIONS

After the actual anti-mount current smart design, this article describes the power socket, capable of real-time identification of household appliances in standby, and then cut off the circuit path. Has a low rate of false positives, the response time is short, simple structure, easy to use and so on. In the contemporary environment protection and energy, must have its broad application prospects.

Fig.8 System real figure

References

[1] Li yi. Household appliances and home standby power saving mode analysis to explore [J] Electrical Building 2013, 2: 39-43.

[2] Zeng Yanguang.States Stand EER analysis [J]. Certification and laboratory .2011, 1:57-61.

[3] Wang Jingjing, Bai Leishi, Yan Hui,Wang Xiaoying. On the standby power consumption of household appliances [J] China Science and Technology Information 2008, 10: 140-141.

[4] Yang ping, Wang wei.MSP43 series of ultra-low-power microcontroller and application [J]. Foreign Electronic Measurement Technology .2008.

[5] Dong Jian huai. Principle and should ACS712 current sensor [J] information Technology.2010,5:94.

The implementation of multi terminal communication research based on Bluetooth

HAN Ming-yang, HU Qiang, LI Wen-ming

(College of Instrumentation and Electrical Engineering, Jilin University, Changchun 130026, China)

***Abstract*—Since the date of birth of bluetooth technology , It has extensive application in the field of mobile communication、 wireless data acquisition、computer network control .In this paper, with the Bluetooth technology as the theoretical basisin, design of control system of multi terminal bluetooth universal with the single chip microcomputer、mobile phone、PDA and PC to realize the communication between hardware platform.After the verification, this system can meet the design requirements and completed the communication among the four platform.**

***Key words*—Bluetooth technology; Multi terminal; Wireless communication; Information transmission**

I. Introduction

BLUEBOOTH is a short distance communication support equipment (usually 10m) wireless technology, wireless information exchange between the support of many equipment. multi terminal bluetooth commun- ication system refers to the system between the various hardware platforms communicating with Bluetooth technology, including the experimental system for microcomputer, mobile phone, PDA, PC, can realize the transmission of any two characters, numbers and receiving. According to the four terminal, development platform including the visual studio ,eclipse, and keil. Design of MCU uses STC89C52 to complete the hardware platform..

II. Procedure for Paper Submission

A. Design for the system

According to the system design and communication requirements, multi terminal bluetooth communication system design as shown in Figure 1, including four modules of MCU system, mobile phone, PDA and PC. MCU system module is based on HC-06 Bluetooth module through the serial port, using low power microcontroller STC89C52 of STC company as the main control chip, peripheral keyboard, LCD. The main control chip to control the keyboard input transmission character and control of liquid crystal display of the receiving and sending character. Mobile phone system module is Meizu MX2 mobile phone, based on the bluetooth4.0, by calling its Bluetooth function, design of communication software, the completion string, digital transmission and the receive, with clear, save, save the file in TXT format storage and memory card. PDA is based on the HP h2210 (FA103A), built-in Bluetooth module JSR-82,system language is Windows CE,VS2005 programming environment. Design and implementation of set, receiving, sending, preservation, removal and other functions. PC based matlab design serial communication software, the parameters can be set to achieve the communication between devices. Eventually, mobile phone, PDA MCU, PC Quartet based on Bluetooth, transmission and exchange of internal information through the serial communication, information processing platform will be received. through the screen is displayed.

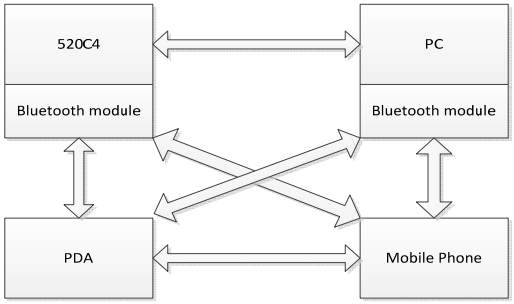

Fig.1 Diagram of the system

B. design for system module

Multi terminal Bluetooth communication system mainly consists of MCU, mobile phone, PDA, PC machine parts. Through serial communication, set the COM port (different equipment settings are different), baud rate 9600, 8 data bits, 1 stop bit and a series of operations, complete the connection, communication, equipment storage, clearance, exit and other operations.

1 MCU design

Using keil4 for programming and debugging, Protues simulation experiment. The hardware block

diagram is shown in figure 2:

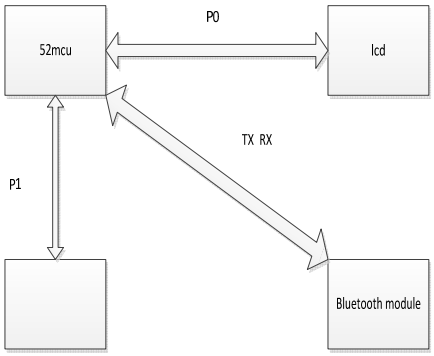

Fig.2 Hardware connection diagram

1.1 Bluetooth module

Bluetooth module using HC - 06 type, interface level 3.3V.The main application of pins VCC, GND, TXD, RXD, VCC connected to the positive electrode, GND grounded, TXD chip RXD and the Bluetooth module RXD is connected with the single chip TXD. Through the Bluetooth module in the MCU Connect the SBUF status register, through the temp=SBUF to receive, send by SBUF=Key_Value.

1.2 keyboard scanning

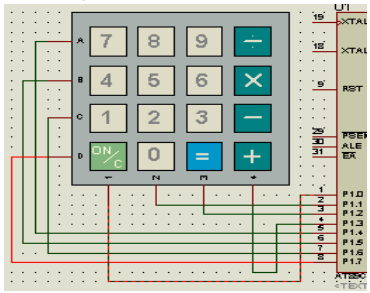

Fig.3 The keyboard circuit diagram

The keyboard using 4x4 matrix keyboard, the matrix keyboard leads pins respectively and 52 MCU P1 port 8 pins connected, hardware connection diagram shown in figure 3,. The scanning process is as follows, P1 port will be one by one to give 0xFE, 0xfd, 0xfb, 0xf7, and then temp one by one to give 0x10,0x20,0x40,0x80, when the first I rows and j columns key is pressed with P1 & temp=0, is recorded by pressing the key position i+4*j.

1.3 display part

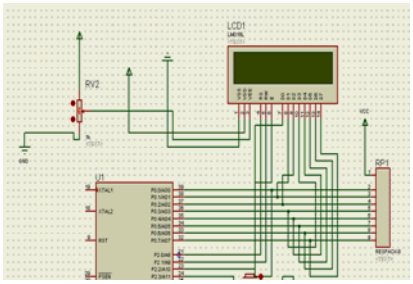

Fig.4 Liquid crystal display circuit diagram

Lcd1602 as a part of display , the data port respectively, and 52 MCU P0, after opening 8 pins connect pull-up resistor, VEE pin sliding rheostat in respectively grounded and positive, VDD and VSS are respectively connected with the anode and the ground, the hardware connection diagram shown in figure 4,. The working process, the program at the beginning of the liquid crystal module for initialization, agreed the display format, display character to be input display character address, then according to the internal character generation memory, input specifies the code to display the character.

2 The design of Mobile phone

MEIZU mx2,is a mobile phone based on the system of Android 4.1. It is designed by using Android language, based on JAVA,and programming software is Eclipse v22.0.5 version to design mobile phone software of Bluetooth.Eclipse is an open source,extensible development platform based on JAVA..

2.1 Mobile phone system hardware

The mobile phone is based on Bluetooth 4.0.It has the advantage oflow peak,average and standby mode power consumption,low cost,interactive devices fro- m differ-ent manufacturers,wireless coverage enha-nceement,The fully backward compatible,Low latency (APT-X).

2.2 The software of mobile phone system

The main interface design system as shown in Figure 5. Including the five controls of connection, transmitting, preservation, clear and exit, two text boxes of sending and receive.

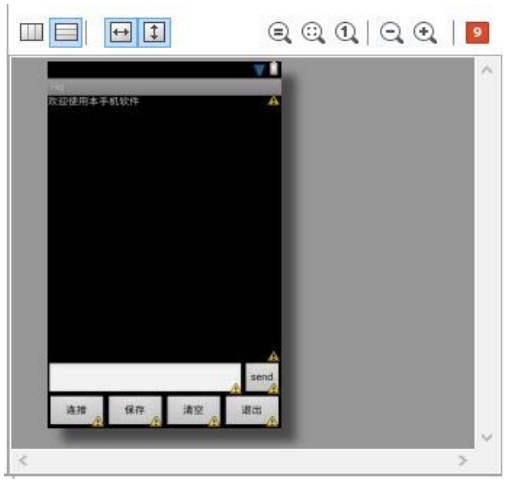

Fig.5 Mobile phone software component design

The design of connection control including custom functions of findViewById and on Connect Button Clicked, to search equipment and respectively connected with the key response function.The design of transmission control use the function of on Send Button Clicked, to achieve send a number or string functions. Other controls the function and the corresponding function as shown in Table 1.

Table 1 Interface design involves the function and parameters

The function	Parameters	Effect
findViewById	R.id.Button03	Search equipment
onConnectButtonClicked	View v	Connect button response
onSaveButtonClicked	View v	Connect button response
onClearButtonClicked	View v	Clear key response
onQuitButtonClicked	View v	Exit key response
Save	( )	The Save button response
onSendButtonClicked	View v	Send the key response

3 Function design of PDA software

3.1 Design platform

About PDA software we need to write a serial communication software. Because the last to be generated MFC file downloads to PDA through Activesync. the PDA for Windows CE operation system, compared several programming language,include Java, VB,andC/C + +, we chose the C + +, because its underlying control ability and it is linked with the Windows system more closely.The environment is vs2005.

3.2 Interface design

We designed to open the main interface,include Bluetooth, turn off Bluetooth, send data , save and remove five controls.there are two text boxes sending and receiving . The ID of part of the above are :

Turn on Bluetooth : IDC_Bluetooth_Open. First determine whether the port is open, then the new serial communication objects.

Turn off Bluetooth : IDC_Bluetooth_Close. Open the serial port so close to end communications.

Sending Data : IDC_Bluetooth_Send;F irst determine whether the Bluetooth connection, the connection will screen the input string line sent.

Save : IDC_Bluetooth_Save; Save PDA interface receives data and character , save directory for my docement.

Clear the screen : IDC_Bluetooth_Clear; Empty the contents of the screen receiver box.

Send box : IDC_Bluetooth_Sendtxt; Display and input characters and data sent via Bluetooth but not sent content.

Receive box : IDC_Bluetooth_ Receive Display the received data via Bluetooth and character.

The main interface is shown in Figure 6:

Fig.6 Application component diagram of the PDA

3.3 Event handlers

When writing the program , we choose CSevil serial class with MFC serial package , we are first prepared by the various control interface , which calls the function were

Turn on Bluetooth : CxianshiDlg :: OnBnClickedBtnOpen ()

Turn off Bluetooth : CxianshiDlg :: OnBnClickedBtnClose ()

Transmit Data : CxianshiDlg :: OnBnClickedBtnSend ()

Clear : CxianshiDlg :: OnBnClickedButton2 ()

Save : CxianshiDlg :: OnBnClickedBinSave ()

OK : CDlgParams :: OnBnClickedBtnOk ()

Cancellation : CDlgParams :: OnBnClickedBtnCancel ()

Then call the serial settings of class :

Serial : CDlgParams :: OnCbnSelchangeCmbComNo ()

Baud Rate : DlgParams :: OnCbnSelchangeCmbComBaud ()

Parity bit : CDlgParams :: OnCbnSelchangeCmbComParity ()

Data bits : CDlgParams :: OnCbnSelchangeCmbComDatabits ()

Stop bit : CDlgParams :: OnCbnSelchangeCmbComStopbits ()

3.4 Generate a MFC of executable file

After compiling the program,we firm executable file of MFC .

4. The part of design for PC

Using matlab GUI to design PC interface software.

Matlab serial port control is through the serial () is mainly divided the implementation class and method of controlling functions corresponding to the four steps:

4.1 create a serial device object and set its properties.

9600b/s communication data asynchronously format for 8 data bits, no parity 1 stop bit.

4.2 open the serial port device object.

Command to open the serial device object.

4.3 read the serial data

Matlab communication data using text ASCII mode to read and write serial device commands are respectively fscanf and fgetl, the fgets fpritf when a Matlab communication data using binary mode to read and write serial equipment command is fread.

4.4 close the serial port device object

The use of Fclose (s) command to close the serial port equipment.

The main function of the operation as shown in table 2:

Table 2 Design of function of PC

The function	Effect
Fprintf	Write function
Fwrite	Write function
Fscanf	Readfunction,with character sreading,terminated by Terminator, with a return function
Fread	Read function, the binary mode read, read the specified number of characters
Fgets	Read function, the binary mode read, read the specified number of characters
Fgetl	Read function, with characters reading, ignore the Terminator auxiliary operation

C Test

Test equipment comprises a MCU, mobile phone, PDA, PC. Serial communication through mobile phone and PC test, PDA test, transmission including strings and numbers. Transmission test chip and mobile phone, PDA is digital.

1. the mobile phone communicates with a PC test. Mobile phone terminal sends a string as a test of character, send the string PC end. The two sides of communication, the experimental results as shown in figure 7.

2. to carry out communication test of PDA and mobile phone machine. PDA end to send the digital, PC end to send the string, the test results are shown in Figure 8, the PDA end and can display and save operation.

3. to test communication between MCU and PDA. As shown in Figure 9.

4. to test communication between MCU and mobile phone. As shown in Figure 10.

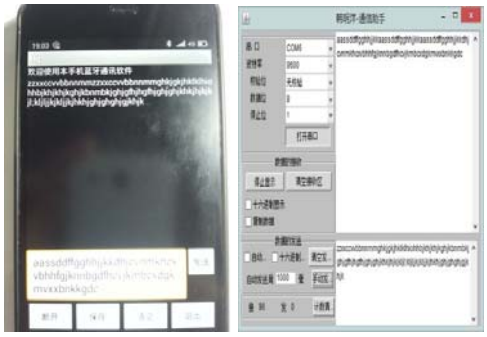

Fig.7 Characters to send and receive test of phone and PC

Fig.8 Characters to send and receive test pattern of PC and mobile phone

Fig.9 Characters to send and receive test pattern of MCU and mobile phone

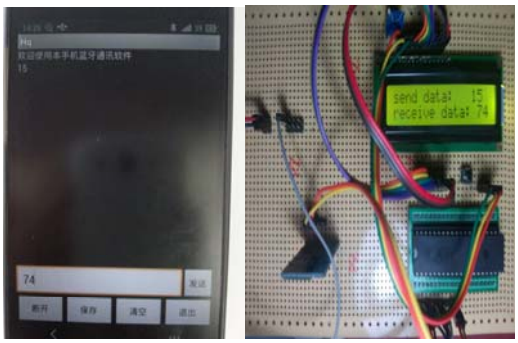

Fig.10 Characters to send and receive test pattern of MCU and mobile phone

After testing, four platform communication in good condition, between the mobile phone, PDA, PC can accurately transmit long string and long string of numbers, and mobile phone and PDA are preserved and clear function. MCU can send two digit, can reach the expected requirements

D Summary

The Bluetooth communication and serial communication technology to design and complete a multi terminal Bluetooth communication system, can realize communication of MCU, mobile phone, PDA, PC machine between the system based on. The MCU and other equipment to realize the digital transmission and reception. Mobile phone, PDA, PC's communication can be a string, inter digital. Mobile phone, PDA has kept clear and other functions.

References

[1] Kin Choong Yow;;Xiaoyu Liu ,Scheduling Mobile Data Services in a Bluetooth, Int'l J. of Communications, Network and System Sciences ,2010

[2] S P Rana;M A Fisher;P F McKee,Group Communication Using Modular Protocol Stacks, BT Technology Journal ,2000

Ultrasonic Ranging System Designbased on STC89C51 MCU

LIU Ke;XIA Yan-long;WANG Huan-yi

（College of Instrumentation and Engneering，Jilin University，Changchun 130021,China）

Abstract: **In view of the current traffic safety and growing problem, STC89C51 chip designed based on the core of the ultrasonic range finder. This system consists of an ultrasonic transmitter receiver module, LCD display module, sound modules and other components. The use of ultrasound to detect the distance of the obstacle in front of the detectable and temperature compensation. Ultrasonic Ranging in order to achieve accurate and intelligent display. The system is low-cost, functional and practical, and can be successful in reducing traffic accidents.**

1. INTRODUCTION

WITH the improvement of the people's living standard, the use of the car number is constantly increasing, the traffic safety problem is faced with more and more severe challenges. In order to constantly improve the safety of the vehicle, involving with the car auxiliary system of traffic safety are graving.

With the increase of the traffic accidents, associated with the Active Safety Systems research is extremely important. Similar design, however, there are many problems, such as the system is easy to damage, the price is too high, the sound is too small, easily distracted the drivers' attention, etc. In order to solve these shortcomings, this paper proposes a real-time detect obstacles around the vehicle, the LCD module is adopted to measure the distance of the value of intelligent display when the distance is less than a certain threshold, risk early warning system. The system can make the driver under the condition of no distraction from the sense of the vehicle information, so as to ensure the vehicle safety. This design is to use single chip microcomputer, sensors, knowledge and so on, to the design of the automotive safety warning device, and reverse travel in cars, help drivers to better understand body environment, avoid the happening of the accident.

2 .The Overall Design of the System

The system is mainly based on the MCU and the ultrasonic sensing technology. In the vehicle before and after ,the installation of the MCU and the ultrasonic sensing module device. Through the microcomputer control ultrasonic module realize the perception of the distance between the vehicles.And can detect the current temperature, realize the temperature compensation of the distance. After treatment, the distance from the LCD module display information and by ringing alarm module.

The block diagram of the overall design of this system are shown in figure 1 , the system consists of main control chip, LCD display and alarm device, ultrasonic receiving modules and ultrasonic emission modules. Distance detection by ultrasonic transmitting and receiving modules, through the master control chip for temperature measurement and temperature compensation, at last, through the LCD display and alarm to report the distance.

Its working principle is as follows: the main control chip control ultrasonic launch module to 40 KHZ sound wave signal, at the same time, start the timer timing. Accept module to accept return of sound waves of the ultrasonicsignal, After receiving the signal, according to the timer to calculate the ultrasonic propagation time t, so as to obtain distance information. If you did not receive acoustic signal receiver, then continue to send ultrasonic, if received acoustic signal, the detection of the current temperature, and the temperature compensation with the main control chip, and the results are the analysis judgment, the precise distance information, and then through the LCD display distance ,temperature. If the calculated distance is less than the threshold, the ringing through the LCD display module and module. On the other hand, the control chip to continue the above judgment.

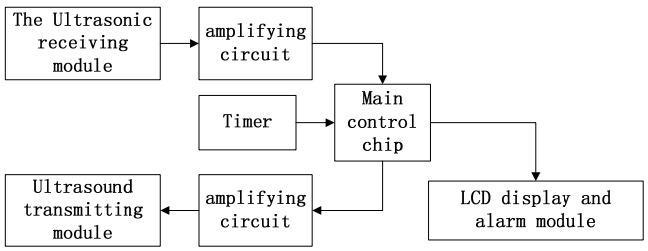

Fig. 1 Over all design scheme diagram

3.The Design of Key Module

3.1 STC89C51

This design chooses the STC89C51 as the core chip system. STC89C51 was developed by the United States on STC company 8 bit microprocessors, embedded 4 KB Flash ROM. Under 3.8 ~ 5.5 V working voltage, the working speed range of 0 ~ 40 MHZ. STC89C51 chips with features include low power consumption, high performance, low price, high speed, high reliability and anti-interference, PLCC encapsulation, 32 programmable multifunction I/O port, three 16 for the timer/counter. This makes it very suitable for used in intelligent system of main control chip[1,2].

3.2 The Ultrasonic ranging module

Ultrasonic transceiver unit adopts high performance embedded wireless transceiver module by wenxuan. Module can work under voltage from 2.4 V to 5.5 V, standby power consumption is lower than 2 mA, performance is relatively stable and are influenced by the outside world is relatively small; Ber is small; the maximum detection Is 5 m, Kbps data rate; Own temperature sensor can realize the measured results are correct. As is shown in figure 2.

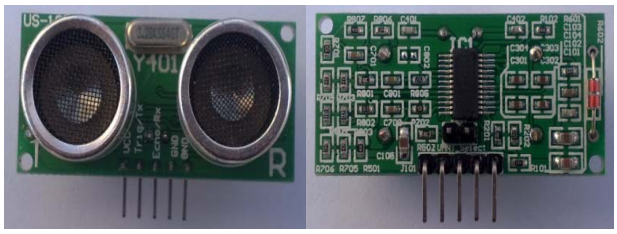

Fig. 2 Ultrasonic Ranging Module

A serial port communication protocol: TX send 0 x55 signal, baud rate to 9600, excluding parity, no flow control.

In this mode, the system sends out eight consecutive 40 KHZ pulse, then the return of acoustic signal detection and the results after temperature correction by Echo output pin. The sequence diagram shown in figure 3 below.

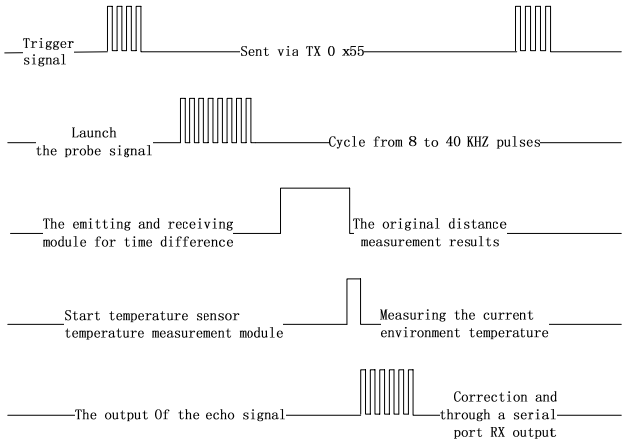

Fig. 3 the timing diagram of the serial interface triggers the ranging

Ultrasonic ranging working process is as follows: Because the ultrasonic is a kind of sound waves, it is related to temperature. If environmental temperature change is not big, the speed of sound change is also not big, the we can approximate that its speed is constant, otherwise you need to compensate the temperature measurement for its. The relationship between the velocity and the temperature in the following table 1.

When the ultrasonic transmitting module detects the trigger signal, the ultrasonic launch module of eight consecutive 40 KHZ pulse signal. INT0 is' 1 ', counter to start counting, the ultrasonic echo signals are waiting for received, when the signal arrives, the microcontroller response interrupt program, close the counter; On the other hand, if the ultrasonic receiver does not receive the return signal, also need to respond to the interrupt program, and start counting, reflected the ultrasonic receiving module continue to wait for the obstacles of acoustic signals. Master control chip, through counter count for the launch and return of acoustic time difference, thus can distance measuring results are obtained. Calculating formula for the distance

$$d=s/2=(v*t)/2$$

Among them: v for sound velocity; t for the round-trip time; d as the distance; s for the sound waves from the distance;

At this point, the start temperature compensation system, the current temperature is measured by the internal temperature sensor. Finally through a serial

port RX output after correction of echo signal.

Table.1 the sound velocity and temperature dependence of the table

temperature（℃）	-20	-10	0
speed（m/s）	319	325	332
temperature（℃）	10	20	30
speed（m/s）	338	349	386

3.3 LCD display and the alarm module

When the MCU received the echo signal after correction, the analysis judgment out of the current information, the design adopts LCD temperature, distance and alarm display (danger). LCD screen has small volume, convenient use, low power consumption advantages. LCD1602 internal character store different lattice character. Show, by operating instructions will need to display the information display on the LCD screen. 1602 LCD screen recognition is ASC Ⅱ yards, by D0 ~ D7 8 bits of data port input data and instructions.

3.4 ringing module

This design set the predetermined risk alert values, when the measured distance is less than the set value, the modules will report.Ringing modules are shown in figure 4 below

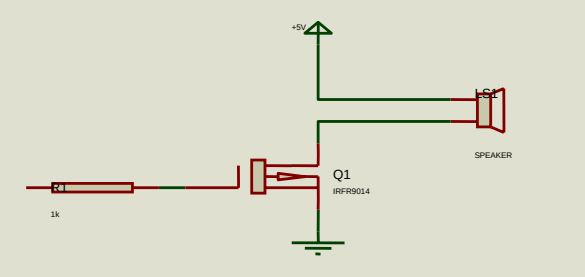

Fig. 4 the ringing module system

4.Software Design

The author designed software program flow are shown in figure 5 below. Software is mainly written using C language, can improve the work efficiency and the procedure of reliability and readability. Design USES the modular design, mainly including ultrasonic ranging module, LCD display and the alarm module and the ringing module. System initialization including master-slave SCM STC89C51 initialized, ultrasonic module[3,4,5] and LCD initialization.

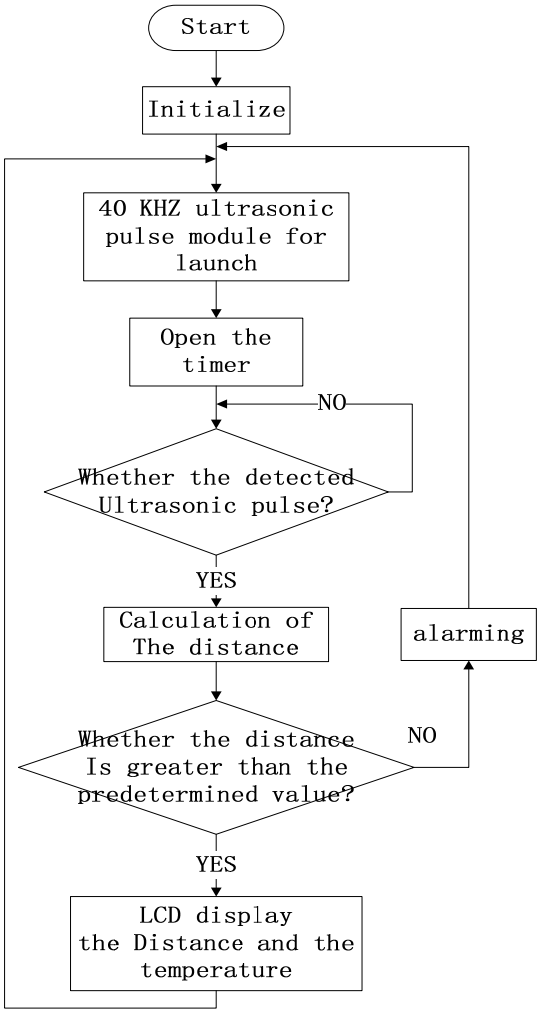

Fig 5 Flow chart of the software

5.The Experiment of System Testing

5.1 Testing the System and Course

Test method: design is completed, the design is made and run functional test. The test system are as follows: set a, b, c, d,e, f, g, h, I, j ,ten points, point spacing is 50 cm, at various points in turn set the baffle. , in turn, observe LCD screen distance, 10 times repeated measurement, record and calculate the error of average, analyzes its error size is in the permitted range.

5.2 the test result and analysis

According to the test method to get the following test results are shown in table 2, table lists the system test experiment mean value of the measured distance. As can be seen from the table, the measured distance meet the system requirements. And the system test experiment, 10 times did not appear without display and repetition.

Table.2 The average distance of the Ultrasonic Ranging record sheet

distance/cm	50	100	150	200	250
Measured/cm	51	101	152	199	252
distance/cm	300	350	400	450	500
Measured/cm	299	351	400	452	503

In the test experiment, the LCD display module display information such as the distance and the temperature, the information of the system are as follows: when the distance is greater than the preset value, the LCD screen display temperature, distance. When the distance is less than the predetermined value shown on the LCD screen flashing "danger!" The ringing alarm module system at the same time. Ten times the system test not present information misstatement in the experiment phenomenon, the system is stable and reliable.

6 Conclusion

The design of ultrasonic ranging system by single chip microcomputer and the ultrasonic transmitting and receiving module has been very mature and widely used technology, based on the idea of modularization of whole building, can realize automatic perception and alarm, accord with the requirement of practical application. Innovation point of this system is to use pulse ranging method and temperature compensation. At the same time, its cost-effective, reasonable design, fast speed, strong anti-jamming capability, complete functions. In order to make the system more human, intelligent,In order to make the system more human, intelligent, and can be modified in the following three aspects to improve: (1) when obstacles movement speed is too large, the error will increase; (2) the precision of temperature compensation to improve; (3) ultrasonic launch receiving probe is strongly influenced by the temperature; After many tests, this system can prove its stable performance and display accurate, is a good way to service for the user.

References

[1] Huabing MCS-51 microcontrollerPrinciple [M] Wuhan: Huazhong University of Science and Technology Press, 2002 .5:47-61.

[2] Li Hua. MCU-51 series single-chip interface technology and practical[M] Beijing: Beijing University of Aeronautics and Astronautics published 1993.6:87-93

[3] Zhang Qian Lin ultrasonic testing Principles and methods [M] Beijing: the National University of Science and Technology Press,1993.10:11-16

[4] Portable design and Implementation of LinWei, Liang Jianing, Lee Ann was versatile ultrasonic range finder [J] Electronic Measurement Technology, 2008, (01): 29-31.

[5] Sue Chang Zan infrared and ultrasonic remote control [M] Beijing: People Post Press, 1993. 7:26 -35

[6] Shi Degang, Liu Wow. Computer Measurement &Control [J].Volume 7 Ultrasonic Rangin Study .2002.10:34-36

[7] Heng Qing, Zhang Jing. Tonghua Teachers College [J]. Volume 5 plus Methods strong anti-interference ability of SCM system .2004 .10:2

[8] Kyushu amplifier circuit Practical Design Manual [M], Shenyang: Liaoning Ningke Science and Technology Press, 2002.5:134-146

[9] Wang Feng, Xue Hongxuan. Using computer software to improve the anti-jamming design Reliability of the system [J]. Electronic products in the world, 2004.1

[10] Zhan Cao,Liang Hou Qin, Yan CaoSCM system software Jamming technology [J]. Electronic technology, 2003.3

Voice intelligent collision prevention system

Kang xiao-meng , Shi lun-shang
（College of Instrumentation and Engneering，Jilin University，Changchun 130021,China）

***Abstract*—Against the worsening the traffic problems, especially the car crash, designed the voice intelligent collision prevention system, this system is based on AT89C51, by ultrasonic relative velocity measurement module, ultrasonic distance measuring module, voice module and display module. To detect the car distance, relative velocity, to judge whether a collision risk and voice warnings in danger. 5 cm of error in the design, can achieve reduce the requirement of the collision.**

I. INTRODUCTION

WITH the rapid development of science and technology, ultrasonic will be more and more widely used in the range finder. But in the current technical level, people can make use of the specific ranging technology is still limited, therefore, it is a burgeoning and infinite prospect of technology and industry. Looking to the future, the ultrasonic rangefinder as a new kind of very important useful tool in various aspects will have very big development space, it will develop in the direction of the more high positioning precision, to meet the social needs of the development of increasingly, such as basic as follows: the development trend of sonar developed the passive ranging sonar has higher positioning accuracy, so as to meet the needs of the water to implement all the hidden weapons attack; Continue to develop the low frequency line-spectrum detection of submarine towed linear array sonar, realize super remote passive detection and recognition; Development work is more suitable for shallow sea submarine sonar, especially solve the problem of shallow sea water target recognition. There is no doubt that the future of ultrasonic range finder will with intelligent automation, and other rangefinder integration and fusion, form a rangefinder. As the range finder technology progress, rangefinder will develop from the simple judgment function to have learning function, eventually to be creative. In the new century, face a new rangefinder will play a more important role.

Becomes more and more popular in recent years, with cars, pitfalls associated with more and more, the collision is one of the safe hidden trouble. When people are driving on the way, because of the rain, fog, speeding, fatigue driving, etc., often occur accident, light caused economic losses, or threaten people's lives. As much as possible in order to reduce automobile collision, to ensure the safety of people's lives and property, prevent collision device is particularly important.

II. ULTRASONIC AND ITS RANGING TECHNIQUE

A. ultrasonic

Ultrasonic refers to the mechanical wave frequency is higher than 20 KHZ. In order to in ultrasonic detection means, must produce and receive ultrasonic super living wave. Complete the function of the device is the ultrasonic sensors, customarily called ultrasonic transducer or ultrasonic probe. Ultrasonic sensor has sender and receiver, but an ultrasonic sensor can also has a dual function of send and receive sound waves. Ultrasonic sensor is to use the principle of piezoelectric effect will power and ultrasonic reciprocal transformation, namely, at the time of launch ultrasonic wave, converts electrical energy to emit ultrasonic; While at the time of the received echo, ultrasonic vibration is converted into electrical signals. The principle of ultrasonic ranging general TOF by transit time method (time of flight). First measured ultrasonic time experienced by returning from launch to meet obstacles, then by ultrasonic get twice the speed of sound source and the distance between the obstacles In the ultrasonic ranging is suitable for high precision distance measurement. Because the ultrasonic propagation in standard air speed of 331.45 m/s, the MCU is responsible for the timing, the singlechip using 12.0 MHZ crystal vibration, so the measuring accuracy of the system theory can achieve millimeter level. Because ultrasonic directivity is

strong, energy consumption is slow, propagation distance in the medium, thus the ultrasonic can be used for distance measurement. Using the ultrasonic detection distance, the design is more convenient, calculation process is simple, and in measuring accuracy can be achieved.

B. Ultrasonic ranging principle

Transmitters of ultrasonic in nu of speed in air, in the object to be tested is reflected back, by the receiver, the round-trip time for t, by the s = n / 2 can calculate the distance of the object to be tested. If the ranging accuracy is very high, it should be corrected by the method of temperature compensation.

C. - US100 ultrasonic module

US - 100 ultrasonic ranging module can realize non-contact ranging function 2 cm ~ 4.5 m, with wide input voltage from 2.4 V to 5.5 V, static power consumption is lower than 2 ma, built-in temperature sensor distance measurement results are correct, at the same time have a GPIO, serial port communication a variety of ways, with watchdog, stable and reliable work.

Real figure is as follows:

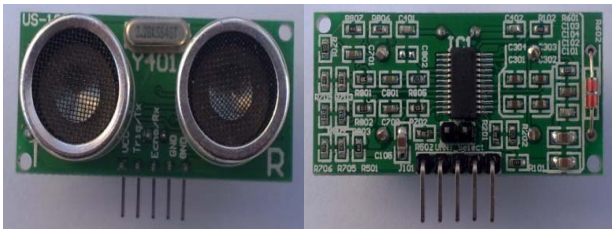

Fig.1 Ultrasonic physical

D. A serial port triggering ranging principle

In this mode only need in Trig/TX pin 0 x55 (baud rate, 9600), the system can send out eight 40 KHZ ultrasonic pulse, then the detection of echo signal. When the Echo signal is detected, the module of temperature measurement, then the distance measuring results are based on the current temperature correction, the correction result by Echo/RX pin output. The distance of the output value, a total of two bytes, the first byte is a distance of eight high (HDate), the second byte of distance low 8 (LData), the unit is mm. The distance value of (256 + LData HData *) mm. A serial port trigger range of temporal sequence as shown in figure 1.2:

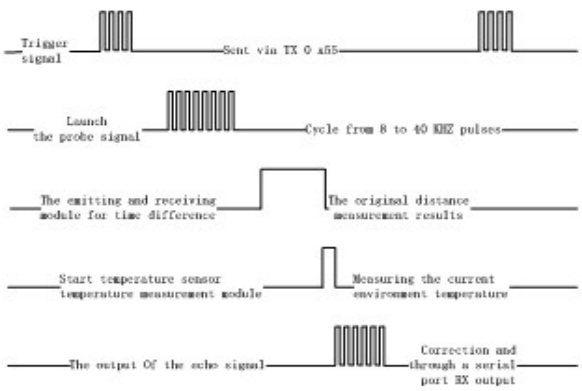

Fig.2 A serial port triggering ranging sequence diagram

Ⅲ .THE SYSTEM DESIGN

For voice intelligent collision prevention device, the specific requirements for the check-out car, two cars relative speed detection, and voice for voice intelligent collision prevention device, specific requirements for the check-out car, two cars relative speed detection, and voice alarm three parts. So we put the system into three modules: ultrasonic ranging - get limber and the distance between the car and speed - based on ultrasonic sensors measure the two cars and relative speed of voice alarm, report if possible collision to the driver. The system total design as shown in figure

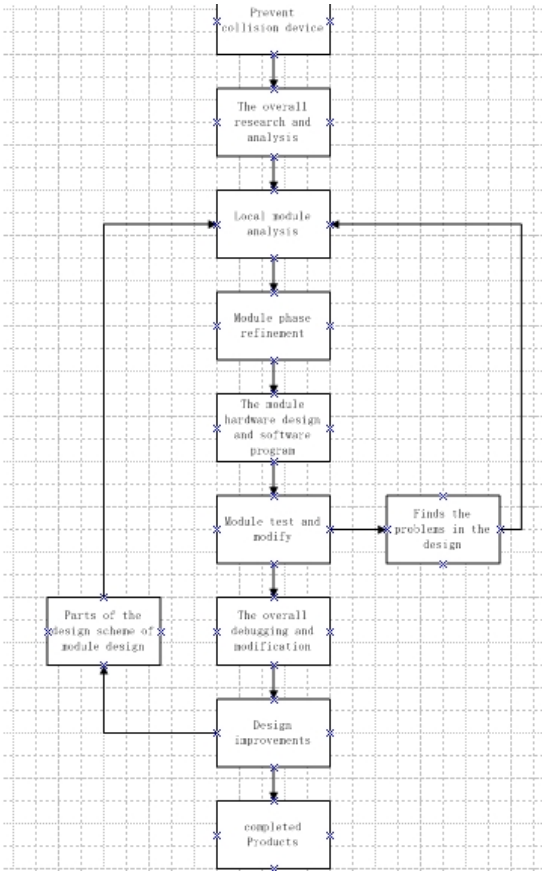

Fig.3The system total design

Ⅳ.SYSTEM IMPLEMENTATION

A. Ultrasonic distance measurement, and the distance between the car get to people.

Using US100 ultrasonic ranging module and peripheral circuit.

B. Speed - based on ultrasonic sensors measure the relative speed of the car

In the experiment, we measure two move relative velocity of the object, and cannot be measured directly. So we use ultrasonic sensors, in a set for a second time, after the measured distance vehicle ahead, and the two cars in a second time of displacement is poor, so can relative speed of the car.

C. Voice alarm, report if possible collision to the driver.

PLAYL: Playback control level trigger. When the end as low electricity at ordinary times, chip into the play cycle; When the end stop playback for high levels.

PLAYE: Playback control pulse triggering end. When the end of the input from high level to low level jump, chip into the play cycle.

RECLED: The tape shows. The termination light-emitting diodes (leds), as the recording light when recording.

REC: The tape control side. The end to the low electricity at ordinary times, recording chip into the state, the client must maintain a low level during the recording.

ISD1420 hardware connection diagram as shown in figure 4. The first to use button control REC pin voice recording, record the three sections of the starting address of the voice, respectively, 00 h, 10 h, 30 h. After the SCM according to the state of light intensity, control chip address for corresponding voice broadcast.

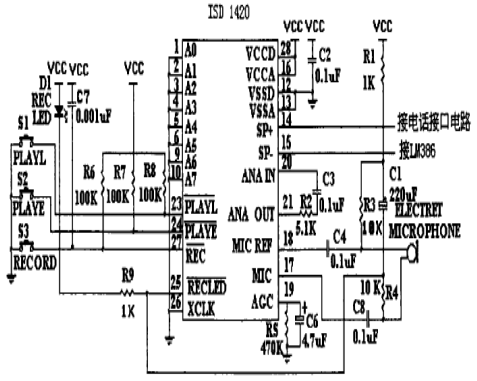

Fig.4 ISD1420The hardware connection diagram

Ⅴ.THE SYSTEM SOFTWARE DESIGN

Software is mainly written using C language, can improve the work efficiency and the reliability of the program and readability. The idea of modular design, mainly including ultrasonic speed measuring module, LCD display and alarm module. System initialization including master-slave SCM AT89C51 initialized, ultrasonic module and LCD initialization. The system software of the main program
flow is shown in figure 5

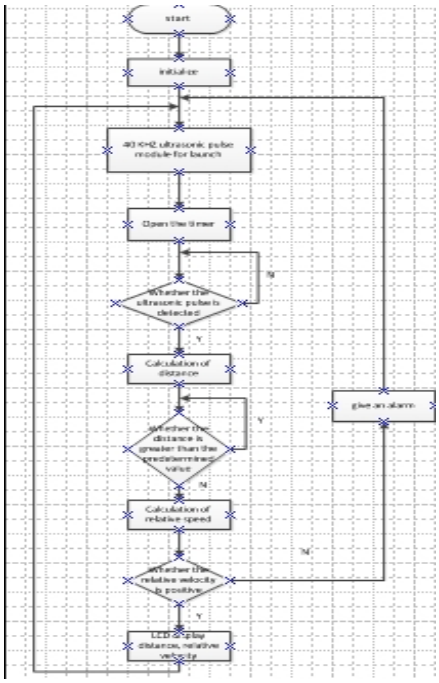

Fig.5Software process

Ⅵ. SYSTEM TEST

A. The test method

After completion of design, the design is made and run functional test. The test system are as follows: choose two car, car mount this device, let two cars at the same speed in the same orbit, by changing the car's speed and distance to observing the distance and relative speed of LCD display and voice alarm in certain circumstances. We assume that the safe distance between the two cars to 1 m, two car relative speed when the car is greater than the speed of the vehicle ahead when is positive, whereas negative. The data is shown in figure 6

distance /m	1.50	1.50	0.90	0.90	0.50	0.50
results /m	1.48	1.49	0.91	0.89	0.47	0.50
The relative	positive	negative	positive	negative	positive	negative
For possible	no	no	yes	no	yes	no
Whether the alarm	no	no	yes	no	yes	no

Table 1 The experimental data in figure

Testing experiment, a LCD display in line with expectations, the relative speed and distance error in the allowed range, and the ability to predict the alarm.

Ⅵ. OUTLOOK：

The design of the system in line with expectations, but there is room to improve: in some special weather, human environment, the rider to steer by transform button, set the same as the driving conditions of safety factor; The system load to the driver of navigation or cell phone, make use more convenient; And the system reliability, practicability and economy.

Ⅶ.CONCLUSION

The author design the system of technology has been mature and have a wide range of applications, and design can realize the distance and relative velocity measurement, and can be personalized by recording speech, and the design of the high cost performance, convenient and practical, low error, strong stability, high safety factor, suitable for a wide range of promotion and application.

Finally thank you give us guidance in the process of design week every word the teacher and classmates give us help.

references

[1] Vizimuller. RF design guide-systems, circuits, and equations [M]. Boston：Artech House，1995.

[2] Keil Software. The Final World On the 8051[M]. Germany： Keil Elektronik Gmbh and Keil software，1997.

Underground metal detectors

Wang fu; Zhang yu; Liang haonan

(College of Instrumentation and Electrical Engineering, Jilin University,Changchun 130012,China)

***Abstract*—With the process of social modernization, the urban construction developprapidly, underground cables and pipelines across the city, resulting in a large number of underground pipeline and communication optical cable has been damaged by the unintentional, more importantly, in the process of urban construction, as a result of the existence of some war wreckage and scrap metal, brought a lot of inconvenience to the modernization of cities. Therefore, the shallow surface of metal detection is particularly important, this paper takes STC89C51RC single-chip microcomputer as the controller, the eddy current sensor module, the signal processing module, A/D module, LCD display and buzzer alarm module of the measuring system, the main use of eddy current sensor non-contact measurement, through the feelings of the change of the magnetic field, to determine whether there is A metal. By non-contact measurement, this system can sense within 5-10 cm below the surface of metal, and can estimate the size of the metal.**

***Key Word*—Metal detector; The eddy current sensor; Non-contact measurement;Low power consumption; Energy saving**

I. INTRODUCTION

AS a security screening equipment, metal detector has been widely used in social life and industrial production in many areas, and it plays an extremely important role in industrial production and personal safety. Metal detectors are widely used in industrial and agricultural production and security, especially, smart metal detectors with high precision, responsive, small, easy to use, etc., favored to use in a variety of occasions. Metal detectors typically using a signal processing circuit for voltage or frequency sensor output signal is processed to detect metal drive when an alarm indicating circuit. Detection principle is broadly divided into beat-style, self-oscillation. Currently metal detectors widely used beat-style and self-oscillation type detection principle, it's circuit generally reference Part 5 oscillators, mixers, amplifiers and alarm circuit. Be applied to intelligent instrument, given its more features, while the error rate significantly lower[1].

Underground metal detector use the principle of metal detectors, the application of eddy current effect, when the metal through the bottom of the eddy current sensor, induced magnetic field, so that the magnetic field sensor is changed, we can see there is a change of metal is present.

II SYSTEM ARCHITECTURE

In this paper, the design of underground metal detectors is made up with STC89C51 controller, A / D 0809 ADC, 12864 LCD display, eddy current sensors, eddy current conversion circuit, and the overall system block diagram is shown in Figure 1. When the eddy current sensor feltthe eddy currents, the eddy current conversion circuit give a voltage signal by A / D 0809 D converter change into a digital signal to the controller to process, then displayed through the LCD display 12864LCD, in order to meet the requirements to detect metal.

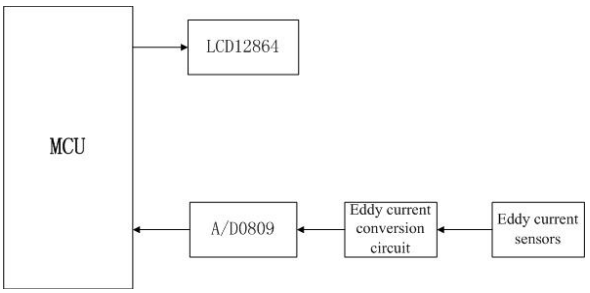

Fig.1 System architecture

III HARDWARE DESIGN

A. Control Module Design

The system uses STC89C51 microcontroller as the system controller, STC89C51 is a class of single-chip 16-bit bus with a band of FLASH. It uses a 16-bit bus, unified addressing peripherals and memory addressing range of up to 64K, you can expand the external memory. A unified interrupt management, with

extensive on-chip peripheral modules. Due to FLASH type, you can online and download to the microcontroller for debugging, because the JTAG port and FET connected directly, without additional simulation tools, convenient and practical, and can operate in low-power mode[2].

The system controller is made up with the peripheral circuit, power, conversion module, LCD display module. The hardware circuit system is shown in Figure 2. Controller acquisition conversion circuit outputs a digital signal, and finally displayed by the LCD display module.

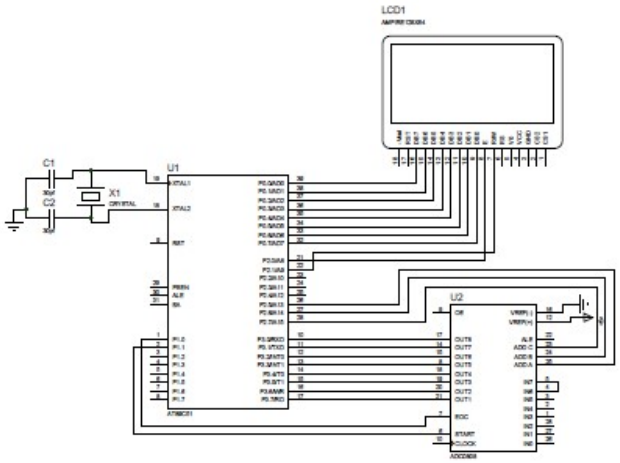

Fig.2 System hardware circuit

B. Eddy conversion module

The eddy conversion module using resonance method, this method will change the sensor coil's inductance to a change of a voltage or current. Sensor coil and capacitor connected in parallel LC parallel resonant circuit. The resonant frequency of the parallel resonant circuit is $f_0 = \frac{1}{2\pi\sqrt{LC}}$; And the equivalent impedance of the resonant circuit is the maximum, is $Z_0 = \frac{L}{R'C}$; In formula, R 'is the equivalent loss resistance of the circuit. When the inductance L changes occur, the equivalent impedance and resonant frequency of the circuit will change with the change of L, the loop impedance can be measured using the method or methods of measurement of the resonant frequency of the circuit of the sensor measured values are measured indirectly[3].

Resonance mainly have AM and FM circuit .Amplitude modulation due to the use of quartz crystal oscillators, so the higher stability, FM and simple structure, easy telemetry and digital display. Therefore, in this system uses a frequency modulation measurement circuit.

FM measurement principle is to measure the change in the circuit caused by a change in inductance of the sensor coil, the inductance changes cause changes in the oscillation frequency. Frequency change is measured indirectly reflect changes. Here coil eddy current sensor is used as an inductive element access oscillators. Figure 4.3 is a schematic diagram of the FM measurement circuit, which consists of two parts capacitance three-point oscillator and emitter follower. To reduce the influence of the sensor output cable to the distributed capacitance Cx is usually adjusted to the sensor coil L and the capacitor Care encapsulated in the sensor, the effects of this distribution capacitors in parallel to the large capacitor C2, C3, and thus significantly affect the resonant frequency reduced.

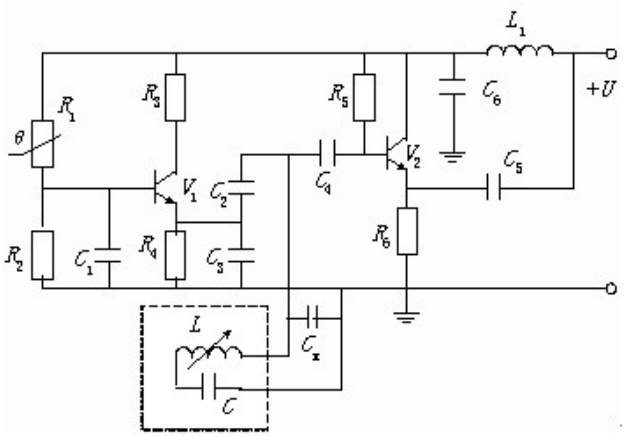

Fig.3 Eddy current switching circuit

C. Eddy current sensor module

The eddy current sensor is consist of probe, extension cable, set the device and measured body composition, high-frequency oscillation current flows through the coil probe extension cable, resulting in the end of the probe coil H1 alternating magnetic field within the effective range of the alternating magnetic field is not measured body close, the magnetic energy is a total loss; When the magnetic field close to the test object, the test surface in this induced current - eddy current shown in Figure 4. At the same time eddy current field test on the body produces an alternating magnetic field H2, H1 direction opposite the direction of H2 due to the reaction of the magnetic field from the current size of the probe coil and phase changes that

occurred in the coil impedance probe change with changes in the impedance of the probe coil is measured to reflect the effect of the eddy current body, eddy current strength of the eddy current reaction changes the equivalent impedance of the probe coil, the measured conductivity of the body, magnetic permeability, geometry, excitation current, frequency of the probe coil and the measured distance between the body and the relevant. Therefore, eddy current sensor is consist of can be viewed as a two-part carrying the probe coil and the sample constituted[4].

The eddy current sensor'swork process is f: when the distance between the probe and the measured body changes, the quality factor Q of the probe coil also changed. Q value caused by the change of the oscillating voltage change after the oscillation voltage detector, a filter, a linear compensation, amplification, normalization into a voltage (current) changes, and ultimately complete the conversion. From the above, eddy current sensor is consist of system measured body of work can be seen as half of the sensor system, namely performance and measured body about an eddy current sensor.

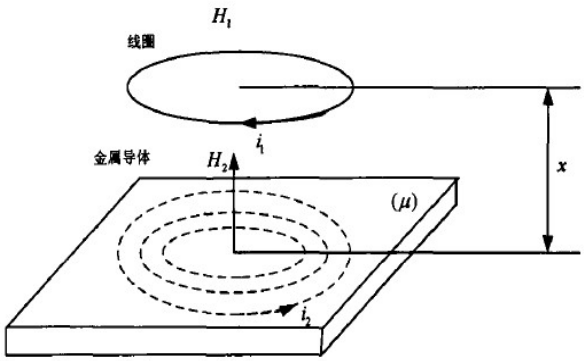

Fig.4Working principle of eddy current

IV Software Design

Master controller program flowchart is shown in Figure 6, the master controller module includes initialization procedure, to obtain a voltage signal acquisition, data processing and so on. The main task of the digital signal coming from the sensor is collected and processed. First, the analog voltage signal coming from the eddy current converter circuit analog to digital conversion, digital signal acquisition after the end of the conversion A / D converter output through the digital signal processing ultimately displayed on the LCD screen. Change the value on the display is the eddy current[5].

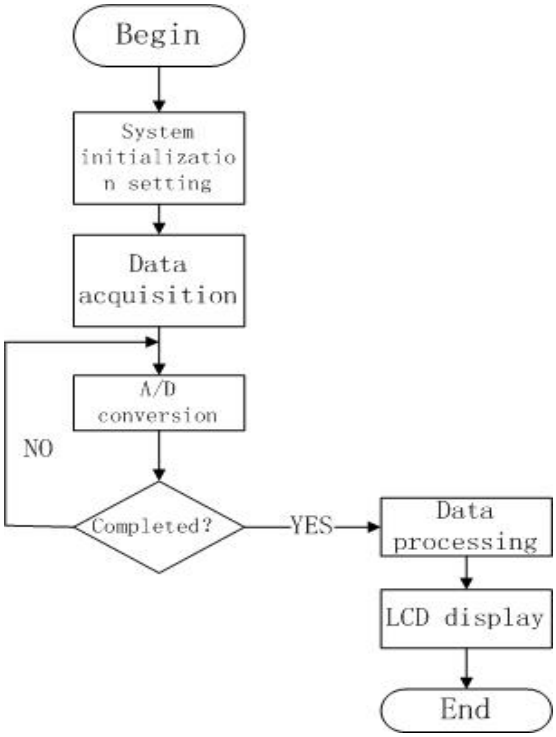

Fig.5 System software flow chart

V Test Results

The experimental prototype in the laboratory for testing: each module is working properly, the use of laboratory test round iron plate as metal, when the sensor probe is placed on top of a round iron 5cm-10cm, the voltage value on the display changes evident in when the voltage value than 10cm small and close to zero. Detailed test results shown in Figure 6.

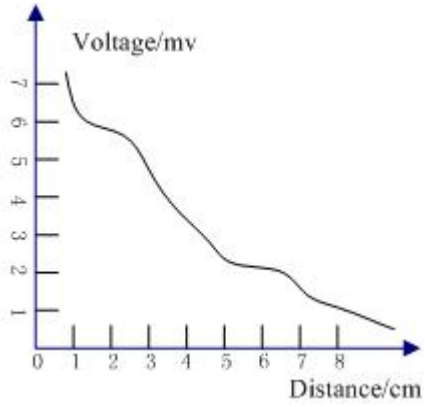

Fig.6 System test result

VI Conclusion

This article describes the underground metal detectors can detect near-surface metal, but can’t detect the deep underground metal, metal detector in the process of carrying out the results in the form of voltage values for display, makes clear, and may determine the metal the edges and center. And conventional metal detectors, compared with small size, light weight, easy to carry features. In addition, the use of eddy current sensor can also size and material of metal detection, due to the constraints, the design did not materialize, but after further research has far-reaching significance.

References

[1] Zhang Xueyong.A metal detector design [J]. Anhui Institute of Architecture Industry, 2007,15 (3) :1-3

[2] Song Fengjuan, Sun Jun, Li Guozhong design 89c51 microcontroller based digital voltmeter [J] Manufacturing Automation, 2007, 29 (2): 89-90.

[3] Kang Huaguang with electronic technology infrastructure (analog part) [M]. Higher Education Press,2006:116-118.

[4] Tung Meng was based on eddy current metal detector characteristics of [D]. Harbin Polytechnic University,2009:18-19

[5] Cheng Defu, Lin Jun and other intelligent devices (second edition) [M].Machinery Industry Press, 2010.

Design and implementation of the Security System for Apartments

Li Fangwei；Wu Qiong；Zhang Di

(College of Instrumentation and Electrical Engineering, Jilin University,Changchun 130022,China)

***Abstract*—In a collective apartment in order to prevent the occurrence of burglary when people sleep at night or go out, this design use infrared sensors and RFID（Radio Frequency Identification）.They can achieve monitoring illegal acts and achieve fast and accurately changing the Armed and disarmed state. This paper introduce the SSA (Security System for Apartments) which STC89C52RC microcontroller, RFID module, LCD display module, sound and light alarm module, UPS (Uninterruptible Power Supply) module and avoiding blocker by infrared, temperature, smoke sensors. The system can achieve accurately alarming in maximum security state, automatic surveillance's USB interface, continuing to monitor when the outages occur. And in order to the actual needs of life, adding the digital thermometer, clock calendar, fire alarm to the SSA .**

Key words—Apartment burglary; Quickly Armed and disarmed; RFID; Continuous monitoring; UPS

0 INTRODUCTION

TRADITIONAL Burglar alarm systems are used for family or business. The number of the main technical solutions is four. First, inductive sensors are always the infrared detector for body. Second, the change of the systems' status is by remote control settings and password button setting. Third, the systems are always armed with a variety of ways to alarm and a variety of types for zone. The last is that the systems can inform the user automatically by telephone, and so on. Technical solutions are mature, and the price is reasonable. Burglar alarm systems are multi-functional, and have stronger universality but poorer specificity in the collective apartment under special circumstances. The design of this paper is a multifunctional security system for apartments which can be disarmed and armed quickly and accurately proceed with identification by RFID RF card. Then, the system is monitoring and alarming automatically when burglary or illegal acts occur. There are two working states that arming and disarming in the system. And multiple sensors are used in each monitoring state. The signal which collected by the sensor will be processed by the single-chip microcomputer, and the processed information will be sent to display and alarm systems. The security system for apartments can not only accurately be a burglar alarm at the maximum security state, and can achieve a variety of useful functions in living disarmed state which can facilitate daily life of the apartment staff.

In the side of power, the system selects the UPS uninterruptible power supply as the power supply. UPS system is an uninterruptible power supply system. It has power storage parts, an AC/DC converter and a DC/AC inverter as major components[1]. In the night, when the device of the apartment is powered down or do it on purpose, UPS would provide power for the entire system. The time is longer than the battery-powered, and the charge-discharge cycle is beneficial to resource saving and environmental protection.

1 SYSTEM ARCHITECTURE

The SSA designed in this paper is made up of STC89C52RC controller, MFRC522 RFID module, sound and light alarm module, automatic surveillance's USB interface, LCD display module, UPS module and avoiding blocker by infrared, smoke, temperature sensors and other components. The overall structure of the system is shown in Figure 1. MFRC522 RFID module uses RF identification card to switch working state. E18-D80NK avoiding blocker by infrared sensor is made up of photoelectric sensor transmitter and receiver modules. It uses the NPN photoelectric switch to output a digital signal. MQ-2 smoke sensor and DS18B20 temperature sensor are digital output too. The signal is detected by single-

chip I/O port. Then it will be for transportation to the microcontroller software to be done with filter and data processing and integration. Then the system goes to produce the corresponding signals to LCD display module and the module for processing alarm by sound and light. So the SSA can achieve the purpose of security and practical function.

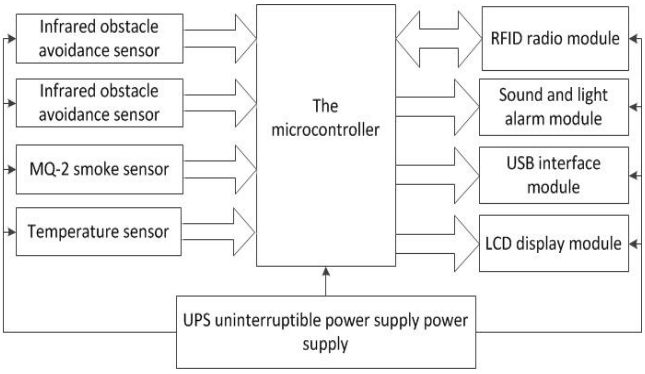

Fig.1 System architecture

2 HARDWARE DESIGN

The system uses STC89C52RC microcontroller as controller. Peripheral interface's circuits consists of UPS module, two avoiding blocker by infrared sensors, DS18B20 temperature sensor, MQ-2 smoke sensor, LCD display module, RFID module, automatic surveillance's USB interface, sound and light alarm circuits and other components, the system's hardware circuit diagram is shown in Figure 2.

2.1 UPS module

UPS uninterruptible power supply be used with 9V turn to 5V three terminal regulator power. It provides a stable 5V supply voltage for the system. 9V turn to 5V three terminal regulator power supply circuit diagram is shown in Figure 3.

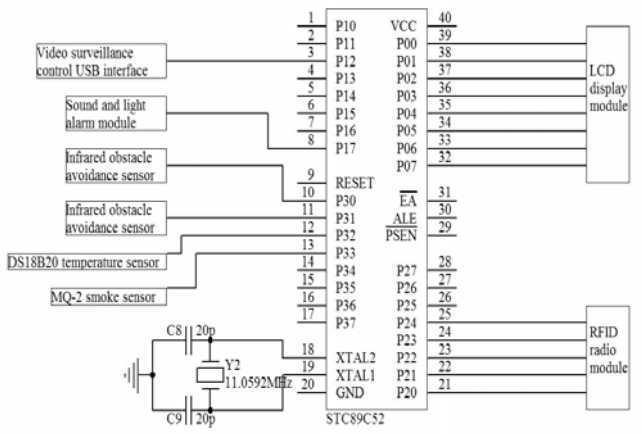

Fig.2 System hardware circuit

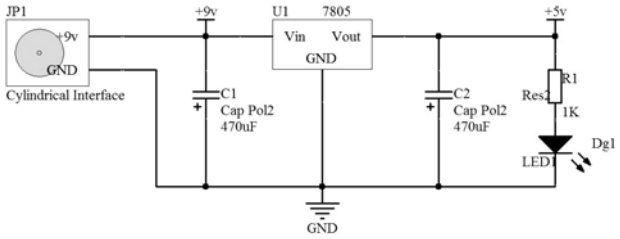

Fig.3 9V turn to 5V three terminal regulator power supply circuit

2.2 Sensor module

2.2.1 The sensors used in armed state

Avoiding blocker by infrared sensor is used. This design uses E18-D80NK two avoiding blocker by infrared sensors. The module is composed of two sensors that the outside sensor and the inside sensor side by side[2]. When someone enters the door, outside sensor is blocked first. The sensor sends low signal to the MCU, after comprehensive analysis of the signal, USB interface output for video surveillance will start. When the door is opened, inside sensor is blocked. At the same time, it sends low-level signal to the MCU, after comprehensive analysis, sound and light alarm circuit will be start. And the system prompts the user through the LCD display module to use RFID radio card to close the alarm.

Smoke detection sensor is used. This design uses the MQ-2 smoke sensor module, the main chip are LM393 and ZYMQ-2 gas sensor. Its operating voltage is DC5V. Schematic diagram is shown in Figure 4. This sensor can detect harmful gases and through the MCU to control the alarm module.

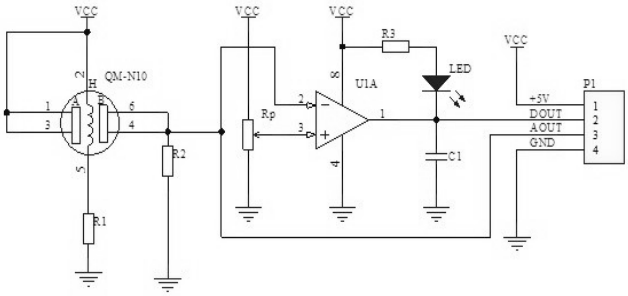

Fig.4 MQ-2 smoke sensor module schematic

2.2.2 The sensor used in disarmed state

Temperature sensing sensor is used. The design uses a DS18B20 temperature sensor. It has high temperature measurement accuracy. What's more, it is greatly improved on conversion time and transmission distance and resolution, and so on[3]. In the disarmed

state indoor temperature is measured in real time, and the data is handled by the MCU and displayed through the LCD display module.

2.3 RFID module

This design uses the MF RC522 non-contact chip card reader and communications antenna circuit. They form the RFID radio module. The chip one kind which is applied to 13.56MHz contactless communication and highly integrated chip card reader. There are a low voltage, low cost, small size and other characteristics in the chip[4]. Complementary antenna circuit is connected to it. The antenna circuit diagram is shown in Figure 5. RFID radio module reads the card information, transmitted to the MCU to process. If the RF card information is identified successfully, the system will switch system working state.

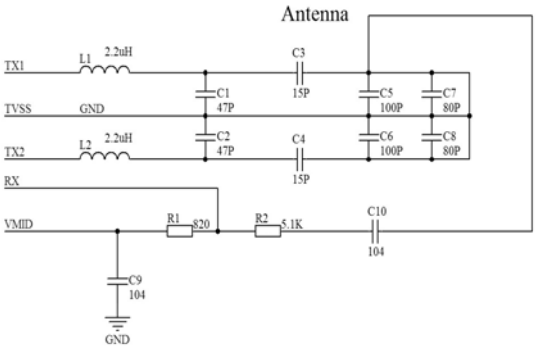

Fig.5 Antenna circuit schematics

2.4 USB interface module

This design uses PNP8550 transistor as the USB interface's drive circuit component. It is PNP silicon transistor with a low voltage and high current and small signal. The maximum collector current is 0.5A, meeting the USB interface driver's working. USB interface driver circuit is shown in Figure 6. By controlling the drive circuit of USB interface, the system can control the video automatically.

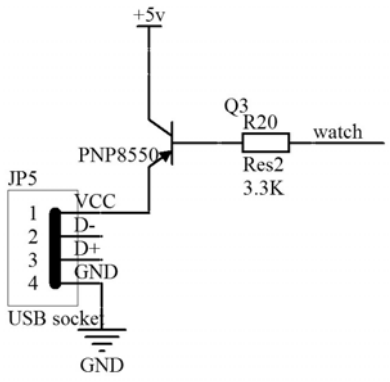

Fig.6 USB interface driver circuit

2.5 LCD display module

This design uses LCD1602. The display is used to letters, numbers, symbols and dot matrix. The LCD module is with micro-power consumption and small size and simple operation display[5]. Master chip on the LCD display module output signal to control the LCD display to achieve clock calendar and sending alarm message to user and other functions.

2.6 Sound and light alarm module

This design uses an active buzzer and LED light-emitting diodes. Master chip's program control buzzer and LED light-emitting diode to work. It can achieve the function that sound and light alarm module first in low-frequency alarming and gradually turning into a high-frequency sound alarm.

3 SOFTWARE DESIGN

Master controller's program flow chart is shown in Figure 6. The program mainly includes three parts. First, it is the main controller's system initialization. Second, it is the identification for RFID cards' data. Third, the master controller deals with the information from sensors and issues control instructions. After system initialization, the main task is the default state which is the disarmed state. The next is identifying the RFID card's information by the RFID module. If recognition success, the system will switch system's working state. In the disarmed state, the master controller deal with the digital signal which comes from the temperature sensor. And the current temperature and clock calendar information is displayed on the LCD display module. In the armed state, avoiding blocker by infrared sensors and smoke sensor's digital signals are sent to the master controller. After digital filtering, the master controller send control signals to the sound and light alarm module and USB controller module.

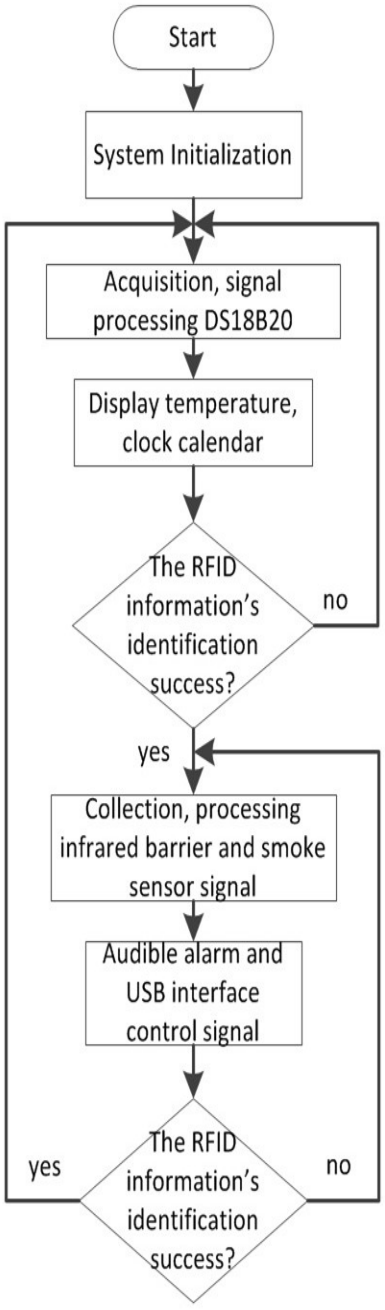

Fig.6 System software flow chart

4 RESULTS OF TEST

The experimental prototype is compared with traditional anti-theft alarm system in the side of armed and disarmed states' speed and accuracy. The result is that under the same operating conditions, the speed for RFID radio identification card switch working condition is more quickly than password. Detailed results for the test are shown in Figure 7.

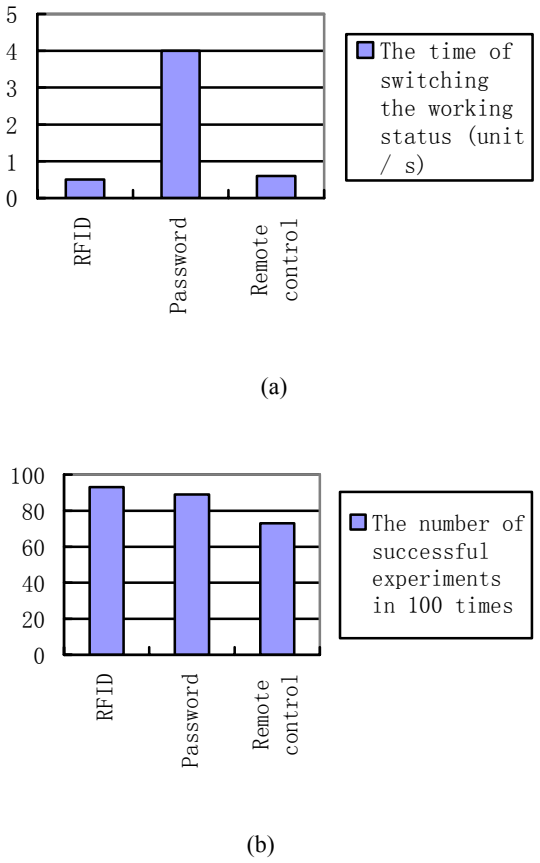

Fig.7 Detailed results for the test

（a）The time of response（b） the accuracy of identification

The experimental prototype is compared with traditional burglar alarm in the side of burglar alarm accuracy. The result is that, under the same collective Apartment working conditions, this system's success rate is more than traditional systems. Detailed results for this test are shown in Figure 8:

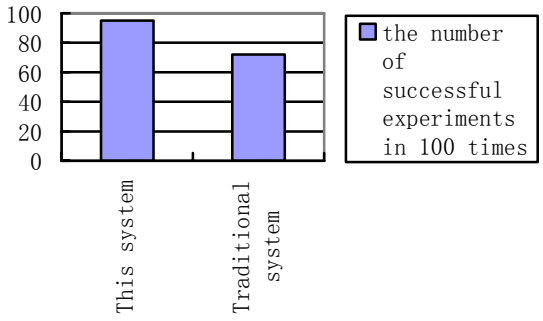

Fig.8 The result of systems' success rate

5 CONCLUSION

This article describes the Security System For Apartments. Under the condition of collective apartments, there is strong anti-interference ability and

in the armed state security alarm's accuracy is above 90%. The speed of Armed and disarmed states' transitions is fast and accurately. And that is convenient and practical. Moreover, when the device of the apartment is powered down in the night or do it on purpose, UPS would provide power for the entire system. So the system can continue to work. In addition, the increased smoke alarm, clock calendar, digital thermometers and other life functions can provide convenience for apartments. According to the analysis of tests' results, the SSA is practical.

References

[1] Zhang Chunyan, Zhang Hongtao. UPS battery pack, calculation, use and maintenance [J]. Chlor-alkali industry, 2008,44 (4) :4-6.

[2] Liu Qian, Ding Huizhu, Wu Chengkui. Intelligent design is based on ARM's apartment Security and Control System [J]. Electronic design engineering, 2011.7, 19 (13) :152-155.

[3] Xiao Huaichun. Fire burglar alarm AT89S51 based on the core of the research and design [D] Jiangxi: Jiangxi Agricultural University, 2011.

[4] GUO Guangling, Wu Huiyun, Zhang Yuefeng. non-contact IC card reader design [J]. Henan Institute of Engineering (Natural Science Edition), 2008,20 (1) :28-31.

[5] Guo Tianxiang. The course for 51 microcontroller C language [M]. Haidian District, Beijing: Electronic Industry Press, 2009.12:147-152.

Software development of near infrared brain imaging system

Xu fenghe,Wu hongmeng,Xie yanni
(*college of Instrumentation and Electrical Engineering, Jilin University, Changchun 130000, China)*

***Abstract*—With the development of science and technology, people pay more and more attention to nondestructive examination . Near Infrared brain imaging system use functional Near Infrared Spectroscopy (functional Near - Infrared Spectroscopy, fNIRS) which is a nondestructive method examination. It is developing rapidly in recent years. Because the major component of blood is a good scattering of near infrared light range 600-900 nm.Based on these data we can speculate the relationship between brain regions of Cognitive activity and other brain regions ,which applied to the study of brain functions.Near infrared brain imaging system is divided into hardware and software part. Hardware circuit is used to launch near-infrared light and collect the output light which go through the cerebral cortex.Software need to control hardware circuit and deal with the gathered signals. Besides,it should achieve calculating cerebral hemodynamic parameters through Lambert - Beer's law and dates' real-time displaying, recording and store.**

0. INTRODUCTION

VARIOUS brain imaging technology is applied in Modern medicine, such as electroencephalogram (EEG), high resolution magnetoencephalography does (MEG), positron emission tomography (PET) [1], the brain functional magnetic resonance imaging (fMRI) and near infrared brain imaging (fNIRS). The EEG is low spatial resolution because of the interference of electrical activity as well as the skull. MEG equipment and inspection charge is expensive. PET equipment is complex, and the imaging speed is slow.In addition, the equipment needs a lot of manpower and material resources, which make the promotion of PET restricted[2]. FMRI equipment is expensive and has a low time resolution. Its experimental environment is not suitable for patients with claustrophobia. FNIRS equipment is small and light. It cost less and have high resolution.Thus, it received extensive attention[3,4].

fNIRS is mainly applied in cognitive science and brain function field. Due to its real-time performance, non-invasive and portability, fNIRS won the broad application prospect in multiple disciplines,especially in clinical medicine [5].

1. Monitoring of brain traumatic intracranial hemorrhage

The rapid diagnosis and treatment of cranial class injury can reduce casualties. By comparing the absorbed light of the cerebral tissue on both sides, Near infrared imaging technology can distinguish this disease [6].

2. Monitoring of dyslexia children

Using near infrared spectroscopy to study the left prefrontal cortex activities of Chinese dyslexia and normal children in phonetic and semantic processing. According to the results, the activation of normal children are greater than dyslexia children [7].

3. Epilepsy location and pathological study

Watanabe et al. [8] monitoring cerebral blood volume of 32 refractory epilepsy people found that 96% epileptic seizures patients has obvious high blood flow perfusion with focal side . So that we can rely on fNIRS for epilepsy positioning.

4. The study of the brain when the man is in motion

Using near infrared spectroscopy to investigate hemodynamic characteristics of the cerebral cortex in the movement,which contribute to reveal the relationship between the movement and the functional activation of the brain cortex ,and to provide empirical evidence for scientific exercise [9].

1. THE PRINCIPLE OF FNIRS

FNIRS use the character that near infrared wavelengths of light have different optical properties to different tissue molecular and good permeability of human tissue[10]. In the cerebral cortex tissues

what mainly absorb near-infrared light composition is water , HbO_2 and Hb . They have different absorptive rate to different near-infrared light . The curve of absorption as shown in figure 1.1.

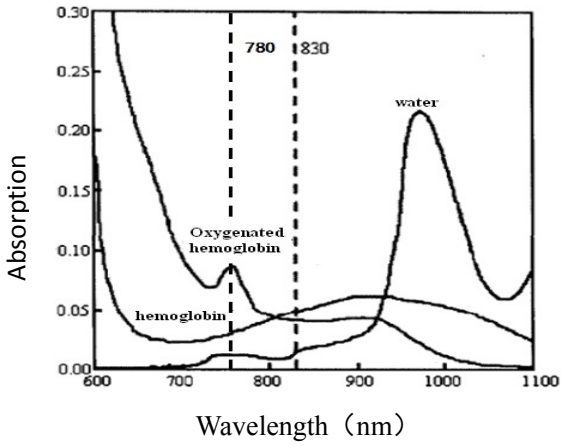

Fig1.1 The curve of absorption near-infrared light

Near infrared light Spectrum phase of Water offer a "window" which can be used as a background for HbO_2 . HbO_2 and Hb have great difference in near-infrared light spectrum in this "window". From the graph, we can see that HbO_2 have absorptive peak in 780nm. HbO_2 and Hb have almost same absorptive rate in 830 nm. Because the absorptive coefficient of this two near-infrared light wavelengths of water is extremely low. Therefore, use the 780 nm and 830 nm of near-infrared light for testing.

Head can be divided into the following sections: skin, skull and cerebrospinal fluid, brain gray matter and cerebral white matter, as shown in figure 1.2.

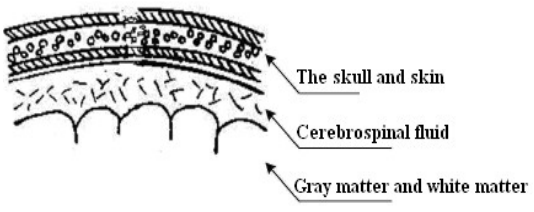

Fig. 1.2 The figure of head

The concentration of HbO_2 and Hb in the brain gray matter and cerebral white matter react the activity of brain. The light go through the skin, skull and cerebrospinal fluid to gray matter and white matter during the test time. And skin, skull and cerebrospinal fluid distribution is full of venous blood capillary . Therefore, the light scattering effect of this part will not change due to the neural activity .So the cortical tissue scattering cause attenuation of light is constant. Optical signal attenuation we have measure is caused by the absorption, which reflects the changes of HbO_2 and Hb during the brain activity. Thus by measuring the scattered light intensity of brain activity area can infer the change of blood oxygen and blood volume in this area. So we can get the changes of HbO_2 and Hb in brain when doing cognitive activity .So we can speculate the relationship between cognitive activity brain regions and various brain regions[11]. The researchers can get the changes of HbO_2 and Hb when brain is active by using fNIRS, and then study the neural mechanism of cognitive activity process[12].

2 THE PRINCIPLES OF TISSUE OPTICS FOR BLOOD OXYGEN MONITORING PARAMETERS

We use near-infrared light to test the hemodynamic parameters of biological tissue, virtually for the optical properties of biological tissue. At present, the study of tissue optical , mainly includes the transmission rule of light through the tissue and the measurement technology for tissue optical properties[13]. This chapter introduces the phenomenon of biological tissue after lighting.Then Lambert Beer's law which is an algorithm for interconversion between the light signal and the cerebral hemodynamic parameters is followed.

2.1 The interaction between light and biological tissue

After thousands of times of random scattering photons will leave the scattering organization.The route can't be known exactly. But we can estimate the distribution of possible paths by meaning of the calculation of probability, as shown in figure 2.1.

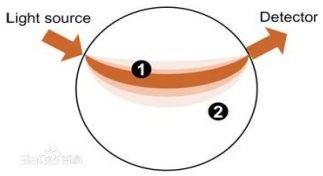

Fig.2 The photon propagation path in tissue

Photons can pass through the part 1 with a high probability.But the possibility is almost impossible through the part 2.

The main forms of interaction between light and biological tissue are reflection (refraction), scattering and absorption. Based on their characteristics we can analyze the atomic, molecular structure. In biomedical photonics research,when dealing with interaction between light and matter,we mainly consider the particle nature of light with ignoring the volatility and the polarization of light effect, etc[14]. Therefore, we usually study that a single photon is absorbed or scattered in the organization.

Because HbO_2 and Hb have unique optical properties in near infrared region.On the basis of the light absorption measurement method, the concentration of these molecular changes can also get the corresponding monitoring[15].

2.2 The basic theory of biological tissue optics

In the initial study, biological tissue spectroscopy of biological tissue is uniform, semi-infinite medium, applying Lambert- Beer's law (Lambert Beer) describe light propagation in biological tissue.However, with the deepening of the research, people gradually realize the biological tissue is a strong light scattering body, light in the organization through multiple scattering to reach the detector from a source[16]. So, some scholars put forward correction lambert beer's law. A brief introduction of the two theories in the following.

1 Lambert-Beer's law

When the light through the homogeneoust and no scattering medium, we only need to consider the medium for the absorption of photons.The relation-ship between the incident light intensity and the emergent light intensity with Lambert-Bill equation described as[17]:

$$A = \ln(I_o / I) = m_a(\lambda)\ r \qquad (2\text{-}1)$$

Here A is optical density, I_o is the incident light intensity, I is the emergent light intensity, $m_a(\lambda)$ is absorption coefficient and r is the distance of the light source to the detector.

$$m_a(\lambda) = \epsilon(\lambda)\ C \qquad (2\text{-}2)$$

Here $\epsilon(\lambda)$ is the molar absorption coefficient of matter in a particular wavelength, depends on the wavelength of light and the nature of the absorption material, C is the concentration of the test material.

2 The modified of Lambert-Beer's law

Basic Lambert-Beer's law is not apply to highly scattering medium of biological tissue. Due to the multiple scattering effect, a photon transmission path length increases in the organization,and greatly increased the probability of photon to be absorbed. In order to reflect the impact of scatter on light loss, Delpy etc[18]. put forward correction Lambert -Beer's law in 1988,namely,

$$A = \ln(I_o / I) = \epsilon(\lambda)\ C\ DPF(\lambda) + G \qquad (2\text{-}3)$$

Here G is on behalf of the loss caused by the background, DPF called path difference factor and used to describe the light propagation path extension caused by the scattering.The related literature also shows the different organizations in the scope of DPF[19,20]. If DPF and G value can be obtained，multiple wavelength absorption spectrum can be used to calculate the concentration of the material under test.

2.3 Measuring the relative variation of hemodynamic parameters

At the time of blood oxygen detection, in order to detect HbO_2 and Hb relative concentration variation, we need to detect the absorbed light of two wavelengths. According to the modified of Lambert-Beer's law to write equations.Then, selecting a base or reference state and detecting the variational concentration of HbO_2 and Hb relative to the reference state.We can calculate the concentration change of the corresponding HbO_2 and Hb, namely,

$$\Delta A^{\lambda_1} = (\Delta e^{\lambda_1}_{HbO_2} + \Delta e^{\lambda_1}_{Hb}) DPF(\lambda_1)\ r \quad (2\text{-}4)$$

$$\Delta A^{\lambda_2} = (\Delta e^{\lambda_2}_{HbO_2} + \Delta e^{\lambda_2}_{Hb}) DPF(\lambda_2)\ r \quad (2\text{-}5)$$

According to the formula (2-4) and (2-5) to calculate the relative hemodynamic parameters variation, namely,

$$\Delta HbO_2 = \frac{(e^{\lambda_2}_{Hb}\Delta A^{\lambda_1} / DPF(\lambda_1)) - (e^{\lambda_1}_{Hb}\Delta A^{\lambda_2} / DPF(\lambda_2))}{r(e^{\lambda_2}_{Hb}e^{\lambda_1}_{HbO_2} - e^{\lambda_1}_{Hb}e^{\lambda_2}_{HbO_2})} \quad (2\text{-}6)$$

$$\Delta Hb = \frac{(e^{\lambda_2}_{HbO_2}\Delta A^{\lambda_1} / DPF(\lambda_1)) - (e^{\lambda_1}_{HbO_2}\Delta A^{\lambda_2} / DPF(\lambda_2))}{r(e^{\lambda_1}_{Hb}e^{\lambda_2}_{HbO_2} - e^{\lambda_2}_{Hb}e^{\lambda_1}_{HbO_2})} \quad (2\text{-}7)$$

Thinking the value of DPF approximately equal in the experiment, the type (2-6) and (2-7) can be simplified into

$$\Delta HbO_2 = \frac{e^{\lambda_2}_{Hb}\Delta A^{\lambda_1} - e^{\lambda_1}_{Hb}\Delta A^{\lambda_2}}{DPF\ \ r(e^{\lambda_2}_{Hb}e^{\lambda_1}_{HbO_2} - e^{\lambda_1}_{Hb}e^{\lambda_2}_{HbO_2})} \quad (2\text{-}8)$$

$$\Delta Hb = \frac{e^{\lambda_2}_{HbO_2}\Delta A^{\lambda_1} - e^{\lambda_1}_{HbO_2}\Delta A^{\lambda_2}}{DPF\ \ r(e^{\lambda_1}_{Hb}e^{\lambda_2}_{HbO_2} - e^{\lambda_2}_{Hb}e^{\lambda_1}_{HbO_2})} \quad (2\text{-}9)$$

From the above two formula, we can know the DPF and the related value of ϵ,and calculated relative variation of cerebral hemodynamic parameters.

3 THE DESIGN OF THE SOFTWARE

This chapter introduces the software design and realize method of the near infrared brain imaging system.Object-oriented designing thought runs through the whole process of the designing.This paper expounds the application framework on macroscopic and introduces the system construction and its realization process in the order of the data to the function modules.

3.1 Software structure analysis

From the aspect of function, the software can be divided into two parts: one is the measurement and control unit.It can set serial port parameters through serial port communication.It can also control the hardware to pick up signals.The other can process signals ,calculate,display in real time and store the data.

1. Control module

PC is connected to the hardware through serial debugging assistants and USB.Then control hardware acquisition signal port by setting the serial port parameters,frequency. And control the signal acquisition to start or stop by sending commands.

2. Detection circuit module

Testing the serial port's connection and wether the port is correct.

3. Data processing module

Data collected by hardware contains two wavelength's information. So, firstly, we must separate the data. In other words, the data must be divided into two groups to store. Secondly, filtering data, then, change light intensity signal to converted information of hemodynamic parameters in real-time.

4. Display

Display the collected data in real-time when hardware begins to collect data.

5. Plotting curve

Plot the curve of HbO_2 and Hb variation according to the time.

6. Storing data

Storing the signal of real-time measured and the curve of HbO_2 and Hb variation for later using.

The software structure diagram as showed in figure 3.1.

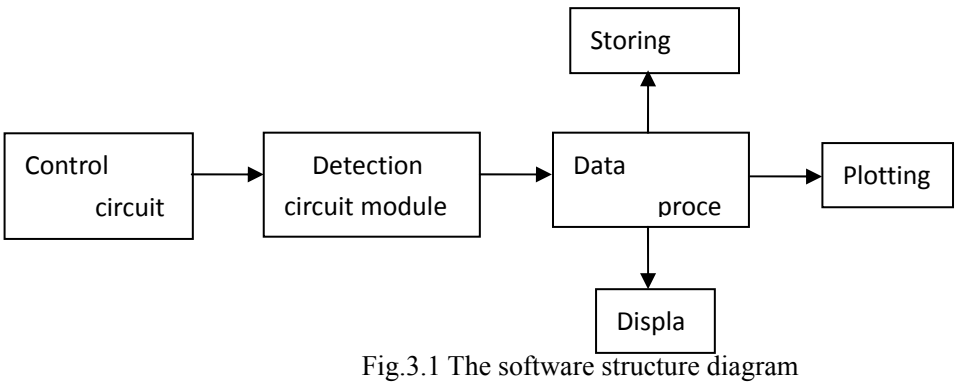

Fig.3.1 The software structure diagram

3.2 The choice of software development platform

Through the analysis, main functions of the bundled software are real-time control, data processing, display and storage. We choose Matlab and Visual Stadio 2010.

1. Matlab and data processing

Matlab is introduced by the American Mathworks company, a powerful numerical calculation and visualization software. Its apply scope covers calculation, algorithm development, system modeling and simulation, digital image processing and other fields[21]. Numerical calculation and analysis function of Matlab are perfect, its computing results can be directly represented in the Matlab environment with 2 d and 3 d even four dimensional graphical .Its grammar struct- ure is simple and the openness is good.Matlab allows the users developing algorithms, and then encapsulate the algorithms to combine with other development tools.

2. Visual Stadio 2010 and Visual interface design

Visual Stadio 2010 is launched on April 12 by Microsoft.In order to interface with hardware conveniently, and processing data better, using Matlab to filter data, etc.And Visual Stadio 2010 is used to divide data, design the Visual interface, display and store data and the dynamic link with Matlab.

4 EXPERIMENTAL RESULT

The Visual interface is designed on the Stadio 2010, the interface diagram as shown in figure 4.1.

Fig.4 surface chart

From this figure,we can see software can select serial port, set frequency,parity, data bits and stop bit of received data.Then click on "open the serial port", if serial port selection is wrong or not connected to the hardware circuit, corresponding prompt will appear. Receiving area can display the received data on real-time, it can also clear and save the received data .

After debugging the system, connect it with hardware the software assistant.Then find some students as experimental objects,collect data and draw the curve of variation of HbO_2 and Hb change over time. The following is one curve of a female student (age 23, height 160 cm, weight 50 kg) .The curve as shown in figure 4.2.

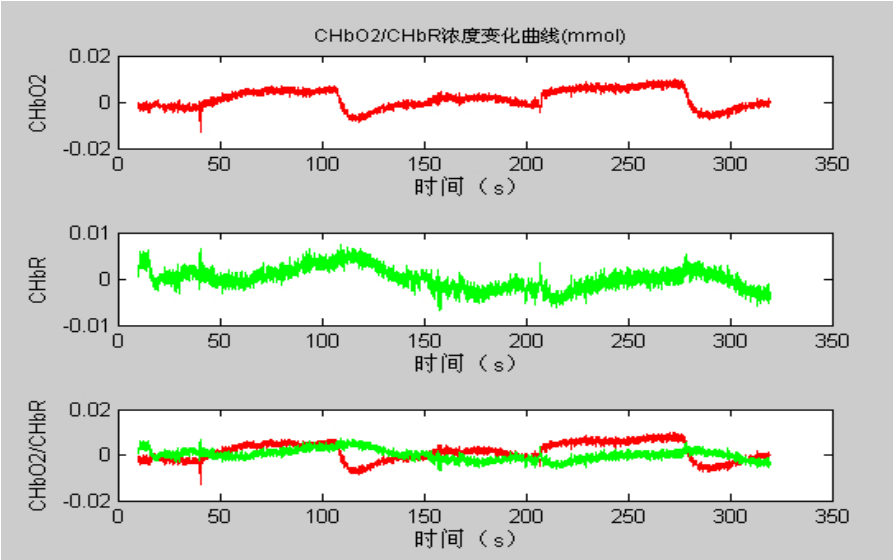

Fig 4.2 Curve of cerebral hemodynamic parameters variation

Experimental method: During the experiment, researchers breath normally for 100 seconds and then breath-hold for 10 seconds ,then breath normally.

Analysis of experimental results:As shown above, we can detect the concentration of HbO_2 and Hb remain stable during the begin 100 seconds. And then , the concentration of HbO_2 fell sharply and the concentration of Hb increase, because the brain lack of oxygen during breath-hold. After the normal breathing, the concentration back to normal,namely, the brain back to steady state.

5 CONCLUSION

As a means of non-invasive optical detection near infrared spectral technology have many advantages, such as real-time, continuous and so on. It have applied extensively in the field of biomedicine. When a region of cerebral cortex is active ,the blood volume of this region will increase or decrease ,which react the degree of activation.Because near infrared spectral brain function detecting system can be real-time and measure the changes of oxygenated hemoglobin and deoxygenated hemoglobin non-invasively in a region of cerebral cortex.This system is convenient to carry and easy to operate.So we can use near infrared spectral technology to research the functional activity of brain region during the cognitive process.

In this paper, we analysis the development and the present of application of near infrared spectrum technology firstly.Then introduces the lambert beer's law and the correction of lambert beer's law,which is a method to calculate the cerebral blood flow hemodynamic changes .The paper also introduces the functions of software and the soft-developing platform have been chosen.Matlab was chosen to calculate the concentration of oxygenated hemoglobin and deoxygenated hemoglobin and plot the curve of cerebral blood flow hemodynamic changes over time.Besides,Visual Stadio 2010 was used to design operating interface and display the gathered dates and graphs.

References

[1] Li wen.The study of Brain imaging technology. [J] Foreign medical archives of biomedical engineering ,1988,22(1): 14-19

[2] Barinag M. New imaging methods provide a better view into t he brain[J]. Science , 1997, 276 (27) : 1974-1976.

[3] Delpy T.Cope M.Quantification in tissue near-infrared spectroscopy[J]. Philosophical Transactions of the Royal Society of London, 1997, 352: 649-659

[4] Villringer A.Chance B.Non-invasive optical spectroscopy and imaging of human brain function[J]. Trends Neurosci, 1997, 20: 435-442

[5] Qian Zhiyu,Li Shitao.The sum of Functional near-infrared spectroscopy (fNIRS) clinical application[J]. Life science instrument, 2013,11(6),45-52

[6] Hu Hanbin. Functional near infrared spectral imaging research and application [D] ..Master's degree in China university of science and technology.2010,5,12.

[7] Liu Baogen,Zhou Jing,Li Feifei. A new method of brain imaging, functional near infrared spectroscopy[J].Psychological Science. 2011,34

[8] Izzetoglu M.Bunce S,C.Izzetoglu K.Onaral B.Function brain imaging using near-infrared technology-Assessing cognitive activity in real-life situations[j].IEEE Engineering in Medicine and Magazine,2007, 26(4),38-46.

[9] Jiang Changhao. Near infrared spectrum technology applied in the study of brain function in movement [J].Acta Biophysical Sinica ,2010,11(26),983-991.

[10] Qian Zhiyu, Li Shitao.The sum of Functional near-infrared spectroscopy (fNIRS) clinical application[J]. Life science instrument, 2013, 11(6),45-52

[11] Gan Zhuo. Near infrared functional imaging of the brain development and its application in dyslexia research [D]. Master's degree in huazhong university of science and technology, 2004, 4,20.

[12] Wanatabe E.Nagahori Y.Mayanagi Y. Focus diagnosis of epilepsy using near-infrared Spectroscopy [J]. Epilepsia, 2002,43:50-55.

[13] Zhang Yan. Based on the near infrared spectrum technology of brain activity signal extraction method research [D]. Harbin industrial university PhD thesis,2011.06

[14] Zhao Jun. Neonatal brain tissue optical parameters of nondestructive testing [D]. The Ph.D. Thesis of Tsinghua university, 2004:1-13

[15] Wang Xiang. Double wavelength of cerebral blood oxygen monitoring signal processing and its clinical application [D].

[16] Wu Xin. Cerebral blood oxygen detection based on near infrared spectroscopy technology research [D]. Harbin industrial university master's degree thesis. 2010,07

[17] Shi Fanzhu,Huang Runheng,Zhou Shijian et al. Wave scattering in random medium and the information of random functional analysis [D]. Fudan university doctoral thesis. 2010,04,01

[18] Delpy DT,Cope M,Vander Zee P,et al. Estimation Time of Flight Measurements[J]. Physics in medicine and biology,1988,33(12):1433-1442.

[19] Duncan A, Meek J H,Clemence M,et al. Optical Pathlength Measurements on Adult Head, Calf and Forearm and the Head of the Newborn Infant Using Phase Resolved Optical Spectroscopy[J]. Physics in Medicine and Biology ,1995,40(2):295-304.

[20] Van der Zee P,Cope M,Arridge S R,et al. Experimentally Measured Optical Pathlengths for the Adult Head,Calf and Forearm and the Head of the Newborn Infant as a Function of Inter Optode Spacing [J]. Advances In Experimental Medicine and Biology , 1992,316:143-153.

[21] Shang Lei.The study of Near infrared brain imaging algorithm [D]. Shandong university master's degree thesis,2008,4,5

Design of the multifunction running test instrument

LiuYang，LiXinquan，LiuXin

（College of Instrumentation and Electrical Engineering, Jilin University,Changchun 130022,China)

***Abstract*—In order to make the runners can immediately understand their state of motion, adjusting running program, and than achieve the purpose of scientific fitness, we design an wearable, multifunction running test instrument. The instrument based on STM32 single chip microcomputer as controller, throug the acceleration sensor, photoelectric sensor acquisition speed, pulse and other information, and then through calculation by the display part of present to the runners. After prototype test, the results show that the measurement deviation less than ± 10% distance, pulse measurement deviation ≤ ± 3 times per minute.**

***Key words*—Running tester function; Acceleration sensor; Photoelectric sensor; wearable; multifunction**

0 INTRODUCTION

IN the past people in running usually need to adjust the running program according to the experience, but in the process of running, often do not understand their own physical condition which can lead to burnout. This not only not fitness function, it is bad for health. Already on the market at present is the speed of testing equipment, mostly rely on GPS mobile phone support software, in a small range, short time measuring accuracy is not high, And pulse measurement equipment for more professional heart rate, blood pressure measuring instrument, the above two devices are there are not convenient to carry, the disadvantage of single function, does not apply to daily running fitness. In this paper, we design a can measure the information such as speed, distance, pulse, and other information feedback by calculation of portable detector running. This design through the acceleration sensor capture the motion information, through the photoelectric sensor collection pulse information. Through the acceleration sensor capture the motion information to be measured values, such as running speed, distance. Its advantage is that can more accurate measurements of small range of motion, which can be widely applicable to the plaza, playground, basketball court and other places of daily running. With photoelectric sensor collection pulse information, its advantage lies in small volume, low power consumption, easy to carry, so in the process of running immediately or at the end of the pulse, in order to understand physical state.

1 OVERALL DESIGN OF SYSTEM

Design of multifunctional running detector by STM32 microcontroller, MPU6050 acceleration sensor module, a pulse detection module, keyboard, display, a total offive parts. As shown in figure 1. Located at the wrist acceleration sensor to judge of arm movements, running and record the information; located in the fingers of photoelectric sensor is responsible for collecting the pulse signals, the last two signal by single chip microcomputer processing, according to the results.

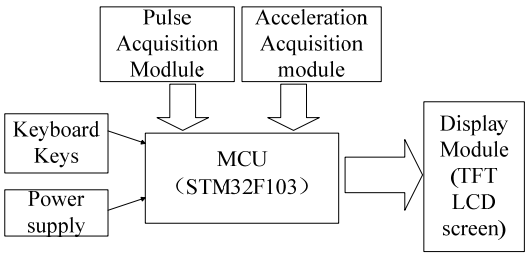

Fig.1 System architecture

Different length, according to the running distance range of established three running modes, can choose to enter the pulse measurement mode after running. Software flow chart is shown in figure 2.

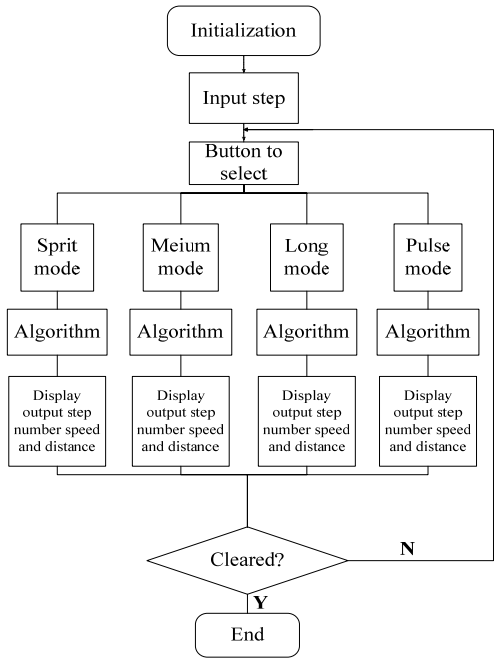

Fig.2 System software block diagram

2 MODULE DESIGN

2.1 Acceleration module

In the design choose MPU6050 chip speed sensor, the design of leading the I2C port in the form of a single data stream, the microcontroller output 6 axis to collect data. Through the analysis of six axisdata, determine the arm motion information, thus determine runners movement situation, through the single-chip microcomputer processing concluded that running speed, distance and other information. The algorithm flow chart shown in figure 3.

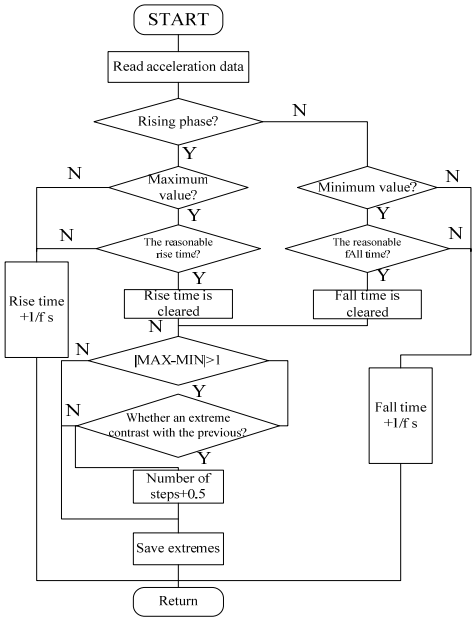

Fig.3 Algorithme flow chart

2.2 The pulse detection module

Of the light absorption in the blood is constant, and in the blood of venous blood pulsing relative to the arterial blood is very weak, can be ignored. Therefore, can think light through the finger after the change is only caused by arterial blood filling, then by detecting under constant wavelength of light irradiation light intensity can be indirectly measured through the finger to the pulse signals of human body. The pulse detection in the design of module adopts photoelectric sensor, analog signal acquisition get approximate triangular wave, through single chip analog signals into digital signals for further processing, finally through the single chip microcomputer and speed information integration, by showing some feedback to the runners.

3 THE TEST RESULTS AND ANALYSIS

3.1 Test scheme

Test number for nine people, nine subjects into three groups, the runway circular runway (400 m) in the test site for sprint (200 meters), medium-range, run (1000 m), m (3000 ft) long running test, tested twice in each group, the end of the running test record runners step length, step, testing pulse.

Table 1 Running Test1

	A	A	B	B	C	C
Number	1.8m	1.8m	2.0m	2.0m	2.1m	2.1m
Step	108	110	98	98	94	95
Real Distance	194m	198m	198m	196m	197m	199m
Distance	200m	200m	200m	200m	200m	200m
Deviation	2.8%	1%	1%	2%	1.5%	0.5%

Table 2 Running Test2

	A	A	B	B	C	C
Number	0.8m	0.8m	0.9m	0.9m	1.1m	1.1m
Step	1170	1157	1063	1089	878	895
Real Distance	936m	926m	957m	980m	966m	984m
Distance	1000 m	1000 m	1000 m	1000 m	1000 m	1000 m
Deviation	6.4%	7.44%	4.33%	1.99%	3.42%	1.35%

Table 3 Running Test3

	A	A	B	B	C	C
Number	0.5m	0.5m	0.5m	0.5m	0.6m	0.6m
Step	5870	5859	5823	5795	4889	4762
Real Distance	2935 m	2929 m	2911 m	2897 m	2933. m	2857 m
Distance	3000 m	3000 m	3000 m	3000 m	3000m	3000 m
Deviation	2.17%	2.35%	2.95%	3.42%	2.22%	4.76%

Table 4 Pulse Test

	A	A	B	B	C	C
Real(time/min)	71	67	74	73	63	60
Test(time/min)	68	66	73	72	61	58
Deviation (time/min)	3	1	1	1	2	2

3.2 interpretation of result

Measurement results as shown in table 1 to table 4, in the sprint test due to the step change is not obvious, so the maximum distance measurement error is only 2.8%, intermediate run test step change is bigger, the maximum error is 7.44%, long distance test step change in little change, maximum error is 3.42%, the pulse test error of a maximum of three times per minute. Above several groups of data shows that the running distance test caused by step length error of the basic control within 10%, the pulse measurement error control within 3 times/per, conform to the anticipated target.

4 CONCLUSION

The design of speed measurement, pulse measurement of two parts, respectively is equipped with accelerometer measurement circuit, pulse sensor, each part are independent of each other, together with the host is linked together, achieve runners running speed and pulse at the same time monitoring purposes. Through practical test, this experiment device and running speed of the pulse error can be controlled within 10%. In addition, the design of small volume, tends to carry, can be used for small sports place, has the good market application prospect.

This project is at the completion of phase encountered all sorts of difficulties and setbacks, through joint efforts of the team finally completed the multi-function running device of the overall hardware connection and the implementation of the related function.

Refer to offer:

[1] Chi Hua, Gong, Juan, Fang Xiuqong , etc. Decreased endurance and running our students lack of education and countermeasures [J]. Chinese Sports Science. 2008, 43(6): 91-94.

[2] Guo Yongfeng. Explore methods of monitoring exercise training intensity measured by heart rate [J]. Qinghai Normal University: Natural Science,2006 (3): 102-103.

[3] Su Liya, Dong Jinming, Zhao Qikuang , Pedometer-based system acceleration sensor [J] , Measurement and Control Technology 2007, 26: 163 -165

[4] Yuan Xianfeng, Zhou Feng Yu, Yuan Tong, et al. Precision pedometer STM32 and iNEMO module design [J]. Microcontroller and Embedded Systems, 2013, 13(9): 42-45.

[5] Shi Xindong, Cheng Yang, Zhang Yu, et al. Based on acceleration, photoelectric sensors fitness partner [J]. Chinese Journal of Medical Instrumentation, 2011, 35(5)

[6] Xu Rui. Pedestrian navigation system algorithm and its application to achieve [D] Nanjing: Nanjing University of Aeronautics and Astronautics .2008

[7] Wang Liying. Pulse measurement methods based on optical technology [J]. Sensor Technology.2006,5(11):32-34.

[8] Li Ping, Liu Ming, Design digital pulse tester [J]. Measurement and Control Technolog. 2009,28(6):28-31.

[9] Fang Zuxiang. Research on the human pulse measurement [J]. Sensing Technology Journal,

2007,20(5):728-730.

[10]Song Haoran, Liao Wenshuai , Zhao Yiming,, ADXL330 accelerometer-based pedometer precision of [J]. Sensing Technology Journal, 2006, 19(4): 1005-1008.

DC-DC DC transformer based on SG3525

Wen Xiaozhe, Xu Linlin, Zhang Facong

（jilin university instrument science and engineering institute, changchun,13002）

***Abstract*—SG3525 is integrated PWM control chip with excellent capability, complete function and high versatility, which is simple and reliable, requiring fewer external components, easy to use and flexible, utilizing push-pull output form, increasing the drive capability. This paper introduces the working principle of SG3525, and deduces the design of feedback loop of the circuit in detail. The experimental results of Buck circuit applications confirm the feasibility of the design.**

***Key words*—SG3525; feedback; Buck circuit**

Ⅰ. INTRODUCTION

WITH the development of power electronics, power MOSFET switching power supplies are widely used. To this end, the United States launched the Silicon General Semiconductor SG3525, to drive the P-channel power MOSFET [1].SG3525 is a current-controlled PWM controller, not only with adjustable dead-time control functions, but also has a programmable soft-start, and in the structure of the voltage and current loop bicyclic ring system, so the performance of switching power supply indicators have improved to some extent. Buck DC converter is a common power conversion technology. Introduced by the SG3525 chip as the control core of Buck DC-DC power module, the power module has a wide application value.

Ⅱ.BUCK DC CONVERTER WORKS ANALYSIS

Buck converter structure shown in Figure 1, the main circuit includes switch VT, freewheeling diode VD, filter inductor L, filter capacitor C and the load R components.

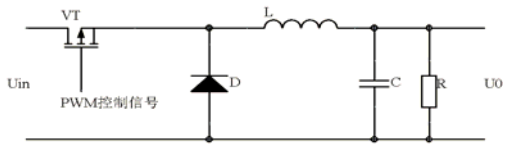

Fig.1 The main circuit of Buck

The output signal of the switching control circuit turns on the tube V_T, U_{in} power supply, the current in the filter inductor L is gradually increased, the energy stored in the inductor is gradually increased while the circuit starts charging the capacitor C. Ignore the MOSFET conduction voltage drop, MOSFET source voltage should be U_{in}, the voltage across the inductor filter should be

$$U_L = U_{in} - U_o = L\frac{di}{dt} \quad (1)$$

Thus it is concluded that flows through the inductor current

$$I_L = \frac{1}{L}\int (U_{in} - U_o)dt \quad (2)$$

Assume that the input voltage U_{in} and output voltage U_o remain unchanged, the switch can be turned on, and the current period is

$$I_L = \frac{U_{in}-U_o}{L}t + I_{min} \quad (3)$$

In the formula, I_{min} is before V_D conducting the instantaneous current in the inductor

When the switch is disconnected because of the control signal, the front voltage of the inductor rapidly drops to zero, but due to the continued flow of the inductor, the current will decrease gradually, in the opposite direction to the original voltage of the induced voltage generated across the inductor L, the induced voltage inductance makes V_D freewheeling diode conduction, inductance L in the switch conduction period transfer the stored energy to the load R by freewheeling diode. If you ignore the

freewheeling diode conduction voltage drop, the voltage across the inductor voltage during the switch off in the production should be

$$U_L = U_O = -L\frac{dt}{dt} \quad (4)$$

It can be concluded

$$I_L = -\frac{1}{L}\int U_0 dt \quad (5)$$

Assuming that the output voltage remains constant U_O, the shutdown-current is

$$I_L = -\frac{U_0}{L}t + I_{max} \quad (6)$$

Where I_{max} is the front switch-off instantaneous current in the inductor.

$$I_{max} = \frac{U_{in}-U_0}{L}t_{on} + I_{min} \quad (7)$$

$$I_{min} = -\frac{U_0}{L}t_{off} + I_{max} \quad (8)$$

Carry on simultaneous solution of the above equation

$$(U_{in} - U_{on})t_{on} = U_O t_{off} \quad (9)$$

$$U_{on} = U_{in}\frac{t_{on}}{t_{on}+t_{off}} = U_{in}D \quad (10)$$

Where, t_{on} the on-time of the switch, t_{off} to switch off time, T is the switching period switch, that $t_{on}+t_{off}$; D ratio for the switch conduction time of the switching cycle, commonly referred to as a conduction ratio or the duty cycle, from the formula (10) we know the duty cycle of the switch signal is less than 1, so the output voltage of the circuit is always less than the input voltage, as the duty cycle decreases, the output voltage decreases, so that the circuit is called a step-down chopper circuit [2].

III.SG3525 ANALYSIS WORKS

SG3525 is an American company producing silicon universal current mode pulse width modulator controller is a universal switching power supply chips, used as PWM generator, and use negative feedback to adjust the duty cycle of the switch, the switching power supply to achieve stable pressure and regulator role.

SG3525 internal schematic diagram shown in Figure 2.SG3525 wide operating voltage range (8V~37V), fine-tuning the internal integration of 5.1V voltage reference, oscillator, error amplifier, soft-start circuitry, shutdown, under voltage lockout circuit and the totem pole output circuit in meeting the basic needs of the switching power supply [3].

A. oscillator circuit

The range of the working frequency of oscillator is wide (100Hz ~ 400 KHz), and the dead zone time is adjustable. Oscillator of the rise time is determined by the timing capacitor and resistor R_T regularly

$$t_1 = 0.67C_T R_T \quad (11)$$

Between pins 5 and 7 there should be an external discharge resistor, which ranges from 0 ~ 500Ω, discharging time is

$$t_2 = 1.3R_D C_T \quad (12)$$

t_2 is the dead time.SG3525 changes dead zone discharge time by adjusting the resistance. Oscillator cycle is determined by the charge and discharge time, oscillation frequency is

$$f = \frac{1}{T} = \frac{1}{t_1+t_2} = \frac{1}{(0.67R_T+1.3R_D)C_T} \quad (13)$$

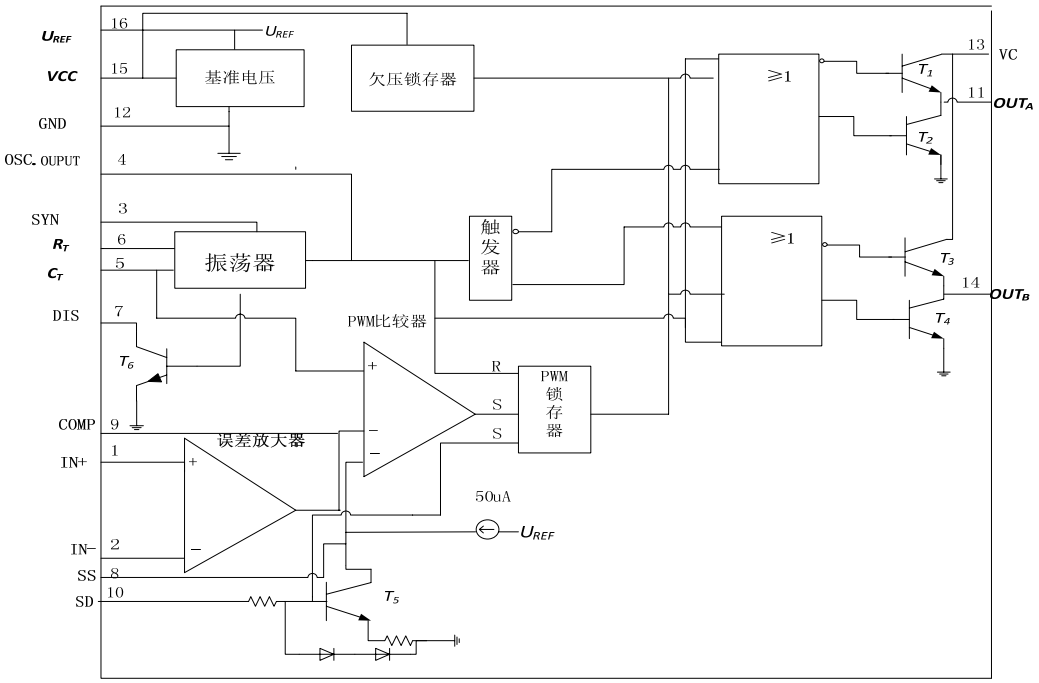

Fig.2 SG3525 internal schematic diagram

B. PWM comparator

As shown in Figure 2, the PWM comparator circuit is constituted by a periodic sawtooth C_T discharge form, an error amplifier, a soft-start circuit.The comparison voltage is introduced by voltage reference pin 16 by dividing resistor to pin 2, while the introduction of a feedback voltage to pin 1, the output of the error amplifier is connected to the PWM comparator's inverting terminal from the output circuit.SG3525 built-in soft-start circuit, the input of the soft-start pin 8 external soft-start capacitor, reducing the impact on the power switch of power [4]; sawtooth signal is connected to the inverting terminal of the PWM comparator. SG3525 supply voltage lower than the voltage of 8V or pin 10 exceeds 1.4V, PWM latch will immediate action to prohibit SG3525's output. Use pin 10 to build the circuit can achieve output overvoltage lock function, the circuit shown in Figure 3.

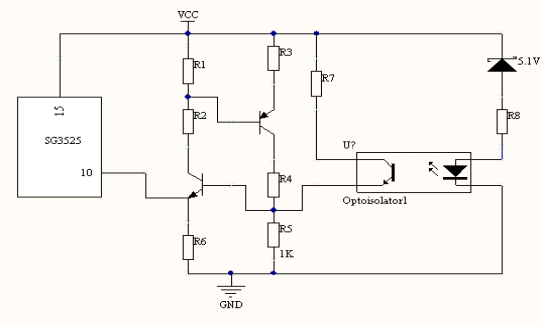

Fig.3 Overvoltage latch circuit

C. The output circuit

AS a dedicated driver chip, SG3525 adopts totem pole output (Figure 2), dual-channel output, shutdown faster.PWM signal of the latch output of the oscillator clock signal and the square wave signal through the NOR logic of the flip-flop control circuit drives the output. When all the signal is low, the output transistor is turned on. Because triggers two complementary outputs Q and $\bar{Q}$ so the output A and output B pin 11 pin 14 alternately outputs a high level[5], current and sink peak current and can provide up to 200mA.A case study in output, T_1 opened, then T_2 shutdown, driving MOS tube opening; T_1 turn-shutdown, T_2 on-resistance of small, provides a discharge circuit for the MOS transistor, MOS tube to achieve faster shutdown.

D. Design of Feedback Loop

SG3525 in the Buck-based feedback loop circuit design process, we must consider the impact of the low frequency of 50Hz frequency interference, but also consider the high frequency noise in the system after being amplified impact on the input side, the use of type II The error amplifier[6] the feedback loop design. Two amplifier circuit shown below:

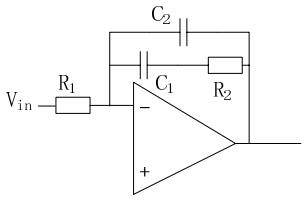

Fig.4 The second amplifier circuit

Transfer function of type II error amplifier is

$$G = \frac{\left(R_2+\frac{1}{j\omega C_2}\right)\left(1+j\omega C_2\right)}{R_1\left(R_2+\frac{1}{j\omega C_1}+\frac{1}{j\omega C_2}\right)} \quad (14)$$

When s = jω, the original formula can organize as follows:

$$G = \frac{1+sR_2C_1}{sR_1(C_1+C_2)(1+sR_2C_2)} \quad (15)$$

Zero point: $F_Z = 1/2\pi R_2 C_1$

Pole point: $F_P = 1/2\pi R_2 C_2$

According to Wiener Boer method selected ratio

$$F_{CO}/F_Z = F_P/F_{CO} = K \quad (16)$$

F_{CO} for the crossover frequency, usually chosen as the switching frequency of 1/4 to 1/5

F_{CO} phase crossover frequency caused by the zero F_Z ahead

$$\theta_1 = \tan^{-1} K \quad (17)$$

Crossover frequency F_{CO} phase lag caused by the pole F_P

$$\theta_2 = tan^{-1}\frac{1}{K} \quad (18)$$

The error amplifier is a 180 ° phase inverter with hysteresis, the initial phase lag due to the pole 90 °, so that the total phase lag

$$\theta_3 = 270° - \theta_1 + \theta_2 \quad (19)$$

Phase shift caused by the LCR filter

$$\theta_4 = 180° - tan^{-1}\frac{F_{CO}}{F_{ESRO}} \quad (20)$$

Relationship between the Buck circuit switch output V_1 and the output voltage V_O

$$V_O = V_1 \times t_{on}/T \quad (21)$$

Peak of the triangular wave is 2.24V, the output of the error amplifier is 1.12V, and the output duty cycle is 50%, the modulator output voltage of the error amplifier between V_O gains:

$$G_m = 0.5 \times 10/1.12 = 4.46 = 12.99dB \quad (22)$$

Using the form in the design of the partial pressure of the output voltage signal acquisition, PWM input of the error amplifier chip reference voltage is 1.7V, so when the output voltage of 5V, the gain between the sampling and output voltages is $G_s = -9.54dB$.So

$$G_m + G_s = 12.99 - 9.54 = 3.45 \quad (23)$$

Corner frequency of the output LC filter is

$$F_0 = 1/(2\pi\sqrt{LC})$$

$$= 1/2\pi\sqrt{1 \times 10^{-3} \times 47 \times 47^{-6}}$$

$$= 734Hz \quad (24)$$

ESR Zero frequency is

$$F_{ESR} = 1/2\pi R_{ESR} C_0$$

$$= 1/2\pi(65 \times 10^{-6})$$

$$= 2500Hz \quad (25)$$

So in addition to the Bode plot outside all aspects of the error amplifier open-loop gain of the total

$$G_2 = 3.45 - 2 \times 40\,log\frac{2500}{734} - 20\,log\frac{7500}{2500} = -27.38dB$$

Therefore, the gain of the error amplifier is $G_2 = 27.38dB = 24$

So choose $R_2/R_1 = 2$, take$R_1 = 1K\Omega, R_2 = 24K\Omega$

Assume phase margin is 45°,$F_{CO} = 7.5kHz, F_{ESR} = 2500Hz$.The phase lag of

108 ° LC filter. Therefore, the error amplifier allows 315 ° -108 ° = 207 ° phase lag for left margin, take K = 5, the phase lag 202 °, then crossing the phase margin frequencies of 360 ° -202 ° -108 ° = 50 °.

When K = 5, $F_z = 7.5/5 = 1.5kHz, F_z = 1/2\pi R_2 C_1, R_2 = 24k\Omega$, $C_1 = 4421pF$;

When K=5, $F_p = 7.5 \times 5 = 37.5kHz$, $F_p = 1/2\pi R_2 C_2$, $R_2 = 24k\Omega, C_2 = 176pF$.

Ⅳ. Experimental results and conclusions

Built in accordance with the circuit schematic experimental circuit, and recorded under different load fixed input voltage (ie, load regulation) and fixed output voltage under load values for different input voltage (ie, voltage regulation) under, as shown in Table 1 and Table 2.

Table 1:The output voltage under different input voltage conditions

$U_{in}(V)$	10	20	25	30	37
U_o	5.01	5.01	5.02	5.02	5.03

Table 2: Output voltage under different load conditions

I(A)	0	0.3	0.5	0.7	1.0
U_o	5.01	5.01	5.02	5.02	5.03

Experimental results show that different input voltages and under different load conditions, the output voltage can be stabilized at a given output voltage, voltage adjustment rate of 0.6%, 0.6% load regulation system to better achieve the regulator.

References

[1] WANG Xiaofeng,WANG Jingmei,SUN Jun,LI Li.Design of a Switching Power Supply Based on Sg3525[J]Electronic Sci&Tech./June.15,2010

[2] Tuo Lifang.Research and Design of Buck PWM DC-DC Switching Power Supply [C].Xi an:Xi'an P.R.China January 2008.

[3] Chen Cunkai. Switching power supply schematic, design and examples [M]. Electronic Industry Press,2012.5,179

[4] Tang Jun,Yin Bin,Ma Lijun, A half-bridge SG3525-based high-frequency switching power supply [J],

[5] LI Guidan GAO Hanying ZHANG Chunxi,The Rearchof DC-DC Convertor Based on SG3525 [J],2008

[6] Abraham I. Pressman, Keith Billings, Taylor Morey. Switching Power Supply Design. Electronic Industry Press.2010.6:363

[7] Abraham I. Pressman, Keith Billings, Taylor Morey. Switching Power Supply Design. Electronic Industry Press.2010.6:367-371.

Photoelectric sensor dark resistance measurement system

Xu-Ya'nan Xu-Wenjie Xiao-Wujian

(Jilin University Instrument science and engineer institute , Changchun 130022)

***Abstract*—Dark resistance is based on the measuring system of photoelectric sensor AT89C51 Intelligent measuring system of single-chip computer and PC can be achieved on the photo sensor P2532-01 dark resistance value measured at different temperatures, on your computer display dark resistance values corresponding to different temperatures. The system is divided into three modules, resistance measurement module, temperature control modules and communication and data-processing module.Measurement module of dark resistors and thermistors to measure the sensor and communication, controlled temperature controller AT89C51 module by single-chip microcomputer control of constant-current source for sensor cooling control. Communication module using the MAX232 chip realization of serial communication between PC and single-chip, to achieve information transmission between PC and single-chip microcomputer, data processing and storage, PC parts made using Matlab GUI software user-interface display and storage. System measurement range: 0-10 MΩ resistance value, accuracy ± 0.5%; 0-1.6A control current, accuracy of ± 1mA, the clarity of the interface, to store a full.**

***Key words*—Photoelectric sensor Dark resistance AT89C51 single-chip microcomputer MATLAB GUI Serial Communication**

0 INTRODUCTION

OUR country is producing the world's great powers photoresistor, but the production equipment and technology and foreign technology is still a wide gap still can not escape the long lineage of inefficient manual processes. With the rapid development of electronic technology and performance requirements for electronic components growing, manufacturers must be able to give a very accurate detailed parameter value of their products to meet the different needs of users. So, how can more accurately and quickly measure the dark resistor is of practical significance. Development of a new dark resistance measuring system to improve the production efficiency is significant. In this paper, the dark resistance of the photosensor measurement system can automatically control the temperature of the photoelectric sensor to measure different temperature rapidly, higher accuracy, and faster measurements.

1 THE OVERALL DESIGN

Design mainly divided between the three modules, temperature control module, measuring and communication modules, the next crew to select AT89C51 MCU, PC and the next crew to achieve information exchange via RS232. The overall design diagram shown in Figure 1.

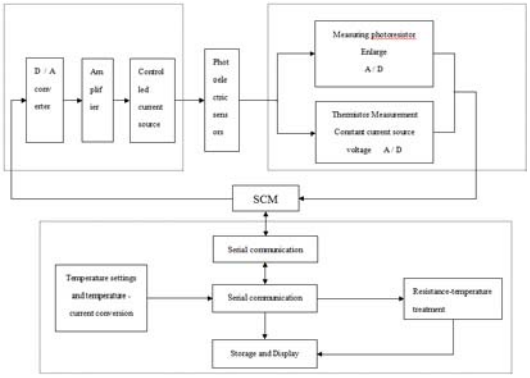

Picture 1.The overall design diagram

First, the PC input set temperature value, converted into the corresponding current value is sent to the microcontroller through the serial port to control the controllable current source output corresponding current value, the photoelectric sensor cooling reaches the set temperature. Start ADC Control Module two dark resistance value of thermistor and sensor measurements, the measurement results sent back to the host computer, after the actual temperature value after processing and signal conversion and

photoelectric sensors corresponding resistance values are shown in dark MATLAB GUI production the PC interface.

Measurement module mainly dark resistance of the sensor and thermistor measurements and communications, mainly by converting amplifier, filter, A / D conversion, AT89S52 microcontroller and serial components.

Temperature control module controlled by the microcontroller AT89C51 control sensor constant current source to achieve the cooling control, including D / A conversion, changing the current source by controlling the gate current output MOS tube. Serial communication using max232 development.

Communication module main transmission between MCU and PC information, data processing and storage, measurement results by matlab software displays the actual GUI interface to graphics and more intuitive tabular form presented to the user.

2 MEASUREMENT MODULE

2.1 Circuit design of data acquisition

Acquisition module measures signals on electro-optical sensor 1, 2 pin and thermistor 5, 6 pin.Sensor resistance's range is from 7K to 10M，The resistance of the thermistor is from 7K to 200K. Signal conversion circuit uses voltage divider circuit and serial respectively at one end a fixed resistor thermo-sensitive resistors and sensors,the sensor resistance value is converted into a voltage of 0 to 5V signal. Single chip microcomputer AT89C51 controls ADC0809 simultaneously AD two resistor voltage signal conversion。

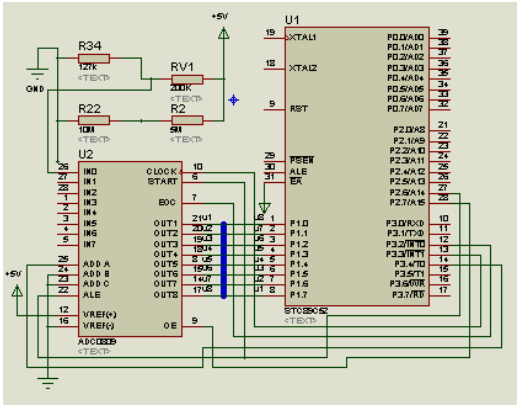

Picture2. The hardware circuit diagram of data acquisition module

Picture2 is the hardware circuit diagram of data acquisition module. ADC0809 uses channel IN0 measuring singnals of thermistor,and uses channel IN1 measuring signals of sensor resistance,conversion results from the OUT1~OUT8 output。ADC0809 with Tri-State output circuit within the buffer, so its eight output cable can be connected directly to the microcontroller bus. Channel address selects signals ADDB, ADDC grounding, ADDA P2.6 received a single-chip, is used to select the analog input IN1 and INO. Because ADC0809 has no internal clock, so it should be coupled with the clock, taking into account the simplification of circuit directly applied programmatically clock signal in the C program.

2.2 The conversion process of ADC

AT89C51 P2.6 receives control signals START of AD0809 and ALE-end, when you receive the computer instruction, open channel INO and IN1 AD conversion, When the microcontroller detects EOC from low level to high level, it ends conversion of ADC. When OE is 1, MCU reads the result. Picture 3 is ADC0809'Conversion process flow chart.

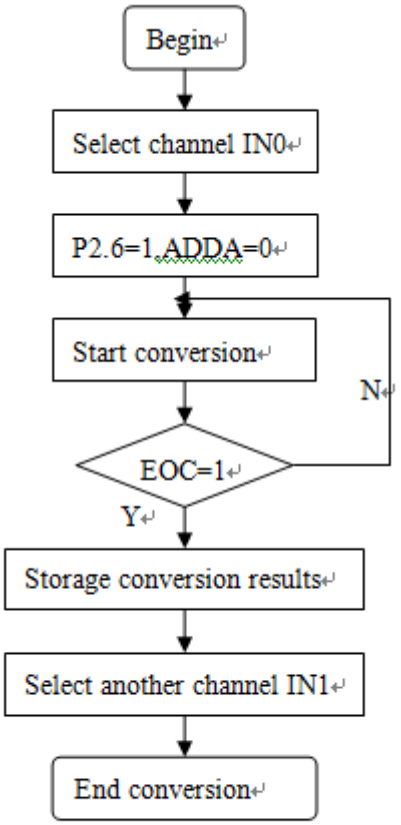

Picture 3. ADC0809'Conversion process flow chart

3 TEMPERATURE CONTROL MODULE

SCM received the PC after the current value of signal sent through data processing, lost by DAC converts the corresponding voltage values entered as part of the constant current circuit, constant current circuit to be converted into the corresponding current photoelectric sensor for refrigeration refrigeration PIN until it reaches the appropriate temperature. Among them, the hardware design of a constant current circuit is the most major part, the part from "high power CMOS OPAMP + tube" structure. Operational amplifiers using OP07, high-power CMOS tube using IRF640. Circuit diagram as shown in Figure 4.

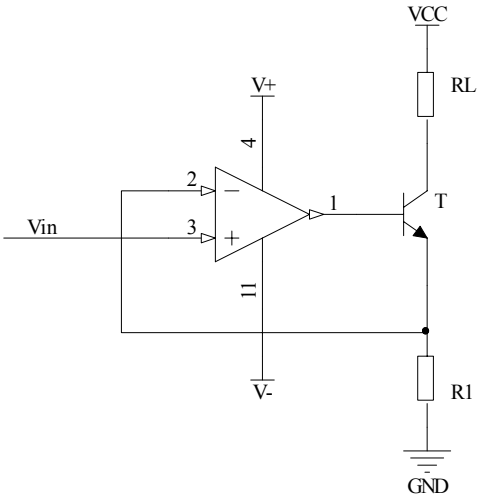

Picture.4.Constant current circuit

Its working principle is current through sampling resistor R1 converts the sample voltage. Sampled voltage voltage Vf as feedback into operational amplifier with OP07 end, compared with the reference voltage Vin, to adjust the grid voltage in order to adjust the output current to enable closed-loop feedback system as a whole is in dynamic equilibrium in order to achieve the objective of stable output current.

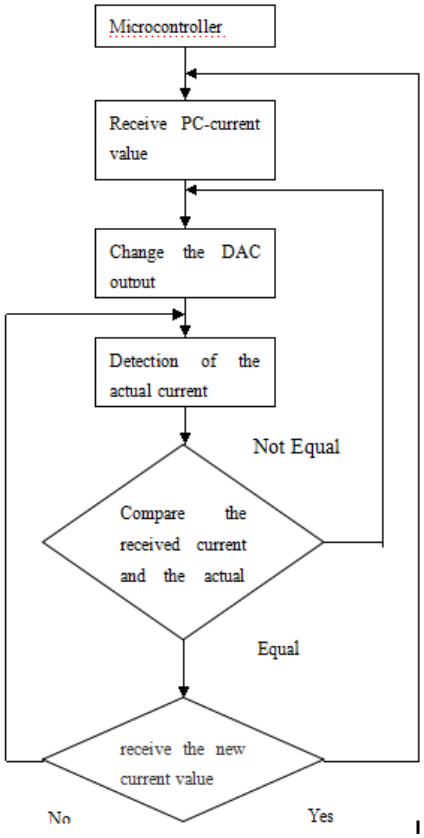

Picture5. temperature control software flow chart

Of information design includes PC software for receiving, processing and starting a DAC to convert the entire flow diagram is shown in Figure 5.

4 COMMUNICATION MODULE

4.1 Serial interface serial design

AT89C51 is used in this system to realize communication between a singl PC and hypogyny computer, and the centralized control of hypogyny computers is achieved.8051 by the serial port serial port control register, the transmission circuit, receiving circuit. When sending data → ACC → SUBF; receive, the receive interrupt proceedings to remove SUBF data. So use MAX232 chip level conversion and upload the data to the PC.

Optional RS-232 connector is DB9, or 9-pin serial port, and its corresponding pin RS-232-C standard interfaces nine common line. Serial circuit shown in Figure 6.

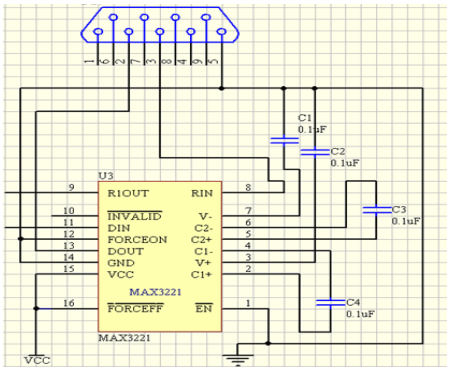

Picture 6.Serial circuit

4.2 Application Interface Design

The system software developed using MATLAB GUI user interface, to achieve mutual information between PC and microcontroller, data processing and data storage display. The system interface is shown in Figure 7.

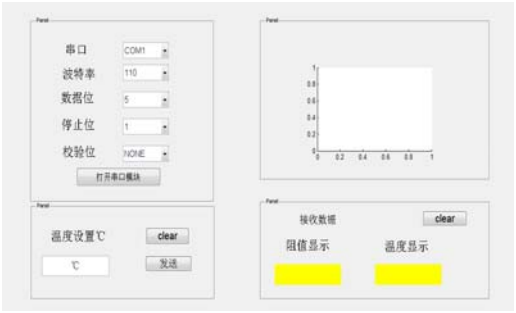

Picture 7.The system interface

Serial port settings include open and closed, serial number, baud rate, parity, data bits, stop bits setting. Reception area display and storage capabilities, and set the temperature and the resistance of the internal algorithms convert the image display. Send district sent to the microcontroller to control the temperature.

4.3 Communication Protocol

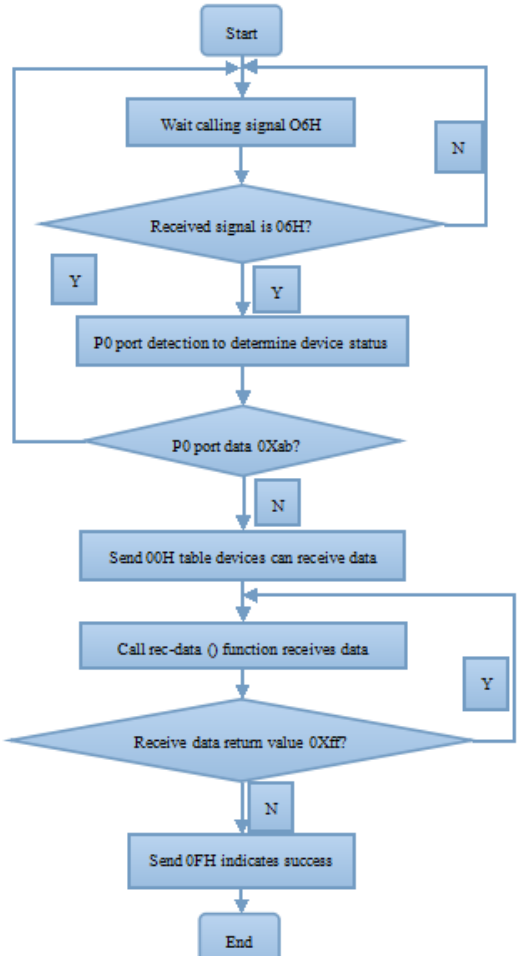

Picture 8.Communication flow chart

Communication agreement provides as follows: Rate of 9.6kbit / s, using a master-slave communication, then hair query. The host sends the handshake process 06H start asking the slave is ready. Reply 00H said slave can receive data back 15H refused to receive. After sending host receives data 00H, 06H otherwise continue to send inquiry slave. After receiving the data from the machine, hair 0FH indicates success; F0H an error, request retransmission. Host receives 0FH communication ends, otherwise retransmit, until receiving 0FH. Communication flow chart shown in Figure 8.

5 SUMMARY

The system uses a PC as the core controller to control the microcontroller AT89C51,dark resistance value of the photoelectric sensor's measurement range is 10MΩ, the error is 0.5%, and a thermistor to measure 200KΩ achieve a range of error of 0.5% , temperature control module constant current source output error is 1mA. PC for data conversion and processing, the temperature corresponding dark

resistor through MATLAB GUI interface displays measured. PC input set temperature and the actual temperature detection error is less than 0.5 degrees, basically meet the design requirements. In this system, since data collection using eight ADC, precision barely meet the design requirements, if you use 12 ADC, would be better.

References

[1] Per Zengmin. Three typical microcontroller AT89S51 with ADC0809 ADC connection [J]. Changsha University,2005,5:75-78.

[2] Fengzhong Ling, Tong Yinghua, Chen Xuehuang. ADC0809 in two-way data acquisition system application [J]. Electronic design engineering, 2011,13:75-77.

[3] Qiao Jianliang intelligent photosensitive resistance detection device research and design [D]. Nanjing University, 2006.

[4] Zhang Guohua precision constant current source circuit design. [J]. Design and Technology, 2001 (8) :37-39.

[5] Chu Danlei, Xue Xiaolong, Hu Guo Qing. Designing computer-based control system Matlab-GUI interface and dynamic simulation Simulink [J]. Detection & Control, 2002 01.

[6] Wang Zhan Jun, Shen Ming. Matlab GUI based implementation of serial communication programming modern electronic technology. 2010 09.

Electronic doctor—Health care system based on video

Luo-Quanquan Dong-Quanrui Zhang-meng
(jilin university instrument science and engineering institute,changchun,130021)

***Abstract*—With the rapid development of medical equipment and the enhancement of people's health awareness, real-time and user-friendly medical devices are more and more popular among people of all ages.At the same time , the modernization of traditional Chinese medical science has received extensive attention. Using modern technology to enable rapid development of traditional Chinese medical science becomes popular. This design is based on the principle of video capture and developes a home-based health care system. It includes the following features. According to the absorption of light by the face captured by the camera, we can caculate the heart rate. It will compare and select face color ,compare and combine different facial features by color feature extraction and classification algorithm to acquire combinations of characteristics and optimal algorithm for optimal space and finally establish a modern diagnosis system with function of preliminary diagnosis of liver disease. Height is measured by camera。This system is of small size and high inteligence ,can achieve the basic health care.**

I. INTRODUCTION

WITH the improvement of material life, people realize the importance of the health. Health is no longer the "patent" for the wealth, ordinary people health consciousness also continue to strengthen.With health issues are addressed, it give birth to the rapid development of health monitoring equipment. More and more portable health monitoring equipment come into the thousands of households.Based on the current domestic and international research and the collection, we design a set of health monitoring system of video.

II. System Design

A. Design Objective

In twenty-first Century, the social life rhythm is rising, more and more workers and housewives in sub healthy state, often under the double pressure of life and work of health risks.Because of the existence of such factors and overcrowded hospitals, it's difficult to have timely medical treatment condition, and the portable health care equipment became the new darling of the times and the "weapon" of health protecting. Portable health care equipment on one hand is to help ordinary non medical staff to monitor their health status, on the other hand is to help medical staff to quickly detect the patient's disease problems, save time for the treatment of late, especially in big city public hospital, the doctors reception are akin to "overload", and portable health equipment can save their valuable time.

B. Working Principle

System acquire images through video recording equipment, access to basic information, and then used the image grayscale or digital processing to remove the impurities, to obtain more accurate information, and through the system internal procedures to calculate the relevant data and then come to the diagnosis of disease or health information presentation.As for the collection and processing of face information, according to the scanning face of light absorbed, calculate heart rate; the face color comparison and selection of the color feature extraction and classification algorithms, face different characteristics are compared and combined, finally arrive at the optimal feature combination algorithm of optimal space and the establishment of modern TCM diagnosis, automatic analysis system are newly diagnosed facial features results by computer, realizing the preliminary diagnosis of liver function. Software architecture as shown in Figure 1.

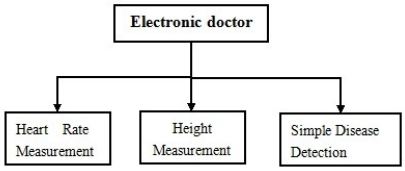

Fig.1

C. Heart Rate Measurement

The human heart is beating all the time, the number of beats per minute is heart rate. Because the blood after sunlight absorption of light in beating heart blood after blood flow volume change, blood absorption amount of sunlight also changing.When the absorption dose increased, the surface of skin reflected light is relatively reduced, this time through the extraction of human blood cycle curve can be informed human heart rate information, determine health through heart rate information can be preliminary.

First of all, by processing the original ECG signal readout waveform, as shown in figure 2.

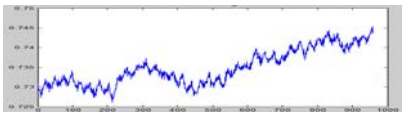

Fig.2

The wavedec calls the MATLAB function on the ECG signal of 8 level decomposition, get the signal s=D1+D2+D3+D4+D5+D6+D7+D8+A8. From Figure 3 we see not hard, the highest level of 8 was obtained by the decomposition scale coefficient, frequency range and baseline drift is approximate component of A8 is the most close to, so the use of A8 as the estimated baseline drift, from the original ECG signal is subtracted from the A8 signal can eliminate baseline drift. To eliminate the baseline drift after ECG waveform diagram as shown in figure 4.

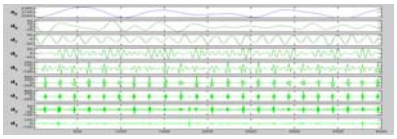

Fig.3

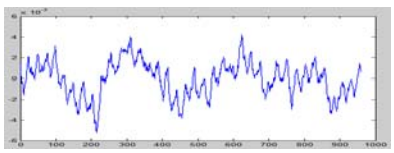

Fig.4

We use sym10 as the scale function of 8 level wavelet decomposition to obtain the signal of ECG signals, components of different frequency, according to the ECG signal frequency distribution characteristic of ECG signal reconstruction. Comparative analysis of spectral analysis and multi-resolution by decomposing the signal, we found that close to the frequency and ECG signal frequency of fourth scale signal components, so that the reconstructed signal s=D4. Through the wavelet transform of ECG signal decomposition and reconstruction, can reduce the impact of other interference. Waveform processed as shown in Figure 5

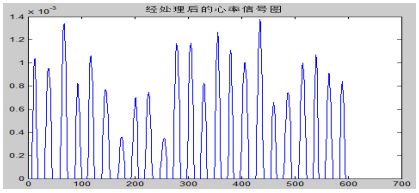

Fig.5

D.Height Measurement

The study on the basis of previous studies, using more advanced image processing algorithms to human image device captured color image gray processing, image pre-processing (including gray normalization, denoising and image sharpening), image edge detection, edge thinning, contour extraction, feature recognition and extraction of the human body image processing, to achieve the purpose of body height.

E.Simple Disease Detection

Acquisition of face information through the camera, according to scanning face of light absorbed, calculate heart rate; the face color comparison and selection of the color feature extraction and classification algorithms, face different characteristics are compared and combined, the optimal combined feature and algorithm of optimal space under the establishment of modern TCM diagnosis system, automatic analysis facial features are the initial diagnosis by computer, realizing the preliminary diagnosis of liver function. The consultation process is shown in figure 6.

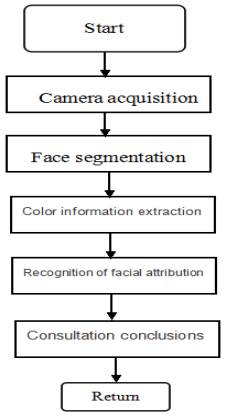

Fig.6

Access to information is mainly the features extracted in the HSV space. HSV (hue, saturation and value) use hue, saturation, brightness to describe a color, more accord with human vision, is a six angle of vertebral model, in the color space for color, H, used in angle measurement, the value range is 0 degrees ~360 degrees; S saturation, the value in the range of 0 ~ 1; V brightness values, values range from 0 to 1.

RGB to HSV conversion formula is as follows:

The value of RGB from 0 ~ 255 to 0 ~ 1, and then seek the maximum of three numbers in MAX,the minimum value of MIN, to the following formula:

$$H = \begin{cases} (6 + \dfrac{G - B}{MAX - MIN}) \times 60, if(R = MAX) \\ (2 + \dfrac{B - R}{MAX - MIN}) \times 60, if(G = MAX) \\ (4 + \dfrac{R - G}{MAX - MIN}) \times 60, if(B = MAX) \end{cases}$$

$$S = \frac{MAX - MIN}{MAX}, \quad V = MAX$$

We advance in the face image acquisition of 50 groups of normal human liver, extraction of the facial color values are averaged, and the average value as the center. Around the 5 expansion units as normal liver reference. Then collect face measured for comparison, if the range is considered the normal liver, or that the liver abnormalities.

III. Conclusion

This work is based on the traditional electronic as application background, designed a home health care system is convenient, practical, camera height measurement, camera acquisition rate and camera interview, through specific parts of the face color information of liver information. Work characteristics and key lies in using the camera to obtain a series of information, such as the acquisition of face of light intensity, can get the heart rate cycle, and can be obtained through location specific parts of face information, through the analysis of these parts of the color, and then the standard comparison, we can get a series of information about liver, through the calculation of pixel scale and height, can measure the height of the human body. Design and implementation of the human body index measuring basic, completed a health care, and the future of the "electronic doctor" has a certain significance.

References

[1] Dai Ruwei. System science and innovation and development of Chinese medicine [M]. Science Press, 2008-04-01

[2] Chen Xin. Huang Wan in clinical electrocardiography (Sixth Edition) [M]. People's Medical Publishing House, 2009-01-01

[3] Gao Yong Li. The Chinese traditional medicine on the development of [M]. Technology Literature Publishing House, 2009-10-01

[4] Shao Yi, Yu Zhilou, Zhang Guihong. The remote health monitoring system for the analysis of [J]. 《Information Technology and Information》, 2013 (01)

[5] Liu Xinhua. The facial color diagnosis and now research overview. Journal of Changchun College of Traditional Chinese Medicine. 2002:18~47

STC12C5A60S2microcontrollerbassource localization system design

Wang Hongchao、Lv Tingting、Peng Yishuai

(Jilin university instrument science and engineering institute,changchun,130021)

***Abstract*—The sound source localization system is based on single-chip host controller STC12C5A60S2 intelligent control system.It mainly consists of moving sound source and sound receiving system.Moving sound source consists mainly car and speaker, microcontroller generates a signal,the signal through the amplifier circuit power amplifier drives the speaker issue fixed audio sound signals, using the car as the speaker carrier,constitute a moving sound source.Audio signal receiving system in a very microphone perceived sound source signal, the pre-amplification, filtering,relatively stable output square wave signal, whereby the square wave signal to control the car to the specified position.Car ambient sound receiving device receives sound wave sat different times, the main controller to calculate the receiving end of the reception time difference and determine the location of the trolley and the midpoint of the deviation,then through thenRF24L01tosend commands from the controller to control the car movement audible sound source,so repeatedly until the sound source infinitely close to the midpoint.After testing,the distance between the coordinate positioning deviation is less than 3cm,meet the design requirements.**

***Keywords*— Voice guidance Sound reception Wireless Communications Difference control**

0 INTRODUCTION

VOICE guidance system can be moved within a certain range of sound source localization and guide it toward a predetermined area, signal and information processing information science discipline is an important part of the development of modern technology to achieve intelligent digital control system is an important development orientation.Voice guidance system to complete the sound monitoring,gathering, processing and other processes,is one of the intelligent direction of development.In this guidance system, the application of both wireless communications NRF2401 achieve information exchange, and thus more precise control car running status and relative positions.In the sound receiving system,make the three reception sensitivity that A,B,C adjustment points consistent with the reception time of the error reduction.Design is simple and practical, with good stability, cost-effective advantages.

1 OVERALL DESIGN

Design is divided into two parts, the main control terminal and from the implementation side, and both use NRF2401 [1] wireless module for information exchange.Overall design diagram shown in Figure1.

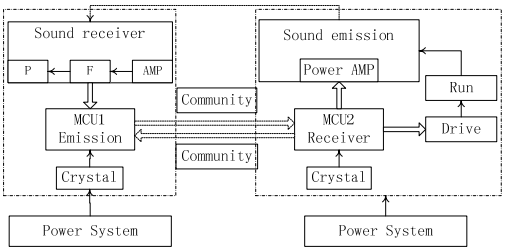

Figure 1 The overall design block

First, the control signal is generated by a wireless terminal chip and it is sent to the sound source on the implementation side, began to sound, then the control terminal receiving the sound source circuit is ready to receive,upon receiving the signal, the microcontroller sends stop sounding signal,received signal according to the difference of the time that the sound source position relative to the midpoint of the motion signal and sends the car, when receiving the control signal terminal is disconnected.When the car running for some time,sending the car stop signal,and continues to send the sound source signal, the receiver receives, once again determine car position, so again,eventually moving to the midpoint of the car.

2 HARDWARE DESIGN

The hardware design of the whole system is divided into three parts, namely,moving sound source section, MIC receiving portion and the MCU peripheral extensions.

2.1 Design of moving sound source

In the design,we use a car to be the sound source moving carrier.When the controller receives a signal occurs, the MCU send a certain frequency square wave signal,the signal after amplification circuit LM386 power amplifier[2], drive a loud speaker audio signal.Amplification circuit design shown in Figure 2.

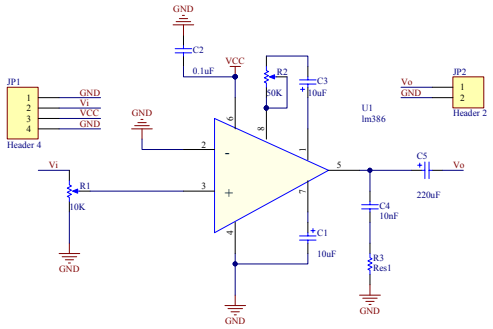

Figure2 Power amplifier circuit

2.2 MIC receiving circuit design[3]

Sound reception in part by the preamplifier, band-pass filtering,shaping three-part comparison,the microphone receives the signal that first pass through the preamplifier circuit that will attenuate the sound signal is amplified, and then filtered through a band-pass filtered signal interference signals, and finally by Compare shaping circuit outputs a stable square wave signal.

2.2.1 The band-pass filter circuit

In order to filter out the interference signal,the sound emitted by the source extraction4KHz valid signal, designed by the high-pass filter and low-pass filtering to form a band-pass filter[4], the high pass cutoff frequency of 3KHz,low-pass cutoff frequency of 5KHz,passband is 4, the circuit design shown in Figure 3.

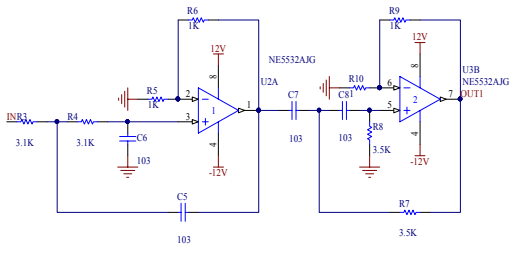

Figure3 Band-pass filter

The Calculation formula of the filter is

$$w_c = 2\pi f = \frac{1}{RC}$$

$$R = \frac{1}{2\pi fC}$$

Chose $C = 0.01uF$

then

$$R_{低} = \frac{1}{2\pi fC} = \frac{1}{2 \cdot 3.14 \cdot 0.01 \cdot 10^{-6} \cdot 5 \cdot 10^{3}} = 3.1k$$

$$R_{高} = \frac{1}{2\pi fC} = \frac{1}{2 \cdot 3.14 \cdot 0.01 \cdot 10^{-6} \cdot 4.5 \cdot 10^{3}} = 3.5k$$

2.2.2 Comparison shaping circuit

In order to make the received signal shaping a microcontroller recognizable square wave,chip design using LM311 comparator circuit,when its input voltage is higher than the set comparison voltage, the output pin will output high, if the input voltage is lower than the comparison voltage, the output is low.Figure 4 shows the circuit schematic of RP is set using the comparison voltage divider.

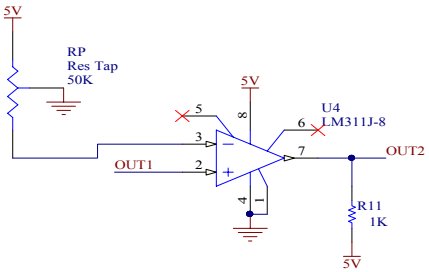

Figure 4 The comparison circuit

3 SYSTEM SOFTWARE DESIGN

Software control is divided into two parts, namely the host control and slave control.Between the host and the slave,we use NRF2401 to transmission information.Software processes and algorithms in Figure 5,Figure 6.

3.1 Host Software Process

First, the host sends to the sound source from the command occurs, then three external interrupt open,waiting to receive sound signals, and then determine whether the receiving circuit receives the sound, if the received corresponding interrupt source is turned off, but will remember receiving circuit chip the sequence of the received signal,and using the control

algorithm to determine the relative position of the sound source, and the calculation result to the slave via wireless transmission to control the relative movement of the trolley.If you did not reach the midpoint of the sound source position, the control car, will go after a certain distance,and then send the car stop signal.So again,in the manipulation stopped at a position as close to the midpoint,as Figure 5.

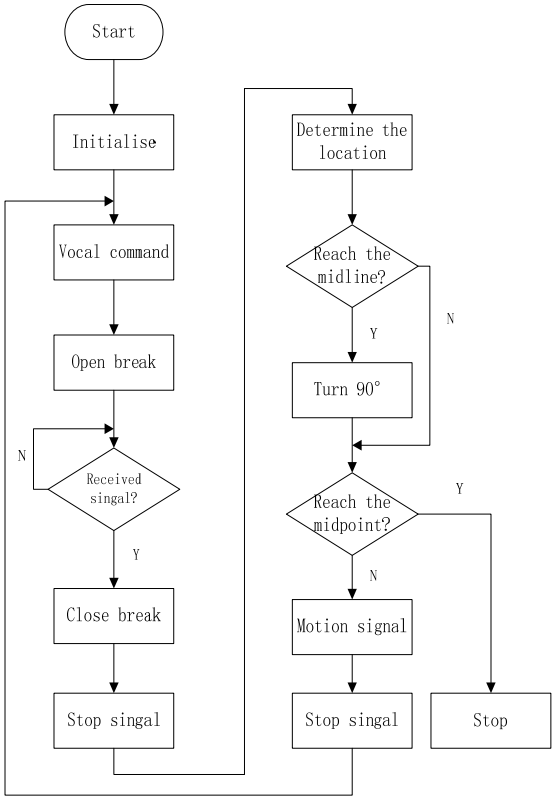

Figure5 Flowchart of Host

3.2 Slave software process

Slave primarily to receive and execute commands sent by the host Line.First, the command to wait for reception has occurred,so that a certain frequency horn,a certain width of the square wave signal,then the host will receive and calculated results from the machine to receive and control the relative movement of the car.

3.3 Positioning control algorithm[5]

Is known,in the three position of A, B, C in the square with three receiving end,in Figure 6:

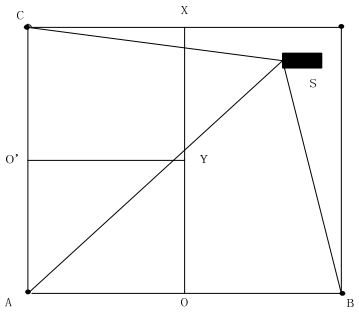

Figure6 Movement diagram

As a result of the distance between the source and receiver are different,so there is a time difference if receive successively.Let A, B, C receives the signal of the time, respectively Dt_A、Dt_BandDt_C .As can be seenfromFigure5,when the sound source is located at the right side OX,first determine the reception time of A, B ,then there will be the following relationship.

$$Dt_A > Dt_B$$

Therefore, it can determine the sound source to the OX direction,i.e.the receiving point A,after the repeated comparison until a time that the arrival line OX,then determine the A point and the reception time point C,as Figure 6, the car is located above OY, can draw the following relationship.

$$Dt_A > Dt_C$$

the Car will run to the OY direction, repeated determine two points until $Dt_A = Dt_C$,then stop moving, and the sound source is located in the midpoint,to complete the design.

4 SYSTEM TEST

Let the intersection coordinates is (50,50),the units is cm.Actually,we test 100 times,intercepted some of the test results in Table I:

Table I Test Results Table

Frequency	Initial	Location	Error	Speed	Yes or No
1	（100,100）	(50 , 49)	<1cm	12.0cm/s	Yes
2	（90 , 80）	(50.3 , 50.1)	<1cm	12.0cm/s	Yes
3	（80 , 70）	(48 , 49)	<1cm	12.5cm/s	Yes
4	（70 , 40）	(49.2 , 50)	<1cm	12.1cm/s	Yes
5	（60 , 30）	(50.2 , 50)	<1cm	12.0cm/s	Yes

Sound source moving distance test,after the movable sound make sound the car moved,when arrived coordinates (50cm,50cm),the car stop.Meter the time that moving sound source movement began to arrive from the designated location is t,the starting position to the designated location is s.With Equation1 can calculate the average speed , the average response rate v.

$$v = \frac{s}{t} \quad (1)$$

The results shown in Table 1,the average speed reach 10m / s or more,meet the design requirements.

Sound source distance positioning error testing.Movable stop after the sound source position and the coordinates (50cm,50cm) distance of positioning error Ds ,according to Table I shows,the actual position error in the range1cm to achieve the desired objectives.

5 CONCLUSIONS

This design use two STC microcontroller as the core control Controller,respectively, as the host receives the sound source signal to determine the location and from the machine as a slave and sound control car movement.Since the host interrupt sources need more,by extending the external interrupt source method to complete the overall system design.Since the signal outside of the signal acquisition system particularly sensitive,as long as the sound can let through the sampling,shaping filter into a square wave signal,the signal testing phase,must be masked out other noise,the system collects the sound of the sound source,where through the filter to the outside world with all the noise shielding to achieve good results,by three points received wave form synchronization correction to reduce the error,so that the test results are accurate and reliable.

References

[1] Hou Tianxing Wang Fengxin. Wireless data transmission system based on nRF2401 [J]. China's agriculture. 2009, 25 (7).

[2] Du Yunjiang BiShuE. LM386 active sonar in small power transmitting and receiving circuit application [J]. Journal of electroacoustic technology. 2010 (7).

[3] Zhang Jianshu Ma Xiaodong, Liu Zhiguo etc. Based on single chip microcomputer voice tracking function of the car control system design [J]. China's new technology and new production

[4] Du Yunjiang BiShuE. LM386 active sonar in small power transmitting and receiving circuit application [J]. Journal of electroacoustic technology. 2010 (7).

[5] Kang hua guang, Chen Daqin, zhang Lin. Electronic technology foundation [M]. Higher education press. 2006.

High density electrical number detector

Liu XinYang Cheng YuanDa Han Dong

(College of instrumentation & Electrical Engineering, Jilin University, Changchun 130061）

***Abstract*—As the high density electric method has such characteristics like small point distance, high data acquisition densities,it has gradually become the commonly used method in geophysical exploration for water and the investigation of geological hazard and engineerings prospecting .Through the analysis with the geological data to find the results have a highly similarity, the scientific and reasonable basis provides convenient for the popularization of high-density electrical method. The number of grounding resistances is large in the exploration of high-density electrical method. If the numbers of the electrodes and the grounding electrode are correct will directly affect the measurement results in actual production. This subject will be based on the single chip microcomputer 430 circuit design detection methods to test the numbers and grounding of electrode.**

***Keywords*—High-density electrical method , Electrode Numbers, test, MSP430 , RS485**

1 INTRODUCTION

1.1 Design background

HIGH density electrical system, distributed electrode existing conversion device is composed of a multi-core cable through the electrode connection box is connected with the electrode, to cover the entire test section, and the machine adopts cascade connection.

Processing now field test personnel of electrode failure is generally made of high density electrical system detects a fault numbering of electrodes, the field staff to determine the fault system terminal numbering of electrodes, electrode and then from No. 1 to several, until the count to fault numbering of electrodes, electrode for processing fault. In the field of hundreds of meters or even thousands of meters away from the search process, that is to find the electrodes along the cable, but also remember electrode number, if forget or error electrode number, field staff will return to the system is research. This approach is time-consuming and laborious, field test and high working intensity, seriously affecting the efficiency of construction.

1.2 Design content

To provide an electrode number detecting device of the design, it can connect point from any machine multi core cable in high density electrical equipment, electrode number the point corresponding to find, in order to find fault electrode number, and the fault phenomenon in fault electrode point to judge, to facilitate the treatment of fault.

Using electrode number detecting device, it can be connected to any machine from the multi - core cable connection point, electrode number the point corresponding to find. For example, in the first K electrode conversion from the machine is broken, electrode number electrode number detection device is connected at a position off to find the corresponding to a point K, in order to find fault electrode number, and the fault in the fault electrode point to judge.

1.3 High density electric characteristics

High density resistivity method is still in the rock, soil conductivity differences as the basis, a method of electrical distribution of conduction current effect of artificially imposed under the steady current field in. The theoretical basis of the same and their conventional techniques, just different. It is actually an array exploration method, field measurement only will all electrode (tens or hundreds of root) each measuring point under observation sections, fast automatic acquisition and conversion microcomputer device and electric engineering measuring instrument can realize data using programmable electrode, the measurement results are transmitted to computer, can also be to deal with the data and gives a geoelectric section distribution of various graphical results. Obviously, the development and application of high density resistivity exploration technology, intelligent degree of electrical prospecting is a great step forward.

Compared with the conventional resistivity method, with the following features:

The electrode arrangement is completed once, which not only reduces the electrode caused by the faults and

disturbances, laid the foundation for the rapid and automatic measurement and field data.

The preprocessing of the detection results and display the profile curve shape, visual result.

The scanning measurement of many kinds of electrodes effectively, it is possible to obtain a geoelectric structure characteristics of geological information more abundant.

The field data acquisition automation, not only the acquisition speed, but also avoids the errors due to manual operation.

The high density electric method of low cost, high efficiency, rich information, easy interpretation, exploration ability to significantly improve the.

2 HIGH DENSITY RESISTIVITY ELECTRODE NUMBER DETECTOR DESIGN

High density electric method in the field test, frequently distributed hundreds of electrodes lay, no rules at all, although the host know each electrode number, but due to the laying of a wide range, and a host of distance, when the need for an electrode of the state, or an electrode without a good grounding words, need to find out the status of measuring electrode, electrode, at the same time in order to facilitate exchanges need to achieve both call. Electrode number detector designed for this occasion. The hardware block diagram is shown in figure 1.

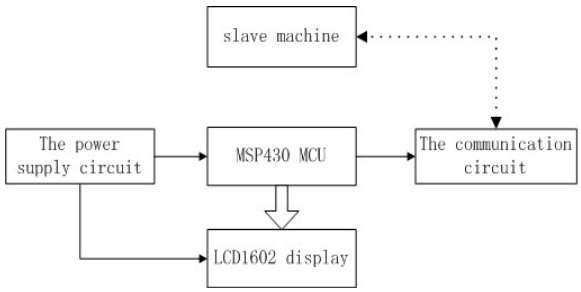

Figure 1 electrical electrode high density number detector hardware block diagram

The power supply circuit comprises a voltage regulator 12V power through the LM7805 transform, 5V power supply, 5V power supply with AS1117 to get 3.3V power source, the voltage in the circuit by the 3 power supply. As shown in figure 2.

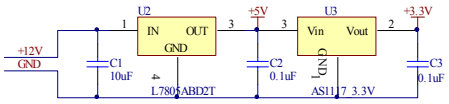

Figure 2 Power supply circuit experiment required

The design of this paper mainly includes following contents: the design of two parts testing code design and voice circuit based on MSP430 mcu.

2.1 Design of MSP430 MCU number detection based on

2.1.1 Introduction of MSP430

MSP430 mcu with 16 bit data bus, with FLASH. It has the features of high cost performance and high integration, so this type of MCU by technology developers welcome. Its peripherals and memory using the unified addressing mode, not only addressing range of 64K, and it can be extended memory, MSP430 MCU with interrupt manager unified, peripheral module on-chip is abundant, the on-chip multiplier is more accurate, the timer uses a 16 bit, the 12 bit analog to digital converter 14.

MSP430 supply voltage is 1.8 ~ 3.6V, current consumption of only 1.6uA standby mode, 64K program memory, 16 bit RISC structure, the 125ns instruction cycle, as well as 3 16 bit capture / compare register Timer_A. Figure 3 is the internal functions of M430F149.

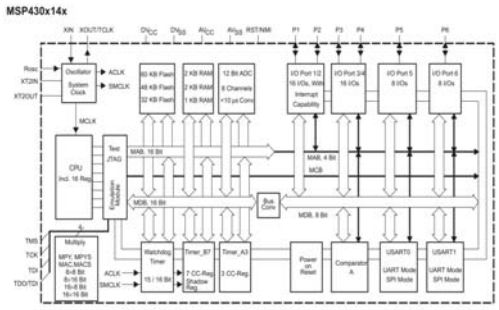

Figure 3 The internal function of Fig. M430F149

The choice of MSP430F149 belongs to MSP430x1xx series microcontroller.

2.1.2 Design of RS485 communication circuit

In the design of electrical measuring instrument, MSP430 mcu is mainly responsible for the operation of data collection, and the PC machine is used for data processing and communication etc.. You need to PC chip timing transmitting large amount of data acquisition. But because the PC and the microcomuputer data acquisition system is far away, and there is the data transmission channel environment

is poor and the need for large capacity electrical equipment to start and cutting operation, process data acquisition transmission brings great inconvenience. Therefore, data can be transferred to the safety of high speed PC machine become the focus of the design, we use RS485 protocol between PC and single chip microcomputer, and the use of RS485 serial communication must install RS485 converter, but due to the equipment is expensive, so we decided to use its own RS485 converter to realize remote communication between PC and single chip microcomputer.

430 MCU to complete data acquisition, and then the host communication, host computer data processing etc.. When at the beginning of the experiment, microcontroller to host sends a large number of data packets. In the experiment, the host and the single work place from a very far distance, electrode scattered near it on foot, far away there are hundreds of meters or even farther, field environment full of uncertainty, when transmitting the data, which is not the ideal environment. In order to ensure the rapid and accurate transmission of data, using RS485 communication. RS485 is a half duplex mode, a send another reception. It allows a two-wire bus sender driven 32 load devices. Station for interconnection can save the signal line, convenient high-speed long-distance transmission.

Pins MSP430 MCU as shown in figure 4.

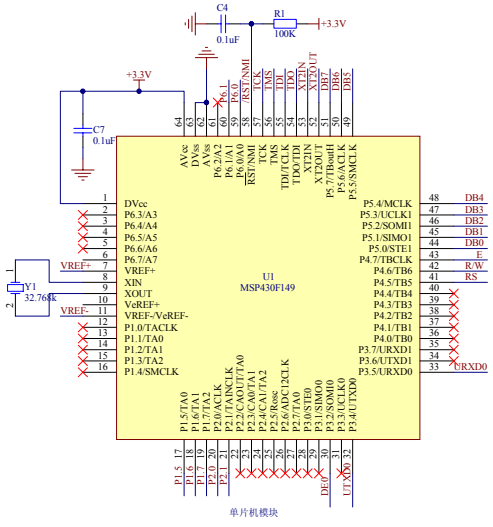

Figure 4 pins of MSP430 MCU

The RS485 communication interface as shown in Figure 5 circuit between MCU and PC.

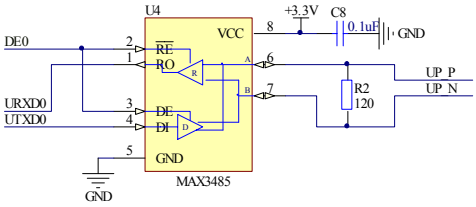

Figure 5 MAX3485 Communication pinout

See from figure 3-4 and figure 3-5, 4 pin single-chip signal from the P3.4 into the RS485 chip, and then through the RS485 interface chip, the chip is connected with the 6, 7 feet and electrode. Electrode through a long cable connected with the host, so as to realize the communication.

The 485 chip output pins without access resistance, signal submerged in noise, could not identify the signal, the host is unable to return data, is a failure experiment. Access resistance, the noise is greatly reduced, the signal which is can be tested is the ideal, so as to realize the communication with the host. So in transmission line RS-485, matched resistors should be one 120Ω.

LCD1602 connected with the MCU pin as shown in figure 6. After MCU host communication, returns the data in the LCD1602 display.

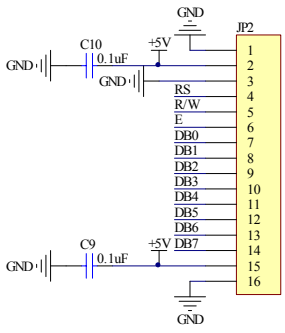

Figure 6 Pins LCD and MSP430 connected graph

LCD1602 the use of 2 groups of power. A group of module power supply, a group of power backlight board, all 5V power supply. RS is the number of liquid crystal have pin, is the command / data selection pin. The foot level is high said it would carry out data operation; low said command operation. RW is also a lot of liquid crystal have pin is read and write selection end, the foot for high level is said to the liquid crystal of read operation; low said to write operation. E also many LCD module has this pin, usually on the bus after a positive pulse signal to inform the data read out, the foot is at high level, is not allowed to change the bus. DB0 ~ DB7 8 bit bidirectional parallel bus, used

to transmit commands and data.

2.1.3 Software programming

The switch is connected with the microcomputer P3.6, when the switch is pressed, it is in the high power level, the microprocessor has to send the packet, it receives a host returns a data packet, the microprocessor receives after its decimal conversion, the results are displayed in the LCD1602. Host the returned data is numbering of electrodes. The flow chart shown in figure 8.

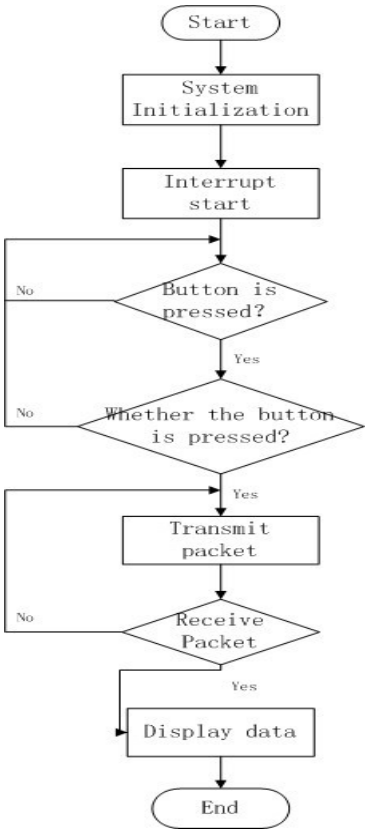

Figure 7 The software flow chart of electrode number query

2.2 Voice circuit design

The former circuit as shown in figure 9. When speaking into the microphone, through the capacitor to remove noise， operational amplifier TL082 is the task of the voice signal sent enough amplification, and then through 2.2 μ F voltage is switched on and the circuit part. The power supply voltage of 12V circuit

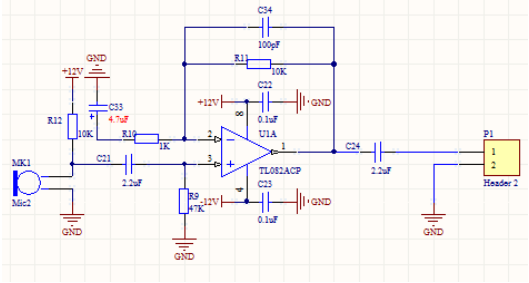

Figure 8 The post stage circuit of Microphone

The post stage circuit is also broadcast circuit as shown in figure 10. The output variable resistance circuit can adjust the speaker. The sound signal level from 1 feet into the audio amplifier LM1875 through the speaker. The 12V power supply circuit, which circuit to realize calling function.

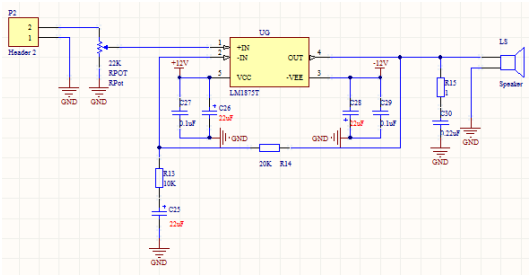

Figure 9 The speaker sound circuit

3. CONCLUSION

In the indoor environment to do experiment, electrode number 5, by aerial plug connected with each electrode, realize the communication with the host, thereby to query the number. The experimental results can accurately detect each electrode number. The 5 electrode (the last electrode) number query, to test the hardware circuit. Figure 10 is the last electrode number query results.

Figure 10 Query results

This experiment has cultivated our ability to research, analyze and solve problems in practice. Meanwhile, it has helped the team finally form good project-researching quality as well as scientific ethics, such as teamwork, communication skills, independent thinking pattern, and ability to capture cutting-edge information. In addition, our project gains and improved team members' hand-working ability, a combination of training theory with practical style as well as creativity.

Reference

[1] Kang HuaGuang. Basic electronic technology

(Analog) [M]. Beijing: Higher Education Press, 2006

[2] Kang HuaGuang. Basic electronic technology (Digital) [M]. Beijing: Higher Education Press, 2006

[3] Xie XingHua. MSP430 microcontroller based and practice [M]. Beijing: Beihang University press, 2008

[4] Cheng DeFu.Ling Jun. Intelligent instrument [M]. Beijing: Mechanical Industry Press, 2009

[5] Liu GuoDong. Electromagnetic and electrical instrument development and application of [J]. oil geophysical prospecting, 2004, S1:46-51+169

[6] Dong Haobin, Wang Chuanlei. Development and application of high density resistivity [J]. Earth Science Frontiers, 2003, 01:171-176

[7] Yu Yanchun, Zhang Lili, Wang Hetao. Multi machine communication MCU [J]. Anhui Agricultural Science Bulletin, 2007, 09:157-158

[8] Chen Shouyuan exchange, improved [J]. experience MCU serial communication in 2004

[9] Cao Linlin, Cao Qiaoyuan [M]. single-chip microcomputer principle and interface technology, National University of Defense Technology press, 2000

[10] Guo Shuhui, Yin Anzhi.485 communication bus reliability design of [J]. defense technology, 2009, 04:9-12

[11] Bu Guangyan. With the realization of serial communication using [J]. electronic components, between PC and MCU homemade RS485/RS232 converter 2001, 06:30-33

[12] Chen Xiaoying, President Guochen. Application of [J]. microcontroller and embedded systems, the stability of multi machine communication system of 2001 single chip microcomputer, 08:20-22

[13] Wang Jun, Zong preserving, Luo Bing, Zhao Jing, Liang Bing, Ling Zhenbao. Enhanced type electrode conversion device [P]. Jilin a high density resistivity instrument: CN201527481U, 2010-07-14

[14] Shen Jianhua, Yang Yanqin. MSP430 series ultra low power 16 bit single chip microcomputer principle and practice of [M]. Beihang University press, 2008

A Design Of Ferromagnetic Detection System Based On The Giant Magnetoresistive Sensor

Cao Xiaoqi, Yuwen Jianguo, and Bi Minghui, Instructor ： Wang Yingji

（College of Instrument Science and Electrical Engineering, Jilin University, Changchun 130022,China）

***Abstract*—This article designed a ferromagnetic detection system based on the giant magnetoresistive sensor by use of giant magnetoresistance. The system uses msp430 microcontroller control signal acquisition and analog to digital conversion,then output the result. Test results show that the giant magnetoresistive sensor not only can satisfy the survey of ferromagnetic objects in human body, but also Effectively avoid the problems of traditional coil detection method.**

***Key words*—Ferromagnet giant magnetoresistance the GMR sensor ADC**

I. INTRODUCTION

AS a means often being used in hospital, MRI examination has great advantages in the diagnosis of disease. However, before doing an MRI we must ensure that the body does not has ferromagnetic objects. If the body has ferromagnetic objects it will cause a shift of ferromagnetic objects when doing MRI, cause injury to the patient. Ferromagnetic objects in human body can also cause distortion of the test results when you do an MRI. Therefore, it is necessary to screen whether there is ferromagnetic objects in human body before doing MRI examination, especially for patients who can not clearly expressed.

Nowadays there are some issues of the traditional method of locating ferromagnetic material in the body: the use of X -rays or CT and other detecting ferromagnetic objects in the body easy to cause large radioactive, actual operation is not convenient and other problems. The hand-held metal detector on the market although easy to carry, easy to operate, but it has a low sensitivity in the ferromagnetic objects detection in the body. So it can not meet the practical applications[1]. To solve these problems, this paper design a high-sensitivity ferromagnetic objects system, preliminary use in the detection of ferromagnetic objects in human body.

II. EXPERIMENTAL PROGRAM

A.Program comparison

Ferromagnetic detector used to probing the ferromagnetic of human body requires high sensitivity, strong anti-interference ability, especially not be disturbed by the human body. By accessing to relevant information, we summed up the following four metal detector design, and compared their advantages and disadvantages:

1. As the most traditional metal detectors, Self-excited induction metal detectors multi-use LC oscillator as a detection circuit. The advantage is low cost, but the drawback is the low sensitivity, and prone to false positives.

2. The difference frequency metal detectors whose probe contains two oscillators. It uses the mixer for mixing and take difference frequency output. The advantage is the detection sensitivity is slightly higher and the anti-jamming capability is slightly stronger than a single probe.

3.The design of metal detector is based on phase principle. The advantage is the use of phase-locked principle, improving the anti-jamming capability. The disadvantage is that the resolution is not high.

4. A ferromagnetic detection system based on the giant magnetoresistive sensor. It is able to meet the requirements which is high resolution, anti-jamming capability, stable circuit and easy to implement the portable.

B. Giant magnetoresistance principle

The so-called giant magnetoresistance is the phenomenon that the resistivity of the magnetic material has a huge change when the magnetic field effect compared with without magnetic field effect [2]. When the magnetic moments of the ferromagnetic layers parallel to each other carrier’s scattering

associated with spin is minimal, the resistance of the material is minimal. When the magnetic moments of the ferromagnetic layers antiparallel to each other carrier's scattering associated with spin is largest, the resistance of the material is largest.

The general structure of the giant magnetore -sistive sensor using of giant magnetoresistance shown below:

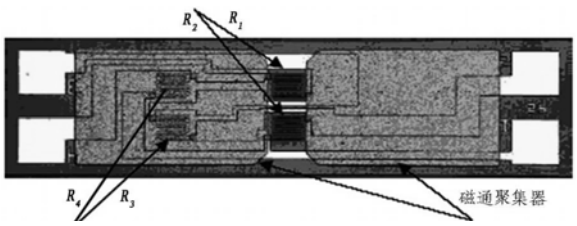

Figure1. The internal structure of the giant magnetoresistance

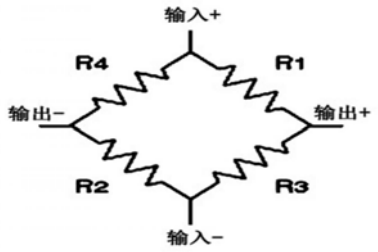

Figure2. The schematic of the giant magnetoresistance structure

As can be seen from the figure inside the giant magnetoresistive sensor is a DC bridge structure consists of four same GMR (R1 = R2 = R3 = R4 = R), R1 and R2 covered and shielded with high perme -ability material. The resistance has no response to the external magnetic. It is the GMR R3 and R4 affected by the external magnetic field. So it is constitute the arms of the bridge relative change in the same direc. –tion. When the sensor is in external magnetic field: R1=R2=R, R3=R4=R-ΔR. ΔR is the amount of resistance change of a single GMR when the magnetic induction intensity of external magnetic field is B[2]. Thus the output voltage can be obtained:

$$Uout=UinΔR/(2R-ΔR) \quad (1)$$

C. System Design

The hardware of ferromagnetic detection system adopts modular design[3], the overall block diagram of the system shown in Figure 3. The system consists of sensors, signal conditioning circuits, A/D converter circuit and alarm circuit. Using the GMR sensor detects magnetic field signals. Due to the voltage signal collected is very weak, the voltage signal is generally millivolt. But the AD converter has a resolution of 6.1mV, through the amplifier is needed to become the voltage signal to which be able to be identified by AD converter. The amplified signal contains high frequency and industrial frequency interference, therefore it need to access low-pass filter to filter out the high-frequency and industrial frequency interference. Then the signal go into the AD converter channel, which will convert an analog voltage signal to digital voltage signal. And then the digital signal is displayed through lcd1602, and the system determine whether alarm.

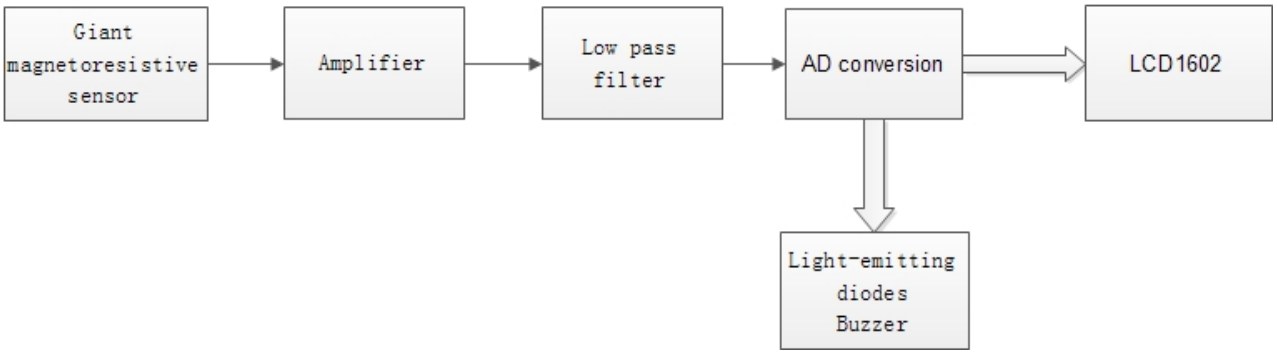

Figure3. The overall block diagram of the system

III. HARDWARE DESIGN

A. Probes

The detection of ferromagnetic substance uses AA series of giant magnetoresistance probe,after amplification, filtering, processing and display.

AA series of giant magnetoresistive sensor as a multi-purpose magnetometers, suitable for a wide field of applications. This experiment uses the AA002-02 giant magnetoresistance.

Table1. magnetic characteristics table of giant magnetoresistance[6]

Part Number	AA002-02	
Saturation field strength（Gs）	15	
The linear range （Gs）	Minimum	1.5
	Maximum	10.5
Sensitivity（*mV*／*V*／*Gs*）	Minimum	3.0
	Maximum	4.2
Resistance（Ohms）	5K±20%	
Die size（*um*）	436×3370	

The sensitivity of giant magnetoresistive sensor is very high. Geomagnetic field to exert some influence, to eliminate the effects of the geomagnetic field, adding zero resistance.as Figure 4 shows, adjust the zero resistance, you can remove the interference. Output of giant magnetoresistive sensor is Huygens bridge differential signal, and the size of signal is on the millivolt level. Specifically at 5V supply, the output of the sensor is:

Min: Vout=5×3.0mV/V/GS=15mV/Gs

Max: Vout=5×4.2mV/V/Gs=21mV/Gs

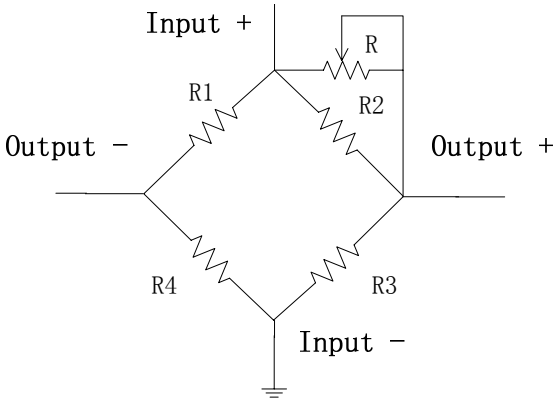

Figure4. zero resistance and sensor

B. Instrumentation amplifier

Improve the sensitivity requires the use of amplifier amplifies the output signal.AD620 is a three op amp instrumentation amplifier with high common mode rejection ratio, a temperature stability, bandwidth amplification, noise coefficient, etc. Suitable for amplifying the differential signal of magnetoresistive sensor. This article selects the basic amplifier circuit[5][7]. As the figure 5 shows:

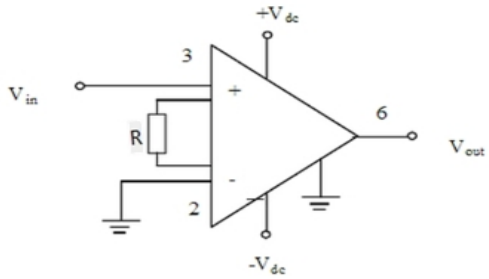

Figure 5. AD620 amplifier circuit

AD620 uses dual power supply, + Vdc and-Vdc select +5 V and-5V power supply. The resistor R is adjustable. 2 pin is connected to ground or negative signal.3 pin is connected to a positive signal. Gain is calculated as follows:

$$G = \frac{49.4k\Omega}{R} + 1 \qquad (2)$$

$$R = \frac{49.4k\Omega}{G-1} \qquad (3)$$

C. Low pass filter

Due to the surrounding environment and internal system may exist high-frequency interference and noise, while in some cases industrial frequency interference will be more serious, so to the part of the filter we use low-pass filter to filter out high-frequency and industrial frequency interference. Through reading relevant literature we know that compared to other low-pass filters, the biquadratic low-pass filter has the advantages of good stability, easy to adjust, etc. Therefore, we use the biquadratic low-pass filter. It's schematic diagram shown in Figure 6:

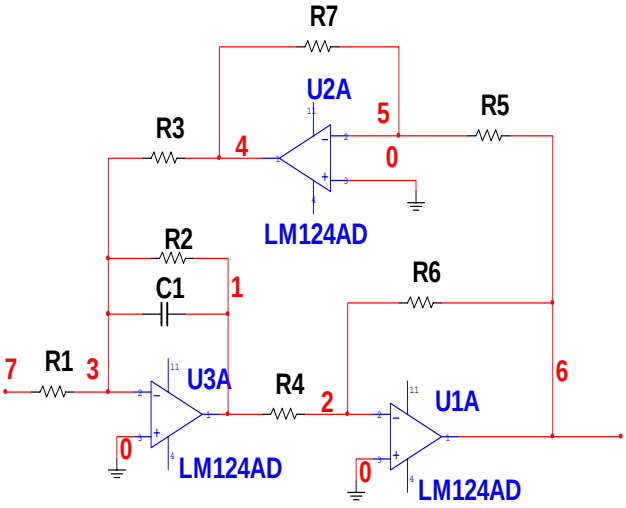

Figure6. Biquad low pass filter

Since the output of the giant magnetoresistive

sensor is less than 5Hz, and the noise of outside is mainly high-frequency interference and 50Hz frequency interference, so the output frequency of the filter circuit of the system set to 0-5Hz, scilicet the filter's cutoff frequency is 5Hz. We set the gain A_{vp} to 1. According to Table 2, we select 0.1uF ceramic capacitor.

Table2. Frequency and capacitance comparison table

f_c(Hz)	1-10	10-10^2	10^2-10^3
C	20-1μF	1-0.1μF	0.1-0.01μF
f_c(Hz)	10^3-10^4	10^4-10^5	10^5-10^6
C	10^4-10^3pF	10^3-10^2pF	10^2-10pF

According to the transfer function $K(S)=\dfrac{A_{vp}w_n^2}{S^2+\dfrac{w_n}{Q}S+w_n^2}$, R1=R3=25K, R2=R4=50K, here R4 take the 51KΩ resistor. R1, R2, R3 are insteaded of sliding rheostats, which easy to adjust the cutoff frequency. The operational amplifier A1, A2, A3 select OP27 precision operational amplifier, whose offset voltage as low as 25 μV, maximum drift is 0.6 μV / ° C, is fully able to meet the design needs.

D. AD conversion

The main features of the AD converter in msp430 are as follows:

(1) 12bits successive approximation;

(2) The maximum conversion rate is greater than 200ksps;

(3) The sampling time can be controlled by software;

(4) Selectable internal or external reference voltage;

(5) single-channel, single-channel continuous, multi-channel, multi-channel continuous conversion mode, etc.

(6) 16 12bits conversion result storage register.

It can be calculated that the input voltage changes between 0 ~ 2V according to the experiment. So we select 2.5V internal reference voltage. It can be calculated the resolution of AD: 2.5/4095=0.61mV. Therefore, using the ADC12 internal the msp430 can meet the design requirements.

IV. SOFTWARE DESIGN

The MSP430 MCU is a 16-bit ultra-low power mixed signal processor which the U.S. Texas Instruments company has began to spread in the market since 1996.The reason why it called the mixed signal processor is that the processor is integrated the analog circuits, the digital circuits and the microprocessor on a single chip. In this way, it can provide a kind of solution to solve problems with only one piece of chip.

The main characteristics of MSP430 MCU is Ultra-low-power, 16bit RISC CPU, high integration, easy to use and code security. The system uses 430c language to design software. The main function is to complete the AD converter, voltage displaying and alarming. The workflow is primarily to convert the input voltage signal by AD conversion. According to the formula(4):

$$N_{ADC}=4095\times(V_{in}-V_{R-})/(V_{R+}-V_{R-}) \quad (4)$$

Translate the average of the conversion results into voltage value and then display by lcd1620. Determining whether there is a ferromagnetic and alarming if the answer is yes. The flowchart shown in Figure 7.

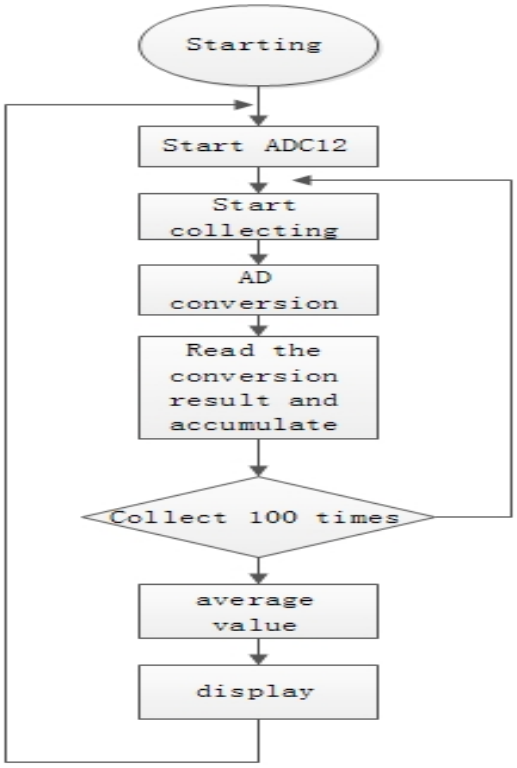

Figure7.Software flow chart of system

Calculate the average data after sampling 100 times so that we can guarantee the stability of the display, as well as to reduce the chance of false alarms.

V. MEASURED RESULTS

In order to verify the feasibility of the system, selecting different size ferromagnetic to test the system at different distances.

Because of the earth's magnetic field and other interference, we need to move the sensor to find a point of 0 magnetic. At this position, the bridge is balance. What's more, this is only a relative value because of the environmental constraints.

In order to ensure the comprehensiveness of the test results, you need to select different objects of different sizes and they can be magnetized in different degree. We select pin, small screws, coins and staples for testing. The pin and the coin are difficult to be magnetized, while the small screws and staples are easily to be magnetized. So we can get more comprehensive test results.

The test results are shown in Table 3:

Table3. Test Results

Measured body	Pin header（1cm）			Small screw（2cm）			
Distance(cm)	1	2	4	2（Interval fingers）	4（Interval fingers）	3	5
Display Voltage (V)	0.58	0.34	0.08	0.41	0.10	0.62	0.27
Warning	Yes	Yes	No	Yes	No	Yes	Yes
Measured body	Staple（1.5cm）			$ 1 coin			
Distance(cm)	2	4	6	2（Interval fingers）	4 （Interval fingers）	3	5
Display Voltage (V)	0.70	0.35	0.09	0.45	0.15	0.75	0.30
Warning	Yes	Yes	No	Yes	Yes	Yes	Yes

As can be seen from the table 3, the different sizes of the ferromagnetic at different distances has different influence on the magnetic field. The greater of the magnetism the stronger of the magnetic field. The closer of the distance, the greater influence on the sensor. The output results of the sensor have relations with the distance of the magnetic sensor and the magnetism of the iron magnet.

Test results show that giant magnetoresistive sensor can satisfy detecting ferromagnetic objects in the human body and effectively avoid the problem of low sensitivity, poor anti-jamming ability which produced in the traditional method of detecting.

VI. CONCLUSION

Through the study of the basic detection of ferromagnetic material, in the small electromagnetic interference, the experiment can be detected within a small range of voltage variation of ferromagnetic foreign bodies interference, to prove the application of GMR sensor can probe a weak magnetic field, the finger can be isolated to detect ferromagnetic material.

The design is to try the giant magnetoresistive magnetic sensor applications in the human body probe objects, to the human body probe magnetic objects provide a new possibility, to provide a new direction.

References

[1] Zhao Liying. Non-invasive Detection System for Metallic Foreign Body [D]. Tianjin：college of precision instrument and opto-electromics engineering, 2010.

[2] Huang Kailian, Li Heng, Mo Haiyun, Liang Jiren. The research of GMR sensor [J]. Journal of Guangxi university for nationalities,2010（16）:p85-89.

[3] Hu Guanhua. A design of ferromagnetic detection system based on Magnetoresistive sensors[J]. Sensorsworld,2011：p26-29.

[4] Zhao Jingliang, Zhang Botao. A design of ferromagnetic detection system based on the

magnetoresistive sensor[J].Technology & Application. 2011, (8).

[5] Sun Jian，Fang Xudong. Research on Detection Circuit for Magnetic Flux Leakage Signals Based on Megnetoresistive Sensor[J]. Journal of Huangshan University. 2011,13(5).

[6] NVE AA002 Giant magnetoresistive sensor[DB/OL]. http：//www.zc-sensor.com.

[7] Wang Yahui, Ding Guoping. Examples & Performance of Low cost, Micro-power Instrument OP Amp-AD620[J].Journal of Electron Devices. 1997,20(1).

[8] Kang Huaguang. Electronic technology foundation (Analog part)[M]. The fifth edition. Beijing: Higher Education Press, 2008: p413-p432.

Intelligent Glucometer with Exercise Intervention

Guangan Ren Wenchang Fan Bing Han
(JiLin University CIEE Class 651004)

***Abstract*—The study shows that positive exercise and proper exercise intervention plan play a significant role on the rehabilitation of patients with diabetes. Based on the study of the relationship among blood glucose in diabetic patients, the exercise situation and the exercise intervention situation, a glucometer with intelligent exercise intervention is developed. We use ADXL345 with high-precision to develop the pedometer which is performed under the control of the MCU MSP430F449. We use glucose-oxidase -type glucose sensor and design the amplifying and filtering circuit for blood glucose testing.Then wesend data via GSM module. Prototype-test-results show that the intelligent glucometer achieves step-counting within 10% error rate, and blood glucose testing within 15% error rate. Finally, the results can be sent to the expert and the patients can get exercise response message via GSM module.**

***Keywords*—pedometer glucometer exercise intervention**

0. INTRUDCTION

POSITIVE exercise and proper exercise intervention plan have a significant effect for the rehabilitation of patients with diabetes. Based on the study of relationship among the diabetic condition and exercise situation and exercise intervention situation, we design this intelligent glucometer.It can detect exercise situation, blood glucose and achieve exercise intervention. It assists the expert to know the exercise situation and blood glucose, and to make effective and proper exercise intervention plan.

This paper first introduces the study of the relationship among diabetic condition, exercise situation and exercise intervention situation.Then we detail the hardware and software designing solutions. Finally, it is the data and results of the prototype.

1. THE STUDY OF THE RELATIONSHIP AMONG DIABETIC CONDITION AND EXERCISE SITUATION AND EXERCISE INTERVENTION SITUATION

Prior to this designing of the intelligent glucometer with exercise intervention function, in order to develop a more rational exercise intervention program to achieve a desired effect for the treatment of diabetes, we investigate the relationship among the diabetic condition, exercise and exercise intervention situations by the way to access the relevant literature.

1. 1 Impact of exercise on diabetes

Through the study of relevant literature on the impact of exercise on the diabetic condition, we sum up the following conclusions:

Exercise can reduce blood glucose because of the combined effects of the exercise accumulation and enhanced insulin sensitivity. Muscle contraction requires a lot of energy, especially in the skeletal muscle. In order to supply the energy, glycogen in muscle and liver breaks down to reduce blood glucose directly. Glucose is the "fuel" to maintain muscle moving. Dietary glucose eventually enters the blood circulation, and there is also a lot of glucose in the muscle. When starting to exercise, the glycogen in muscle and liver is the "fuel" of body. When these storage runs out, the muscles will absorb glucose in the blood for their own [1]. Therefore, the blood glucose level decreased during exercise. After exercising, body stores the glycogen in muscle and liver again, then, the level of glucose decreases more. So insisting on long-term exercising benefits on controlling the level of blood glucose and reducing the risk of cardiovascular disease [2]. Meanwhile, studies show that walking and other aerobic exercise have a good effect on reducing blood glucose. It enables muscle uptake of more glucose, and increase oxidation

and utilization. Thereby, it reduces blood glucose and glycosylated hemoglobin, and the toxicity of chronic hyperglycemia [3].

With regarding to the exercise intensity, the survey results show that, 1 h after breakfast, walking for 3000 steps briskly outdoor, with step speed controlled to 1000/10 min, can effectively regulate and control blood sugar levels. And it is well tolerated by patients with diabetes which can be used as a safe and effective exercise therapy [4].

1. 2 Impact of exercise intervention on diabetes

There are 34 relevant literatures about the impact of exercise intervention on the fasting plasma glucose of diabetes. 2697 cases were concerned in the 34 literatures. They consist of exercise-intervention group for 1422 cases, control-group for 1275 cases. The result shows that: the intervention group had more advantages in reducing fasting glucose in patients with type 2 diabetes, compared with control group; there are 27 relevant literatures about the impact of exercise intervention on the postprandial blood glucose of diabetes. 2124 cases were concerned in the 27 literatures. They consist of exercise -intervention group for 1099 cases, control-group for 1025 cases. The result shows that: the intervention group had more advantages in reducing postprandial blood glucose in patients with type 2 diabetes, compared with control group; there are 25 relevant literatures about the impact of exercise intervention on the glycosylated hemoglobin of diabetes. 1925 cases were concerned in the 25 literatures. They consist of exercise-intervention group for 1025 cases, control-group for 900 cases. The result shows that: the intervention group had more advantages in reducing glycosylated hemoglobin in patients with type 2 diabetes, compared with control group; there are 18 relevant literatures about the impact of exercise intervention on the BMI of diabetes. 1462 cases were concerned in the 18 literatures. They consist of exercise intervention group for 1422 cases, control group for 1275 cases. The result shows that: the intervention group had more advantages in reducing BMI in patients with type-2 diabetes, compared with control group.

2. OVERALL STRUCTURE OF INTELLIGENT GLUCOMETER

2. 1 Hardware Structure

The hardware of the intelligent glucometer is divided into the following sections, which are power-supply module, control module, the pedometer module, glucometer module, GSM module and displaying module. Wherein the power-supply module provides different power supply voltage for the system; Control module is used for coordinating and initializing other modules; Pedometer module and glucomerer module are used for detecting exercise situation and blood glucose. GSM module is used to achieve exercise intervention function; Displaying module is used for displaying related information when system running. Overall system hardware block diagram is shown in Figure 1:

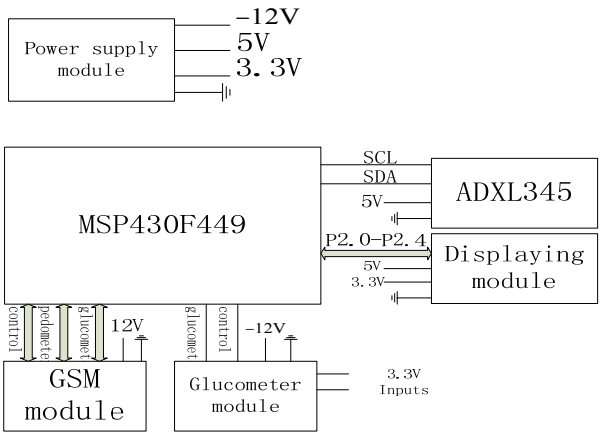

Fig. 1 The overall system hardware block diagram

First, the power supply module uses 12V battery as the power source. It achieves conversion between different voltage levels including 12V, -12V, 5V, 3.3V and so on through 7805 and 1085. Power supply module schematic is shown in Figure 2:

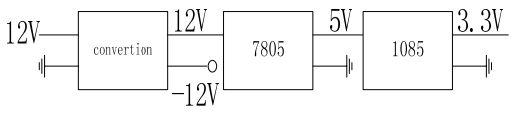

Fig. 2 Power supply module schematic

Second, as for the control module part, we choose MSP430F449 MCU produced by TI to control the entire system. The main reasons for using this MCU are as followed: first, the low-power mode is

suitable for portable devices:processor power consumption (1.8V ~ 3.6V, 0.1 ~ 400 μA , 250 μA/ MIPS), maximal leakage current through serial line is 50nA, which can greatly reduce power consumption and extend battery replacement cycle. Second, MSP430 transient response characteristics are important to ensure the system's low-power event-driven approach. Finally, this single-chip is small and light, which meet the design requirement for portable glucometer.

Third, in the designing of the pedometer module, we use an acceleration sensor named ADXL345 to count steps. The sensor is a small, thin, ultra-low-power, 3-axis accelerometer with high precision. The digital outputting is 16-bit twos complement. It can be accessed through the SPI or I^2C. ADXL345 is well suited for mobile devices. It could detect gravity and dynamic acceleration. It can measure angle variation less than 1.0°. Its functional block diagram is shown in Figure 3:

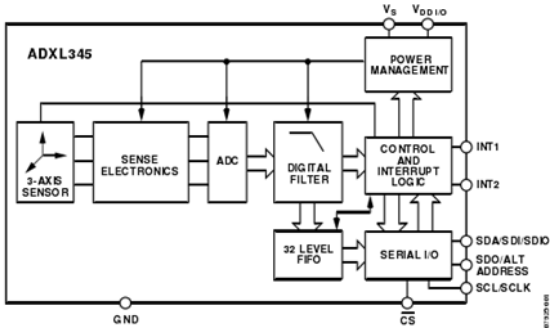

Fig. 3 ADXL345 functional block diagram

Fourth, in the glucometer module, the weak signal processing circuit is made up of amplifier and filter. The glucose detection circuit is shown in Figure 4. The input voltage is 3.3V. The voltage enters the voltage follower then divided to 0.2V. the second stage is an amplifier and filter. The current is converted to the voltage through the resistor. Since the current won't flow between the terminal and the inverting terminal phase. The voltage collected from A/D converter is produced by the current from the electrode. It will ensure the accuracy of the system [6].

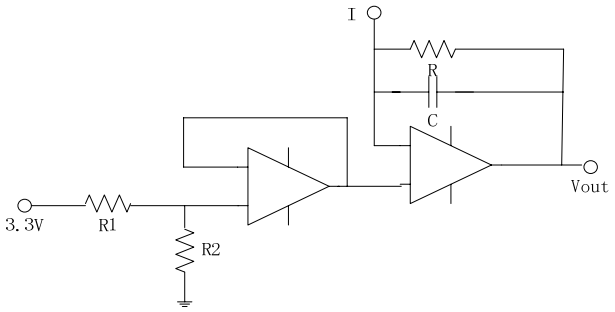

Fig. 4 The glucose detection circuit

Fifth, the short message function is achieved through the GSM module. It is an industrial grade module supporting Chinese short message. It works at the dual band of EGSM900 and GSM1800. The power is in the range of DC 3.3 ~ 4.8V. The current is 3.5mA in dormancy, 25mA in idle, 300mA in emission. It can transmit the signal in the form of voice and data. The power consumption is 2W in EGSM900 and 1W in GSM1800. The SIM card reader is connected via the interface connector and the antenna connector via the antenna. The GSM module data interface (CMOS level) can transmit bi-directional instructions and data via AT commands. Selectable baud rate is in the range of 300 b/s~ 115 kb/s and automatic baud rate with 1.2 kb/s ~ 115kb/s. It can send short message in the form of text and PDU. In addition, it can restart and achieve recovery through AT commands or shutdown signal.

Sixth, we use NOKIA5110 as the display screen. The LCD screen that can display Chinese, English, numbers is designed for mobile devices. And it has the feature of low power consumption that meets the design requirements of portable blood glucose meter.

2. 2 The architecture of software

2. 2. 1 Overall algorithm process of system

Considering the complexity of the algorithm and the using-order of each module, we regard the pedometer algorithm as the main program. The program first runs pedometer algorithm. When it reaches a specified number of steps, it will call GSM module to send the data to the expert's phone. If the switch is on, it will carry out blood glucose detection and send it as the above. It will go into a waiting status until receiving exercise intervention plan message. This message will trigger interrupt to display the content. The chart of algorithm flow is shown in Figure 5:

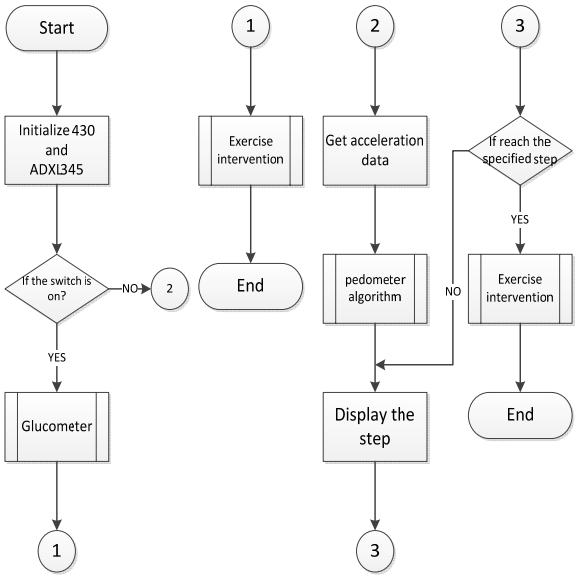

Fig. 5 System algorithm flow chart

2. 2. 2 The design and implementation of the algorithm pedometer:

The research on human gait :

In the feature that can be used to analyze running or walking, we choose acceleration as the relevant parameters. The movement can be decomposed into three components including forward, vertical and lateral direction as shown in Figure 6. ADXL345 accelerometer will detect acceleration from x, y, and z-axis. Pedometer is in an unknown direction, the measuring accuracy won't depend heavily on the direction relationship between the axis of movement and the measuring axis [7]. Foot, leg, waist, arms are in motion when walking, they will produce an acceleration with a peak at a certain point. To detect from the acceleration of the foot steps is the most accurate. But considering the convenience, we choose to use the waist motion. Figure 6 shows the acceleration direction from Pacers. In any case, there is a usable acceleration direction at least. So you can count steps based on this principle.

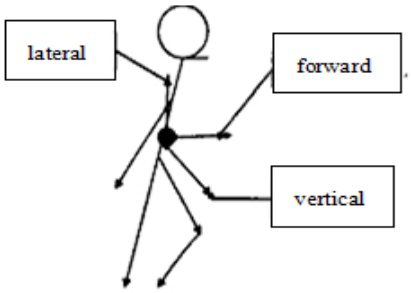

Fig. 6 Three-axis when walking [7]

The parameters of pedometer:

Digital filter: First, we require a digital filter to smooth signal waveform. Four registers and a summing unit can be used as shown in Figure 7. Of course, you can use more registers to enable smoother acceleration data, but the response time will be slower.

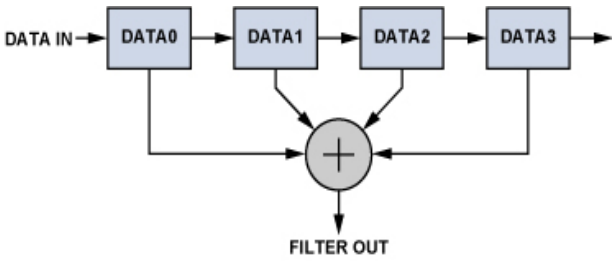

Fig. 7 Digital filters

Dynamic threshold and dynamic accuracy System continuously updates the maximum and minimum acceleration axis every 50 times and the (Max + Min)/2 is defined as dynamic threshold. This threshold value is to determine whether an invalid step has taken. It is dynamic because it refreshes every 50 times. This choice is adaptive and fast enough. In addition to the dynamic threshold, it also uses dynamic accuracy for further filtering.

Taking a step is defined that when the acceleration curve goes below the dynamic threshold, the value is negative.

The peak detection is that Pedometer selects an axis with the biggest accelerometer from the x, y, and z-axis to calculate the number of steps. If the acceleration is too small, pedometer will be ignored.

Pedometer with the help of this algorithm can work well with the help of this algorithm, but sometimes it seems too sensitive.

When the vibration is similar to walking, pedometer will regard it as the pace. The use of "time window" and "counting rules" can solve this problem. "Time window" is to exclude the invalid vibration. Assuming that the fastest walking speed is 5 steps per second and 1 step every 2 seconds is regarded as the slowest. Thus, the "time window"is between 0. 2s and 2. 0s. This algorithm data rate is 50Hz. The times of data updates between two steps is recorded in a register. If the interval is between 10 and 100, it proves thar the two steps are in the valid window. Otherwise, this is an invalid step. The counting rule is to determine whether the pace is a part of the same rhythm pattern. Pedometer has two operating states including search rules and validation rules. It is started with search

rules. After four consecutive valid paces, if it exists a certain rule, it will go into the second work. In this mode, the pedometer will increase one after an efficient pace. But, it will go back to the first work when it detects an invalid pace.

2. 2. 3 The principle of the glucometer

Using glucose oxidase sensor and a circuit for weak signal amplifying and filtering, we can get the relational between the voltage and the blood glucose concentration. With the aid of the cf tool in MATLAB, we can achieve quadratic curve fitting. We got a fitting formula for the two data. The SCM converts the A/D value to the blood glucose concentration through this formula and displays it.

3. THE EXPERIMENT RESULT

3. 1 the experiment result of pedometer

The experiment result of pedometer module is shown in table 1

Table 1

The experiment result of pedometer module

	Actual steps	Measuring steps	Error	Error rate
1	10	14	4	40%
2	50	58	8	16%
3	100	110	10	10%
4	200	213	13	6.5%
5	300	530	30	6%

3.2 The experiment result of glucometer

3. 2. 1 Testing data

The experiment result of glucometer is shown in table 2.

Table 2

The experiment result of glucometer module

time / mmol/L	2s	4s	6s	8s	10s	12s	14s	16s	18s	20s	22s	24s	26s	28s	30s	32s	34s	Sum	ave.
23. 7	112	116	110	103	97	92	88	85	83	81	79	77	75	74	73	72	71	1498	88 1
22. 3	98	96	95	92	90	88	86	84	82	81	79	77	75	74	73	71	70	1411	83
16. 6	96	96	90	85	80	76	74	72	70	68	66	64	63	62	61	60	60	1243	73.1
12. 8	85	82	78	75	71	68	66	64	63	62	61	60	60	59	58	58	58	1128	66.4
8. 3	70	69	65	60	57	55	53	51	49	48	47	46	45	44	43	42	42	886	52.1
7. 3	62	59	56	53	50	49	48	46	45	44	44	44	43	43	42	42	42	812	47.8
3. 6	42	39	35	34	32	32	31	30	29	28	28	28	27	27	26	26	26	520	30.6

3. 2. 2 MATLAB curve fitting and expression

Quadratic fit curve is shown in Figure8:

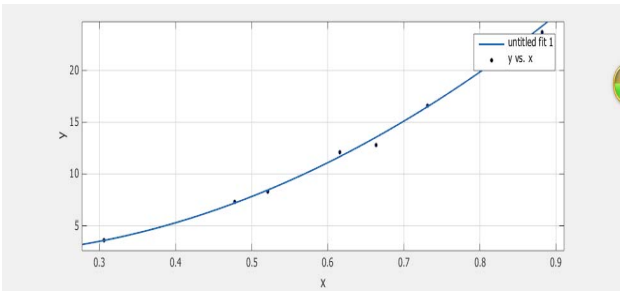

Fig. 8 Quadratic curve fitting

The expressions generated by the MATLAB toolbox cf tool is shown in Figure 9:

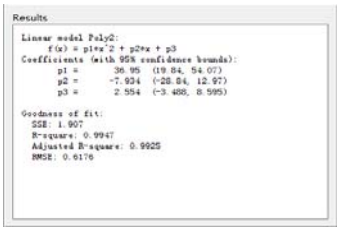

Fig. 9 Curve fitting function expression

Curve fitting expression:

$F(x) = p_1*x^2+p_2x+p_3$

p_1=36. 95; p_2=-7. 934; p_3=2. 554

3. 3 The experiment result of the exercise intervention

GSM module experiment is divided into three parts, including sending blood glucose data and

pedometer data, receiving exercise intervention plan message from the expert. Firstly, the module can send a SMS on the blood glucose data to the expert's phone when the test is completed. Secondly, it also can send pedometer data as planned. When completed, it will go into a waiting status until receiving exercise intervention plan message. Then, it will display the content of the message.

4. CONCLUSION

In this design ，the intelligent blood glucose meter with exercise intervention function can carry out a accurate detection of movement under less than 10% error. And, it can test blood glucose concentration under less than 15% error. Meanwhile, it can send this two data to the expert's phone in the form of text messages through GSM module. Then, it can receive exercise intervention plan message from the expert in order to achieve exercise intervene.

References

[1]. Lu DJ, Kexin He, The development and application of sports health management system[J], The Chinese health management, 2008，1:84-86

[2]. Lu DJ, Yoshino H, Ryo T. The effect of exercise prescription by applying walking intervention using pedometer for the non insulin dependent diabetes mellitus patients among elderly in Shanghai, China [J]. Japan Journal of Lifelong Sport, 2007, 5 (1) :35-43

[3]. Lu DJ, Therapeutic Effectiveness of Three Exercises Intervention for Type 2 Diabetes. Medical research, 2012, 41（10）：51-56

[4]. JIA Ke-bao, WANG Li. Influence of different walking exercise intensity on postprandial blood glucose among type 2 diabetes patients [J]. Chinese Journal of Health Education， May 2013, 29（5）：450-452

[5]. Sha Luo, Shan Luo, Aixia Ma, Meta analysis on effect of exercise intervention on type 2 diabetes mellitus patients' blood glucose controlling[J]. China Journal of Pharmaceutical Economics. 2011，1：32-42

[6]. Meiling Yang, Research and Development of a Portable Wireless Glucose Step Count Instrument [D]. 2013，6

[7]. SONG Hao-ran, LIAO Wen-shuai, ZHAO Yi-ming, Using 3-Axis Accelerometer ADXL330 to High Accuracy Pedometer [J], Chinese Journal of Sensors and Actuators. 2006, 19（4）：1005-1008

Design and Implementation of Auto-control Seesaw System based on the Intelligent Electric Car

WAN Yunxia[1,2] ZHANG Xiaoyu[1] ZHANG Hongfei[1] HU Haiyang[1]

(1.College of Instrumentation and Electrical Engineering, Jilin University, Changchun 130026,China;
2. Key Laboratory for Geophysical Instrumentation of Ministry of Education, Jilin University, Changchun 130026, China)

***Abstract*—Aiming at the ships and moon exploring vehicle is difficult to balance in particular environment, we design a set of electric vehicles on the seesaw automatically and put forward a method based on automatic controlling theory, and through the way of theory and experiment verified the feasibility of it. Automatic controlling system of the intelligent electric car on the seesaw is based on 51 microcomputer, use the intelligent vehicles as the motion carrier ,assisted the sensor of acceleration HC-SR04 diastimeter to reaction the state of motion and the slant motion on the seesaw ,adjust the state of motion between the two cars on the seesaw to achieve the goal of balance. The simulation result and experiment indicated that the system can keep balance automatically in a preset time.**

***Key words*—Automatic control Intelligent car Angular transducer Ultrasonic sensor**

Ⅰ INTRODUCTION

NOWADAYS with the growing importance of the production and life, a lot of large equipment devices are required to keep balance at work. For example, the weight of the plane and air can't make the plane keep balance ,if couldn't ,the speed of the plane can be changed and turn around the center of gravity, it's not conductive to flight safety. The intelligent electric seesaw in the car as a carrier, using automatic control technology, with the combination of tracking, distance measurement, display and control module. According to the collected information of the seesaw angle to control the running status and make the system to be balanced. The system provides a feasible scheme to solve the problem of maintain and adjust the balance.

Ⅱ INTEGRATED DESIGN

The intelligent electric vehicle [2-3] seesaw automatic control system is based on the theory of automatic control technology and through the following hardware module to realize, such as: the power module, the driver module of electric motor, the tracking module, the display module ,the angle measurement module, the ultrasonic ranging module and the voice module. Figure 1 is the principle diagram of the system as a whole.

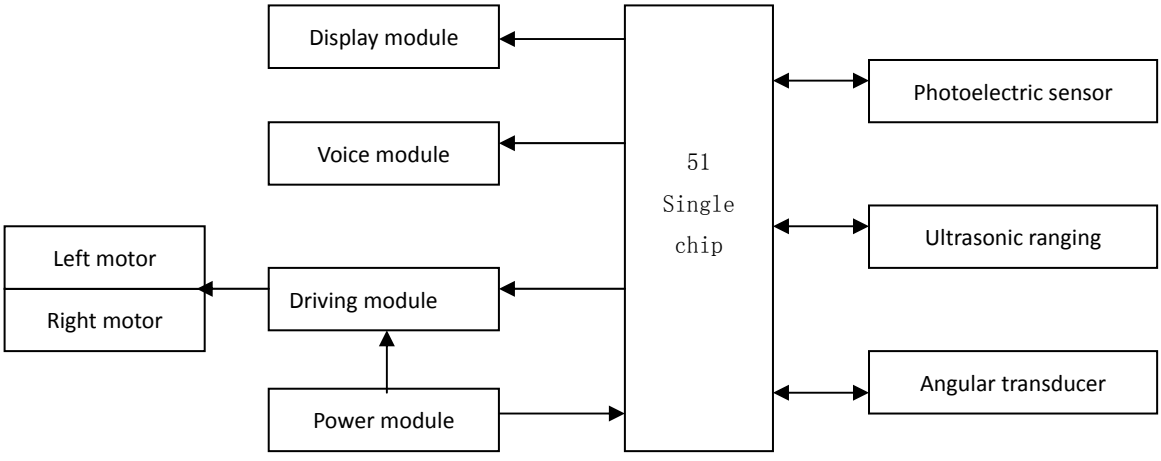

Figure 1 The whole hardware architecture diagram

The core of the balance to be sought by the intelligent electric seesaw automatic control system is

the angle measurement module, it brought the collected signal transmission to the microcontroller, the SCM according to the signal of the car's running status to distinguish the car's motion up to the system to be balanced. The tracking module ensured the car can travel along a straight line when the balance and at the same time, ranging module to ensure the car won't collide. The principle diagram of figure 2 for the system balance.

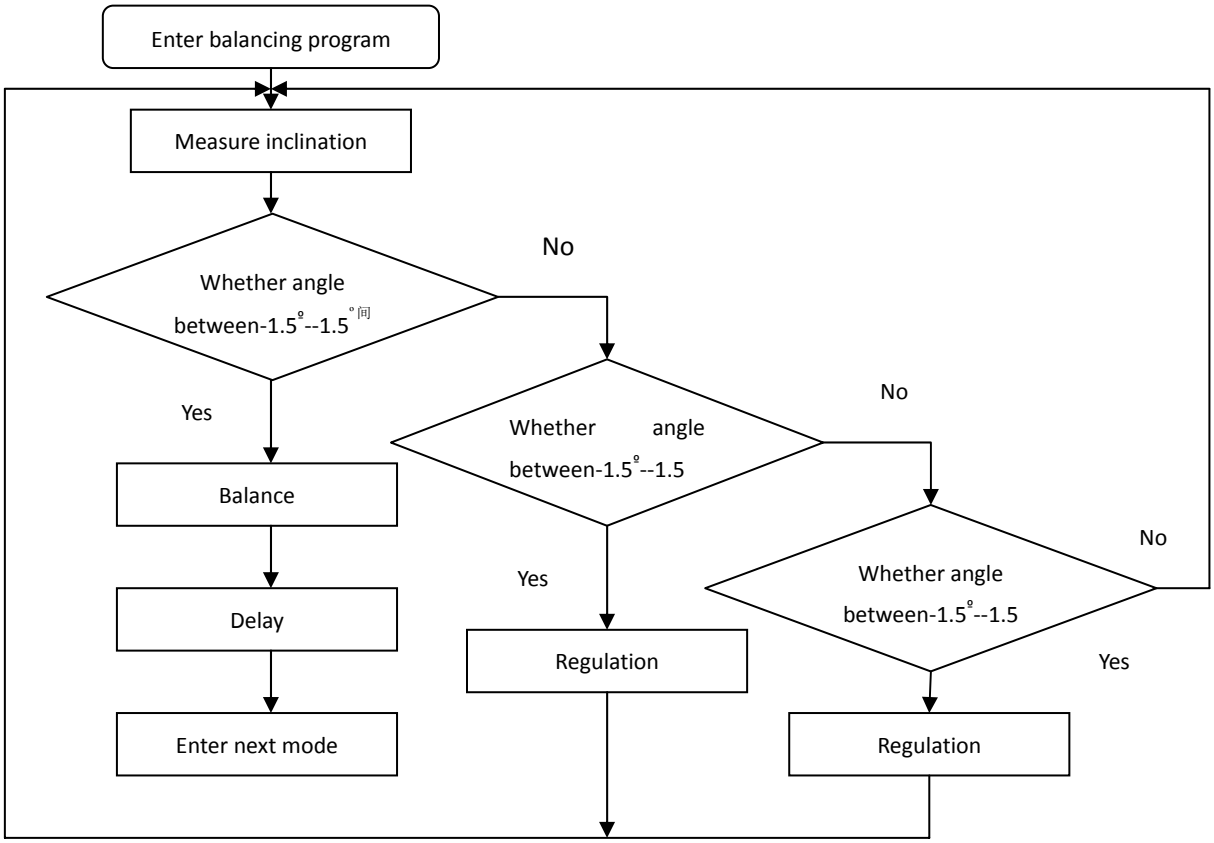

Figure 2 Schematic diagram to seek a balance

III MODULE DESIGN

A Motor drive module design

Driving part is the most basic part of intelligent electric seesaw automatic control system, this part adopts L298N. FIG. 3 for L298N drive circuit.

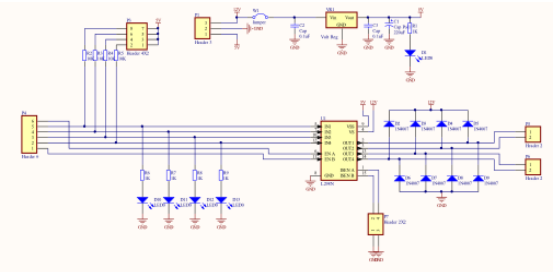

Figure 3 L298N driver circuit

Driving mode was shown in table 1

Table 1 Drive mode

	Left front	Right front	Left rear	Right rear
Ahead	1	1	0	0
Back	0	0	1	1
Stop	0	0	0	0
Turn left ahead	0	1	0	0
Turn right ahead	1	0	0	0
Turn left behind	0	0	0	1
Turn right behind	0	0	1	0

In figure 1，The first column represents the way of car movement, in the first line, 'left' showed the electrical machine let the left wheel of the car to go ahead. "right front", "left rear", "right rear" showed the direction of the wheel. "1"showed the motor to work in the state, "0"showed the motor shall not be electric. In the case of the car ahead: when the motor drives the car to the left or right ahead, the car would have been along a straight line.

B Tracking part design

The part of the tracking was realized by the photoelectric geminate transistors[4-6], the schematic diagram was shown in figure 4.

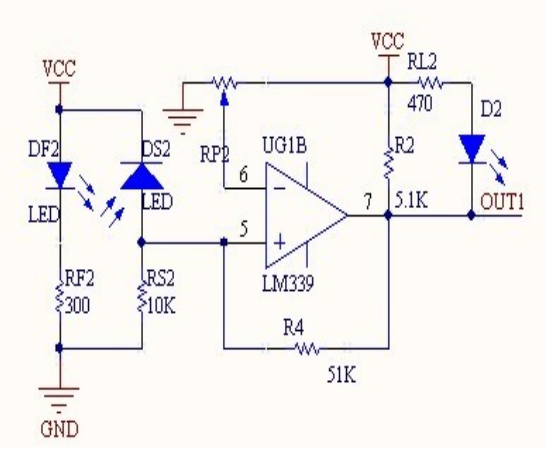

Figure 4 Photoelectric tube schematic diagram

DF2 is infrared (light blue), DS2 is photo diode(black). Its working principle was shown in figure 4, the figure 5 is for tracking.

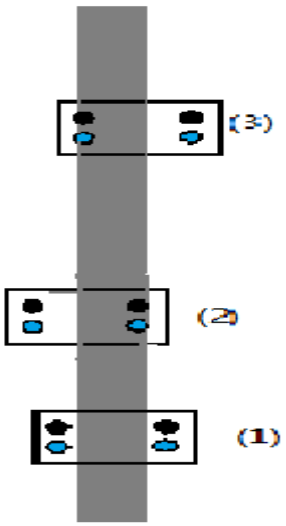

Figure 5 Tracking map (note: 1 go straight and turn right, 2, 3 left)

The car tracking has three states: Left, right, and not off track。Using the numerical value according to the photoelectric tube and judge the car is in which state, then use the SCM to control the car moves, after a while to collect the car status, then to adjust the car moves, rotated around so and the car can realize tracking function.

In figure 5 the grey line represents the moving trajectory，the black rectangle on behalf of the car，On either side of the circle represents two infrared tube(the black is photo diode, the blue is Infrared emitting). With right into the case, As is shown in figure 5 (2), The car was left off the track, on the right side of the photoelectric tube tests for detecting the black line, put the signal into the microcontroller，the SCM on the basis of the signal control to drive the car on the right and then back to the track. The car tracking flow chart was shown in figure 6.

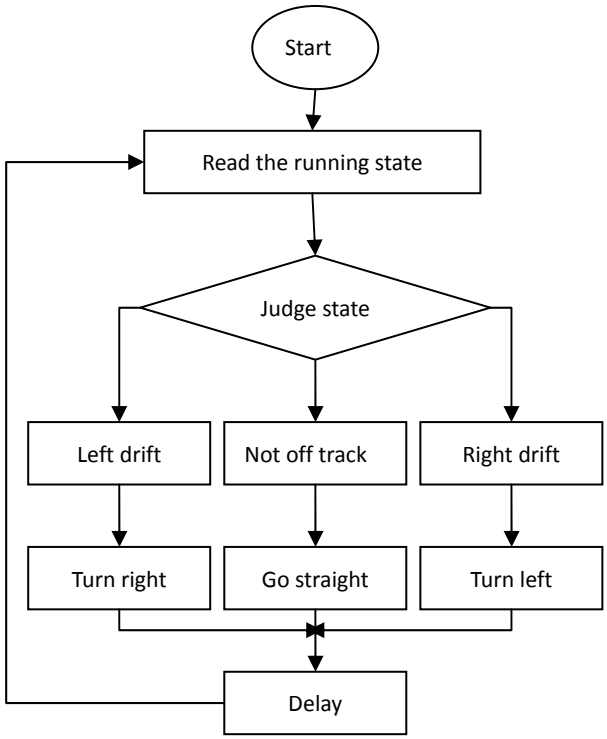

Figure 6 Flow chart of tracking

C Ultrasonic ranging module design

The ranging part use the HC - SR04 ultrasonic rangefinder [7-9],when ranging，start timing first，then decide whether detected the echo signals ,if not, timing rest, if tested it, read this time, then change with time multiplied by the speed of sound is the distance from a small workshop .Ultrasonic ranging

principle diagram was shown in figure 7.

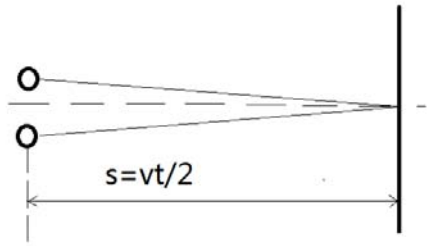

Figure 7 Ultrasonic ranging principle diagram

Ultrasonic flow chart was shown in figure 8.

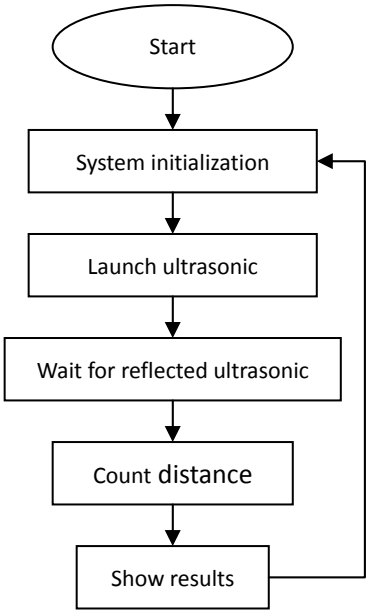

Figure 8 The flow chart of distance

D Angle measurement module design

Using ADXL345 acceleration sensor [10-11] can measure the acceleration value, angle values can be obtained by calculation. The sensor can measure 3 axis acceleration, its measuring range is – 16 g – 16 g, the measurement precision is 0.25. Angle sensor measured data into the microcontroller, after decided, corresponding action according to the results and get balance.

Calculated by the acceleration value, the value of the formula is as follows:

$$\begin{cases} \varphi = \arctan \dfrac{\sqrt{A_X{}^2 + A_Y{}^2}}{A_Y} \\ \sqrt{A_X{}^2 + A_Y{}^2 + A_Z{}^2} = 1G \end{cases}$$

AX, AY, AZ respectively the X, Y, Z axis acceleration.

E Voice and display module design

The voice module mainly adopts ISD1400 or ISD1420. After the car balanced, the voice module issued a “balance” prompt.

Figure 9 is the voice module circuit diagram.

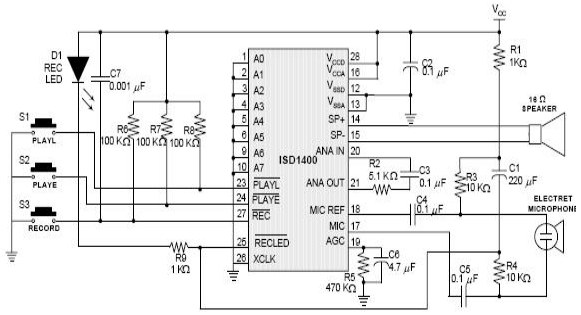

Figure 9 Voice module circuit diagram

The display section we prefer to use LCD12864.First decide whether 12864 is busy ,if yes, wait until 12864 was not busy; if not, we can read the data(acceleration sensor, ultrasonic rangefinder)from sensors, then use the transformation formula of corresponding to the data and show that in 12864.

Ⅳ SYSTEM TESTING AND ANALYSIS

The experimental determined that the system can be balanced by adjusting the movement of two cars on the seesaw in a short time. The following is the test result of each module. Power supply module, motor drive module and tracking module can work normally. Three coordinate travel can make the car along a certain path and conform to the design requirements. Display module can display Chinese characters such as "Angle", "distance", and revealed properly. Voice module can send prompt after the balance. Ultrasonic ranging module, distance and the actual value can be measured according to the experiment with 3 mm error, The reasons are as follows: ultrasonic transmission and reception all need certain time, the ultrasonic sensor has blind area [12], we have to improved. The angle sensor module can measure the seesaw angle more accurately, but the measurement speed is slow, we proposed to adopt the method of software to improve angle measuring sensitivity [13].

Ⅴ CONCLUSION

In view of the system need to keep balance, this paper proposes a balance method based on 51 single chip microcomputer. This method can to seek a balance system more quickly, which can be widely used in the equilibrium system, for similar systems, we just need to improve the corresponding parameters and use the suitable hardware to be balanced. Next step we will improve the balance of speed and accuracy of balance by efforts.

Reference documents

[1] Zhangguan Yu, Automatic control technology and application. Harbin Institute of Technology,2007（02）.

[2] Zhengping Xu, Wenqi Ge, Xiaokun Wang, Youyi Li, Yongsen Xu,Jun Li. Huangpu has LCD display and voice prompt function of intelligent electric vehicle design [J]. LCD to display.2010(04).

[3] Yonggang Chen, Simple intelligent electric design of ultrasonic automatic obstacle avoidance system [J].Gansuscience and technology aspect.2005(02).

[4] Jianping Wu, Zhanguo Yin, Sirong Cao, Kunyuan Li. Infrared reflection type sensor in the application of the autonomous tracing the car navigation[J]. China Measurement Technology .2004(06).

[5] Yafeng Zhu, Shugang Li. Smart car design based on the infrared laser tube [J]. information technology.2010(06).

[6] Liang Jing. A path recognition based on photoelectric sensor intelligent car [J]. Science, technology and engineering.2011(01)

[7] Guo Rong,Liao Na,Guo Li. The ultrasonic ranging system based on STC89C51 microcontroller design and implementation[J]. Petroleum instruments. 2010(05).

[8] Dongyan Yang. Ultrasonic ranging system for mobile robot obstacle avoidance [J]. Inner Mongolia science and technology of economy.2008(16).

[9] Liying Guo. The design of ultrasonic distance measurement circuit based on MCU [J]. Automation technology and application.2010(06).

[10] Yufa Tang, Zhang He, Jianjing Liu. Based on the composite magnetic resistance sensor and accelerometer attitude Angle detection technology[J].Transducer and Microsyste Technologies. 2013(01).

[11] Yufa Tang, Zhang He, Guotai Xu, Jianjing Liu. Based on the weighted moving average to examine the measuring technique [J]. Chinese Journal of Scientific Instrument.2012(08).

[12] Liru Han. Improving precision of ultrasonic distance measurement method were reviewed [J]. Telecommunication Engineering.2010(09).

[13] Zhuquan Bai, Xiaoming Zhang, Liu Jun, Wang Yu, Zhao Lu. The digital inclinometer based on accelerometer error modeling and analysis [J]. Chinese Journal of Structural Chemistry.2013(08).

A TSC Localized Reactive Power Compensator for Asynchronous Motor

Wang Shilong[1], Shen Feng[2], Guan Qiao[2], Cui Hailong[2]

(1.Laboratory of the Earth Information Detection Instrument, Jilin University, Changchun 130026, China 2. College of Instrument and Electrical Engineering, Jilin University, Changchun 130026, China)

***Abstract*—In this project, we try to design and realize the method of localized reactive power compensation by the experiment and analysis of the no-loading power factor characteristics of the asynchronous squirrel cage motors in the laboratory of College of Instrument and Electrical Engineering in Jilin University. The TSC localized reactive power compensator for asynchronous motor is based on STC89C51 microcomputer as its core control chip; use LM393 and CD4013 chips forming a power factor acquisition module; and choose the compensation capacitor by the switch module consists of thyristors and diodes with inverse-parallel connection, in order to improve the power factor. The results of computing and analysing indicated that this compensator can improve the power factor of the asynchronous motor in no-loading situation.**

***Key words*—Asynchronous motor Reactive power Localized compensation**

I. INTRODUCTION

THE three-phase asynchronous motor is the major prime mover in electrical machinery, which takes away 60% of the total electricity of the whole country, can cause huge burden by its runtime reactive power for electrical grid. The technical parameters of the three-phase asynchronous motor used in the laboratory of Jilin University includes rated voltage of 220V DC, rated current of 0.6A, rated power of 120W, rated rotated speed of 1380n/min, 50Hz working frequency, and power factor between 0.75 and 0.8 when it is running smoothly and regularly. When several motors run at the same time, great loss will be caused. The asynchronous motor runs with inductive load, by using parallel capacitors as localized compensation, the power factor can be improved greatly. This project regards the localized compensation as the study object, aims at providing a scheme of the localized compensation for the motors in the laboratory.

II. OVERALL DESIGN

The TSC localized reactive power compensator takes the compensating capacitor as its major functional unit, the thyristor as its hurl-slices switch and the STC89C51 as its kernel control chip. The compensator is consisted of following modules: the real-time collection module for the currents and voltages, the managing module for the power factor, the controlling module and the switching module. The schematic diagram of the overall system is shown in figure 1.

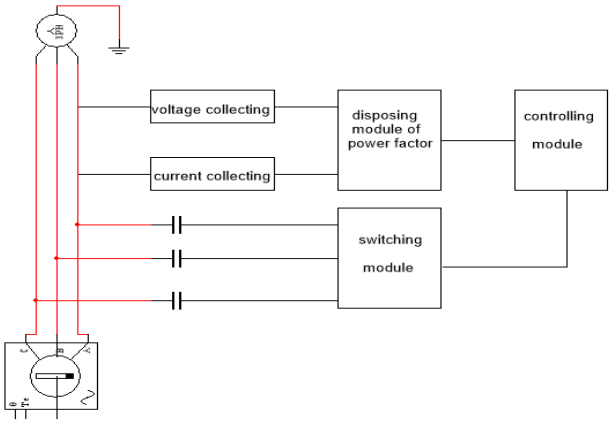

Figure 1 The diagram of the overall design

III. MODULE DESIGN

A. Real-Time Collection Module For The Currents And Voltages

The real-time collection module for the currents and voltages is the basic of the power factor calculating. It collects the phase voltage and phase current for phase A of the motors major by voltage transformers of ZDPT-101 series and HWCT (5A/5mA) micro precise current transformers.

The circuit of voltage collection is shown in figure 2,

the proportion of voltage collection $K = R1:\ R2 = 20k\Omega/2k\Omega$.

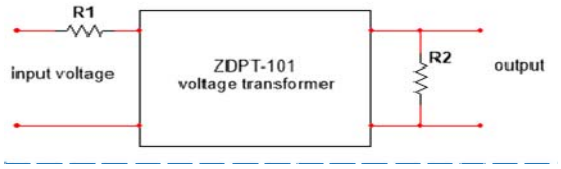

Figure 2 The circuit of voltage collecting

The circuit of current collection is shown in figure 3, the proportion of current collection is 1000/1, and the voltage of the output current signal is $U_2 = i_2 R = \frac{1}{1000} i_1 R$, in which $R = 1k\Omega$.

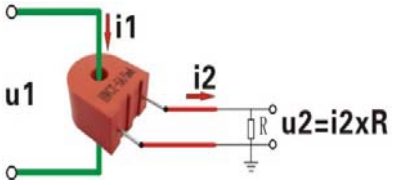

Figure 3 The circuit of current collecting

B. The Disposing Module For The Power Factor

The disposing module for the power factor is the most important module in power factor calculating, which consists of the zero voltage circuit and zero current circuit. Then output a 50Hz square wave with duty ratio n after comparing and disposing the zero voltage and the zero current. The power angle of it is $\varphi = 2\pi n$. The zero voltage circuit is shown in figure 4, the zero current circuit is shown in figure 5, the managing module for the power factor overall circuit is shown in figure 6.

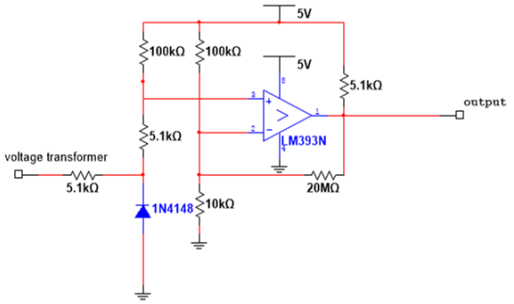

Figure 4 The zero voltage circuit

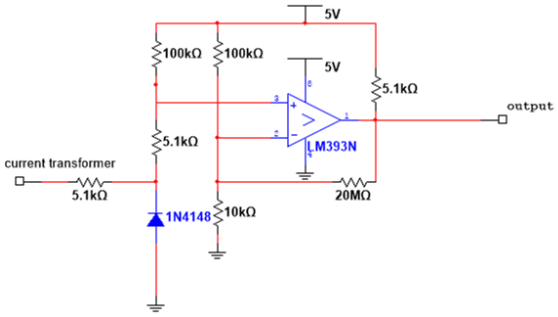

Figure 5 The zero current circuit

The core chip of the zero passage circuit is LM393, the waveform of output voltage and current after zero passage will be compared and disposed by chip CD4013, then the pulse waveform of its corresponding power factor can be received.

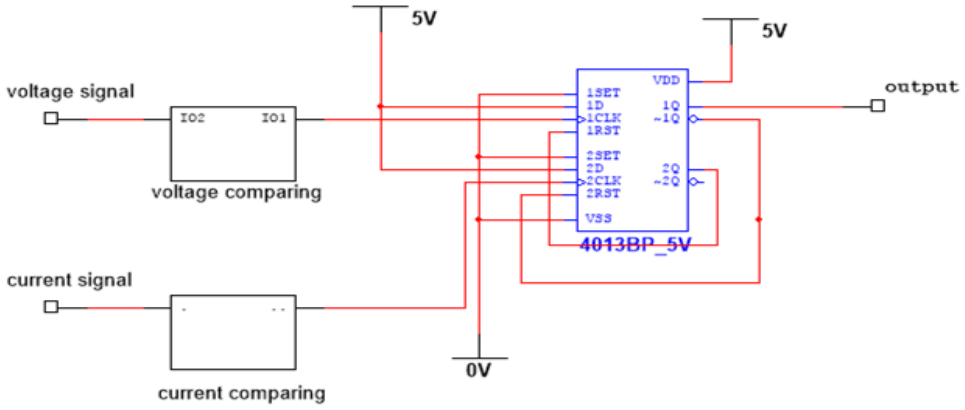

Figure 6 The managing module for the power factor overall circuit

C. The Controlling Module

The controlling module is based on the microcomputer STC89C51, and form a micro system with the microcomputer to collect the pulse signal output by the disposing module for the power factor and calculate the power factor and the present reactive power that need to be compensate, then output 3 pulses and choose the thyristors which need to be switched and correct the switching time in order to get rid of the current impact caused by inappropriate switching time. The flowchart of the controlling module is shown in figure 7.

The microcomputer will calculate the power factor after it has collected the signals, and then output the first pulse to choose compensation capacitor of phase A, $\frac{\pi}{3}$ period later, output the second pulse to choose compensation capacitor of phase B, one more $\frac{\pi}{3}$ period later, output the third pulse to choose compensation capacitor of phase C. When finishing the 20 cycles of compensation, the microcomputer will scan the input signal again, the switching processing will be restart when the collection of power factor is finished, and work repeatedly. Ensure that the compensating capacitance is appropriate with different power factors in order to get rid of the loss caused by overcompensation.

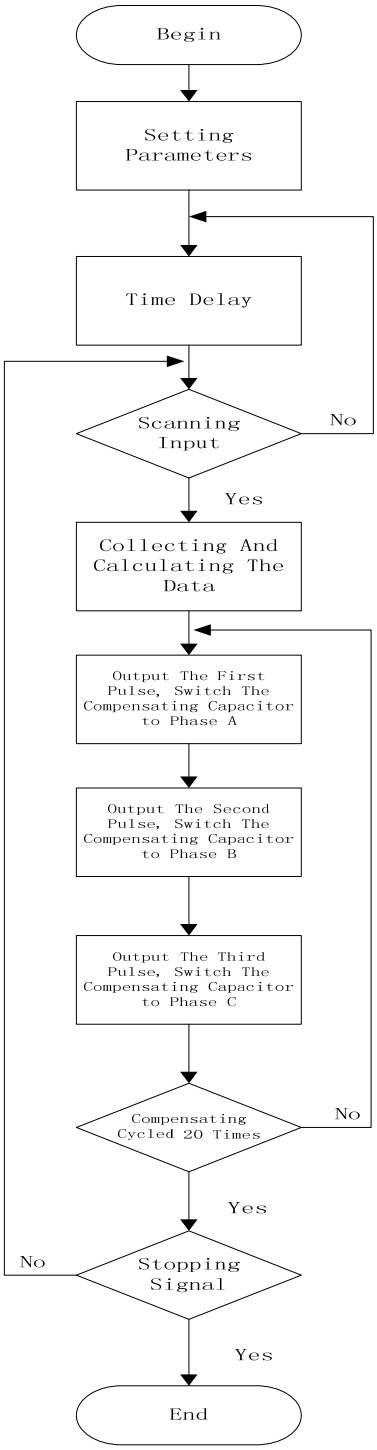

Figure 7 The flowchart of the controlling module

D. The Switching Module

The switching module is mainly consisted of: switching thyristors and reflow diodes in inverse-parallel, compensating capacitors, buffer inductors and over-current protection resistors, etc. The circuit diagram is shown in figure 8.

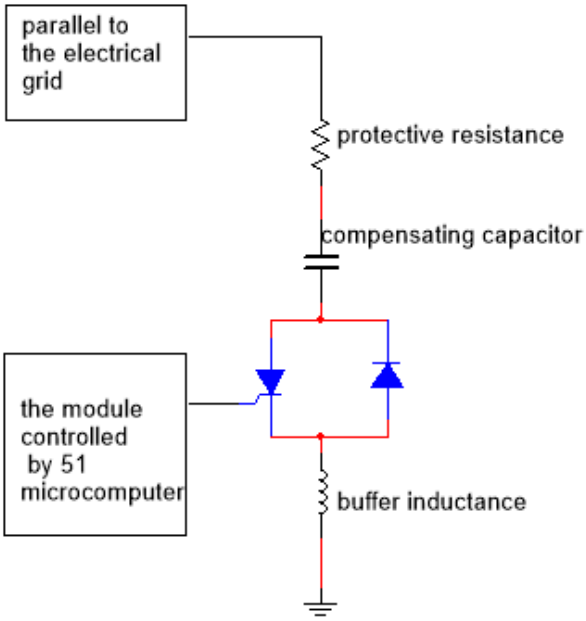

Figure 8 The circuit of the switching mode

The switching mode of switching thyristors and reflow diodes in inverse-parallel in the switching module simplified the structure of the circuit and reduced the burden of the controlling system. In order to absorb the impulse current appropriately but not influence the compensation when switching, the buffer inductance should be 5% of the compensating capacitance.

IV. The Calculation Of The Compensating Capacitance

The calculation formula of compensating capacitance includes the method of no-load current, target power factor and experience. In this project, it is calculated by the method of target power factor.

The method of target power factor can calculate the compensating capacity and ensure the size of the capacitor.

i. The calculation formula of the compensating capacity:

$$Q_C = P(\sqrt{\frac{1}{\cos\varphi_e^2}-1}-\sqrt{\frac{1}{\cos\varphi^2}-1})K_2$$

Q_C is the compensating capacity needed(kvar);

P is the rated power, P= 0.12KW;

K_2 is a coefficient, $K_2=\frac{U_{N1}^2}{U_{c0}^2}=\frac{0.4^2}{0.22^2}=4.18$;

$\cos\varphi_e$ is the rated power factor, $\cos\varphi_e=0.8$;

φ is the power factor angle expected after compensating, $\cos\varphi=0.95$;

U_{c1} is the rated voltage of the capacitor 0.45kV;

U_{c0} is the real voltage of the capacitor 0.22kV;

It can be calculated that $Q_C=0.228$Kvar.

ii. The formula of the size of the capacitor and the compensating capacity:

$$Q_c=0.314CU_{c0}^2$$

C is the size of the capacitor (μF);

It can be calculated that $C=15\mu F$.

As a result, the macro capacity of compensating capacitor is $15\mu F$.

V. Device Testing And Analyzing

The starting process of the laboratory motors is different from the motors in factories, the process of the laboratory motors is to start the motor smoothly by increasing the voltage of the asynchronous motor progressively. When it runs without load, the motor won't start under the circumstance that the voltage is less than 50V. Meanwhile, the power factor is also low, about 0.5-0.85 (errors could be made in experiments by choosing different motors), and the current of the rotor is also high. Then, the motor starts when the voltage is higher than 50V. During

the process to the rated speed, the current decreases, and the power factor falls smoothly then stabilized at about 0.7.

After the compensating device connected to the circuit, when the motor voltage is less than 50V, the power factor is not so well as 0.95 we required, because the voltage of the capacitor is low, the compensation effect is also far too low to reach the target. With the voltage increasing, the compensation effect becomes better and the power factor comes to more than 0.95and could be overcompensated a bit.

VI. CONCLUSION

Aiming at the phenomenon of producing reactive power when experimenting, this project puts forward a method of localized compensating by switching paralleled compensating capacitor. With this method, basing on different compensation capacity, the thysistor can be switched intelligently to choose different compensating capacitors, provide reactive power to motors effectively and decrease the load of the electrical grid. Also, this device can be used in inductive load which is similar to asynchronous motors. The next target is to study farther about improving the precision and effect of the compensation.

References

[1] Li Yuan. Research on Control Method of Static Var Generator [D]. Beijing: Beijing Jiaotong University, 2008.

[2] Lv Chongwei. The Usage of Controllable Transducer in Reactive Compensating of The Pumping Unit [D]. Beijing: Beijing Jiaotong University, 2006.

[3] Cheng Hanxiang, Liu Jian, Yin Xianggen, etc. Research of Single Bridge SVG Control System for Reactive Power Compensation [J]. Electric Power Automation Equipment, 2004,24(2):5-8.

[4] Niu Yinan, Feng Ting, Wang Yang, Li Chengbo. Review on The Reactive Power Compensation of Power System [J]. Information & Communications, 2011.1:48-51.

[5] Zhang Qian, Liu Yingyi, Jiao Zhixing. An Investigation on Local Compensatory Technology of Reactive Power of An Alone Asynchronous Machine [J]. Journal of Nanjing Engineering Institute, 1999.14(1):74-79.

[6] Shang Debin, The Localized Reactive Compensation of The Pumping Unit Motors [J]. Electrification in Rural Area, 2013.10.

An acquisition and preliminary processing system of vibration signal

Sun Feng[1, 2],Xue Yu[1], Gao Zi-Yun[1],Chen Zhang-Ze [1]

(1.College of Instrumentation and Electrical Engineering, Jilin University, Changchun 130061,China;
2. Key Laboratory for Geophysical Instrumentation of Ministry of Education, Jilin University, Changchun 130061, China)

***Abstract*—In the process of geological survey ,the traditional acquisition and analysis system of vibration is too large ,it is hard to move the system and we could not observe or analyse the data online.In this project ,we use a sensor ,a Single-chip Microcomputer and laptops to build a smaller acquisition and analysis system of vibration , we can observe and analyse the data online with it ,thereby solving problems of devices moving and real-time analysing in the process of geological survey.**

I .FOREWORD

GEOLOGICAL survey and its relative domains are related to the development of the energy sources, it's the foundation of the development of the economical society with the features of guiding、fundamentality、comprehensiveness and exploratory etc., in which domains it is used almost refer to every aspect of the construction of the national economy. However, in the actual procedure of geological survey, people utilize artificial ways to generate small-scale controllable artificial earthquake and acquire the underground geological information with a series of acquisition and processing system. The design of an acquisition device of vibration signal is the key issue .The cost of mature technology which is used around the world now is too high, the efficiency of the programming is very low, and its expansibility is not very well. Therefore, we want to design a set of portable and easy-operated acquisition system of earthquake vibration signal which can show the real-time wave form

II.OVERALL DESIGN

In order to acquire the vibration signal of earthquake exactly , we use the accelerometer to detect the vibration signal. The whole system covers the acquisition section, the data transformation and storage section and the after-treatment section, the fig.1 is the overall framework map. As follows

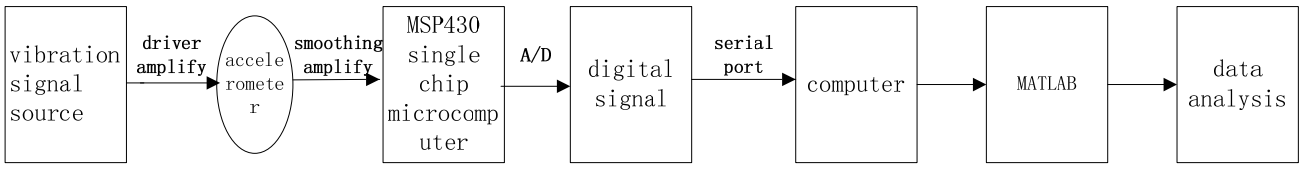

Fig.1 Overall framework map

III. MODULE DESIGN

A.the acquisition section

The accelerometer is single signal output, so it can transfer the signal to the single-chip Microcomputer immediately after passing the processing circuit without differential treatment. The acquisition of the weak vibration signal needs pre-amplifier and low pass filter, because its amplitude and frequency are low. The second-order low-pass active filter is consist of two RC filter link and operational circuit which is synclastic and proportional, we can use it to bring in moderate positive feedback, it can make the magnitude-frequency characteristic and filtering effect better ,and its circuit is easier, so we select it .

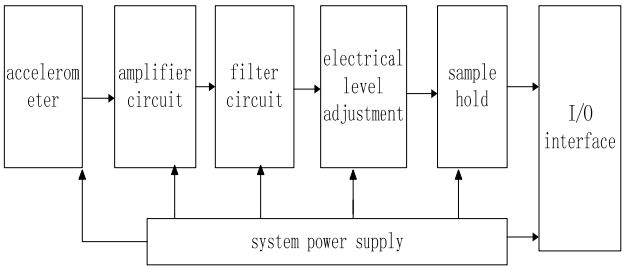

Fig.2 Collection framework map

B. The design of the amplifier circuit is as follows:

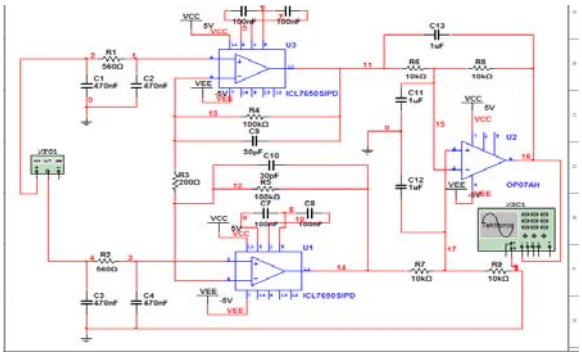

Fig.3 Amplifier circuit

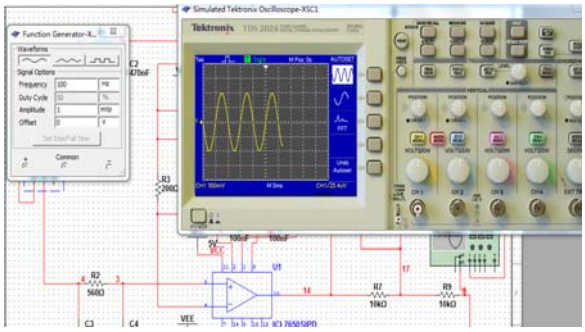

Fig.4 Simulation results

complement：

The design of the filter circuit is as follows:

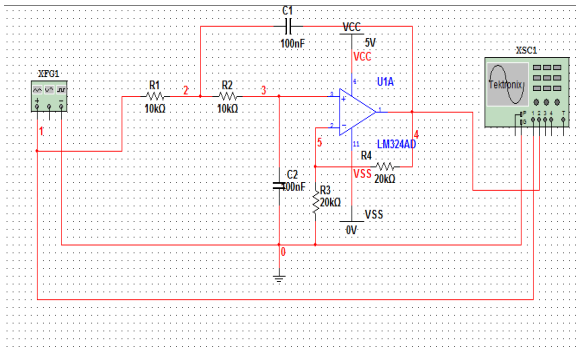

Fig.5 Filter circuit

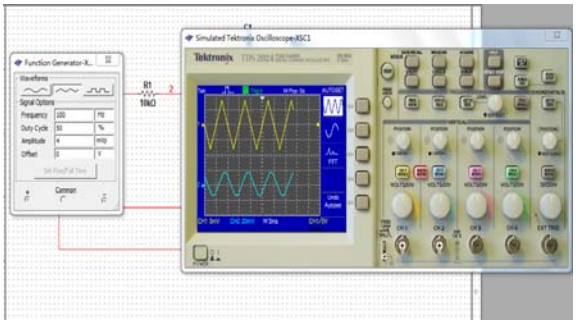

Fig.6 Simulation results

The simulation results show that the designed circuit can achieve the expected effect.

C. the data transformation design

The vibration signal changes fast, so it can be saved in the single-chip Microcomputer only after passing the sampling holder, then we take the A/D conversion, the designed sampling holding rate is 9600B/S. We use only one channel to acquire ,then sampling conversion will be taken and at the same time, digital signal will be transferred to the upper computer .One digital signal is consist of two 8-bit binary numbers, but only the last 12 bit is valid, we use the parity bit “0011”as complement .

Fig.7 A / D Converter block diagram

Upper laptop saves the data in txt format.

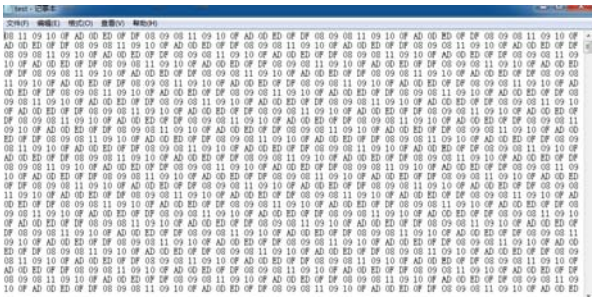

Fig.8 Data storage figure

D. The MATLAB data processing model

The data will be read from the txt file, then we use the Matlab to restore the waveform and analyse the data.

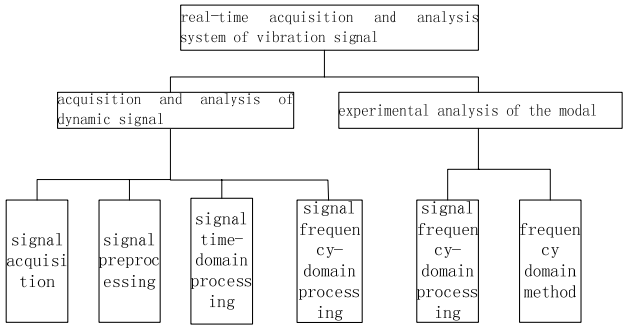

Fig.9 MATLAB data processing framework map

We use the front GUI interface to control. The GUI

interface covers the waveform display、the count 、the restoration、the frequency-domain analysis and the time-domain analysis etc.

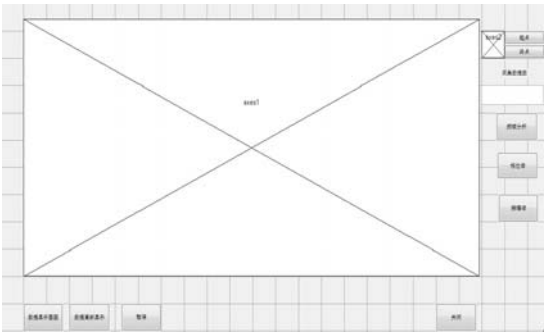

Fig.10 GUI interface

The underlying programming of the GUI interface includes the smoothing ,the delay and the algorithm routine of data restoration.

IV. SYSTEM TEST AND ANALYSIS

All the sections can almost achieve the functions, such as acquiring the real-time data and transforming the analog quantity to digital quantity. The accuracy rate is 99.63%, so it has a little effect on the waveform display. Because the program which we have wrote is a cycle collection program, the data may lose. At the beginning of each cycle, there will be a calibration process to test if the data is as same as the 16-bit binary number when the acquisition started, the calibration number may lose in the real process.

The trial GUI interface

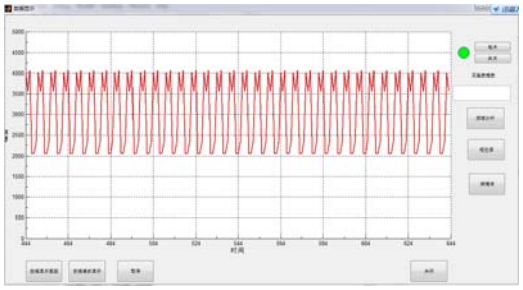

Fig.11 Vibration waveform chart

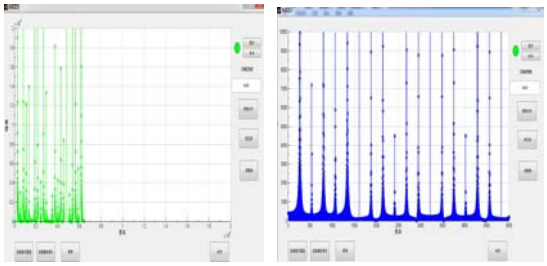

Fig.12 Frequency domain, time domain analysis

We used the system to acquire the vibration of a board which is fixed at one end as a experiment and compared it with the result of the simulation. Here is the simulation figure which we have got:

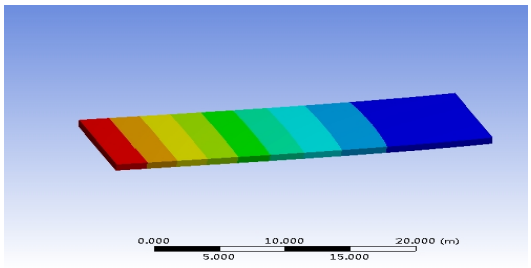

Fig.13 Simulation figure

We measured ten points in turns from the left end to the fixed end of the board .The data is as follows:

Table 1 Simulation and measurement of displacement values

Sequence number	Vertical displacement	
	Simulation value	Measured value
1	130.84	2015
2	112.64	1807
3	94.573	1756
4	76.691	1765
5	59.512	1677
6	43.434	1437
7	28.990	1311
8	16.778	1198
9	7.454	990
10	1.7179	980

The measured value does not represent the real displacement value, the relative value measured by the system shows the vertical vibration of one equilibrium position. So we verified if the measurement task has been completed by comparing the relative vibration between the measured value and simulation. In the simulation section we set up the indicators for the optima without taking the external vibration interference and electromagnetic interference into consideration.

The two sets of data are showed by making curves .It is as follows:

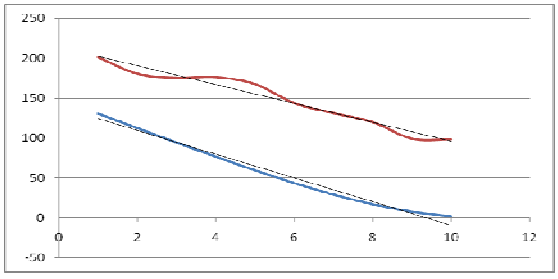

Fig.14 Comparison of measurement and simulation curve

The measured value curve upon the fig.14 and the simulation curve have similar trends in general. It shows that the system can mainly complete the measurement task and the fluctuation in the curve may caused by the external vibration interference.

V. CONCLUSION

Contraposing the vibration signal of the earthquake, we use accelerometer and matlab to acquire、show and analyse the vibration signal. Then we will try to increase the accuracy rate of the data saving and improve the analytical method of the system.

References

[1] Jiang Jitong,Tang Shizhen, A Vibration Signal Acquisition and Analysis System Based on MATLAB[J]. Proceedings of the ninth national academic conference on vibration theory and application in 2007, 2007.10.17-19：9-95—9-99

[2] Yang Jinchao, Zhao Difei, Xu Donglin, the discussion of the function and significance of the geological survey to the development of the national economy[J].Charming China,the second phase, 2011：87

[3] Hu Yelin, Zhang Wenli, Wang Zune, Research on electric measuring and instrument system in geological exploration engineering network[J].Coal science and technology, 2004.2,32(2)：17,18,23

[4] Ding Kang, Xie Ming, Wang Yanchun etc., DAS－1 Dynamic Signal Analysis and Fault Diagnosis System[J]. Journal of Vibration Engineering, 1993.6,6(2)：199—204

[5] He Yuxuan, Chen Run, Zhu Te etc., Earthquake Monitoring System Based on MSP430[J].Electronic Measurement Technology, 2009.7,32(7):78-80

[6] Hong Li, Zhang Yang, Li Shibao, Principle and application example explanation of the MSP430 single chip microcomputer[M].Beijing University of Aeronautics and Astronautics Press, 2010.7

[7] Liu Jun, Yang Junhua, Yang Mengli etc., Vibration Signal Acquisition and Analysis System of Wind Turbine Gearbox Based on Matlab and VC [J]. Guangdong Electric Power, 26(6)，2013.6:70-75

[8] Yuan Yun, Bai Jie, Wang Lin, Zheng Huihui, The design and research of the acquisition system of the signal of the piezoelectric accelerometer [J]. Science & Technology Information, 2011 , 27:138

[9] Tang Jun, Guo Tao, Shi Yunbo, Liu Jun, . Journal of Transducer Technology, Design of signal process circuit of high precision accelerometer [J].2005,24)7):52,53,56

Dynamic analysis and implementation for Memristor

Zhang Chun, Huang Yizhao, Zhao Tianhui

（jilin university instrument science and engineering institute,changchun,130021）

***Abstract*—Memristor is a nonlinear resistor with memory, which is considered as the fourth basic passive element and has a broad prospect. In order to research the dynamic characteristic of memristor, we establish a new quadratic flux-based equivalent circuit and analyze the influence of frequency to the memristor's i-v curve. We use resistors, capacitances, operational amplifiers and multiplying units to design an equivalent circuit. The equivalent circuit model has been emulated in PSIM to observe the memristor's i-v curve in different excitations and frequency. Additionally, we build a breadboard model for experiment. The experimental results are in agreement with the simulation results, which have verified the effectiveness and validity of the mathematical model and the relevant circuit design.**

I. INTRODUCTION

IN circuit theory, resistance, inductance and capacitance are common elements, which are always characterized by voltage, current, magnetic flux and charge. The concept of memristor is first present by Chua in 1971, under the structural integrity of the relationship between circuit components ports. L Chua pointed out that there should be six mathematical relations to connect the four basic physical quantities. Based on the five existing relations, we conjecture the four basic circuit components from the perspective of symmetry, which is memristor, used to reflect the functional relationship between charge and magnetic linkage. Memristor comes from the two words, memory and resistor. According to the meaning of these two words we can probably understand the concepts and functions that the memristor is a nonlinear resistor with memory function.

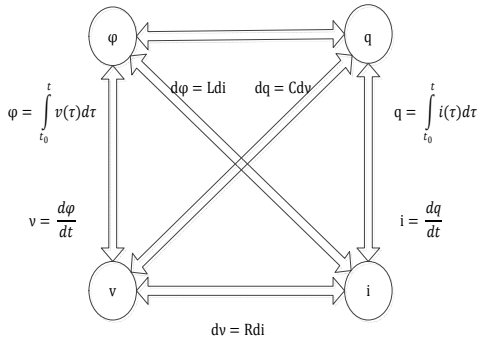

Fig.1 The relationship of four basic variables

Due to lack of experimental support, the theory of memristor made within two decades, did not cause extensive attention among the scholars .Until the researcher of HP Labs proved the real existence of memristor in reality, this technology became famous overnight. As people's deeper understanding of memristor, the physical models and properties successively presented in various research areas makes memristor into reality. Currently, the implementation model and mechanism of memristor are mainly including Transference Model, Electron-spin Blocking Models, Metal-insulator Transitions, redox reaction and so on. Presented in the literature [5], the magnetron memristor, determined by the non-linear curve with a three times monotonously declines in the φ-q plane , has Voltage-current Characteristic curve like a ramp characters "8" hysteresis loops. Smooth magnetic memristor and negative conductance can constitute active memristor and the mechanism of the active model and realization circuit of this paper is more simple and fit into our study compared with that presented in the literature [4] .So we chose the active memristor as our research object to study its dynamic behavior .

II. MODELING SIMULATION AND MATHEMATICAL PECULATION

The active memristor described in literature [5] is realized by Chua circuit with three non-linear characteristic curves, showed in Fig.2. It's characteristic figure is showed in Fig 3. In the picture, the operational amplifiers U1act as a voltage follower, U2 and R1C form as Integrator with and its output complete nonlinear operation through the back two analog multipliers , the circuit formed by U_3,R_3 andR4

make the resistance of R2 to become negative.

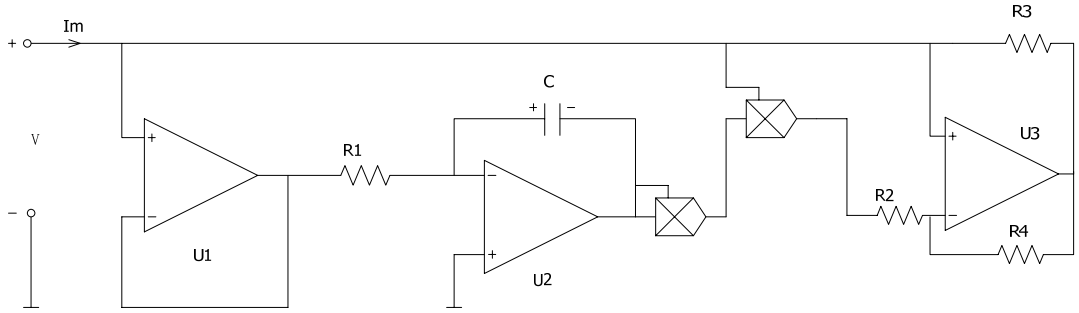

Fig.2 The equivalent circuit of Active Memristor

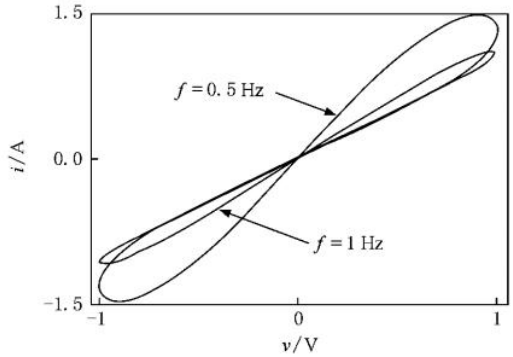

Fig.3 The i-v character figure of active memristor

Through research on the characteristics of a memristor, we make some improvement and innovation on the equivalent circuit above. In literature [5], the author define a magnetic memory with a smooth monotonous increasing cubic nonlinear curve, that is,

$$q(\varphi) = a\varphi + b\varphi^3$$

After simplification, we can give a model of magnetic memory with a monotonously increasing conic nonlinear curve, that is

$$q(\varphi) = a\varphi + b\varphi^2 \quad (1)$$

The conductance of memristor is $W(\varphi)$

$$W(\varphi) = \frac{dq(\varphi)}{d\varphi} = a + 2b\varphi \quad (2)$$

$$i_m = W(\varphi)v = (a + 2b\varphi)v \quad (3)$$

In the formula,

$$\varphi(t) = \int_{-\infty}^{t} v(\tau)d\tau$$

Here , a > 0， b > 0.

As we decrease power from the cubic nonlinear curve to the quadratic nonlinear curve in the equivalent circuit after removing a multiplier and replace negative resistors as ordinary ones. So the modified equivalent circuit of active memristor is

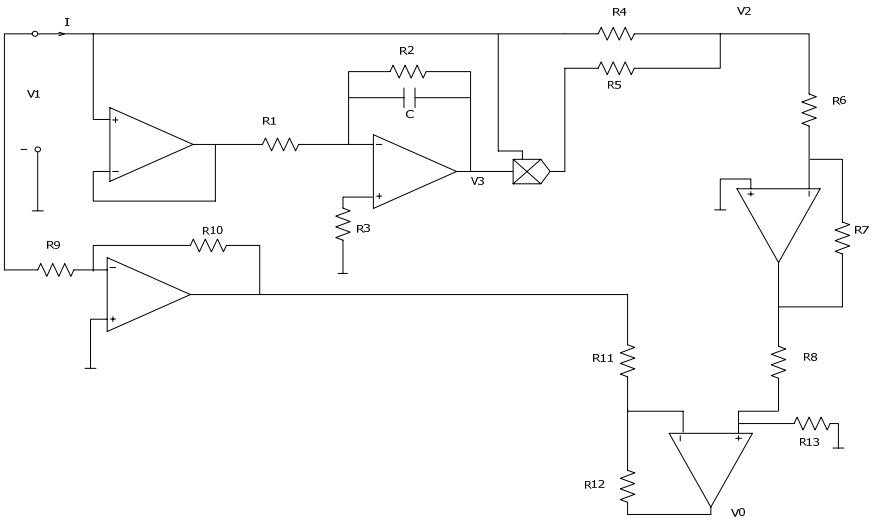

Fig.4 The modified equivalent circuit of active memristor

From Fig.4, we can conclude that

$$V_2 = -\frac{1}{R_1C}\int_0^t v\,dt = -\frac{1}{R_1C}\varphi \quad (3)$$

$$V_1 = V \cdot V_2 = -\frac{v}{R_1C}\varphi \quad (4)$$

$$i = \frac{v - v_1}{R_4} = \frac{v + \frac{v}{R_1C}}{R_4} = \left(\frac{1}{R_4} + \frac{\varphi}{R_1R_4C}\right)v \quad (5)$$

Compared with equation (3), we get that

$$a = \frac{1}{R_4} \qquad b = \frac{1}{2R_1R_4C}$$

It shows the relationship between parameters of circuit. Since the current value of the memory resistor circuit is too small to measure, we observe the relationship between the voltage across the resistor R_4 and the input voltage to replace $i-v$, as is showed in Fig.5, confirming the feasibility of this alternative approach.

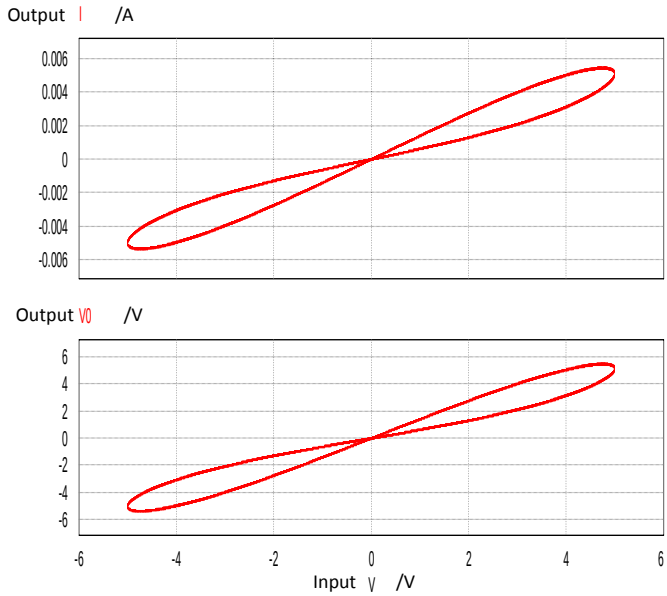

Fig.5 The comparative map of $i-v$ and v_0-v

We use PSIM simulation software to generate the improved circuit showed in Fig.4.The result is showed in Fig.6 and Fig.7. From the pictures, we can see clearly that the model of active memristor with quadratic nonlinear characteristic curve suits the Chua's definition on memristor perfectly. Furthermore, the simulation result is same with that shown in Fig.3, proving the correctness of the improved circuit.

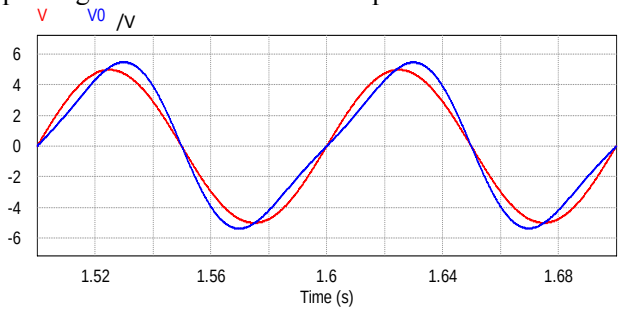

Fig.6 The oscillogram of modified equivalent circuit

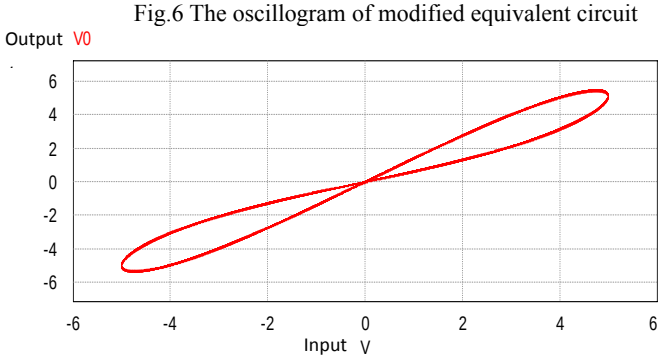

Fig.7 The memristor's character figure of modified equivalent circuit

Based on the above experiments, we confirmed the feasibility of our modified circuit under the simulating condition.

III. THE DYNAMICS ANALYSIS AND MATHEMATICAL DEDUCTION OF THE MEMRISTOR'S MODEL

In order to analyze the memristor's dynamics characteristics ,we use the above proposed new circuit model as the equivalent circuit model of memristor, by changing the parameters of the equivalent circuit to get the corresponding experimental circuit waveform.

A. The frequency parameter

Frequency parameter has a great influence on properties of memristor, the higher the frequency the narrower the characteristic curve of memristor. When the frequency is too high, the *i-v* characteristic of memristor's figure will fit tightly together. In this case, the memristor's nonlinear characteristic may become very weak. Obtained by mathematical deduction frequency f and the memristor's i-*v* characteristic figure as follows:

When a = 1 and b = 1, then the equation (2) describes a normalized magnetic control memristor.as in

$$W(\varphi)=\frac{dq(\varphi)}{d\varphi}=1+2\varphi \qquad (6)$$

Using unit sine wave as the equivalent circuit's input signal $v=\sin 2\pi ft$

By equation (3)

$$i=(1+2\varphi)v=\left(1+2\int_0^t v(\tau)d\tau\right)v$$

$$=\left[1+\frac{1}{\pi f}(1-\cos 2\pi ft)\right]\sin 2\pi ft \qquad (7)$$

For $v=\sin 2\pi ft$ *and* $\cos 2\pi ft=\sqrt{1-v^2}$ or

$\cos 2\pi ft=-\sqrt{1-v^2}$

When $\cos 2\pi ft=\sqrt{1-v^2}$, then

$$i=\left[1+\frac{1}{\pi f}(1-\sqrt{1-v^2})\right] \qquad (8)$$

For $\frac{di}{dv}=1+\frac{1}{\pi f}-\frac{1}{\pi f}\cdot\frac{1-\varepsilon v^2}{\sqrt{1-v^2}}$, when $v\to\varepsilon,\varepsilon\to 0$,

then $\frac{1}{\pi f}\left(1-\frac{1-\varepsilon v^2}{\sqrt{1-v^2}}\right)>0$

This shows that the slope is increasing until endless. The above proved is the figure which is under the horizontal axis when the v > 0.When

$\cos 2\pi ft = -\sqrt{1-v^2}$,we can prove the figure that is above the horizontal axis. About opening size and the relationship with the frequency is proved the following:

$$\frac{dt}{dv}\Big|_+ - \frac{dt}{dv}\Big|_- = \frac{2}{\pi f}\cdot\frac{1-2v^2}{\sqrt{1-v^2}} \tag{9}$$

We can conclude that the slope decreases with the increase of the frequency *f*. The input frequency *f* respectively set to 10 Hz, 50 Hz, and 150 Hz. Through the software PSIM's simulation, we has obtained and recorded in a wide range of input frequency *i-v* diagram as shown in figure 8 to 10.

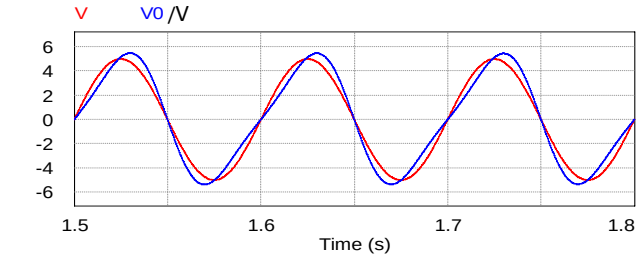

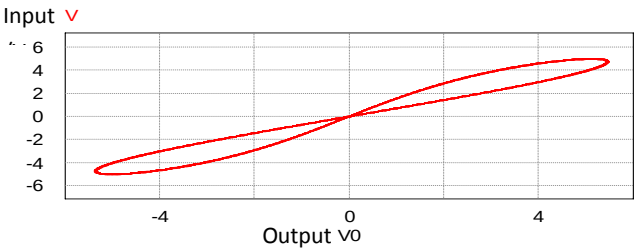

Fig.8 The memristor's character when v = 5V f = 10Hz and the input signal is sine wave

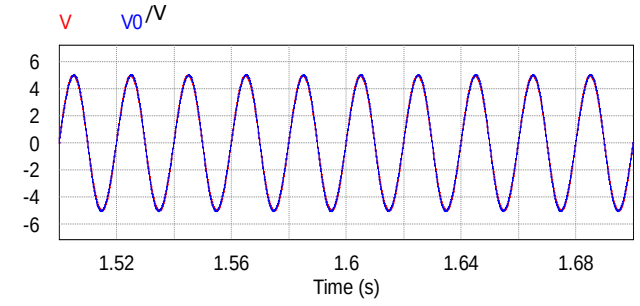

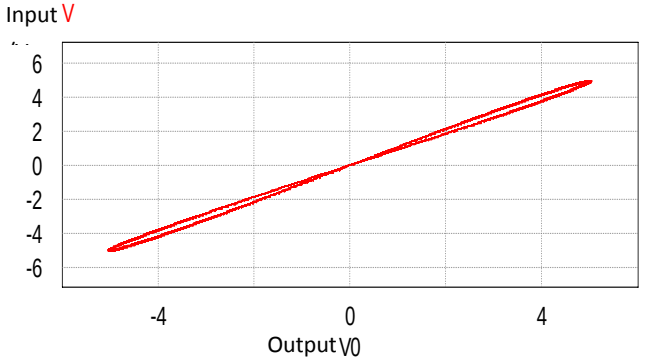

Fig.9 The memristor's character when v = 5V f = 50Hz and the input signal is sine wave

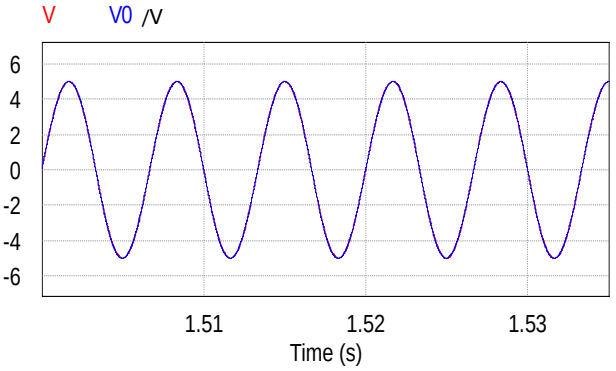

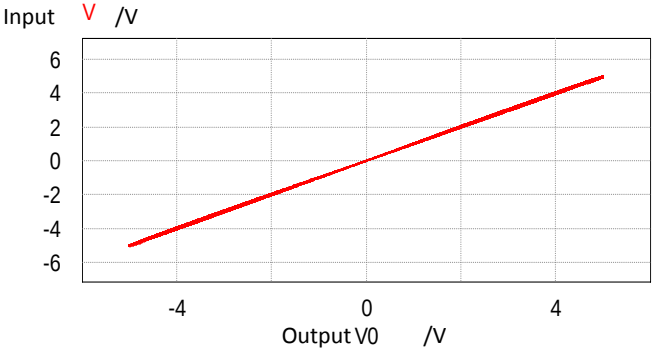

Fig.10 The memristor's character when v = 5V f = 150Hz and the input signal is sine wave

B. Input signal

As the result of the triangular waveform is similar to sine wave waveform, we change the type of the input signal as triangular wave. When the frequency of is 10 Hz triangle wave as input, the simulation can still get the nonlinear characteristic of the image rendering "8" glyph curve. Only in extreme turning point mutations, it is not the same as a sine wave as the input signal curve smoothing, particular case shown in figure 11.

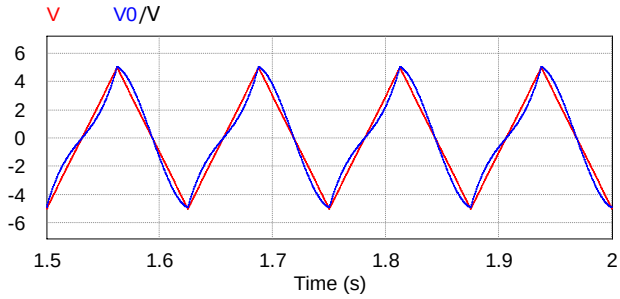

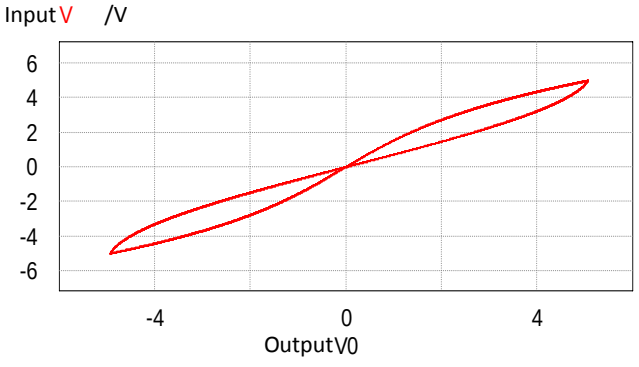

Fig.11 The memristor's character when v = 5V f = 10Hz and the input signal is triangular wave

We dispatch the triangular wave frequency is 15 Hz and 50 Hz, and we get the characteristic curve of memristor as shown in figure 12 and 13. It can be seen when the higher the frequency, the narrower the characteristic curve of memristor .When the frequency reaches a certain limit, characteristic curve can fit tightly together, which is meant that the nonlinear characteristic of memristor is fade away. By setting the triangular wave frequency, we once again verify the frequency parameters' influence of memristor's dynamic characteristics.

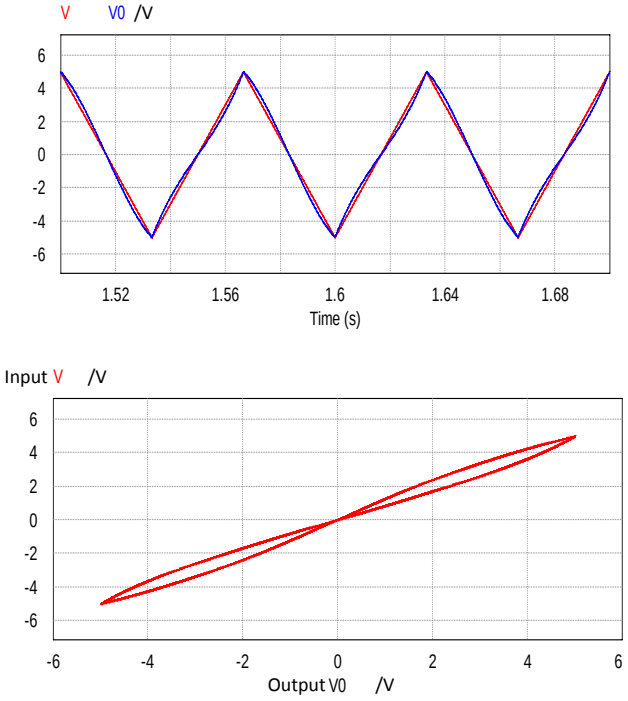

Fig.12 The memristor's character when v = 5V f = 15Hz and the input signal is triangular wave

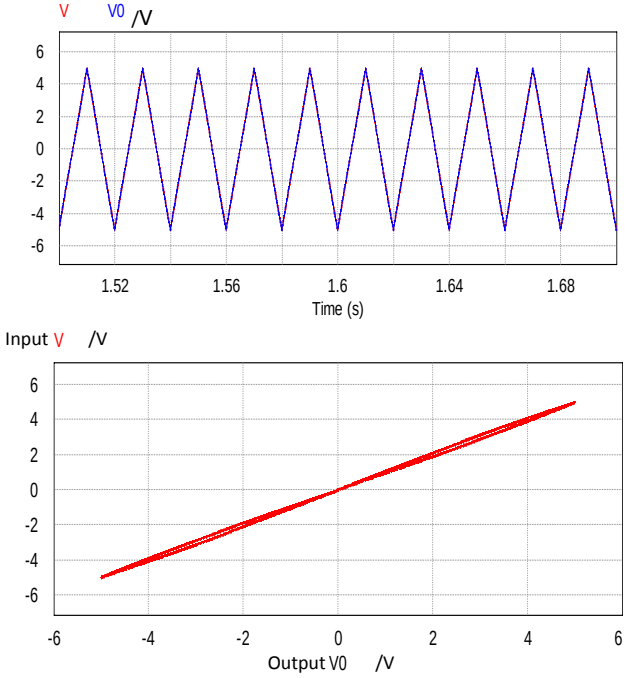

Fig.13 The memristor's character when v = 5V f = 50Hz and the input signal is triangular wave

IV. The actual results of the circuit model of memristor

On the basis of PSIM software simulation and the derived mathematical formula, we successfully build the analog circuit of the memristor on the bread board. By the simulation and circuit experiment, we demonstrate the validity of the circuit design. By using the oscilloscope measurement, we obtain the consistent with the simulation output waveform as shown in figure 14 to 19.

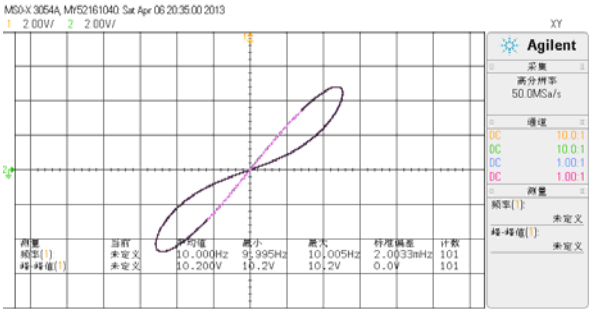

Fig.14 The memristor's character when v = 5V f = 10Hz and the input signal is sine wave

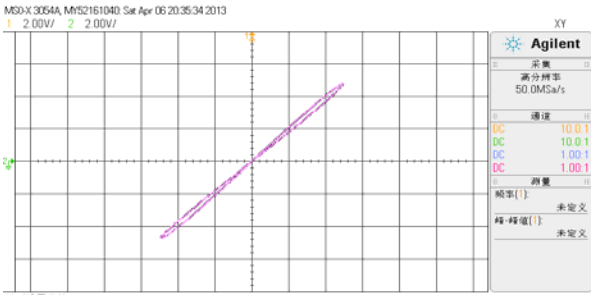

Fig.15 The memristor's character when v = 5V f = 50Hz and the input signal is sine wave

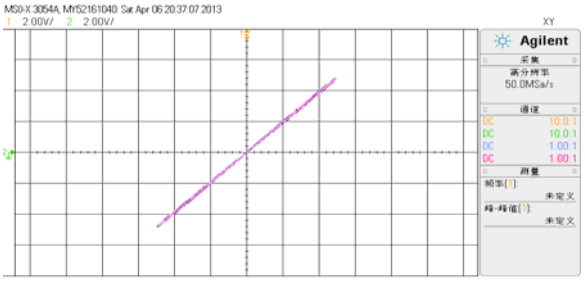

Fig.16 The memristor's character when v = 5V f = 150Hz and the input signal is sine wave

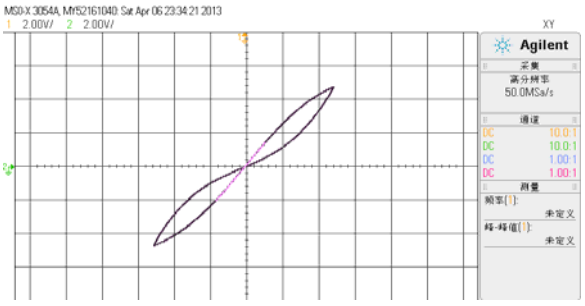

Fig.17 The memristor's character when v = 5V f = 10Hz and the input signal is triangular wave

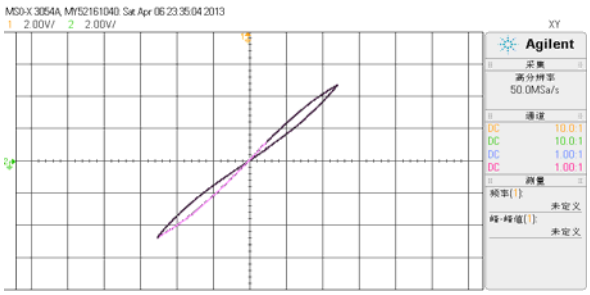

Fig.18 The memristor's character when v = 5V f = 15Hz and the input signal is triangular wave

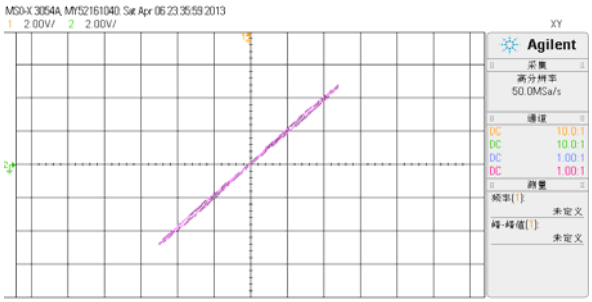

Fig.19 The memristor's character when v = 5V f = 50Hz and the input signal is triangular wave

V. Conclusion

In the process of study, we propose a new memristor's model which is controlled by smooth quadratic nonlinear magnetic characteristic curve. Besides, on the basis of original analog circuit we innovate our model's analog circuit. The test result of the circuit which is got by software simulation and set up the actual circuit is similar with the expected result. It has proved that the proposed circuit is correct. By the result of the experiment, the new memristor's model is completely meet L Chua's definition of memristor.

During the study of memristor's dynamics characteristics, we mainly research the frequency characteristic and influence of different input signal. In terms of frequency, as we can see by the result of the experiment, the memristor has a frequency threshold. When the frequency of the input signal is more than this threshold, the memristor will lose nonlinear property and began to show the linear features, and the nonlinear property with the increase of the input signal frequency will decrease. In terms of the influence of different input signal, as we can see by the result of the experiment, in the case of different input signal we can find that the characteristic of memristor has changed. The experiment uses sine wave and triangle wave as input signal, and we found that the memristor's characteristic curve in the extreme value of the turning point have weaker nonlinear characteristics. The mainly reason is that the triangle wave can be represented as a large number of sine wave superposition, and the high frequency part of sine wave makes memristor lose nonlinear property and have resistance characteristic .So the memristor's characteristic also related to the type of input signal, which is considered that the higher harmonic frequency sine wave of input signal, the weaker of memristor's nonlinear characteristic.

This time we research the memristor's dynamics behavior from two aspects which are the frequency of input signal and the type of the input signal. Finally, a satisfied result is obtained. However the other dynamics characteristics of memristor need subsequently research.

References

[1] CHUA L O. "Memristor – the missing circuit element" .IEEE Trans Circuit Theory, vol. 18, no. 4, 1971, pp. 507-519.

[2] Wang Qinghua, Song weiping . "Reallization of Memristor by Two-port Mutator".Journal of Elestrical & Electronic Engineering Education, vol. 33, no. 3,2011,pp. 56-57.

[3] Ralph Rajola. "The application of memristor". Electronic Products China, no. 11, 2008, pp.52-53.

[4] Cai Kunpeng, Wang Rui,Zhou Ji, "Research progress on memristor and its applications as the fourth passive component". Electronic Components And Materials, vol. 29,no. 4,2010, pp. 78-82.

[5] Bao Bocheng, Hu Wen, Xu Jianping et al., "Analysis and implementation of memristor chaotic circuit", Acta Phys. Sin., vol. 69, no. 12, 2011, pp. 58-65.

Aerogeophysical Instrument Recycling Airbag Damping System

Liang Shaomeng, Xu Jie, and Luo Xiaochun;
(College of Instrumentation and Electrical Engineering, Jilin University, Changchun 130026, China)

***Abstract*—In order to avoid aerogeophysical instrument in aircraft landing impact and damage, we use recycled airbag shock recovery mode to control airbag inflator and inflatable volume when it reaches the set height and speed through the microcontroller, and collect data of altitude between the bottom of aerogeophysical instrument and ground, falling speed and acceleration. The data is transmitted to the ground and displayed on the PC. Experiments show, the buffer system preferably has a cushioning effect for aerogeophysical instrument.**

Key words—Aerogeophysical instrument Airbag Damping

I.INTRODUCTION

AEROGEOPHYSICAL instruments was based on the aircraft or airships as carriers, in upper air sounding instruments of the underground information. In order to avoid electromagnetic interference and improving detection, Instruments are often installed on the bottom of the aircraft or hanging below the aircraft, so expensive aircraft may be damaged during the landing of geophysical instruments, therefore it need to be equipped with a safety recall system. Subject to location restrictions, it should adopt airbag shock absorber landing recovery.

Airbag have been widely used in aviation and aerospace as an effective tool to ease the impact and absorb energy, for example, heavy equipment airdrop buffering, UAV recovery, Space capsule lands protection and so on. First applied to recycled airbag dampening system in foreign countries, Including the drone recovery, missiles and spacecraft recovery recovery [1-3]. The reliability of airbag recovery is strong，thus it have broad application prospects in the field of aerospace. In the domestic, air damping technology is mainly used in airdrops, but in China, airbag shock absorber technology was not mature enough, application of airborne aerogeophysical equipment recovery is still in its infancy stage.

II OVERALL PROJECT DESIGN

Recycled air suspension system is divided into two parts, respectively is the air and ground part. Acquisition aerogeophysical high from the ground at the bottom of the instrument and falling velocity and acceleration data, when developed set data, control pump gas, using the data from the wireless communications will launch to receive part of the PC on the ground, and through the serial asynchronous communication display data and charts. The overall flow chart shown in figure 1, the overall structure is shown in figure 2.

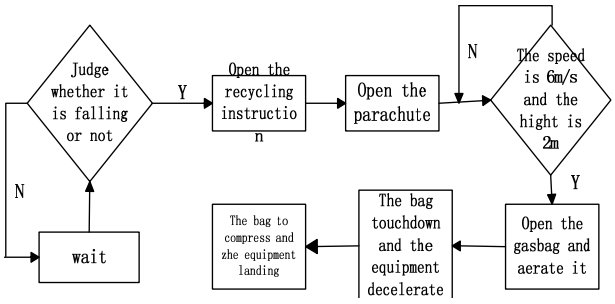

Fig.1 Integral flow diagram

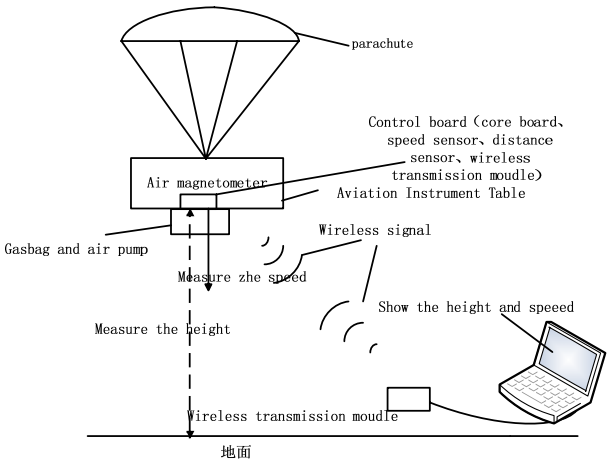

Fig.2 Integral structure diagram

III. EACH PART OF THE DESIGN AND IMPLEMENTATION

This design is aerogeophysical instrument recycling airbag damping system, including air wireless transmission, data acquisition, data processing, device control. In the air, microcontroller core monitoring are ultrasonic ranging module, ADXL345 accelerometer module, LCD1602 display module, wireless transmission module, relay control inflatable devices, alarm module.

Ground segment mainly consists of MCU control module, wireless module, a serial display. The main function, through the wireless module, receives the data collected of the air and through a serial asynchronous communication to make the data transmission to a PC, PC machine through Labview decode the data extracted the data of height and acceleration in three directions and then plotted charts.

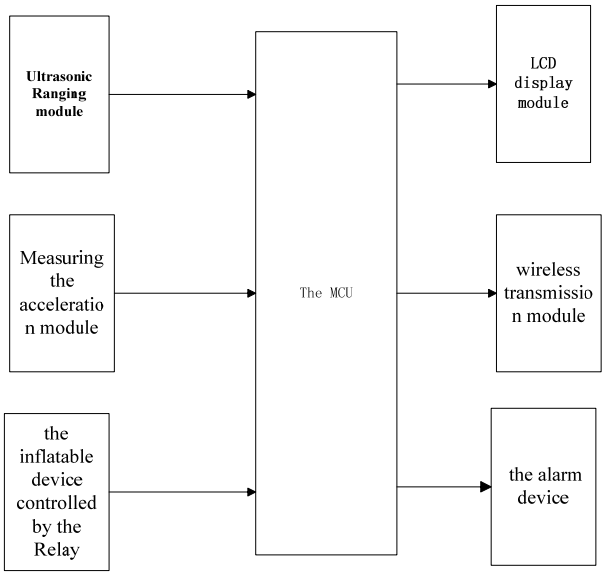

Fig.3 The hardware design diagram of air system

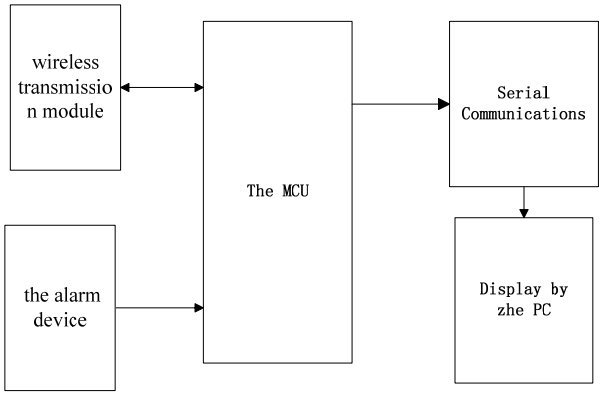

Fig.4 The hardware design diagram of ground system

A ADXL345 acceleration measuring module

The ADXL345 is a small, ultralow power, 3-axis accelerometer with high resolution (13-bit) measurement up to ± 16g. Digital output data is formatted as 16-bit twos complement and is accessible through either a SPI (3-or 4-wire) or I^2C digital interface. Its high resolution enables measurement of inclination changes less than 1.0^o.

B The ultrasonic ranging module

The trig pin must be input a high level more zhan 10us when the US-020 module works, and then the system will send eight ultrasonic pulse of 40KHZ and check the echo signal. The echo pin will send zhe data after zhe echo signal has been checked. We can get zhe distance according to the high level's time sanded by the echo pin. The formula is multiply the time of high level and two, and then divide it by two. By this way we will get the distance. The flow chart is showed as figure 5.

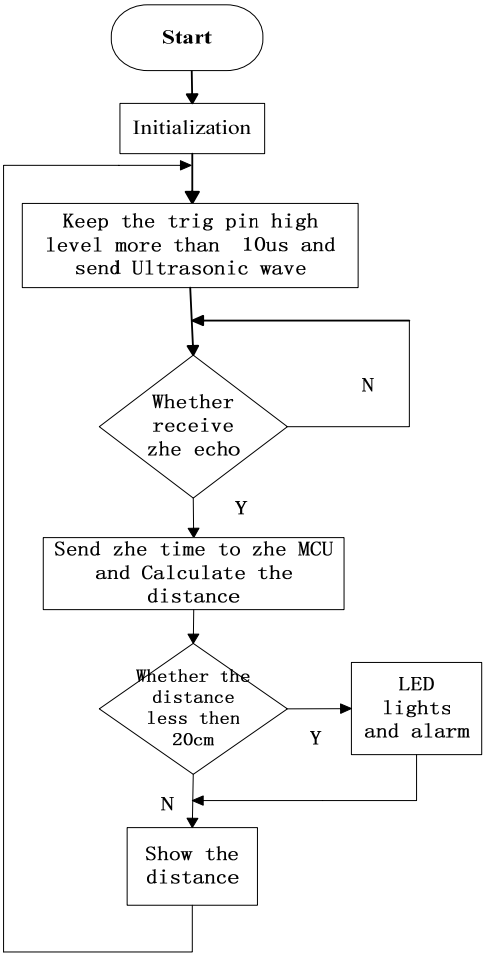

Fig.5. Flow charts of the measured distance

C. LCD1602 display module

Display section use LCD1602, when the LCD1602

displays the first is determine whether it is busy, if LCD1602 busy, waiting until 1602 can woke so far, 1602 is not busy if you can read the resulting data of the sensor (acceleration sensor, ultrasonic range finder), and then use the appropriate conversion, the obtained data shows in 1602. The process is shown in Figure 6.

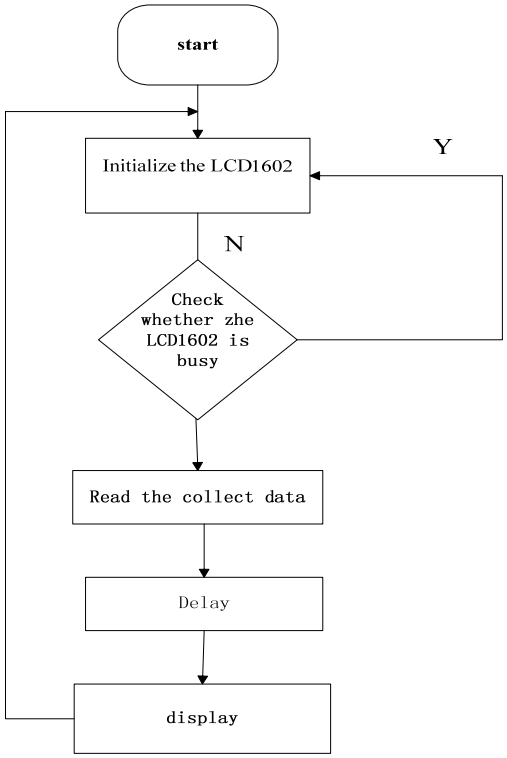

Fig.6 Flow diagram of display

D. NRF24L01 wireless transmission module

Wireless transceiver comprising: a frequency generator, the controller of enhanced SchockBurstTM mode, a power amplifier, a crystal oscillator, a modulator, a demodulator. Setting the output power, channel selection and protocol can by the means of setting the SPI interface. In receive mode nRF24L01 can receive data from six different channels. Each data channel using a different address, but share the same channel.

All channels can be set to Enhanced ShockBurst mode. After confirming receipt of data nRF24L01 recorded address, then this address is the destination address and sends a response signal. On the transmit side, data channel 0 is used to receive the response signal, therefore, the receive address of data channel 0 is equal to the transmission mode address to ensure that the received signal is a correct answer.

Ⅳ. TEST AND ANALYSIS OF SYSTEM

By the experimental determination, the system can be completed within a short time of data collection, data transfer, data processing and analysis, the control of the airbag inflator by the two control modules. The following is the test result of each module.

(1) The system can capture every moment of the model from the height of the ground and the current three-dimensional acceleration by air microcontroller and peripheral circuits, and displayed the data on the LCD screen.

(2) The height of the air from the ground and the three-dimensional acceleration data transmitted by wireless communication to the ground, then receiving and transmitting to the PC via a serial asynchronous communication.

(3) Through labview PC machine will analyze the four data and processing, then respectively display by the waveform.

(4) Air controller can automatically control the relay to control the airbag inflator, the entire control system and the hardware model and the peripheral circuit have completed basically.

The experimental data processing and analysis, to remove distorted data, drawing smooth curves in Figure 7, Figure 8.

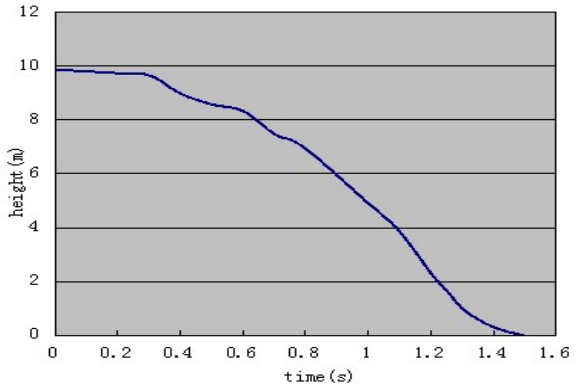

Fig7. The curve of time-height

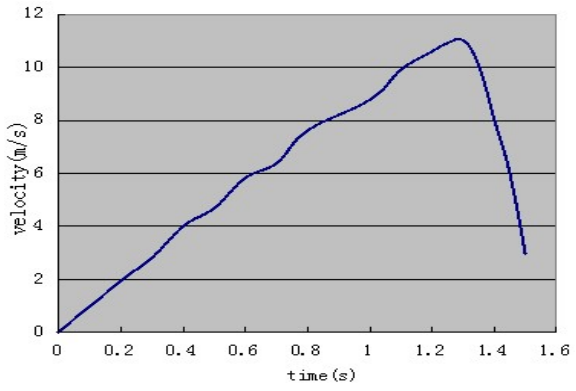

Fig8. The curve of time-velocity

Ⅴ .CONCLUSION

Suspension system is designed based on MSP430 single chip microcomputer as control core, while mainly based on ultrasonic distance measurement to measure the acceleration of display and acquisition data processing and analysis for wireless transmission. Through the analysis of theories and practices, Design is basically feasible. MSP430 achieved the major control core. This system is at work by distance sensor and acceleration sensor to collect data. It controlled by the microcontroller core quickly calculates distance and obstacle and display the results through the LCD to achieve the goal of safety warning, and transfer it that ultrasonic measurement data and acceleration data in the air to the ground through wireless module. At the same time, send it on the computer through a serial port. PC use labview software to receive data frames and solution，then separate height data and three directions of acceleration data，meanwhile make a graph.

In the course of work，there may be interference between signals，Therefore wireless communication interference is the focus of the whole system.

References

[1] Zhang Yuan Ming .the study of the theory of the recycling suspension airbags of the unmanned plane. Hydromantic and pneumatic, 2005.1:7-9

[2] Sun XiRen.GB2019-94, the general requirement for the unmanned aerial vehicle recovery system.

[3] Fan Bangkui. Unmanned .aerial vehicle books abroad, Beijing press，2001.

[4] Tamer C T, Girard Jr L A. Air bag impact attenuation system for The AQM-34VRP.AIAA 81-1917R, 1981, 1-2.

[5] Wang guorong. Overview of the composite materials. Harbin. Harbin industrial university press, 1999.8.

[6] Shen jianhua, Yang yanqin, Zai xiaoshu.The16 ultra-low and singal-chip microcomputer principle and application .Bijing, Tsinghua university press.2004.11

[7] Qin long .The design: SCM c language application of the MSP430.Beijing: Electronic industry ress, 2006.5

[8] Zhang xi, Wang deyin, Zhang chen. The practical language c program design of the MSP430. 2005.9

[9] The review to improving precision of ultrasonic distance measurement. [J].The telecommunications technology.2010 (09)

[10]Li jiawei,Wang yizhi. The testing of the ultrasonic [M].Mechanical industry press.2000

[11]Ding shoucheng. The design and implementation of the ultrasonic ranging system based on MSP430 MCU. Modern scientific instruments.

Intelligent System for Charging and Discharging of Battery

Sun Caitang; Sun Jianlong; Liu Huichang; Che Jingfeng
（College of Instrumentation & Electrical Engineering, Jilin University, Changchun 130012）

***Abstract*—Today's battery life is short, and its efficiency is low. In order to improve battery life and efficiency, this paper designs an intelligent system to charge and discharge the battery. The system can process the battery charging and discharging. Charging process is divided into two stages named constant current charging and constant voltage charging. It can detect the voltage, current and temperature during the charging and discharging, and can intelligently control battery by comparing these parameters. If the voltage, current or temperature exceeds the settings, the system will send out alarm signal. The experimental results show that the system can accurately monitor the working status of battery.**

***Keywords*—intelligent control, constant voltage source, constant current source, parameter detection, alarm**

I. INTRODUCTION

AS people increasingly pay attention to resources, in order to improve using of resources more efficiently, people began to study the technology of the battery in more depth.

From the end of the 20th century, many scholars began studying. He Gang studied additives for lead-acid batteries [1]. In the 21st century, with the development of science and technology, people studied on the battery in more depth. In 2003, Zhang Xiaodong used the MSP430 microcontroller monitoring methods to achieve a real-time measurement of the percentage of battery charge remaining [2], and it could accurately control the charging and discharging process. Xu Lihua selected the three-phase voltage-type PWM inverter main circuit as topology, and established a mathematical model of a three-phase PWM converter to realize a semi-intelligent battery control system [3]; Wei Lan put forward an intelligent design to lead-acid battery charging and discharging which developed the intelligent electrode system [4]; Zhang Baokai designed an intelligent lead-acid battery charge controller based ATmega16 microcontroller, and it resolved common technical problems about battery charging [5]; Liu Weijie designed a distributed control system for battery, It can collect the battery status parameters in the charging process [6].

Studies on charging abroad also have a great achievement. European countries have made some new charging methods, such as fractional charge constant flow, pulse charging method, given the state of the chemical reaction method, variable intermittent current constant voltage charging method and variable intermittent voltage constant current charging method [7]; American Battery Monitoring System(BMS) technology applications in the power industry. BMS systems can provide information about the remaining power of information to staff performance and battery alarm when approaching the limit state; American scientists discovered the effect of temperature on battery charging characteristics and found that the battery charge index of current trends. American scientists found gassing phenomenon when studying the battery charging, and the charging process of the embodiment of the charging voltage control [8]; German scientists Peukert discovered different rates affect the discharge rate of the battery capacity when using the battery discharge [9]; In addition, there are people studying the VMS (VRLA Battery Management System), it can control functions.

This article designs an intelligent systems for charging and discharging, it can manage battery's charging and discharging process. Constant voltage and constant current charging process is divided into two stages, in the charge-discharge process can detect the status of voltage, current and temperature. The system can control the charging and discharging by monitoring the state of the battery.

II. THE OVERALL DESIGN

Battery charging process consists of two stages, that

are constant voltage and constant current. When the battery voltage is lower than that in the normal state, the resistance of the battery is lower. In order to prevent that the charging current is too large to cause battery's damage. The first stage is constant current charging. With the charging time increasing, the resistance will increase. When the voltage of the battery reaches the predetermined value, it will switch to constant voltage charging status. The overall design diagram shown in Figure 1:

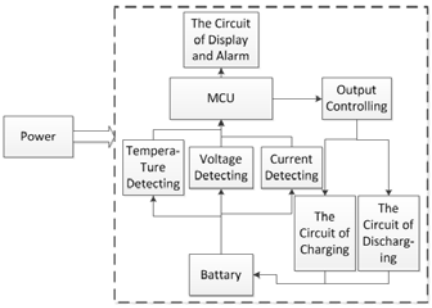

Fig. 1. Design block diagram of overall system.

System includes the following modules: voltage, current and temperature detection module, a display alarm module, a power supply circuit module, charge and discharge module and external control module. In order to achieve the system's intelligence, we need a microcontroller as the master chip. We can use these module to monitor battery parameters. And it can switch constant voltage and constant current status.

III. Circuit Design

A. Constant Voltage Source

At first, we use the rectifier circuit to converting AC to DC. Then we use the filter capacitor for filtering, transport the rest of the DC to LM7805 to achieve producing the constant voltage. The voltage follower operational amplifier KA741 plays the role of ensuring that the output voltage constants. Adjusting R3 can change the output voltage, and the output voltage reaches 14V. The constant voltage source circuit is shown in Figure 2:

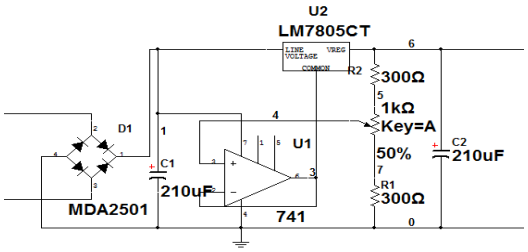

Fig. 2. Circuit diagram of constant voltage source

B. Constant Current Source

Constant current source circuit is to provide constant current to ensure other circuits working stability. In this part, we use BJT to achieve the function of constant current. The constant current source circuit is shown in Figure 3:

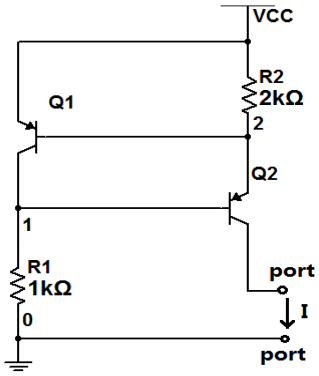

Fig. 3. Circuit diagram of constant current source.

In order to ensure the transistor having a stable output current, it must satisfy two conditions: a) The voltage of input should be stable; b) Resistance of the output transistors should be as large as possible. The constant current source power is provided from the constant voltage source.

Wherein, transistor 8550 is used as Q1 and Q2, it is a kind of low voltage, high current and small signal PNP type transistor. Q1 provides a stable voltage to Q2, and Q2 provides the current.

C. Voltage Collection

Voltage collection circuit mainly consists of a differential amplifier and a voltage follower, as shown in Figure 4. OP07 and LM358 are selected to be as the Operational amplifier.

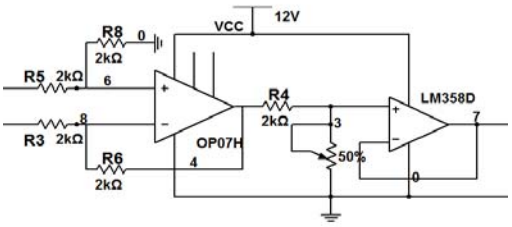

Fig. 4. Circuit diagram of voltage acquisition.

D. Current Collection

Current collection circuit is shown in Figure 5. First, it uses the current transformer ACS712ELCTR to convert current value into voltage value. Then, it send the resulting voltage signal to the microcontroller.

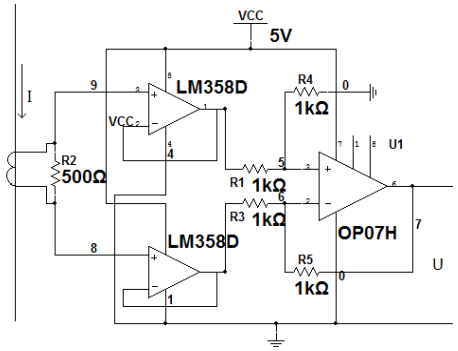

Fig. 5. Circuit diagram of current acquisition.

E. Temperature Collection

Temperature collection circuit is shown in Figure 6. It has a unique single-wire interface mode.It can achieve the two-machine communication with only one serial cable between the MCU and DS18B20. The temperature range is from -55 ℃ to +125 ℃.

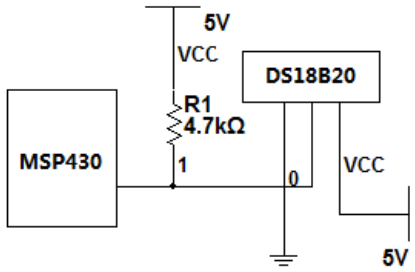

Fig. 6. Circuit diagram of temperature acquisition.

F. Alarm Circuit

Alarm circuit is shown in Figure 7. When the voltage exceeds 14.6V, the current exceeds 1.2A or the battery surface temperature exceeds 60 degrees, the red LED will light, and the buzzer will sound as the alarm signal.

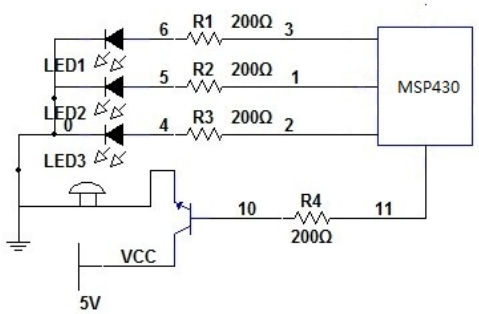

Fig. 7. Alarm circuit diagram.

IV. Intelligent Control

The voltage sources and current sources are switched to control by using MSP430. In the constant current charging process, the battery internal resistance increases, and the charging voltage will increase. When the voltage value increase to a certain value, it will generate a lot of bubbles inside the battery, causing the battery loss.

In the charging process, when the voltage reaches 14.7V, it will converted to constant voltage charging. Thus, we can achieve the intelligent control.

V. Experimental Analysis

The system can determine the voltage and current according to the battery charging parameters. There is a 7Ah-12V battery, when the battery is in constant current charging, the current will be maintained at 700mA, and the charging voltage will increase. When the voltage reaches a predetermined value, it will switch to the constant voltage charging process, and the voltage holding at 14V. Then the charging current will decreases until the battery is filled. Thus the whole charging process is completed. TABLE I shows the data collection of constant current charging; TABLE II shows the data collection of constant voltage.

TABLE I

Data Collection of Constant Current Charging

Charging time(h)	1	3	5	7	9
Voltage(V)	12.2	12.7	13.8	13.9	14.0
Current(A)	0.72	0.72	0.72	0.69	0.60
Temperature(˚C)	20.1	24.6	24.6	24.6	24.6

TABLE II

Data Collection of Constant Voltage Charging

Charging time(h)	9.1	9.3	9.5	9.7	9.9
Voltage(V)	14.0	14.0	14.0	14.0	14.0
Current(A)	0.60	0.54	0.32	0.11	0.11
Temperature(˚C)	24.5	24.5	24.5	24.5	24.5

From the above table, it can be seen that in the charging process, the internal resistance of the battery becomes larger.And when the battery power is nearly saturated, its resistance is almost unchanged.

VI. Conclusion

This article designs an intelligent battery charging and discharging system, which can detect the battery status in the charge-discharge process. It can switch the charging mode according to the working status.

However, this system also has some shortcomings. For example, voltage and current instability during the charging, and the testing results would be affected by the element's performance and environment. These are the next areas for improvement.

References

[1] He Gang, *Synthesis of Ethylene Carbonate by One-Step under Pressure* [J], Chemical Industry and Engineering, 1990,19(1) :7-8

[2] Zhang Xiaodong, *Battery Monitoring's Domestic System Status Quo and Development Trend*[J], Agricultural Mechanization Research, 2002, (3) :18-19

[3] Xu Lihua, *Research on Charge-discharge Divice of Storage Battery Based on PWM Technology*[D], Chengdu: Southwest Jiaotong University, 2005. 5.

[4] Wei Lan, Yue Yan, Liu Qizhong, *Research on the DC Traction Power Supply of the Urban Rail Transit* [J], Power Electronics, 2009, 43(9)：9-10

[5] Zhang Baokai. *Design of Intelligent Charging and Discharging Controller for Battery Based on Single-chip computer* [D]. Dalian: Dalian Maritime University. 2013. 6

[6] Liu Weijie, *A Design for Lead-acid Battery Smart Charge and Discharge System Based on STM32*[J]. Research and Design. 2013, 4: 33-36

[7] Chen Yuhong, Wu Ling, Ren Chao. *Study status of lead-acid battery from European Lead Battery Conference*[J] .Chinese Labat Man. 2000, 4: 35-37

The automatic choreographed PC software design and realization of the humanoid robot

Cao Mingming Kang Lili Hu Xueyan

(Collage of instrumentation & Electrical Engineering, Jilin University, Changchun 130022,China）

***Abstract*—To design a humanoid robot to the robot motion for automatic arrangement of PC software, based on the Windows 7 operating system with Visual Basic 6.0 as development environment to design and development of software, PC software can control the robot real-time robot the rotation Angle and speed of the steering gear, plus the orchestration of the robot motion for automatic integration, at the same time using a serial port debug and robots to communicate. To complete the debugging and control of the robot.**

***Keywords*—Robot PC software Serial port communication**

1.THE INTRODUCTION

THE robot is a comprehensive strong discipline, have a wide range of research and application field.

The humanoid robot is an important research topic in the study of robot technology, and bipedal robot is the prelude to a humanoid robot research. Walking technology is a movement of people and most of the animals have, is a kind of highly automated movement, Because the bipedal robot has multiple joints, drives, and the characteristics of the multi-sensor, and generally have redundant degree of freedom, has done a lot of difficulty, the characteristics of its control problem for control and optimization methods provide an ideal experimental platform.

Humanoid robot motion of debugging is a quite complex process, The program will undoubtedly is very complex, is not conducive to real-time observation action effect, Therefore, to develop the robot dynamic debugging software, PC for editing and debugging action provides a quick and easy way. Make it a remarkable research direction, the existing PC software are mostly to the steering gear of a single robot debugging, not integrate the motion of the humanoid robot, and are not able to automatically generate C language for the robot program download. So the design and production of a robot movement can be automatic layout and can be automatically generated for the robot directly download the PC software of C language for robot control and the experiment has very important practical function.

2.MENTALITY OF DESIGNING

PC software based on Windows 7 operating system using Visual Basic to write, so can make the humanoid robot has good man-machine interface. PC software by adjusting the progress bar to adjust the operating parameters of the steering gear, and add parameters to the operation of the PC interface, PC can realize change at the same time, reset, add interval, delete, save, and other functions, after completion of the experimental run successful data can be automatically generated c language program for robot operation, so as to realize the automatic layout of humanoid robot motion control.

2.1 The choice of the ways of communication

Single chip microcomputer common USB, Ethernet communication module, asynchronous serial communication port (hereinafter referred to as a serial port), of which the most serial common and easy to use "from basic C51 series 8-bit microcontroller to 32-bit MCU is integrated with a serial port module" project and desktop computers and notebook also has general serial port, for there is no serial notebook turn can use a USB serial port "rate of serial port communication is usually between 9600 BPS to 9600 BPS, state to send and receive enough instruction. The system debugging is commonly the scene debugging, 15m serial port communication distance also meet the requirements.

Therefore, this paper use a serial port for PC software and MCU communication way of communication. PC software execution in P C end, through a serial port line, receiving MCU of state information, and transmitted via a serial port to the single chip microcomputer instruction. Write special status information for single chip microcomputer sends the service procedure and instruction processing function.

2.2 The choice of design software

As non-professional application developer, may be the Basic C/C + + programming, but Windows environment programming, need to use a lot of API, directly in C/C + + Win32 SDK design which has the function of display software, time-consuming and there is no need to, so the design choice of development tools should as far as possible to simplify the underlying knowledge of Windows, common Visual programming software are VisualC++, Java, Visual Basic, Labview, which VisualC++ and Java powerful but not enough is easy to use, not suitable for professional application developers use, Labview is easy to use, but is not flexible, Visual Basic in achieve a better balance between ease of use and flexibility "for the design, more powerful and easy to use, its characteristic is an important, using Visual programming, window design as simple as drawing, PC software design are introduced in this paper, precise and easy to understand language, its generated program can independently execute on other computers.

2.3 The realization of the function of automatically generated C:

The control using 8-bit STC12C5A60S2CPU, its resolution is 28 = 256. Through experiments, the limit of the steering gear parameters should get can be divided into 250, 2.5 ms - 0.5 ms = 2 ms = 2000 us, so the PWM control precision of 2000 ms / 250 = 8 us. So we will take us to control the steering gear rotating the smallest unit of 8. Steering gear convertible largest Angle of 185 degrees, 185 degrees available for steering gear control precision present 250 = 0.74 degrees, 0.74 degrees each defined as a position each position 1 DWT. Do we calculate the robot steering gear rotating the pulse width, thus conducive to the following procedure realize the function of the automatic generation of C language.

```
For i = 0 To List1.ListCount - 1
If Mid(List1.List(i), 1, 2) = " The steering gear " Then
For j = 0 To 7
If Val(Mid(List1.List(i), 5 + 9 * j, 2)) <temp(j)
temp(j) = Val(Mid(List1.List(i), 5 + 9 * j, 2))
Print #fn, "chang(" + CStr(j) + "," + CStr(temp(j)) + ");"
Print#fn, "sleep(" + CStr(Val(Mid(List1.List(i), 3, 4))) + ");"
```

3. A SERIAL PORT RECEIVES THE DATA IN VB

3.11Receive data in the OnComm event

This way can be fully MSCOMM control features. OnComm event can also check and deal with the communication error; Check the value of the CommEvent property to query events and error; For variable length data and the data processing is more complex, this method is not very convenient.

3.12 Round robin method to collect data:

For sending and receiving data packets way and do not require immediate response, by using the round robin method is better. Actually the biggest benefit of round robin law depends on the concentration and less CPU processing data. Round robin method should pay attention to timing acquisition time fragment size; Here in binary transceiver model; Make the attribute RThreshold, SThreshold is 0, shielding ONCOMM event.

3.2 VB serial port receiving the choice of sending data

Considering the experiment data are not particularly complex, USES the receive data in the OnComm event, fully using MSCOMM control features, can be convenient to check and manage communication errors can also by checking the value of the CommEvent property to query the events and errors, so convenient for experimental data transmission.

3.3 The realization of the MSComm control in the upper machine

In VB5.0/6.0 to create a new project file. Add Microsoft Comm Control 5.0 components, add the Command in simplified Form1 named Command

buttons and CmdTest, named MSComm Control MSComm1, and through the following main function of MSComm Control statements.

Private Sub cmdTestClick () 'open the serial portSet Com2 MSComml.Com mPort = 2 '

If MSComml. PortOpen = False Then

MSComm1. Settings = "9600, n, 8, 1" '9600 baud rate, no check, 8 data bits, one stop bit.

MSComm1. InputLen = 0 receives a binary numberMSComm1. An InputMode = ComInput ModeBinary

Buffer = MSComm1. InputNeed special attention is that when send character array data note ByteArray containing must define the assignment in advance, as shown in figure is the main process of using VB to a serial port communication.

4. ROBOT PC MAIN MODULE

4.1 The joint servo motion value adjustment module

The power source of the robot to complete all kinds of action is the steering gear.Steering gear control signals to cycle 20 ms pulse width modulation (PWM) signal

The pulse width from 0.5 to 2.5 ms, corresponding to the position of the steering wheel of 0 ° ~ 180 °, a linear change. To realize the robot has done all kinds of action points by steering gear control principle. Specific to each points of the steering gear to define an Angle variable pulse width, and give the initial value for the middle of the steering Angle, to the timer setting initial value is both a steering gear PWM wave pulse width of the initial value. Every time when the timer interrupt time to overflow, after entering the terminal service subroutine, first put down all of the steering gear control output, to a certain position is high, and to give the timing time of PWM pulse width. Last shift make next, enter the interruption to a high position, equivalent to pass time slice to the next steering gear drive. When each is steering gear control output loop set high timing once, fill again on 20 ms cycle for the rest of all the control mouth lock down time, in this way the analog output 20 ms for the cycle of PWM wave, to control the steering gear rotation. Figure 1 for PC in each corresponding to the pulse width of the steering gear.Variable numerical control module, through Vb VScroll controls to implement for numerical control.

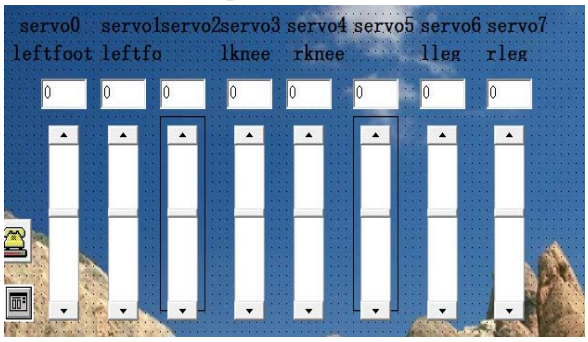

Figure1 The corresponding numerical control pulse

4.2 Robot PC software function module

Through PC function module as shown in figure 3, robot can be a corresponding action steering gear pulse width of the variables of the corresponding numerical integrating, automatic layout and convenient robot movement, but also can modify the motion of the required changes, delete, and save functions such as, at the same time can be automatically converted into the corresponding action by the robot available directly download the C language program, more convenient robot debugging and the experiment, effectively save the programming time.

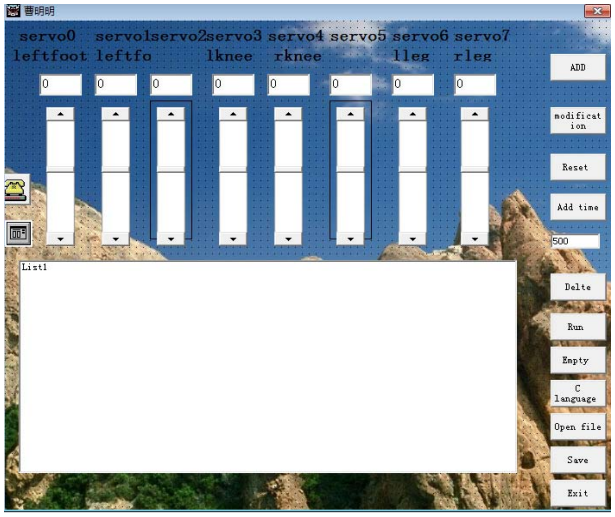

Figure2 as the ultimate PC software interface.

5. THE SYSTEM TEST

The software debugging process for assembling test software, the first test a basic module, test after the completion of the next one to test the module assembly to the module test in the test, all the modules together, step by step and complete the test. Regulation value of the software is divided into robot

joint steering gear motor module, robot PC software function module, serial communication control module debug respectively, and finally integrated debugging, software and stable operation. Some problems in the process, such as the steering gear control module debugging, abnormal part of the steering gear control work, but after the follow-up program changes, has improved. Test surface, the system has realized the reserve requirement, can pass the PC to control the robot programming. Figure2 as the ultimate PC software interface.

6. CONCLUSION

The software finally realizes the following functions: (1) the robot PC software can use a serial port debugging and robots to communicate; (2) the PC software can control the robot real-time robot steering gear rotation Angle and speed, so as to complete the action of the robot. (3) local server PC software can be through a serial port and 51 single-chip microcomputer experiment board communication, and can be run through wireless communication control robot, convenient to experiment on the 51 SCM experiment board. In the design, due to the limitation of time and personal ability, the function of the software system are not perfect. So in the future study, we will continue to improve the robot PC software, and beautify the PC software interface, increase the number of steering gear control, simplifying the operation process, strive to do better the robot PC software.

References

[1] Chen Xianting, Dong Jingang , a PC software design and implementation of teaching robot, high-tech products and research and develo-pment, 2012167-2012167

[2] Tan Lingyan , the wu army, wen yi first, since the balance of the humanoid robot motion controller design, electronic science and technology, 2010100-2010100

[3] LiChanglin.Visual basic serial communication technology and the typical example [M]. Beijing: tsinghua university press, 2006.

[4] Kong Xu, humanoid robot joints innovation platform design and development [A] 3-9767-2011100

[5] Dehong Cong, Ning Xu,Design and Implementation of Contest Robot Control System

[6] Zhang Rui,Altium Designer 6.0 schematic and PCB design,Beijing: Publishing House of Electronics Industry, 2007.

[7] Tao Junyuan , Li Desheng, Jin Ming Harbin Institute of Technology, China,Novel Electromagnetic Driving Soccer Robot Platform,2010

Research on rapid charge and discharge characteristics of supercapacitor

XuFei; DongXuefeng; WuHaifeng

(College of instrumentation andElectrical Engineering, Jilin University, Changchun130022, China)

***Abstract*—This article briefly introduces the principle of super capacitor and current development at home and abroad. Focus on super capacitor charging and discharging characteristics are studied and presented to the evaluation of the pros and cons of super capacitor charging methods. In the experiments, we use constant voltage charge mode and constant current charge mode for charging experiment. We also research for a single super capacitor rapid charging and discharging characteristics or more super capacitor series-parallel combination characteristics. Charging time, Charging efficiency and energy storage are both considered. We use the mathematical tools such as MATLAB to consolidate the obtained test data and sum up a series of super capacitor charging and discharging characteristics and the best charging mode.**

***Keywords*—super capacitor charge and dischargecharacteristic leakage current**

Ⅰ. INTRODUCTION

ALONG with the development of society, energy production and other aspects of life is becoming more and more importance, and electric energy storage device that will directly affect electrical equipment for the application. Super capacitor also could be described as electric double-layer capacitor, gold capacitor or farad capacitor. It has large capacity, fast charging and discharging, little energy loss and high charging efficiency and less pollution, longer cycle life, power density, and many other advantages. With the materials science breakthrough, these new type of power electronic components have appeared in recent years. Super capacitor has the characteristics of general nature of capacitors and batteries. Ordinary capacitors are characterized by high power density, low energy density. The characteristic of battery is higher energy density, low power density. Super capacitor came into being in the background that People are looking for high energy density and high power density of the energy storage components. By the virtue of its own merits, super capacitor has a very wide range of application spaces. Super capacitors have been used in the transport, industry, communications, renewable energy industry, military field. For example, in the Iraq war, the United States applied "microwave bomb" that equipped with Super capacitors made of ultra strong electromagnetic pulse into the bunkers damaged internally, the force of attacking is extremely powerful. At present, the United States, and Japan, and Russia, and France and other developed countries leader in super capacitor research. In China, the super capacitor development started a little late. Domestic research development still needs to be improved as a whole. In many places, it also needs a great deal of fundamental research. This article has researched and summarized super capacitor charging and discharging characteristics of activated carbon as electrode materials, reference to other research workers.

Ⅱ. PRINCIPLE OF SUPER CAPACITOR

Super capacitor energy storage principle is different from ordinary battery, the charging and discharging process conditions such as temperature restrictions, and charging and discharging currents play a decisive role. The most widely used of these are activated carbon. Carbon-based super capacitor electrode material performance depends in large part on activated carbon. These kind of super capacitors using organic electrolytes for medium, formed electric double-layer between the electrolyte and activated carbon , as shown in Figure 1.

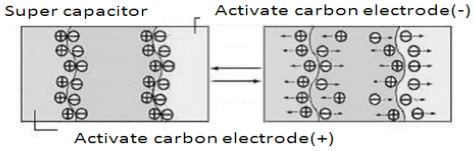

Fig.1 the principle of super capacitor

Super capacitors can be seen as two suspended in

electrolyte reactivity of porous electrode plates, power at the plate, positive plates attract negative ions in the electrolyte, cathode plates attract positive ions, actually formed two capacitive storage tier, the separated positive ions at the cathode plate near and negative ions close to the positive plate. Super capacitors store energy in the charge separated, their energy storage is affected by electrode materials for surface area, porosity of porous electrode and electrolyte activity factors and so on. The more area used to store charge and more crowded the separated charge, the more capacity it has. Due to the specific surface area of super capacitor based on porous carbon materials, porous structure of the material allow its area of 1500-3000m^2/g, so this huge surface areas coupled with a very small charge-separated from make super capacitors have enormous capacitance than the traditional capacitors.

Ⅲ. INFLUENCE ON DISCHARGE CAPACITY OF THE CHARGING SYSTEM

Super capacitor equivalent of the internal structure is shown in Figure 2. Super capacitor equivalent series resistance ESR(entrails series resistance) primarily by the internal resistance of the electrode material ,the internal resistance of solution, contact resistance and other compositions. The ESR of capacitor is to reflect an important indicator of its performance. Equivalent series resistance performance for: when the electrodes are charged at a constant potential for a long enough time, capacitor begin to discharge and electrode potential will be a dump ΔU.

It is because:

$$U = U_c + \Delta U \quad (1)$$

$$\Delta U = I \times Res \quad (2)$$

In the equation, U is the capacitor's voltage, Uc is the internal equivalent capacitance voltage, I is charging current, Res is the equivalent series resistance. When the charging current has disappeared, the ΔU disappear, the Terminal voltage will have a voltage drop.2.7V/400F super capacitor charging test results as shown in the figure 3.

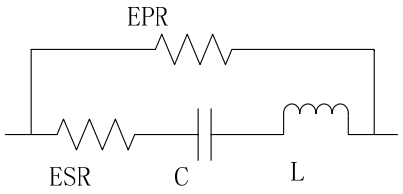

Fig.2 the entrails equivalent model of super capacitor

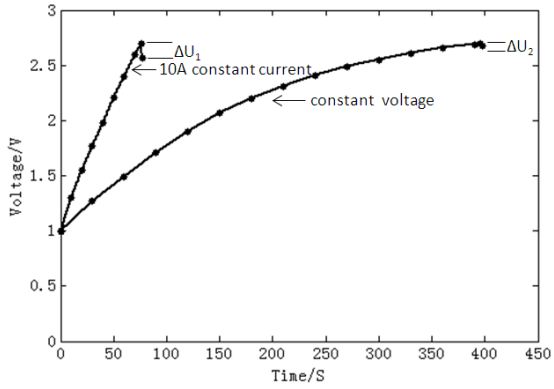

Fig.3 the terminal voltage change of super capacitor

In Figure 3, 10A constant current charging, the charging time required for the 77S, landed upon completion of charging capacitor voltage to Δ U1=0.13V; 3.0V voltage charging, the charging time is 400S, landed upon completion of charging capacitor voltage to Δ U2=0.02V.

For super capacitor, there is:

$$E = \frac{1}{2}CU^2 \quad (3)$$

That is: super capacitors store the energy associated with the capacitance and voltage.When charging is complete, both ends of the capacitor smaller pressure drop, indicating that larger capacitors store energy. As far as the charging voltage, constant voltage charging method can greatly reduce the Δ u. This is because when the voltage is close to the rated voltage, the charging current is very small, inside the capacitor correctly activated carbon pore structure of full contact with the electrolyte, resulting in capacitor inside a stable potential. Charging time, constant current charging time required significantly less constant voltage charging time required. Take charging time and store energy aspects into account, for a single super capacitor, high current switch constant voltage charging after constant current charging mode works best.

Ⅳ. MORE SUPER CAPACITOR SERIES-PARALLEL

COMBINATION OF CHARACTERISTICS

When using super capacitor in series or in parallel, the super capacitor combination can be taken as a whole to research which characteristic does it different from a single super capacitor with different charging current. Due to the combination of greater practical value of, so for the combination of characteristics, main charge time and charge and discharge efficiency.

A. Charging system on super capacitors series combination of effects

Using three 400F/2.7V capacitor in series, respectively use the 5A and 10A constant charging current to do a experiment. By LM2587 chip discharge the booster circuit for resistive load. Test results are presented in Figure 4.

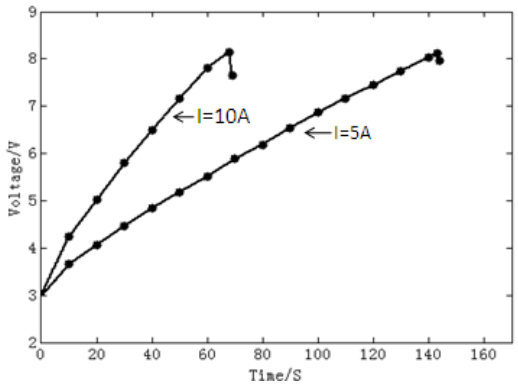

Fig.4 the terminal voltage change of super capacitor by constant current charging

As can be seen in Figure 4, when we use 10A current charging, the series combination charging time is not significantly different from a single super capacitor charging time.

This is because:

$$Q = CU \qquad (4)$$

For n in-line super capacitor series; there is:

$$Q_n = \frac{C}{n} \times nU = CU \qquad (5)$$

That is: when the same super capacitor in series, its ability to store charge remains unchanged. Theoretical analyses and experimental data can be seen in constant current charging case, super capacitor in series combination with super capacitors monomers in charge there is no difference between the time, and this feature is consistent with ordinary capacitors.

B. Analysis of super capacitor charging and discharging efficiency series-parallel combination:

The charging process, energy consumption is:

$$E_1 = \int_0^t U_i I_i dt \qquad (6)$$

In the equation (6), the Ui is super capacitors and Ii respectively the input voltage and input current.

Discharge test, the release of energy to the load is:

$$E_2 = \int_0^t U_o I_o dt \qquad (7)$$

In the equation (7), Uo and Io, respectively were super output voltage and the output current of the capacitor.

The super capacitor charging and discharging efficiency is:

$$\eta = \frac{E_2}{E_1} \times 100\% \qquad (8)$$

Using MATLAB to fit charging voltage versus time curve and do integral calculation, after several tests, the results as shown in table 1.

Table1 the efficiency of super capacitor by constant current charging

Current (A)	Time (S)	Efficiency(%)
2	701	46.2
4	378	48.5
6	244	53.3
8	190	58.2
10	156	64.7

This suggests that as the current increases, within certain limits, super capacitors series combination of charging and discharging efficiency will increase.

Ⅴ. ANALYSIS OF SUPER CAPACITOR LEAKAGE CURRENT

Due to the existence of internal shunt resistors EPR （entrails parallelresisrance）, super capacitor in case of power will produce an electric current flows through the EPR, the current known as the leakage current. Due to the presence of leakage current, super capacitor internal shunt resistance is determined by the size of in-line distribution of super capacitor voltage of the unit. Due to the super capacitor capacitance is large, so when the test super capacitor leakage current, regulations imposed on the test capacitor voltage

30min the measured current is the leakage current of the capacitor. Test as shown in the figure, ambient temperature of about 16 ° c; applied voltage to the operating voltage of the capacitor; and during the test power supply voltage fluctuations not exceeding 0.01V; Charging time is 60min; final leakage current test data from the effects of size sampling resistance Ro, it provides sampling resistance Ro=10Ω, leakage current test chart (in the Figure 5) the leakage current is calculated as:

$$I_L = \frac{U}{R_0} \qquad (9)$$

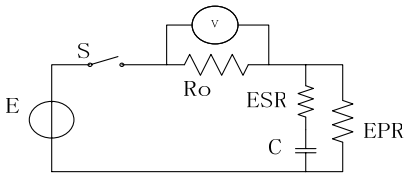

Fig.5 the leakage current test circuit of super capacitor

After many test, leakage current curve as shown in Figure 6. As can be seen, along with extended hang time, leakage flow decreases, and leveled off after 30min. As can be seen, as the number of tests increases, stable super capacitor leakage current value decreases. This is because in previous cycle process, when charging although there has large charge accumulated in electrode surface formed double electric layer, due to electrolytic liquid in electrode internal passed charge of speed more slow, makes activated carbon within cavity in the many pore is not get full uses, part charge just is electrostatic attracted in "electrode/solution" interface, this part charge in discharge moments release, led to a big of leak current. With the cycle frequency increased, super capacitor leakage current is reduced to a smaller value, indicating that the super capacitor in the loop after using for a long time, performance to stabilize.

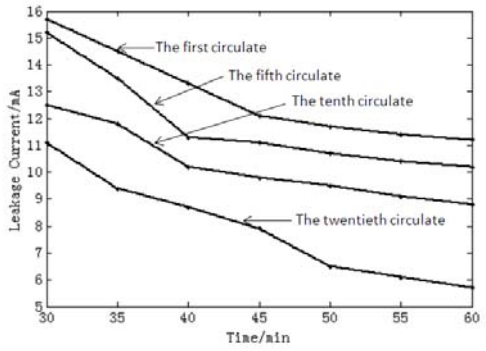

Fig.6 the leakage current test curve of super capacitor

VI. CONCLUSION

For a single super capacitor, high constant charging current has a distinct advantage in charging time. But as the current increases, landed in both ends of the capacitor voltage when charging is complete also increases. In order to solve this problem, you can use constant current charging voltage switches then to the constant voltage charge for some time. Leakage current measurement test shows that the super capacitor performance after a number of recycling has improved and stabilized. For more super capacitor combination, when super capacitor used in tandem, their capacitances are same with the single super capacitor. While in charging and discharging efficiency, within certain limits, as the charging current increases, efficiency will improve. Evaluate the pros and cons of super capacitor charging system, charging time, charging efficiency, discharge capacity, three major aspects to consider.

ACKNOWLEDGEMENTS

Thanks for Professor Cheng Defu help the author specifies the direction of research and patiently guide and assist in writing this article. Through this research opportunity, by experimenting and writing this article, I learned a lot not only in the knowledge and practical competence, but also learning benefit.

References

[1] ZhaiNansong,ZhangDonglai,TongQiang.Research and application status of supercapacitor[J],Chinese Journal of scientific instrument,2007,24(8):1-4

[2] LI Zhong-xue,PENG Qi-li,CHENJie.Study on the dynamical characters of supercapacitor terminal voltage,Battery,2005,35（2）：85-86

[3] TIAN Yan-hong,FU Xu-tao,Wu Bo-rong. Development of porous carbon materials for electric double-layer supercapacitor .Power supply technology.2002,26（6）：466-479

[4] CaiGuoying, Wang Yajun, Xie Jing. Study on the characteristics of super capacitor energy storage power supply of [J]. world, 2009:33-38

[5] WangXianquan, Zheng Zhonghua. Super capacitor charging and discharging characteristics of [J].ship electric power technology, 2011, 31 (4): 54-56

[6] XiongRui, He Hongwen, Zhang Xiaowei. Modeling of ultracapacitor test data based on [J]. vehicle& power technology, 2010, 4:25-28

Remote Air Quality Detecting System Based On GPRS

Zhang Wen-jun,Tian Ji-yu, Lv Ting-ting, Zhao jing

(College of instrumentation and Electrical Engineering, Jilin University, Changchun130021)

***Abstract*—Air quality testing system uses sensor technology, GPRS wireless communication technology and air quality intelligence analysis software to achieve the air quality testing, analysis and alarm. There are five components of air to be detected: carbon monoxide, sulfur dioxide, nitrogen dioxide, ozone and particulate matter. And then we use five gas sensors to convert corresponding gas concentration to analog signals. Then after a signal conditioning circuit, making analog signals access to analog to digital conversion channels of controller. The controller will process signals and display it on the LCD screen, while making remote transmission of data by GPRS network. Then display the measured data on the host computer.**

***Keywords*—Gas sensor Dust Sensor GPR wireless communication**

1 INTRODUCTION

1.1 Research significance

REFERS to the surrounding air around the earth gas, it maintains the survival of humans and creatures. Throughout the atmosphere play an important role in humans and creatures of the air layer is 12 km away from the ground, namely the troposphere, the clean air is made up of 78.06% nitrogen, 20.95% oxygen, 0.03% carbon dioxide and other gases, the three gas make up about 99.04% of all air, other gases sum is less than one over one thousand. Air is one of the necessary conditions for the survival of humans in the human body need 10 ─ 12 cubic meters of air inhaled every day. A person who don't eat in five weeks or five days without drinking water, to be able to sustain life, but more than 5 minutes without breathing air, will die. Air has certain self-purification ability, pollutants by natural or artificial process into the air, by air purification process to remove from the air itself, so as to maintain a clean air [1]. However, with the continuous development of industry and transportation industry, a large number of harmful substances emitted into the air, beyond the self-purification capacity of air, which changes the composition of the air, the air quality is bad, so that our health is affected [2]. Then we need an air quality detection system to detect air quality at any time, is that people can better understand the general levels of air pollution, so as to make preventive measures. According to the national standard, we need to test the content of the following five kinds of air composition, carbon monoxide, nitrogen dioxide, sulfur dioxide, ozone and particulate matter. What has been discussed above, we need to use high-precision sensor to test the air quality at any time, to this end, and we performed the design of the air quality detection system based on GPRS.

1.2 Research status

Existing technology for a small number of individual household family air detector, the late used in decorating a building air quality inspections to assess whether the habitable. There are all kinds of particle detector, gas detector and air are targeted strong individually detection and cannot show that air quality as a whole. For example, the different factory inspection on different gas pollution index. But especially since the recent air pollution fog poison the emergence of the phenomenon such as to make people more need to understand their air quality around [3]. So the air quality detectors should be spread around so that people can understand the change of air quality.

On October 11, 2012, Wu Xiao-qing, vice-minister of environmental protection stressed that the first stage to carry out the new standard of air environmental quality monitoring in 74 cities, to carry out monitoring and publish data on schedule, national and local air quality information release system should be established and make full use of the TV, newspaper, Internet, mobile phone and other media release in time

according to the new standard of monitoring data, the public can conveniently from a variety of sources to obtain information of air environmental quality. To establish a regional atmospheric environmental quality forecast system, improve the ability of risk analysis and early warning information [4]. So air quality detection system is an indispensable tool, conducive to national detection at the same time also bring about air quality reliable message to people everywhere.

2 OVERALL SYSTEM DESIGN

Air quality testing system uses sensor technology, GPRS wireless communication technology and air quality intelligence analysis software to achieve the air quality testing, analysis and alarm. There are five components of air to be detected: carbon monoxide, sulfur dioxide, nitrogen dioxide, ozone and particulate matter. And then we use five gas sensors to convert corresponding gas concentration to analog signals. Then after a signal conditioning circuit, making analog signals access to analog to digital conversion channels of controller. The controller will process signals and display it on the LCD screen, while making remote transmission of data by GPRS network. Then display the measured data on the host computer.

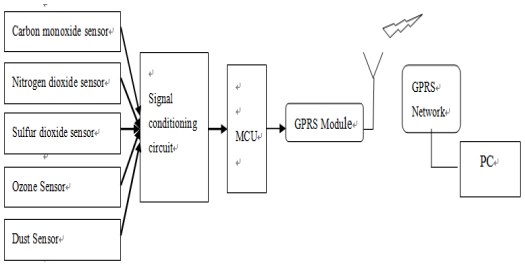

Figure 9 System structure chart

3 SYSTEM HARDWARE DESIGN

3.1 Master's choice

Under the existing laboratory conditions and system functional requirements, we d1eveloped three master's options:

（ 1 ） STC89C52 microcontroller, this microcontroller have fewer resources, and larger size, such as the master system needs to connect A / D converter.

（ 2 ） MSP430F149 microcontroller, this microcontroller’s resource meets the system requirements, has more external pin, and comes with 12 A / D conversion [5].

（ 3 ） STM32F101 microcontroller, this microcontroller has rich resource, complex functions, being applied to this system will result in a waste of resources.

Overview, select MSP430F149 micro- controller as the master controller of system, thus can meet the needs without wasting resources.

3.2 Select the sensor

According to market resources and the function of systems I select the following sensors: MQ-7 carbon monoxide gas sensors, 2SH12 sulfur dioxide sensor, WSP1110 nitrogen dioxide sensor, MQ-131 ozone sensor and DSM501 dust sensor [6].

3.3 Sensor network architecture model

This section consists of three components: filter circuit, to temperature drift circuit and signal conditioning circuit. As follows (Carbon monoxide sensor as an example):

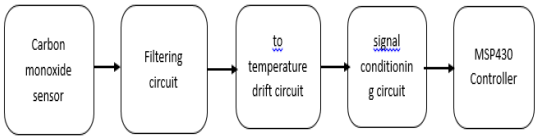

Figure 10 Signal conditioning circuit for carbon monoxide

To temperature drift circuit follows [7]:

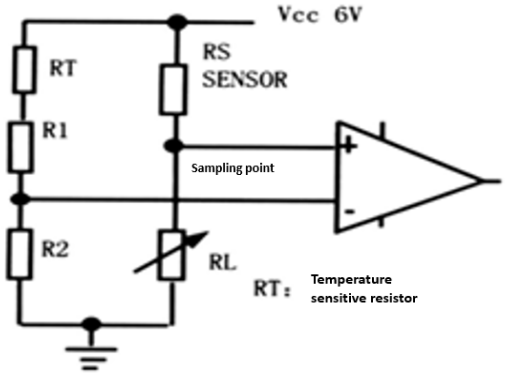

Figure 11 To temperature drift circuit

3.4 Data remote transmission part

To achieve long-distance transmission of data, I chose GPRS module as a medium, GPRS data transmission module has a very wide range of applications. Although GPRS is a transition technology of second-generation GSM mobile communications technology to third-generation mobile communications (3g), it is based on mobile packet data services, has always online、free switching, higher transfer rates, the advantages of cheap and flexible billing. In the case of

3G licenses has not yet been issued, using GPRS module for data transmission has become an ideal choice for the information market. GPRS data transmission module suitable for communication requirements in many areas, improve work efficiency, reduce the consumption of human and material resources, has the advantage of less cost, small size, wide distribution and the use of flexible [8].

4 System Software Design

The software Section consists mainly of signal acquisition sub, data processing subroutine, LCD sub program, data sending subroutine, data receiving and filing of PC. Signal acquisition of which is carried out by msp430f149 MCU owning A/D. Through setting the control register ADC12CTL0, ADC12IE, ADC12IFG and ADC12CTL1, regularly collecting data in data memory ADC12MEM0 ~ ADC12MEM4. Then by formula $N_{ADC}=(4095*(V_{In}-V_{(R-)}))/(V_{(R+)}-V_{(R-)})$ Collected voltage value V_{In} can be calculated. The data processing is based on the sensor output voltage and the measured gas concentration response curve. Take characteristic curve of sulfur dioxide and dust sensor for instance:

Sulfur dioxide sensor response curve follows：

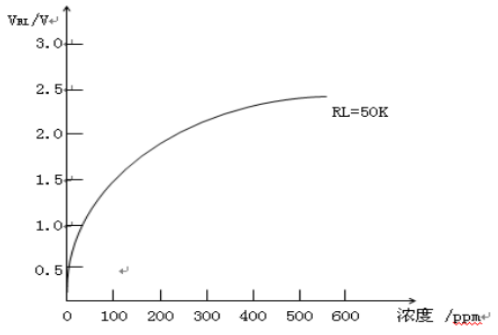

Figure 12 Sulfur dioxide sensor response curve

Voltage value V_{In} collected in the signal acquisition part can be converted into sulfur dioxide concentration of detection Points via this response curve. The output waveform and characteristic curve of the dust sensor follows [9]：

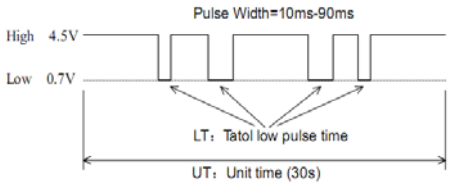

Figure 13 Dust sensor output waveform PWM

Low pulse rate：RT=LT/UT*100%;

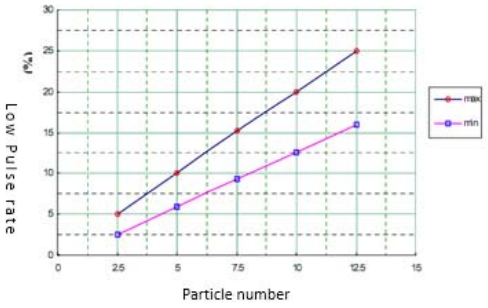

Figure 14 Characteristic curve of the dust sensor

Respirable particles can be calculated by PWM output waveforms and characteristic curve of the dust sensor.

Data transmission can be achieved via GPRS module. It can be achieved using AT commands to send data. Flow diagram follows [10]：

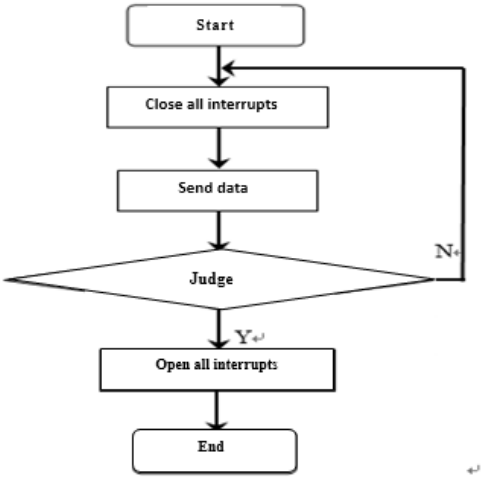

Figure 15 Data flow diagram

5 Conclusion

The remote air quality detecting instrument designed by the author provides a more comprehensive air quality detection and display, versatile and suitable for most environments requirements on air quality testing, and also this detecting instrument itself is small, lightweight, easy to detecting of moving anywhere, operate and maintain, largely to meet people's needs. Thus on people's physical health play an important role.

References

[1] Liu Wei, Han Yu. Discussion on criteria index system of urban air pollution in the haze weather.

Tianjin Environmental Monitoring Center. China Environmental Monitoring 25 No. 3 June 2009.

[2] Zhou Zhibo. Talking about the air pollution index and ways to improve air quality. Environmental monitoring stations of Muping. Yantai. Yantai .264100

[3] Lv Jian, Li Dingkai. Research status and development of respirable particulate matter. Key Laboratory of thermal power engineering and thermal sciences, Tsinghua University. Beijing .100084

[4] Chen Chaochang, Qu Zhangqi, Huang Zuo-hua. Atmospheric suspended particles detection and analysis methods in China. Electrical Engineering Technology. Volume 36, No. 03 .2007.

[5] Wei Xiaolong. MSP430 series single - chip microcomputer interface technology and system design [M].Beijing: Beijing University of Aeronautics and Astronautics Press, 2002.

[6] Cheng Defu, Wang Jun, Ling Zhenbao. Sensor Principles and Applications. Beijing: Mechanical Industry Press, 2008.

[7] Kang Huaguang. Fundamentals of Electronic Technology (part of analog). Beijing: Higher Education Press, 2005.

[8] Lv Xin, Wang Zhong, Design and Implementation of GPRS data transmission module (School of Electrical Engineering and Information, Sichuan University, Chengdu. Sichuan 610065)

[9] Gong Ruikun. Development and application of dust sensors. Dynamic.

[10] Li Changlin. Visual Basic serial communication technique and typical examples [M]. Beijing: Tsinghua University Press, 2006: 56 - 78.

Nuclear magnetic resonance for Any position within the excitation field measuring device design

SUN Hui , HU Xiao-jie , LIU Lei

(College of Instrumentation and Electrical Engineering, Jilin University, Changchun 130061, China)

***Abstract*—In nuclear magnetic resonance (NMR) detection range, according to a study in has the use of coil in the underground tunnels for water inrush detection of excitation field calculation and simulation method, know the geomagnetic field Angle and coil toward the impact on excitation field, in order to verify whether the nuclear magnetic resonance (NMR) stimulate the sinusoidal electromagnetic field in the space in conformity with the calculation and simulation results, the paper design a able to accurately measure different distance, coil toward the impact on excitation field measurement device. Excitation field characteristics for 1 k ~ 3 kHz sine signal. Coil after receiving signals, preamplifier and adopt AD574 to convert the signal collection, main controller AT89C51 for signal processing and displayed on the LCD. After the test, the device is measured by the electromagnetic induction intensity change trend in conformity with the calculation and simulation.**

***Keywords*—magnetic resonance imaging; excitation field; electromagnetic induction**

0 PREFACE

ACCIDENTS in China's coal production is still very serious, ranking second after gas explosion in water column. In recent years , frequent water inrush accident occurred in China's coal mines, tunnels, not only led to a large number of casualties, but also has caused great economic losses , it is important to determine a ahead of forecast method of water gushing in coal mines, tunnels is particularly important. Methods currently used to hang water ahead of the forecast is mostly indirect measurement [1-3], formed a direct NMR method of non-invasive geophysical technology to detect mines, tunnels, water , compared with the traditional method with high resolution, informative and efficient settlement of unique advantages , Underground water is a very promising technology.

Nuclear magnetic resonance excitation field measurements anywhere within the detecting device, is a validation of the experimental device. Has been studied using the coil water inrush detection in the underground tunnels of excitation field calculation and simulation methods and magnetic inclination and coil toward the stimulating effect of [4], design theory of measuring devices to verify and match. Design by receiving coils, and after a simple LC filter, and then through the preamplifier circuit will signal an initial amplification, and then with double quadratic bandpass filter to eliminate interference from other signals, then again with a main amplifier amplifier, next AD conversions, ultimately adopted LCD displays the size of the magnetic field strength. The device can detect 1k~3kHz of low-frequency weak signals, high measuring accuracy, sensitivity is strong, and relatively small and easy to carry.

1 PRINCIPLES AND METHODS OF DESIGN

1.1 Design principles

In accordance with the concept of displacement current, and any change over time of electric field, all fires in adjacent space magnetic field. In accordance with the concept of induced electric field, magnetic field of any changes over time, fires in adjacent space induction electric field. Maxwell's equations showed that electric and magnetic fields of inspiring, interconnected with each other to form a uniform electromagnetic field [5]. Integral form of Maxwell's equations are as follows:

$$\oint_l H \ dl = \int_s (J + \frac{\P D}{\P t}) \ dS \qquad (1)$$

$$\oint_l E \ dl = -\int_s \frac{\P B}{\P t} \ dS \qquad (2)$$

$$\oint_s B \ dS = 0 \qquad (3)$$

$$\oint_S D \ dS = q \qquad (4)$$

To convert the measured voltage value of magnetic induction, conversion formula is [5]:

$$E = NBSw \quad (5)$$

E : Electromagnetic induction electromotive force, unit:V

B : Magnetic induction ,unit:T

S : Coil size,unit:m^2

w : The signal is angular frequency, units:rad/s

1.2 Design methods

Design by receiving coil and coil on a LC filter and preamplifier circuit using OP37 instrument amplifier consisting of 210 times magnification, with double quadratic bandpass filter to filter the signal to eliminate signal interference, and then use the μA741 Signal 500 times magnification, making signals meet the AD conversion range, analog to digital conversion using AD574 chips, take the conversion result to AT89C51 microcontroller processing end LCD LCD display. Hardware design are presented in Figure 1 shows:

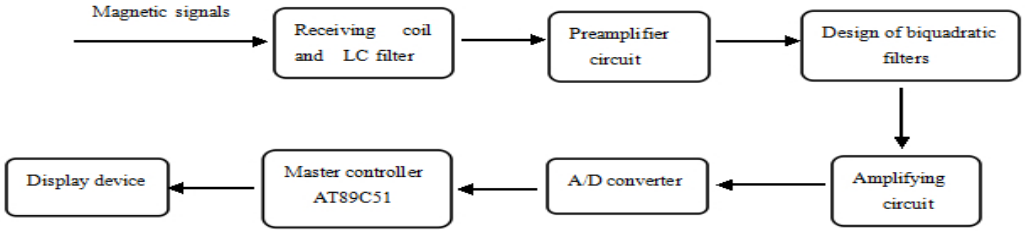

Fig.1 The hardware design

2 HARDWARE DESIGN

2.1 Receiving coil design

Receiving coil with enameled wire, coil winding parameters calculation formula looks like this:

$$l = \frac{0.01 \cdot D \cdot N^2}{\frac{L}{D} + 0.44} \quad (6)$$

l : Coil inductance, unit: micro-Heng

D : Coil diameter,unit:cm

L : Loop length, unit:cm

N: the number of coil, unit: the turn

According to Ohm's law, in order to balance current and the size of the resistor, and selects material conveniently, coil winding, enameled wire diameter is 0.27mm. Because you want to measure the magnetization of longer distances and measuring coils should not be too large, so select the diameter 10cm. Based on experience, coil coil diameter length 0.7 times can improve the Q value, intensive wound 85 when hit, achieve the desired value.

After measuring, get the inductance of the coil 836.5 mH .Coil quality factor is $Q = w\frac{L}{R}$,The coil Q =1.9112.Theory Q greater selective induction coils is considered better, traditional method of winding coil Q is less than 10. Induction coil output voltage signal, due to weak magnetic field to be measured, the Induction coil output voltage signal signal noise is superimposed, for extracting signal from noise, using RLC series resonance circuits to filter the input signal,R1 to receive the equivalent resistance of the coil,L1 to the equivalent inductance,C1 for the equivalent capacitance. Coils and filter circuit connections figure 2 shows:

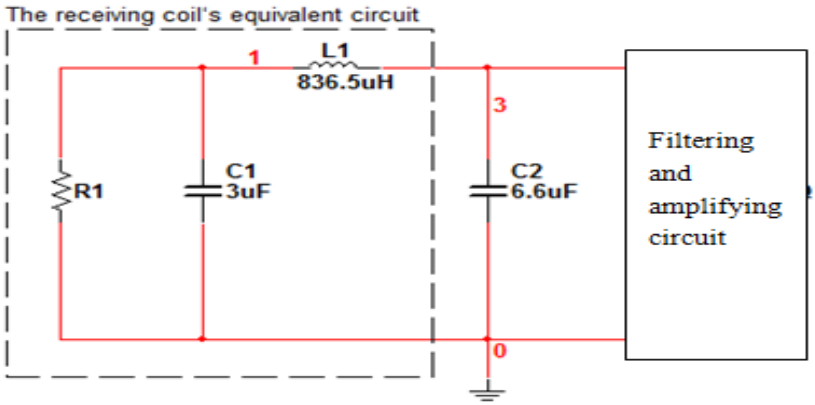

Fig .2 The receiving coil's equivalent circuit

Because of the resonance frequency for 2kHz, LC resonant circuit resonant frequency formula:

$$f_0 = \frac{1}{2p\sqrt{LC}} \qquad (7)$$

Get resonant capacitor for 9.2 mF .

2.2 Preamplifier circuit design

Since tiny signal is received, and some equivalent input noise, overwhelmed by noise in order not to make small-signal circuit, the circuit must be preceded by a grading Amplifiers , as Figure 3 shows. Because OP37 is a high performance, low noise operational.

Is the amplifier also has excellent output drive capability, as well as High small-signal bandwidth, the input offset voltage 10nV,And wide supply voltage range, low prices, so the Choose OP37.

Gain formula is: $A_v = -\frac{R_4}{R_3}(1 + \frac{2R_2}{R_1})$,

Select R1=R3=1K,R2=R4=10K, due to the design of circuit diagram, R7=R3,R5=R4,R6=R2, magnification of 210 times.

Known measurement conditions, the launching coil current is 0.5A Shi, the magnification can guarantee that zoom in close range of induction electromotive force, and will not be made into AD574A voltage is out of range.

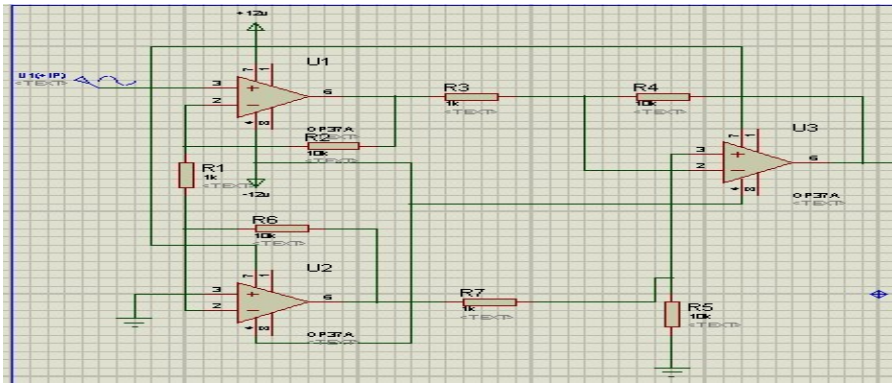

Fig.3 Preamplifier circuit

2.3 Design of filter circuit

Because the signal of a single frequency, using band-pass filter, and second-order filters can effectively filter out noise better,With double quadratic bandpass filter, and the circuit components and easy to adjust, center frequency 2kHz, in order to guarantee the purity of signal, no noise, select the bandwidth 10Hz. According to

$$f_0 = \frac{1}{2pc\sqrt{R_3R_4}}, Q = \frac{R_2}{\sqrt{R_3R_4}}, A_{vp} = \frac{R_2}{R_1}$$

And design requirements for selected R1 =16K,R2=160K,R3=8K,R4=8K, Design of circuit R3=R4=R5=R7=8K. Because LM324 four transports puts the electric circuit has a wide power supply voltage range, small static power, single-supply, low prices and so, so choosing LM324 used in the circuit. Circuit shown in Figure 4 shows:

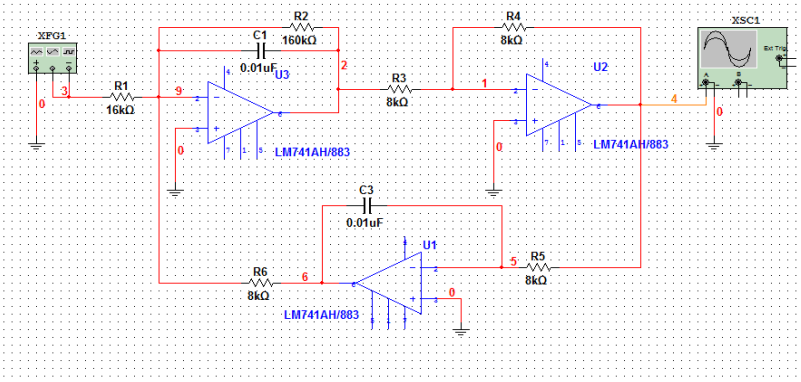

Fig.4 The Design of Biquadratic Filters

2.4 Amplifier design

Because they are not considered common-mode input signals, selecting reverse proportional amplifier circuits, in order to ensure that signals can be in AD within range, preliminary magnified 100 times enlarged 5 times.Two series were magnified 500 times, and then through the voltage follower output. chip choose UA741, the circuit in Figure 5 shows:

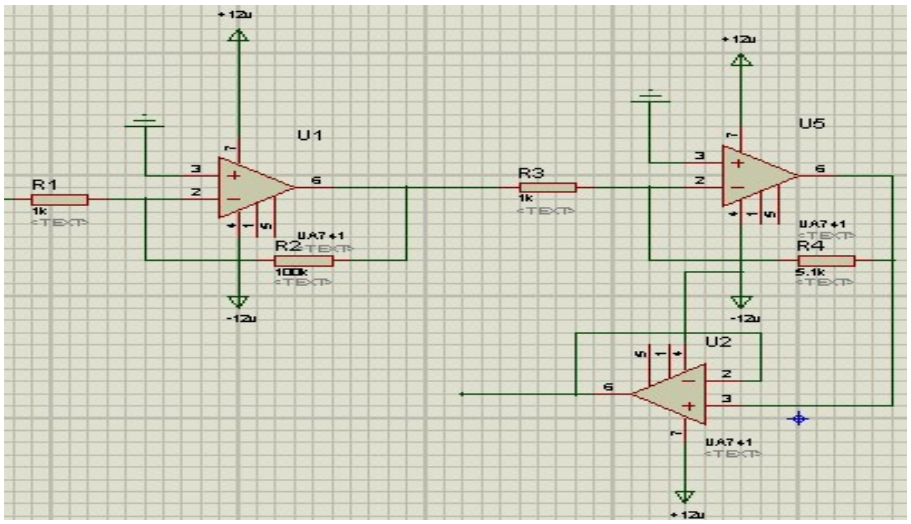

Fig.5 Amplifying circuit

2.5 Design of the analog to digital conversion and display circuit

AD574A Is a single-chip high-speed 12 -bit successive-type a/d converter, convert built-in bi-directional hybrid integrated circuit chips as well as sample and hold, with fewer external components, low power consumption, high precision, and with auto zero and auto-polarity conversion feature, simply add-amount of resistive and capacitive components to form a complete set of a/d converter. 12 -bit mode, the conversion rate for 25us.

Host controller AT89C51, display LCD1602. Circuit shown in Figure 6 as shown:

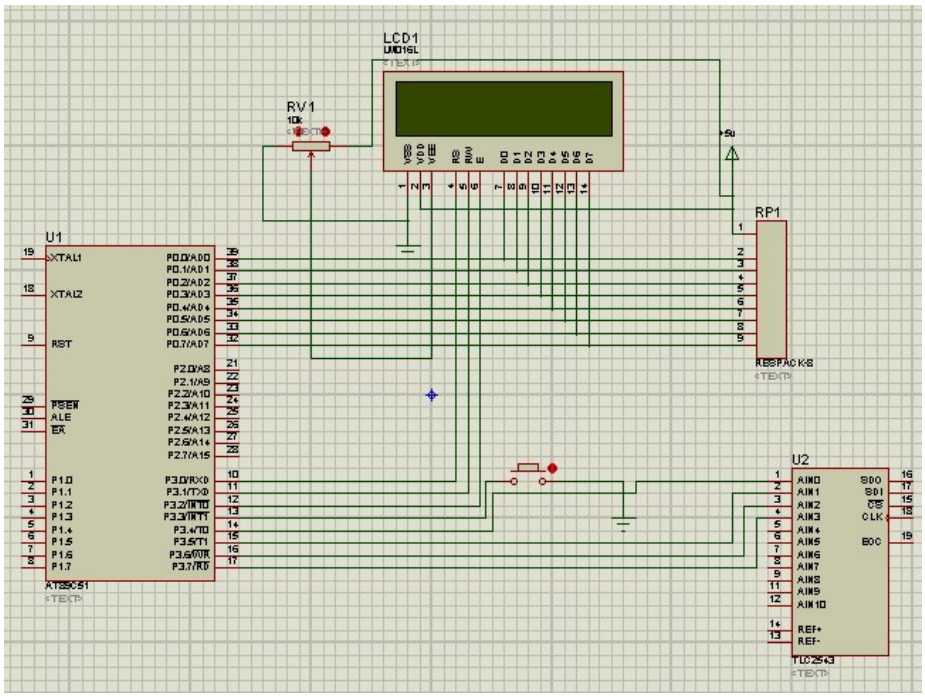

Fig.6 The circuit of Signal acquisition and display

Software design process, as shown in Figure 7 shows:

3 SYSTEM SOFTWARE DESIGN

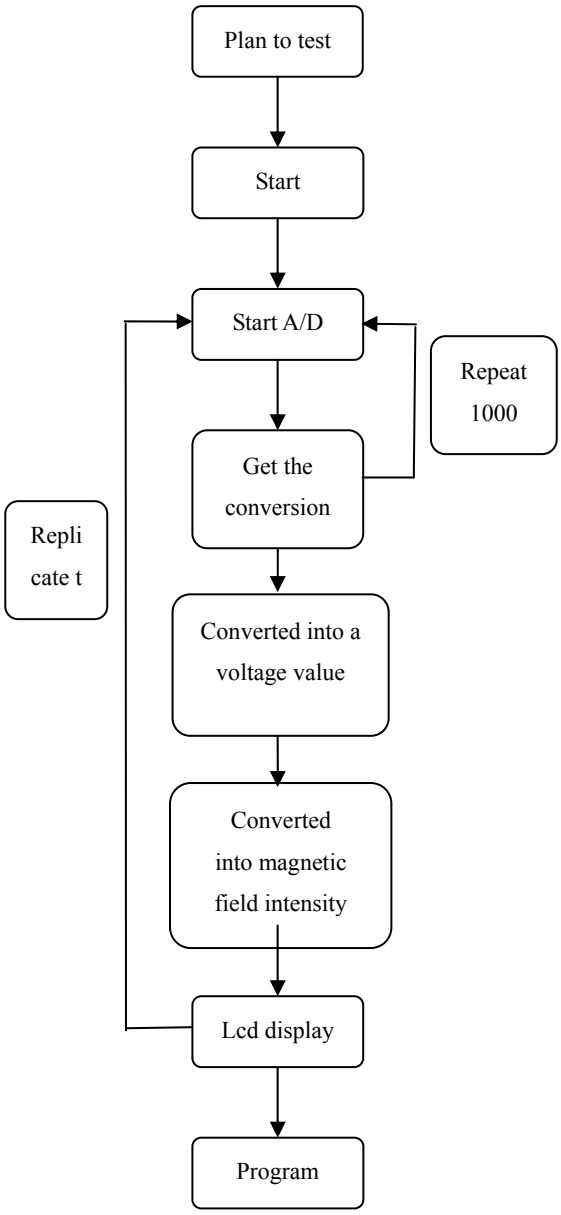

Fig. 7 The software design procedure

Start the a/d converted, after 1000 tests, make 1000 sets of data, derive Max Vmax as well as minimum value Vmin, differential peak-peak value is the measured signals.

4 TEST RESULTS

Launching coil excitation of magnetic field generated $\boldsymbol{B}_T$ With Earth's magnetic field $\boldsymbol{B}_0$ Vertical plane projection of the component $\hat{\boldsymbol{B}_T}$ Fires on NMR is valid [4,6]. Thus $\boldsymbol{B}_T$ AndEarth's magnetic field $\boldsymbol{B}_0$ In a relationship, because detection coil toward the different results $\boldsymbol{B}_T$ With Earth's magnetic field $\boldsymbol{B}_0$ Vertical component $\hat{\boldsymbol{B}_T}$ Projection in different locations, so $\hat{\boldsymbol{B}_T}$ Magnitude and direction in addition to launching coil dimensions, number of turns, current and power conditions impact, also vary with geomagnetic inclination angle and loop towards the change. Here, we studied the receiving coil magnetic variations at different distances.

When launching coil diameter of 1M, current 0.5A Shi, offline at different distances were measured, respectively on the plane of the maximum voltage value, again with this location for the baseline, measured voltage values upwards and left in different places, measurement data as shown in the table.

Table1 Measurement data

Distance from the coil center point (z)	Measure the position (x,y)	Reading (Vp-p)
1.2m	Center maximum value (0,0)	12.8
	The left 30cm(30,0)	12.2
	The left 50cm(50,0)	10.6
	Bias on 30cm(0,30)	11.6
	Bias on 50cm(0,50)	10.0
	Bias on 70cm(0,70)	8.40
	Bias on 90cm(0,90)	6.00
1.8m	Center maximum value (0,0)	7.20
	The left 30cm(30,0)	7.00
	The left 50cm(50,0)	6.40
	Bias on 30cm((0,30)	6.80
	Bias on 50cm(0,50)	6.40
	Bias on 70cm(0,70)	6.00
	Bias on 90cm(0,90)	4.24
2.4m	Center maximum value (0,0)	3.92
	The left 30cm(30,0)	3.88
	The left 50cm(50,0)	3.40
	Bias on 30cm(0,30)	3.90
	Bias on 50cm(0,50)	3.44
	Bias on 70cm(0,70)	2.88
	Bias on 90cm(0,90)	2.16

Table1 Measurement data (Cont.)

Distance from the coil center point (z)	Measure the position (x,y)	Reading (Vp-p)
3.0m	Center maximum value (0,0)	1.90
	The left 30cm(30,0)	1.88
	The left 50cm(50,0)	1.54
	Bias on 30cm(0,30)	1.86
	Bias on 50cm(0,50)	1.52
	Bias on 70cm(0,70)	1.44
	Bias on 90cm(0,90)	1.02
3.6m	Center maximum value (0,0)	0.792
	The left 30cm(30,0)	0.786
	The left 50cm(50,0)	0.712
	Bias on 30cm(0,30)	0.736
	Bias on 50cm(0,50)	0.664
	Bias on 70cm(0,70)	0.600
	Bias on 90cm(0,90)	0.512

Based on the measurement results can be analyzed, different from a central location on the launching coil (the xy plane central location), the magnetic fields are the strongest, as far away from the Centre, magnetic fields weaker, electro-magnetic flux density distribution maps plotted as shown in the following figure:

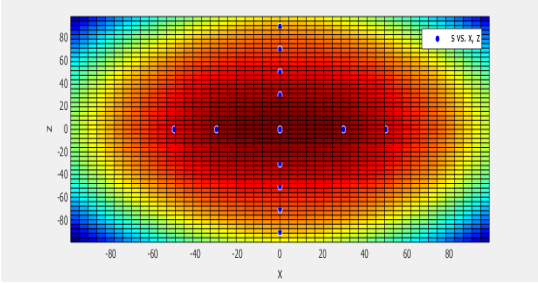

Fig.8 The magnetic field distribution in the XY plane

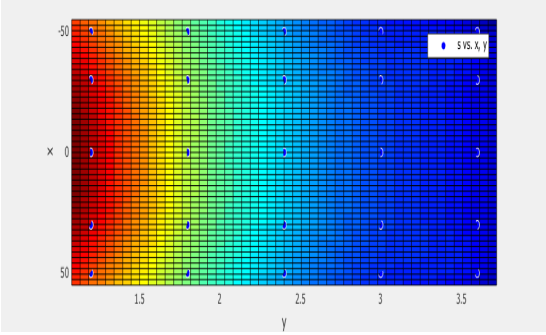

Fig.9 The magnetic field distribution in the XZ plane

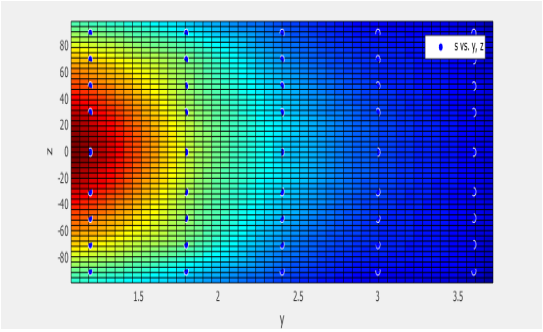

Fig.10 The magnetic field distribution in the YZ plane

5 CONCLUSION

NMR detection range fires anywhere in the field for the distance of the measuring range of the measuring device can be stabilized launch loop 4 times diameter. According to the measurement results of simulation data, emitting electro-magnetic induction coil various distances decreases with distance calculation of trends and match the simulation results. In addition, we measured on the launching coil centerline 4.2m peak peak voltage at 430mv, as far as you can measure to 4.8m, due to interference is large, measured voltage peaks peaks around 190mv or so. It can be seen that the device also has a lot of room for improvement, and poses greater challenges for improving the measurement precision.

References

[1] Zhang Lixin and Li Changhong, Zhao Yu . Research status and developing trend of mine water inrush prediction [j]. China's mining industry,2009,18(1):88-108.

[2] He Jishan, Liu Jianxin . Study on advanced detection technology and its application in tunnel [j]. Journal of Engineering Geophysics, 2004,1(4):293-298.

[3] Zeng Zhaohuang . Advanced forecasting of tunnel seismic emission law [j]. Chinese Journal of geophysics,1994,37(2):218-230.

[4] Wang Yingji, Zhao Yue, Lin Jun . Adit water detection by NMR study of excitation field [j].Progress in geophysical ,2013,28(1):468.

[5] Feng Cizhang, Ma Xikui . An introduction to engineering electromagnetic fields [m]. Beijing: higher education press,2002.

[6] Sun Huaifeng, Li Shucai, Li Xiu . NMR feasibility of deep geological prediction in tunnel [j]. Journal of Shandong University (engineering),2013,43 (1): 92-103.

The Whole Point of Headlights Control System That Can Improve the Driving Safety at Night

Yuhong sun Wenjia jia Rong jiang

(Jilin university instrument science and engineering institute,changchun,130021)

***Abstract*—This paper introduces the design and manufacture of the car headlights intelligent steering system based on MSP430F149.The system has two parts, including level steering and pitch angle adjustment. The system uses WDD35D4 angle sensor as the direction signal of input.It has two buttons,one on behalf of the accelerator ,another on behalf of the brake,what control the speed of input. After the input data has been processed by MSP430, 3128A motor drive makes two stepper motors rotate angle accordingly in the vertical direction and horizontal direction.So it can eliminate lighting corner by adjusting the irradiation angle of light ,makes driving at night safer. The angle value and speed in the operation will be displayed in real-time by LabVIEW.**

Ⅰ.FOREWORD

As the important automotive safety most of components, most of the current automotive headlamp illumination angle is fixed. As the traditional way of lighting and vehicle direction consisten so when cornering light still shine to the front, so that the Inside of the curve will inevitably become the lighting of the dead. Light may be projected onto an oncoming vehicle, we can not illuminate the front, but also cause glare to other drivers, making driving at night there is a big security risk.

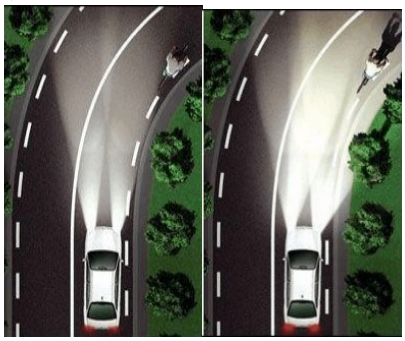

Figure. 1. Comparing before and after the installation of smart lights in the corners

In addition to the highway when the vehicle is traveling or more open terrain, the driver will increase the speed, Therefore, the braking distance will grow, so drivers need to be on the road to predict further afield to ensure road safety.

Therefore, the need to design an intelligent control system auto headlight, used to adjust the irradiation direction lights.

Ⅱ. THE OVERALL PROGRAM DESIGN

The project consists of two main parts, That is, by measuring the angle of the steering angle control level lights and by measuring the speed of vehicles traveling to control the pitch angle of the lights. System block diagram program follows:

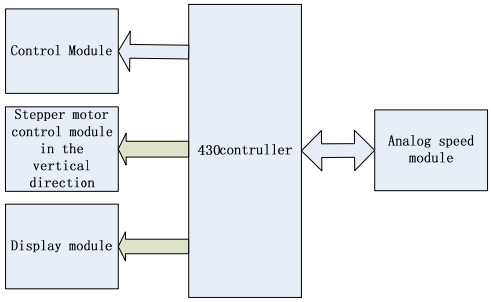

Figure. 2. Tilt angle of the motor control system diagram

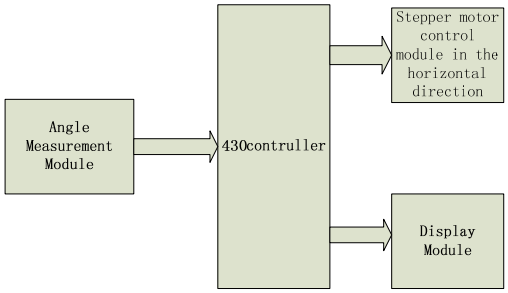

Figure. 3. Horizontal angle of the motor control system diagram

Tilt angle of the motor control system includes an analog tachometer module, speed control module, vertical stepper motor control module, display module; Horizontal angle of the horizontal motor control system comprising a stepping motor control module, display module, the angle measuring module.

III. HARDWARE DESIGN

A. DC Motor Speed Module

DC motor speed module block diagram is shown in Figure 4:

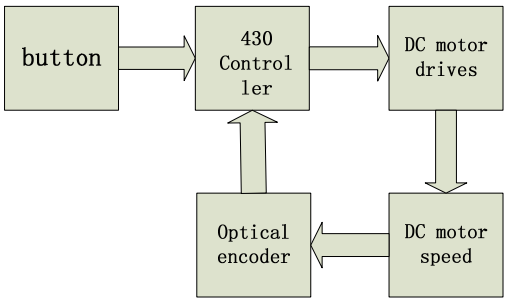

Figure .4. DC motor speed module

Two buttons represent the accelerator pedal and the brake pedal of the car, as the vehicle speed input value. Comes with MSP430 chip timer calculates the speed is increasing or decreasing. Then to control the DC motor speed by controlling the frequency of the DC motor drive signal.

Measured using optical encoder DC motor speed, as the speed of the input signal, the speed value to the 430 controller.

B. Stepper Motor Control Module

Stepper motor driver module includes MSP430F149 chip, 3128A high stepper motor drives, stepper motor 42. The drive up to 128 segments, namely (1.8 ° / 128) degrees, fully meet the design requirements for accuracy.

Table1. Breakdown mode selection table

M1	M2	M3	Subdivision
0	0	0	1
0	0	1	2
0	1	0	4
0	1	1	8
1	0	0	16
1	0	1	32
1	1	0	64
1	1	1	128

Figure 4, the control unit is the input section MSP430 chip, then two pulse signals, the direction of the signal input connection 3. Public segment connected to the chip leads to 3.3V power supply, DC + and DC- can access the DC 10 ~ 36V.

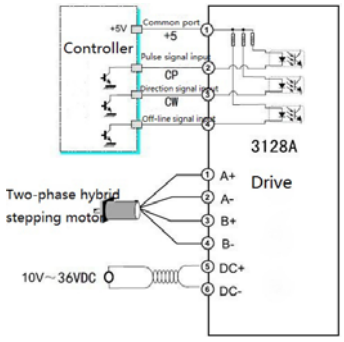

Figur.5. 3128A High stepper motor drive hardwear Connection diagram

IV. THE SOFTWARE DESIGN

A. Display Module

The display module includes LABVIEW serial communications and display module. Using MAX232 level converter chip 430 serial communication between the controller and the host computer, Mining and packaged by the sensor signal of the direction and speed of the signal processing is sent to the PC via serial communication, And displayed on LABVIEW software on the PC.

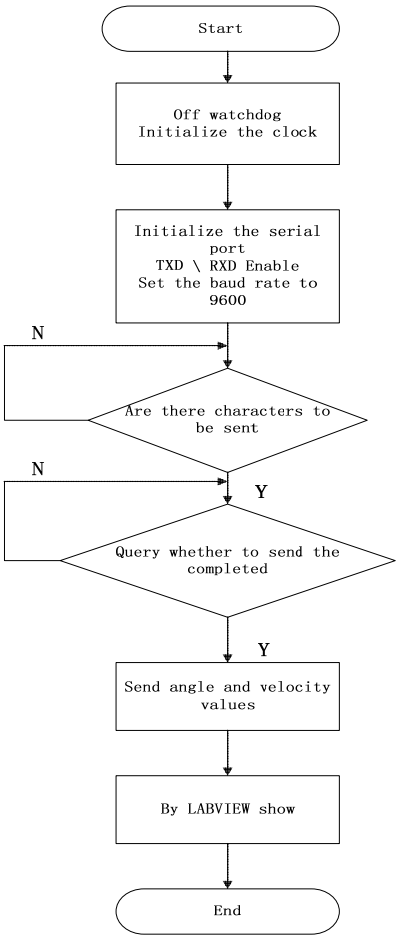

Figure.6. Display module program flowchart

B.Angle sensor module

Vehicle turning direction and angle are controlled by the steering wheel, we use an angular sensor to get the angle value. After processing by ADC12 built in the MSP430, we will get the steering wheel steering angle.

We need to collect only one channel signal that comes from the angular displacement sensor signal,so you can choose single channel sequence conversion mode.

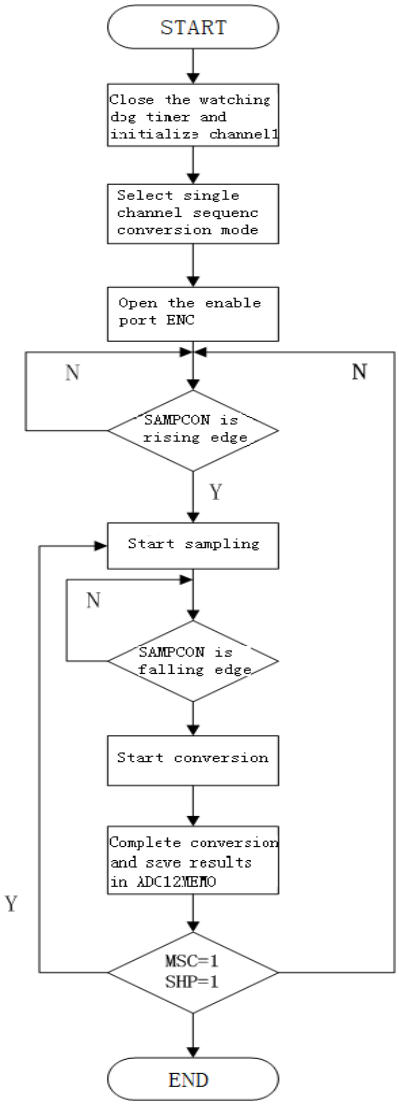

Figure .7. The flow chart of angle sensor module

Ⅴ.MEASURING AND ANALYZING THE RESULTS

Setting the steering wheel angle is 360 degrees, i.e., the left or right turn 180 degrees.The actual steering wheel inside the vehicle is generally the largest angle (35 ~ 40) ° about,Here steering angle set headlights 40 °, ie left or right to turn a maximum of 40 degrees each.Lights should be turned to the relationship between the degree of steering angle proportional.

The car model is fixed at a point,put a piece of paper in 25.5cm away vertically. When light swing or pitch, we can determine its swing angle by observing the location of light spot.Then test its performance. Test results as follows:

	The distance betwee the lamp and the graph paper (cm)	Expect ed turn angle (°)	Expecte d spot offset distance (cm)	The actual spot offset distance (cm)	The actual turn angle (°)
1	25.5	0	0	0	0
2	25.5	9	4.04	4.15	9.24
3	25.5	18	8.29	8.50	18.43
4	25.5	27	12.99	13.25	27.46

Ⅵ.CONCLUSION

Through the test we know, the precision of the system has reached the expected standard, so it can satisfy the actual work needs.And through the display module we can see the vehicle's running status intuitively. As a result, the system has achieved the goal that can reduce the lighting conner, improve the traffic safety.

References

[1] Ting Li.The intelligent car lighting technology [J]. Journal of automotive electronics.31.2011.

[2] Wei Wang. The research of automobile headlight servo steering control and dynamic characteristics simulation [D]. Wuhan polytechnic school.2012.

[3] Xinliang Liu;YongBin Chi. AFS headlights servo steering law research [A]. Mechanical design and manufacturing period.8.August.2011.

[4] Haiye Qiao. Light rotation system based on adaptive control design [A]. Computer technology and development Vol. 22 7 July 2012

[5] Yuming Wei ;Xuan Wu;Yafei Ou. The car intelligent servo positioning and analysis of the steering lighting system [J]. Science and technology. 2008

[6] Di Wu. Car headlights active safety research [J]. Science and technology monograph. 2011

[7] Y. H. Xu; M. Ahmadian . Study on the performance of active front steering system . International Journal of Automotive Technology 2013.8

[8] H Hogrefe . Adaptive Frontlighting Systems for Optimum Illumination of Curved Roads, Highway Lanes and Other Driving Situations . S.A.E. transactions .2000.6

Study on electro-control system for home security

Liu Hongwen; Zhang Lin lu; Li Xin; Liu Changying

(College of instrumentation and Electrical Engineering, Jilin University, Changchun130021)

***Abstract*—The safe use of electricity control system is installed on a home power lines, used to detect security of household electricity and automatically cut off electrical devices with problems and can be remotely controlled. In the household electricity security system, at first to use the current sensor to monitor the total household electricity current in the circuit, when due to a short circuit or overload the circuit causes the circuit current is too large.the system will automatically cut off the problematic branch to maintain the remaining working properly with appliances, but also to protect the safety of household electricity lines; At the same time send the probable point of failure to the user's mobile phone terminals via GSM wireless module, so that people can timely maintain, further eliminate safety hazards. People can remote control home appliances via mobile terminals which greatly facilitates people's lives.**

***Key words*—electricity Remote control GSM Household electricity**

1 INTRODUCTION

WITH the continuous improvement of people's living standards, and electrical equipment also increased safety for household electricity line also had the more severe test. Common faults of electrical wiring: insulation damage, poor contact, overload, breakage, lack of space, protective conductors for live, these failures may lead to power outages, electrical shock, fire and other accidents. For example, wiring insulation damage based on the different levels of damage, short-circuits, leakage may occur both hazards. Insulated full damage will cause a short circuit. Short circuit, current flows through the circuit to increase several times to 10 times the number times the normal operating current. The calorific value of the wire is proportional to the square of the current, leading to sharp increase in heat, a short period of time may cause a fire burning. ARC discharge and high temperature arcing would burn nearby personnel may also directly cause a fire; In addition, under short-circuit conditions, some with dangerous fault voltage bare conductors, may give a fatal electric shock. If the insulation is not completely broken, will lead to leakage, leakage is the most common cause of electric shock accident. Leakage of local heating, local temperature too high may lead directly to a fire, may also prevent further damage of the insulation, form a short circuit and cause a fire. If a grounding conductor, the heat produced by the Earth current and arc, could lead to a fire at the ground. Contact contact resistances caused by poor connection increases, under the action of electric current produces heat, can make metal discoloration or even melting, it is easy to become an ignition source, causing electrical wiring insulation, close to combustible materials and combustion of heavy combustible dust accumulation. When the wires heat proportional to the square of the current, heat often exceeds the allowed limits, ranging from accelerated aging, resulting from the heavy insulating layer the burning fire. Overload or increases the voltage loss on the wire. Disconnection could cause a fault line, mixed and multiple accidents such as short circuit, broken wires fell on the ground or the grounding conductor may result in electric shock accidents; produce sparks when disconnecting or pulling off the wire, can ignite nearby combustible materials.

With the rapidly growing popularity of GSM mobile communication network and intensified competition, development and application of new technologies and services have been referred to a very important position.

For household electricity supply line fault detection and protection of many studies, direct with electrical short circuit, overload, overpressure protectors, easy to damage, there is no hint feature, not human. For this design more humane, intelligent, and added GSM remote control of home electrical safety control

system.

2.SYSTEM INTEGRATED DESIGN

Home security system can be divided into two parts, the system block diagram is shown in Figure 1

Safe use of electricity: electric current sensor detection circuit, detects the signal into the controller and safety values in contrast to cut immediately to monitor excessive current issues branch, and guarantee the remaining branch appliance is working properly, and by launching the receiver handset and send questions to the user information to facilitate timely repair

Remote controls: mobile user terminals can be done by launching the receiver to the controller for an order, it can be turned on or off for a particular electric, to conserve electricity and to facilitate people's lives.

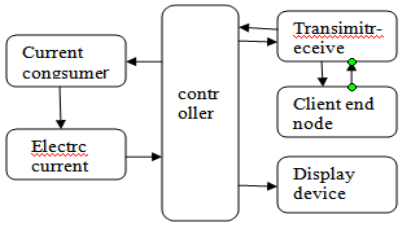

Figure 1 system integrated design

3 OVERALL SYSTEM DESIGN

3.1 congtroller

SCM is a TI company started in 1996 to market of ultra low-power microprocessors, in addition he also integrates a number of modules, allowing a MSP430 chips to complete the chip to complete features, greatly reducing the size and cost of the product. It of main features: low power voltage range, 1.8~3.6V; super low power, has 5 species low power mode; flexible of clock using mode; high-speed of operation capacity, 16 bit RISC schema, 125ns directive cycle; rich of features module, MSP430 chip Shang including JTAG interface, simulation debugging through a simple of JTAG interface conversion players on can convenient of achieved as set breakpoint, and single step Executive, and reads and writes left-players, debugging; fast flexible of into way, To the CPU via JTAG and BSL in two ways in a program.

Based on its high speed, low power consumption, fast and flexible way of debugging, 0~5V voltage and current sensor output values needed for AD conversions, MSP430F149 micro channel is integrated in 10-14-bit AD converter, eliminating additional AD conversion device.

3.2 current sensor;

Current sensor MIK-DJI-0~50A transducer for alternating current sensor using the current transmitter can be measured directly converts AC current in the primary circuit by linear DC 4~20mA output (by 250 ω resistor converts DC 1~5V) constant current loop standard signal after AD conversion continuous conveyor onto a single chip. Former Vice height electric current transducer insulated isolation, two-wire and three-wire output connection mode. Wire system transmitter with auxiliary power supply +24V the positive end and negative end and signal outputs.

-Current transmitter performance advantages:

(1)It less vulnerable to parasitic thermocouples and pressure drop and drift along the wire resistance effects of transmission lines is available very cheap thin twisted wire;

(2)It is in current source output resistance is large enough, by the magnetic field coupling the voltage sense wire loop will not have a significant effect, as sources of interference caused by electric current is extremely small, twisted resistance to reduce interference;

(3)Permissible cable length longer than the voltage telemetry system farther;

(4)4mA to zero level, making judgments-circuit or sensor damaged (0mA) is very convenient;

3.3 transmit-receive unit

New version of the transmit-receive unitSiemens industrial GSM module is an industrial grade GSM modules support Chinese SMS, It work in EGSM900GSM1800 double band, power range for DC 3.3~4.8V, current consumption--Hibernate State for 3.5mA, idle state for 25mA, launches State for 300mA (average), 2.5A peak; can transmission voice and data signal, power in EGSM900 (4 class) and GSM1800 (1 class) respectively for 2W and 1W, through interface connection players and antenna connection players respectively connection SIM card reader and antenna. Via AT commands can be bi-directional transmission instructions and arrays, selectable baud rate of 300B/s~115kb/s,Format it supports Text and PDU

SMS (Short Message Service, SMS), may be achieved through AT commands on and off signals to restart and failback. As main processing core baseband processor of the TC35i GSM terminal for voice and data signals, and covered with a cellular radio frequency equipment for all analog and digital functions

4 System Software Design

Software part of the system mainly include data acquisition, data processing, display, data sent and received. Signal acquisition of which is carried out by msp430f149 MCU owning A/D. Through setting the control register ADC12CTL0, ADC12IE, ADC12IFG and ADC12CTL1, regularly collecting data in data memory ADC12MEM0 ~ ADC12MEM4. Then by formula $N_{ADC}=(4095*(V_{In}-V_{(R-)}))/((V_{(R+)}-V_{(R-)}))$ Collected voltage value V_{In} can be calculated. Remote sending and receiving of information is key.

SCM can use right AT instruction initializes the TC35 module and receive short messages. To control three-short messages: Block, PDU mode and Text mode. Use Block mode require cell phone manufacturers to provide driver support. This system uses PDU mode SMS sending and receiving. Single chip computer controlled through the following series of AT commands for SMS. Figure (4) for the process of transmitting and receiving Note the short message center number might be different due to different mobile phones or in different regions. If you read the short message service centre using the command AT + CSCA =? < CR >, the module should return < CRL f > + CSCA: ″ 8613800531500, ″ < CRL f >.

Message receive: (3) prompted automatically sets the short message arrives AT + CNMI = 1, 1, 0, 0, 1 < CR >, set the correct module returns < >OK< CRL CRL f f >. Set this command makes the module in the short message upon arrival to the MCU sends commands < CRL f > + CMTI: ″ SM ″, IN2DEX (information store) < CRL f >. After receiving text messages short messages to arrive, SCM can receive instruction < CRL f > + CMTI: ″ SM ″, INDEX (where information is stored) < CRL f >, AT+ CMGR = INDEX < CRL f >, the module returns, just received a short message is read.

5. Conclusion

Tested monitor line current access total power at around 1.5%, and can better achieve overload power users remote control functions. This design system was installed on the home line to test the safety of home energy, detect and control devices, and can be remotely controlled, greatly facilitates our lives, conforms to the modern society moved closer to intelligent direction, improving the quality of life of the family electrical safety issues of great significance to the promotion.

References

[1] Cheng Defu, Wang, Ling Zhenbao. principle and application of sensor. Beijing: China machine press, 2008.

[2] Cornwallis light. electronics (analog section). in: higher education press, 2005.

[3] Wang Jimei. Successful development of short-circuit current limiting switching devices [j]. grid technologies, 2004 (10).

[4] Zhao min. short-circuit protection principle of power system based on current rate of change [j]. grid technology 2008 (04)

[5] Li Changlin. Serial port communication technology and typical examples of Visual Basic [m]. Beijing: Tsinghua University Press, 2006

[6] Wu Yutian. TC35 GSM module and its applications [j]. the computer measurement and control, 2002, 10 (8)

[7] Yang Peng, and Yang Sui. using GSM network and wireless sensor network design and realization of intelligent home system [j]. Micro-computer information, 2012,28 (10)

[8] Kaplan E D. Understanding GPS: principles and applications [M] .Boston : Artech House ,1996. 75～132.

[9] Spilker ,JrJJ . GPS signal structure and performance characteristics[J]. Nav-igation , 1978 ,25 (2) :121～146.

Design of Simulation System for Remote Signaling and Telemetry of Computer Relay

Zhao Yifei; He Xiaotian; Li Yongheng

(College of Instrumentation and Electrical Engineering, Jilin University, Changchun 130012,China)

***Abstract*—With the development and the extensive application of smart grid, traditional relay protection devices have been unable to achieve remote monitoring, control and other requirements. In order to overcome the defect of traditional protection devices of power system，microcomputer protection device combined with remote signaling telemetry has been widely applied in the smart grid. The system is based on the basis of 51 SCM, achieving the computer monitor and data collection by the technology of serial communication. Using the SCM LCD to display the real-time data and monitor the status of the circuit. Design the interactive interface by Visual Studio. In addition, running and canceling the system, setting and changing the data by the method of remote signaling and telemetry. This paper presents the design of hardware and the program of software functions and simulates the functions of the system of microcomputer protection. The remote control of the device is really important for the stable running of the power system, providing reliable power quality and voltage stability.**

***Keywords*—microcomputer protection; remote signaling telemetry; Visual Studio**

0 FOREWORD

WITH the proposed，research and application of the smart grid， constantly enhance the level of power system application ability，we also need to present new challenges to power system protection device and requirements simultaneously. In order to guarantee whether we the electric components work normally and ensure the stable operation of power system，we need to understand the operational status of the protection device better. Microcomputer protection device has become the mainstream of relay protection and network and it can provide the mutual connection and the channels of communication for the modular distributed system. Networks can bring a new and innovative idea for microcomputer relay protection development and design. It will greatly simplify the hardware design and enhance the reliability of the hardware. With the rapid development of power system and computer technology and the progress of the communication technology, relay protection technology will face the trend of further development. The foreign orientation of relay protection development is to be computerization , networked and integration (measurement, control, protection, integrate data communication)and artificial intelligence. In a word, delay protection will be more wildly used with the development and progress of all kinds of technology.

1 THE OVERALL DESIGN AND WORKING PRINCIPLE

To design a simulation of power system microcomputer protection device prototype hardware, complete remote operation and control system. The most important is to achieve the remote settings and modification according to the instruction of the software. Then display the real time parameters.

The first is the completion of the convergence and communications between the computer and hardware devices, Hardware device can receive and identify the directives issued by the computer, it also can automatically accomplish these instructions for action（LCD display， data storage, and so on）. In the aspect of hardware, design "distance/local" circuit control hardware devices，device with the computer through the serial port for data transfer. As for software , based on the Windows Form (c #) design human-computer interaction interface，use C/C + + language. Write single-chip microcomputer control program （ Remote control and communication functions）. Computer as the PC, 51 single chip microcomputer as the machine， through the human-computer interaction interface and the serial port communication single to achieve the

communication between PC and MCU，PC sends instructions to MCU data, MCU makes different response by judging the PC's instructions. The above can achieve the purpose of the experiment remote software control hardware.

2 HARDWARE DESIGN

2.1 A serial port communication solution

In the aspect of serial communication， 51 single-chip microcomputer has a special buffer， Serial port to send and receive buffer，namely, SBUF buffer. SBUF buffer can receive data and send data at the same time. However, the serial receive buffer and send buffer are independent in physics. It is attentive that the receive buffer can only read but not write. On the contrary, the send buffer can only write but can't read. According to this, we design the single-chip microcomputer serial port TXD MAX232 chip and RXD pin connection，then connect to the 9 needle， make the single-chip microcomputer and computer serial port have a consistent level， constitute a standard RS-232 interface ， realize serial communication between single-chip microcomputer and computer. The concrete method is using a MAX3221 chip TXD come from single chip output signal level after converting to the PC，sending a signal sent over from the PC to the RXD. Figure 1 shows the design of RS - 232 interface circuit connection diagram

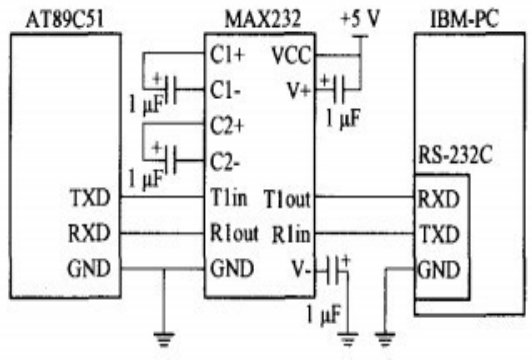

Figure 1 PC and single chip microcomputer communication interface circuit design

2.2 Local control circuit

This part mainly includes the data acquisition module, A/D conversion module, control module, display module and other modules. Take AT89C51 as the control module，the core of ADC0809 as A/D conversion module, ADC0809 has 8 analog input ports, through the C, B, A three address input and achieve select one way to complete the conversion from 8 path. If change the address if the 3 bit input in turns, then we can measure the input voltage of the 8 ports. LED dynamic display uses software decoding， it can choose 8 roads to circulate through the key module operation as well as choose one of the single road to show, all these can realize the circuit of data display and monitoring. Figure 2 shows the local circuit diagram of the circuit.

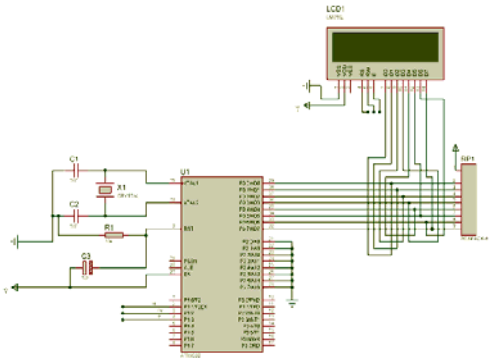

Figure 2 the circuit connection diagram

2.3 The distance control circuit

Remote control circuit needs to realize the remote communication between MCU and PC. The design includes two big modules: sending and receiving. The sending part includes RS - 232 interface circuit, MAX232 interface circuit referring to the corresponding pin is linked together and the corresponding software program into circuits. When the circuit is relatively independent, it can be directly call circuit parameter values, its influence and interference is low. After meeting the requirement of transmitting and receiving module, we can adjust control independently. Both by sending parts to set parameters and modifying threshold operation to control the MCU module, and can receive real-time data by receiving module, monitoring circuit, realizing the PC to the remote microcomputer control. The specific circuit has shown in figure3.

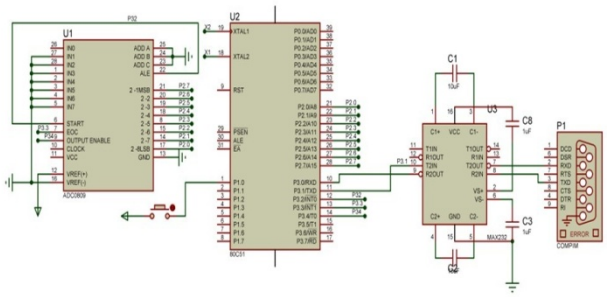

Figure 3 remote control circuit

3 THE SOFTWARE DESIGN

The main program of the system includes electricity initialization, self-check, interrupt (data acquisition), fault detection, alarm display and circular self-checking, etc. After the system power-up or manual reset, initiate first. During the initialization process, shut global interrupt, interrupt enable, interrupt flag are set to 0. Initialize PIE, PIE interrupt vector table, as well as peripherals and resources required configuration (including the initialization of each compilation amount of register initialization, various flag is cleared, etc.).

After the initialization, here comes a self-test, including the RAM area to read and write checks, value checks, input and output circuit self-test. If the self-test has no error , then open interrupted to achieve the sampling and serial communication functions (by the data sampling procedures, and serial communication program and PC communication program and several subroutines). Next it needs to determine whether a fault exists, and if so, the amount of output through the switch protection, and alarm and fault information is displayed on the LCD screen; If there is no fault, the cyclic self-test, continue the previous work.

3.1upper computer interface design

In the design, Visual Studio 2005 is used to design and write the upper computer interface. The design requires adding button controls that is the most important part is using Serial Port controls to debug serial port. As long as you set up the baud rate of serial port communication, data, and then open the serial port, you can realize all functions. Next is the program serial port communication:

```
spCOM.PortName = "COM1";
spCOM.BaudRate = 19200;
spCOM.DataBits = 8;
spCOM.Open();
spCOM.Write ("6");
```

3.2 Design of single chip microcomputer serial communication program

This design requires us to realize serial communication of upper computer and single chip microcomputer. The upper computer sends the command while microcontroller can take orders and make corresponding action. So the key point of the single chip microcomputer serial communication program design focuses on the single chip microcomputer serial port receiving part. It needs a serial port initialization and the initialize needs to establish communication baud rate, single chip microcomputer works by timer way, because this project only needs the single chip microcomputer to accept data, so the next is the main serial communication program of single chip microcomputer :

```
while(1)
{
  while(RI==0);RI=0;
  b=SBUF;
  if (b==0x36)   p16=0;
}
```

4 CONCLUSION

This project has completed the design and implementation of microcomputer remote control system based on the serial communication between computer and single chip. The study of reclosing device remote control system has very important significance for the stable operation of power system, reliable power quality for power grid and the stability of the voltage . At the same time, the circuit system also has important significance when the malfunction occurs and resumes. With the development of computer, the highly intelligence and highly integrating of grid technology have become a very important aspect. Although the study technology has the limitation, the study still has very important significance because of the same direction with the

development for smart grid.

This design has a very wide application because it implements the control-by using upper machine and lower machine communication .Design a kind of instrument needs communication with the computer because the scientific design is designed for users.

In order to simplify the operation, serial communication between upper machine and lower machine has solved the problem. In addition, the use of relay also has great significance, the connection of electronic circuit and control circuit not only have good control, but also achieve good isolation by relay, because the normal operation of the high voltage large current circuit may not require people to control directly. The interaction between a man and a computer will become more and more important with the development of science and technology.

Reference

[1] Wang liang, Zhao Wendong. The present situation and development trend of microcomputer relay protection [J]. Science and technology development and economic information,2006,16(18)：150-151.

[2] He Jiali Present situation and the development of power system relay protection technology [J]. Electric power in China.1999,32(10)：39-40.

[3] Gao Liang Power system microcomputer relay protection [M]. China electric power press

[4] Tian Ji Cao Junbiao, Wang Fulin. A general microcomputer relay protection device development [M]. Proceedings of the annual meeting of the relay protection and automation industry in China. 2007:119-122

[5] Luo Shiping. Microcomputer protection principle and device [M]. China electric power press, 2001

[6] FengMingBao, walker. New type of microcomputer protection device of hardware and software research [J] shandong university of science and technology, 2006.

[7] Xu Jianan. Microcomputer relay protection power system [M]. Beijing: China water conservancy and hydropower press, 2007.

[8] Li Youguang Lin Dong. Power system relay protection principle and new technology [M]. Beijing: science press, 2003.

[9] Ding Gang. Power system microcomputer relay protection simulation research [D]. Nanjing university of science and technology, 2007.

[10]Cai Xiaoye. Wide-area relay protection system based on grid computing research [D]. Shanghai jiaotong university, 2007.

[11]Lan ZhiHui,Xu YongHai, Xiao Xiang-Ning . Research of the Influence to the Pickup Unit of Microcomputer relay protection from Electric Locomotive Loads. 2008 IEEE Electrical Power & Energy Conference，2008，32：1-6.

[12]Gangjun Zhai,Ying Wang,Longzhi Li,et al.Development of Power System Relay Protection Experiment in E-Learn[J].Procedia Engineering，2012，29：2975-2979.

[13]Liu Yucheng,Liu Yubin.Design Strategy of Anti-Electromagnetic Interference for Microcomputer Relay Protection System[C].Information Technology and Applications (IFITA),2010，401331：180-183.

[14]WANG HaiZhu, CAI ZeXiang, SU ZhongYang,et al.The Analysis of Relay Protection Communication Mechanism Based on IEC61850[C].The International Conference on Advanced Power System Automation and Protection，2011，510641：223-227.

Intelligent House Leakage Detection and Alarm System

Li Suyi, Wang Duoqiang, Bai Yang, Zhang Weijie
(College of Instrumentation & Electrical Engineering, Jilin University. Changchun, Jilin, China)

***Abstract*—This study designs a kind of discontiguous reflected liquidometer system which has the characteristics of low cost, high-resolution, high sensitivity and high anti-interference capability. It fits for the minimum liquid height and can be applied to the house-leaking. The photoresistances that are linear set on the liquidometer are used to receive the laser signal to improve the resolution. The discontiguous reflected liquidometer system consists of sensor, MCU, GSM and power supply. The hardware circuit design, software design, detection principle and testing result are introduced. By data analysis we can get the conclusion: sensor resolution 3mm, average error 0.19mm, standard error 0.51mm. This system can measure several kinds of house-leaking and run normally at least 72 hours.**

***Key words*—house-leakage, discontiguous, reflected, GSM, liquidometer**

0. INTRODUCTION

THE house-leaking happens frequently and causes property loss especially in apartment. It may cause other secondary disaster such as fire, electric shock and short circuit. The technology about intelligent alarm system is mature but lack for a kind of system that is cheap and high-resolution. In order to solve the problem, we develop a system that can measure the liquid level fast, accurately, conveniently and can be used in ordinary family.

There are several detection methods to measure the liquid level: sonic detecting technique[1], liquid short-circuit method, flow detection method, Magnetic Float Gauge[2] and Diffused Silicon Pressure Transducer technique[3]. But all of these instruments must contact the liquid directly that can be covered by the dirt leading to the inaccurate measuring result.

And the majority of current non-contact liquid level detection devices use ultrasound as propagation medium. The devices always get bulky, expensive, complex and can't be used in common family. Although the non-contact level detection method[5] based on the refraction of light can achieve the aim, the liquid which is measured must be transparent and depends on the optical imaging lens. In order to achieve the rise or fall of the water level , the linear array CCD [6] or the linear arrangement of fiber optic sensors [7]is used, so that the detection resolution is improved, but the cost is greatly increased.

In conclusion the contacting liquidometer has the defect of easy hanging dirt, short working life, high price etc. And the caustic liquid can't be measured. The refracted detection equipment can only measure the transparent fluid and depend on the optical imaging lens and its anti-interference capability is weak. In order to overcome the defect talked above, this study designs a kind of discontiguous reflected liquidometer system which has the characteristics of low cost, high-resolution, high sensitivity and high anti-interference capability.

The application of GSM technology makes it possible to detect the house leakage and alarm in distance when no one in the house. Once the water-level changes, the system can measure the signal immediately and send the alarm message to the user's mobile phone.

1. HOLISTIC STRUCTURE

The holistic design is shown in Figure 1, the system is consist of discontiguous reflected sensor, MCU, GSM, LCD screen and power supply(is not shown in the figure). The output of the discontiguous reflected sensor is connected to the MCU input, the outputs of the MCU are connected to the LCD screen and the GSM. The sensor will send the water-level information to the MCU when it detect the water. Then the MCU module classifies and treat the information to judge the

water-level and control the GSM to send alarm message. The LCD screen display the water-level instant.

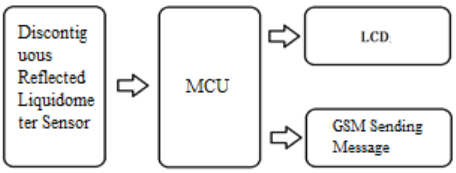

Figure 1. Fundamental Structure

2. THE HARDWARE DESIGN

2.1 The design and manufacture of the discontiguous reflected sensor.

Seen in Figure 2, the schematic diagram shows the theory of the discontiguous reflected sensor: when the laser diode send laser toward the liquid surface as a certain angle, the reflection happened. The reflected laser spot will move toward the laser diode parallelly as with the rising of the liquid. On the other hand, if the liquid level drops, the laser spot will move closer to the laser diode parallelly. The photoresistances are set on the trajectory of the spot linearly to perceive changes in light intensity. By measuring the logic level of the photoresistances, we can know the difference of the liquid level.

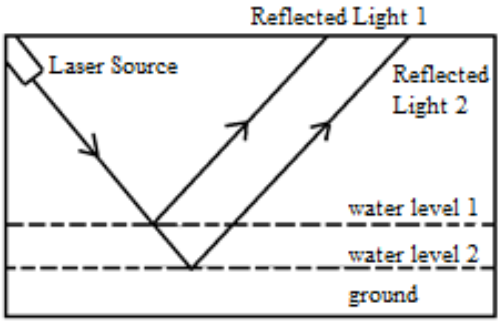

Figure 2. Collecting Theory

However, the diffuse reflection of the laser and other light source cause interference so that the photoresistance can't be used as the device to measure the liquid individually. To meet the requirements of the high-resolution, high sensitivity and high anti-interference capability, the receiving pipe is used. It obviously improves performance that is required and can be applied to detect the house leakage. The photoresistance is mounted in the receiving pipe to dampen the interference caused by the diffuse reflection of the laser and other light source so that the anti-interference, resolution is improved and the resolution ratio has reached 1 mm. The figure 3 is the discontiguous reflected sensor design drawing.

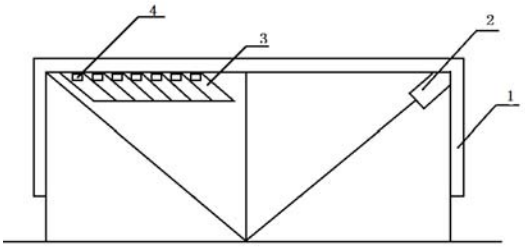

1.Plastic casing 2.Laser source 3.Receiving pipe 4.Photoresistance

Figure 3. Light reflex non-contact liquid level detection sensor module schematic diagram

2.2 The MCU Control Module

Figure 4 is the schematic diagram of this module. As shown in figure 4 α is the angle of incidence, H is the height of the equipment, h is the water-level, L is the length of the apparatus, x is the displacement of the laser spot on the sensor.

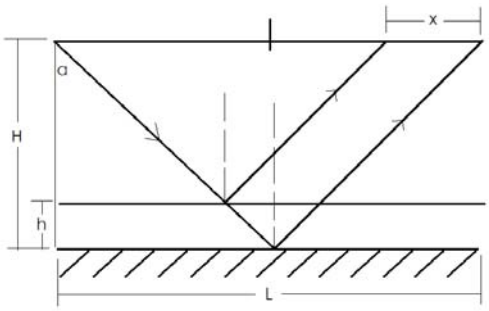

Figure 4. Signal Processing Module Calculation Principle Diagram

The formula derivation process is as follows:

$$\tan\alpha = (L/2)/H \quad (1)$$

$$\tan\alpha = (x/2)/h \quad (2)$$

$$x = (L/H)\,h \quad (3)$$

By geometric analysis we can get: $x=(L/H)/h$. The distance of the laser spot is decided by height of the equipment, water-level, the length of the apparatus. Once x is known, the water level is detected.

In order to detect the water level in time, this design uses a linear array of photoresistance array and receiving pipe to receive laser signal. The resistance(10 kΩ)is in series with photoresistance to low down voltage. If the photoresistance is illuminated by laser, the MCU will receive low level form the I/O so that we can know the distance of the laser spot and the water

level.

2.3 GSM sending module

Through market research, we have chosen SIM300 GSM SMS module which is consumption and widely used. Just insert a SIM card when using the module to the module slot. If the system start, GSM SMS sending module will wait for the alarm signal, when the water level changes controlled by the MCU to send alarm SMS.

3. SOFTWARE DESIGN AND IMPLEMENTATION

Software design of the system is consist of signal processing and SMS module.

3.1 The software of signal processing

This section consists of two programs:

Firstly, the initialization of I/O port and interrupt are defined, and then enter the main loop. The program in the main loop is used to display the water level at the time and detect changes. It will send water level signal immediately once water level increase or decrease, simultaneously start the message counter. The program continues to display water level if there is no change of it.

When the level changes, program start scanning from the furthest photoresistor away from the laser source. If low potential signal is detected, the alarm signal is generated and read out the current level. At the same time the system stops the scanning. If high potential signal is detected, illustrating there is no laser spot. The system continues scanning until the first high is detected. After the water level signal is sent the program will restart the c\scanning. Loop detection is achieved.

This program uses the 60ms timer interrupt, the interrupt subroutine count 6s (used for experiment, it can be adjusted). Whenever the interrupt is triggered, the SMS counter is checked. If the value is less than or equal to 2, program sent to the GSM module to send message and the message counter plus 1. Otherwise, immediately disable interrupts. The specific process is shown in Figure 5.

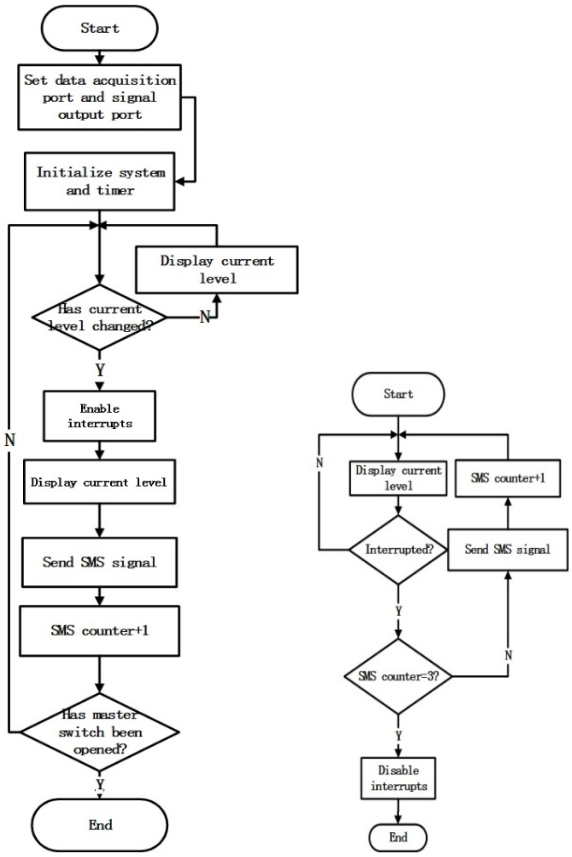

Figure 5. Signal Processing of The Software Design

3.2 SMS software design

MCU control the GSM module through the serial port. The procedures of this paragraph by the operating instructions of the GSM communication module AT command manual [13] query.

First, the LCD display module, single-chip control module, and GSM SMS sending module is initialized. After the successful launch of the GSM module system enters detecting water cycle. Secondly, GSM module extracted from the single-chip serial I/O signal sequence length of three. If a "000" is returned the microcontroller continues to detect, otherwise wait. If the I/O signal sequence is maintained for a period of time and then becomes "000", meaning checksum is correct, the I/O signal sequence is valid, otherwise invalid. Finally, the MCU identify the I/O signal sequence content to determine the corresponding water level and control the GSM module to send alarm SMS. After the sending of the alarm message the program continues to detect code circular. Software process is shown in Figure 6.

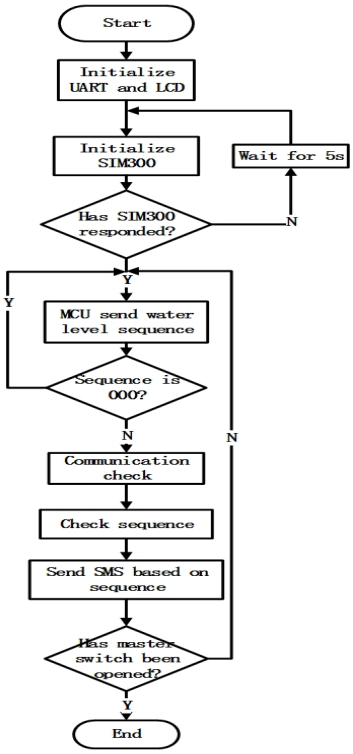

Figure 6. SMS Sending Part of The Software Design

4. PROTOTYPE TEST AND ERROR ANALYSIS

The fluctuation of the liquid surface will produce errors. The liquid level is likely to produce a level change of 1mm while measurement, in order to enable the detection and alarm system to be stable and reduce the false alarm or alarm frequently the water level is divided into 6 level, each level interval 3mm. As the level increases, reaching the corresponding level, LCD screen will display the current level (display 0 when there is no water), at the same time GSM module will send an alarm SMS to the users' phone.

4.1 Laboratory Instrument

Sink, Homemade home flood alarm system, caliper.

4.2 The measurement of the accuracy and resolution .

4.2.1 Measurement method

Inject the liquid into the sink slowly, stop the injection while the LCD screen displays the level variation, the current level is measured with a caliper and recorded. Continue to inject water until it reaches level 6. Through this method, 10 groups of measurement data as shown in Table 1, error analysis are shown in Table 2, which Δh is the difference between the measured value and the actual value of the unit mm.

Table 1. Measurement data table

actual value	measured value	Δh	actual value	measured value	Δh	actual value	measured value	Δh
1.00	1.00	0.00	4.00	4.00	0.00	7.00	6.80	-0.20
1.00	1.20	0.20	4.00	4.20	0.20	7.00	7.10	0.10
1.00	1.20	0.20	4.00	4.10	0.10	7.00	7.10	0.10
1.00	1.10	0.10	4.00	4.20	0.20	7.00	6.90	-0.10
1.00	1.10	0.10	4.00	4.20	0.20	7.00	7.00	0.00
1.00	1.20	0.20	4.00	3.80	-0.20	7.00	7.10	0.10
1.00	1.00	0.00	4.00	4.00	0.00	7.00	7.10	0.10
1.00	1.10	0.10	4.00	4.10	0.10	7.00	7.10	0.10
1.00	1.10	0.10	4.00	3.20	0.80	7.00	1.90	0.90
1.00	1.20	0.20	4.00	4.90	-0.10	7.00	6.90	-0.10
10.00	9.80	-0.20	13.00	12.70	-0.30	16.00	15.90	-0.10
10.00	10.00	0.00	13.00	12.60	-0.40	16.00	15.80	-0.20
10.00	9.20	-0.80	13.00	12.20	-0.80	16.00	16.20	0.20
10.00	9.70	-0.30	13.00	12.80	-0.20	16.00	15.50	-0.50
10.00	9.70	-0.30	13.00	12.90	-0.10	16.00	15.80	-0.20
10.00	9.80	-0.20	13.00	12.90	-0.10	16.00	15.90	-0.10
10.00	10.20	0.20	13.00	13.40	0.40	16.00	16.20	0.20
10.00	9.80	-0.20	13.00	13.20	0.20	16.00	16.40	0.40
10.00	10.20	0.20	13.00	13.20	0.20	16.00	16.00	0.00
10.00	9.70	-0.30	13.00	13.00	0.00	16.00	15.90	-0.10

Table 2. Error analysis table

actual value	average error	standard error	actual value	average error	standard error	actual value	average error	standard error
1.00	0.12	0.14	4.00	0.13	1.30	7.00	0.10	0.32
10.00	-0.19	0.35	13.00	-0.18	0.15	16.00	-0.04	0.26

4.2.2 The measurement results

According to Table 2, the average of average error -0.01mm; the average of standard error - 0.42mm.

The measurement can be approximated with an average error of 0.01mm; standard error of 0.42mm. Gaussian theory of accidental error shows that 68.3% of the measurement error is between 0.42mm.

4.2.3 The system false alarm rate experiments

i . Detection Method:

Under laboratory conditions, simulate no water, water seepage (smooth flow), the leakage (medium flow rate of water flow), water pipes burst (turbulent flow) four cases. Detect the alarm system whether works normally under these four cases . Different alarm system live to work 72 hours to observe the stability.

ii . The test results:

No leaking: don't send alarm SMS . System false alarm rate equals 0.

iii . Leaking: water seepage, leakage and water pipes burst in the three different situations can send alarm SMS properly.

5. CONCLUSION

This study designs a kind of discontiguous reflected liquidometer system. The system is applied to design the alarm for house-leaking. The innovative use of the linear array of photosensitive resistor as the light receiving member, not only improves the resolution and accuracy, but also reduces the cost. The experiments show that the system is suitable for domestic use low-cost, long-range flood alarm system.

6. ACKNOWLEDGEMENTS

This project is supported by the Jilin University. Special thanks to Ms. Li Suyi of College of Instrumentation & Electrical Engineering, Jilin University, for their invaluable assistance in the design suggestion. The author also thanks to College of Instrumentation & Electrical Engineering, Jilin University.

References

[1] Liu, Zhiqiang & Sun, Yujing. Application of Sonic Detecting Technique in Regional Water Leakage Detection [J]. *WATER TECHNOLOGY*. 2009, 3(1):47- 49.

[2] Zhang, Feng. Magnetic Sub-level of Design and Installation [J]. *Meter Sensor* .2001.1:42-43.

[3] Ning Rulong. Invested Diffused Silicon Level Gauge Principle [J]. *ZI DONG HUA YU YI QI YI BIAO*. 2000. 4:51-52.

[4] Wang, Hongbo. Chen, Xi. Qian, Lisha & Zhou, Leijiao. Non-contact Ultrasonic Level Measurement Method [J]. *Fujian Computer*. 2011.2:11-12.

[5] Gao, Yue. Refraction of Light Non-contact Ype Liquid Level Monitoring Device and Use the Device Detection System. China Patent: CN 201600171U [P]. Announcement Date: 2010. 10.16.

[6] Wang, Weiqiang. Linear CCD Level Measurement and Optical Path Design [D]. Harbin Engineering University. 2011. 3.15.

[7] Huang, Yanping. Pei, Li & Jian, Shuisheng. Description on optical fiber liquid level sensor (OFLLS) [J] *Optical Communication Technology*. 1995. 2:131-136.

[8] Zhan, Yang. Variable Condenser Water Level Switch [P]. Chinese Patent: CN201869184U，2011-06-15.

[9] Sun, Qingdian. Li, Canxin & Cheng, Yong. Research and Design of Water Supply Pipeline Leakage Warning Monitoring Device [J]. *Water*

Resources and Power .2010, 28 (10): 125 - 127.

[10]Yu, Hongbo. On the Leakage Alarm System [D] Beijing: *National Library of The Center of the Fire Control Room*.2006.

[11]Li, Yuan & Tie, Yong. Water Leakage Detection Algorithm Based on LMS Denoising Algorithm [J]. Journal of Inner Mongolia University. 2008.39 (2): 172 - 176.

[12]Yu, Qixiang. Leak-proof Safety Lock and Water Leakage Alarm Systems [P] China Patent: CN202329950U.2012-07-11.

[13]*AT Command Manual*

Double-fed Induction Wind Generator Rotor Side Prolapse of PWM Inverter Control Strategy Research

Xing-xing Fan, Yu-jun Wang, Shuang-wei Wang
（jilin university instrument science and engineering institute,changchun,130021）

***Abstract*— Based on the running characteristics of doubly-fed asynchronous wind power generation system, and compared with the traditional cross - straight - to pay the converter system, this paper puts forward to a droop control strategy for the rotor side converter in order to maintain the stability of power grid voltage and frequency, which is applied to two level voltage type double PWM inverter of doubly-fed asynchronous wind power. In this paper, the principle of PWM inverter in the rotor side is introduced and by the way of sagging power control, inverter for wind power generation system model is simulated .Besides, this paper achieved the voltage and current harmonic analysis of the double-fed induction wind generator rotor side and the results analysis of the rectifier. Finally it is concluded that the simulation results and the PWM inverter control of the rotor side scheme is verified the feasibility.**

***Key words*—Wind power Inverter PWM Droop control.**

I. INTRODUCTION

THE current mainstream of wind turbine model is double-fed induction wind generator in wind power generation system, its operation control is through the control of ac excitation rotor side converter to achieve[1].When the doubly-fed asynchronous parallel operation of wind power system, the frequency of wind power generation and power grid frequency requirements are consistent, which requires constant wind power frequency. The current wind power system is mainly divided into constant speed constant frequency motor system (CSCF system) and the variable speed constant frequency motor system (VSCF system).If we take measures to keep in the process of wind power generator speed constant to get and the grid frequency is consistent, the constant frequency power is the constant speed constant frequency motor system. This system adopted by the general generator synchronous generator is the main and squirrel-cage induction generator [2]. However, variable speed constant frequency (VSCF system) of the generator motor system speed change with wind speed is in the process of wind power. We get consistent and power grid frequency constant frequency power by other control ways. The grid inverter is part of the frequency converter, it is in the rotor side and asynchronous wind power generation system is essential to maintain a constant voltage frequency in the wind power system. The present study focuses on improve the grid side of the grid inverter power factor and reduce the current total harmonic distortion (THD) to solve the problem of the large capacity power control the transformer. And it requires that the inverter has the certain grid fault ability to adapt in order to realize through the operation of power grid failure under. It mainly introduces a kind of active inverter output of feed forward compensation on the basis of switching function method is used to control the output voltage and filtering inductance current double loop feedback scheme 3 in the literature. But the inverter output current harmonic distortion; It has established the single cycle control three phase high power factor of grid inverter simulation model in this paper, four and mainly to its principle were expounded; This paper puts forward 5 voltage type PWM rectifier direct power feed-forward decoupling control new strategy based on power control mathematical model. It solves the issue of active power and reactive power are coupled. But it is not involved inverter power control. It can realize the current rapid dynamic tracing power grid voltage instantaneous current tracking control technology to in 6, the thesis then keep sine wave inverter current waveform and voltage low efficiency.

To solve above problems and research direction, we will be in the micro grid inverter power tracking droop control strategy is applied to the doubly-fed asynchronous wind power generation system according to the micro grid in a dissertation 7, 8 class power droop control theory. Simulation research for

control strategy through simulation software Matlab/Simulink, we hope that we can realize the maximum utilization of wind power and intermittent control. This article is mainly around the PWM converter and its related control technology in doubly-fed asynchronous wind power generation system. It set up two level voltage type double SPWM inverter technology of the rotor side converter and inverter model on the basis of the traditional hand in rectangular converter. It was carried out on the model simulation and analysis of control method in the matlab/Simulink before the system design and debugging. To verify the feasibility and effectiveness of the control strategy..

II THE STRUCTURE AND WORKING PRINCIPLE OF THE ROTOR

With the rapid development of power electronic technology, PWM control technology is widely used in high power inverter circuit. Now the single machine capacity has reached megawatt wind turbines, although its rotor ac excitation only need to the size of the slip power capacity, but the large capacity transformer capacity of wind turbines can still achieve megawatt. Figure 1 is a dual PWM converter rotor side of the inverter circuit structure. If the sine wave as N connected to other waveform of pulse sequence, then the pulse width is equal, but not equal amplitude, and pulse at the top is not horizontal, the pulse amplitude according to the sine law of change. It is the so-called SPWM technology that makes the pulse width according to the sine law of change and equivalent of sine wave. We are on the VT1 - VT6 in figure 1 of the inverter bridge SPWM control according to the sine signals and triangular wave comparison method. It can produce a sine wave modulation in the dc input terminal of the AB inverter bridge. In the Uab, Uab JiBo component and high frequency harmonic and switch frequency. The appropriate control Uab can make A, B phase current and voltage in phase, to achieve power factor to 1.In the same way can control the Uac and Ubc, make the current and voltage in phase. According to the circuit in the properties of dc power supply, the voltage type inverter circuit is divided into two kinds of inverter circuit and the current type inverter circuit.

This paper mainly introduces the voltage source PWM inverter circuit. As shown in figure 1 of this three phase inverter Bridge IGBT power/diodes three-phase Bridge in the Universal Bridge module, DC on behalf of the DC power supply, RLC on behalf of the load circuit of the inverter.

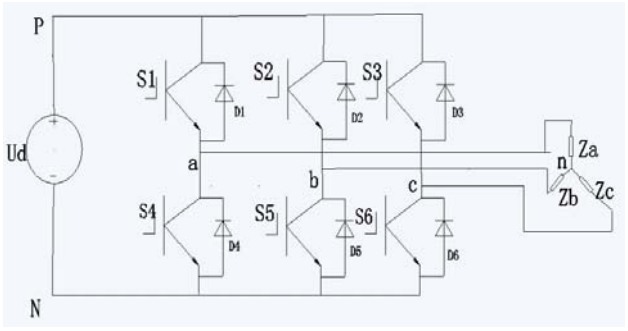

Fig.1 PWM Inverter main circuit

The three-phase bridge inverter circuit adopts dual polarity control mode in figure 1, U, V three-phase PWM control Shared a triangle wave carrier, three phase modulation signal are in turn 120 radians. Carrier signal is symmetric triangular wave, the frequency of 50 Hz, the modulation signal is a sine wave. The frequency is zero. Each phase of the control laws of power switch device is the same. Its upper and lower bridge arm took turns to conduction to get bipolar PWM waveform.

III. THE LOW FREQUENCY AND HIGH FREQUENCY MATHEMATICAL MODEL OF THREE-PHASE GRID INVERTER

When the column to write KVL equation of three-phase filtering inductance, we can get the state equation of three-phase grid inverter in ABC stationary coordinates as follows:

$$\begin{bmatrix} L\frac{di_a}{dt} \\ L\frac{di_b}{dt} \\ L\frac{di_c}{dt} \end{bmatrix} = \begin{bmatrix} -R & 0 & 0 \\ 0 & -R & 0 \\ 0 & 0 & -R \end{bmatrix} \begin{bmatrix} i_a \\ i_b \\ i_c \end{bmatrix} + \begin{bmatrix} 1 & & \\ & 1 & \\ & & 1 \end{bmatrix} \begin{bmatrix} v_a \\ v_b \\ v_c \end{bmatrix} - \begin{bmatrix} 1 & & \\ & 1 & \\ & & 1 \end{bmatrix} \begin{bmatrix} e_a \\ e_b \\ e_c \end{bmatrix} \quad (3\text{-}1)$$

The mathematical model of low frequency inverter in alpha beta coordinates:

$$\begin{bmatrix} L\frac{di_\alpha}{dt} \\ L\frac{di_\beta}{dt} \end{bmatrix} = \begin{bmatrix} -R & 0 \\ 0 & -R \end{bmatrix} \begin{bmatrix} i_\alpha \\ i_\beta \end{bmatrix} + \begin{bmatrix} 1 & 0 \\ 0 & 1 \end{bmatrix} \begin{bmatrix} v_\alpha \\ v_\beta \end{bmatrix} - \begin{bmatrix} 1 & 0 \\ 0 & 1 \end{bmatrix} \begin{bmatrix} e_\alpha \\ e_\beta \end{bmatrix} \quad (3\text{-}2)$$

The PWM converter ac status under the dq coordinate system as follows:

$$\begin{bmatrix} L\frac{di_d}{dt} \\ L\frac{di_q}{dt} \end{bmatrix} = \begin{bmatrix} -R & wL \\ wL & -R \end{bmatrix} \begin{bmatrix} i_d \\ i_q \end{bmatrix} + \begin{bmatrix} 1 & 0 \\ 0 & 1 \end{bmatrix} \begin{bmatrix} v_d \\ v_q \end{bmatrix} - \begin{bmatrix} 1 & 0 \\ 0 & 1 \end{bmatrix} \begin{bmatrix} e_d \\ e_q \end{bmatrix} \quad (3\text{-}3)$$

The mathematical model of three-phase grid inverter state variable expression in ABC stationary coordinates as follows:

$$\begin{bmatrix} L\frac{di_a}{dt} \\ L\frac{di_b}{dt} \\ L\frac{di_c}{dt} \\ L\frac{dv_D}{dt} \end{bmatrix} = \begin{bmatrix} -R & 0 & 0 & S_a - \frac{1}{3}V_D\sum_{k=a,b,c}S_k \\ 0 & -R & 0 & S_b - \frac{1}{3}V_D\sum_{k=a,b,c}S_k \\ 0 & 0 & -R & S_c - \frac{1}{3}V_D\sum_{k=a,b,c}S_k \\ -S_a & -S_b & -S_c & -\frac{1}{R_Z} \end{bmatrix} \begin{bmatrix} i_a \\ i_b \\ i_c \\ i_d \end{bmatrix} + \begin{bmatrix} -1 & 0 & 0 & 0 \\ 0 & -1 & 0 & 0 \\ 0 & 0 & -1 & 0 \\ 0 & 0 & 0 & -\frac{1}{R_Z} \end{bmatrix} \begin{bmatrix} e_a \\ e_b \\ e_c \\ e_d \end{bmatrix} \quad (3\text{-}4)$$

The high frequency model under the three-phase coordinate system conversion to high frequency model under two-phase static coordinate system:

$$\begin{bmatrix} L\frac{di_\alpha}{dt} \\ L\frac{di_\beta}{dt} \\ C\frac{dv_D}{dt} \end{bmatrix} = \begin{bmatrix} -R & 0 & S_\alpha \\ 0 & -R & S_\beta \\ -S_\alpha & -S_\beta & -\frac{1}{R_E} \end{bmatrix} \begin{bmatrix} i_\alpha \\ i_\beta \\ v_D \end{bmatrix} + \begin{bmatrix} -1 & 0 & 0 \\ 0 & -1 & 0 \\ 0 & 0 & \frac{1}{R_E} \end{bmatrix} \begin{bmatrix} e_\alpha \\ e_\beta \\ E \end{bmatrix} \quad (3\text{-}5)$$

The high frequency of the three-phase grid inverter model under two phase rotation system as follows:

$$\begin{bmatrix} L\frac{di_d}{dt} \\ L\frac{di_q}{dt} \\ C\frac{dv_D}{dt} \end{bmatrix} = \begin{bmatrix} -R & wL & S_d \\ -wL & -R & S_q \\ -S_d & -S_q & -\frac{1}{R_E} \end{bmatrix} \begin{bmatrix} i_d \\ i_q \\ v_D \end{bmatrix} + \begin{bmatrix} -1 & 0 & 0 \\ 0 & -1 & 0 \\ 0 & 0 & \frac{1}{R_E} \end{bmatrix} \begin{bmatrix} e_d \\ e_q \\ E \end{bmatrix} \quad (3\text{-}6)$$

By formula (3-1) ~ (3-6), we can find out the model corresponds to the quantity. The general mathematical model of PWM rectifier using switching function description is accurate description of the switch process, therefore very suitable for wave simulation.

IV. Droop Control Principle and Model

This article will make PQ droop control is applied to the wind turbine rotor side converter in parallel system, the combination of PQ droop control method to improve the overall performance of the inverter parallel system. According to droop theory of the electric power system, the rotor side converter made prolapse of active and reactive power control, at the same time it will pass own active power and reactive power signal signal to the network side of the inverter through the network telecommunication lines. network side inverter will weight average after get used to droop control power signal own the active and reactive power signals and the rotor side of the inverter power , as the control of the inverter trigger pulse signal. The wind power inverter parallel system based on network control and PQ droop control ,and the network side of the inverter power control signal associated with the rotor of the inverter, so the system as a whole are mobility can be similar to the parallel control system, and when the transmission line failure it does not like have a wire in the parallel control system failure, weaver inverter can still be in accordance with its own power droop control work. The PQ network control in the wind power generation system not only can improve the inverter parallel system, and the effect of weaver implementation can be close to have a wire in the parallel control of weaver flow effect. According to the rotor of the inverter output active power P and reactive power Q, it collected its output current and voltage, the power output of the active power and reactive power is equal to the reference power. As shown in figure 2 to droop control chart; Figure 3 in the Matlab simulation software to build the droop

control model diagram.

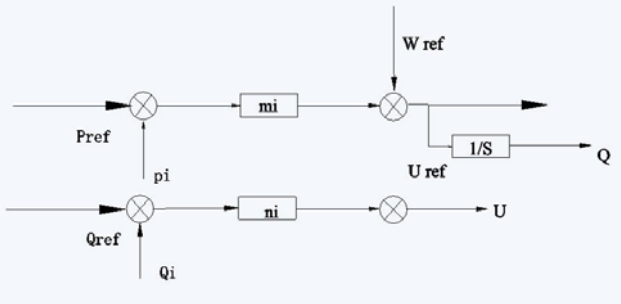

Fig.2.Droop control block diagram

According to the PQ droop control strategy, we establish the MATLAB/SIMULINK control simulation model as shown in figure 3.The node voltage and current as the output signal, through the active power and reactive power feedback, finally we get the trigger pulse to control the power switch device
to shut off.

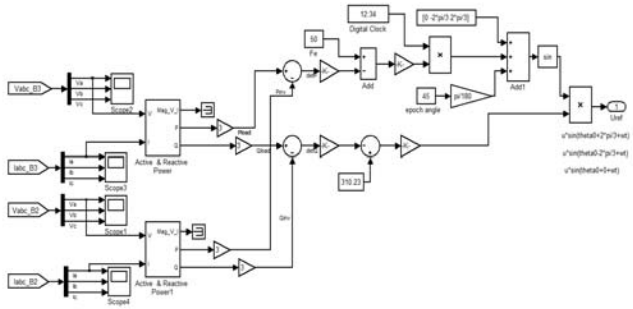

Fig.3. Droop control model in matlab

We get the active power P and reactive power Q through the grid feedback of the three phase line voltage and the phase line current, thus forming a power tracking control to generate the trigger pulse signal to control the three-phase inverter, realize the droop control of the inverter.

V. THE SIMULATION ANALYSIS OF THE THREE-PHASE PWM INVERTER

The simulation parameters are as follows: power grid voltage is 1000 V, 50 Hz, load for 50 kW, three-phase grounding load 380 V RMS, 50 Hz;

The simulation time starts from zero moment. In order to observe clearly the waveform, and the simulation time is set to 0.08 s. Figure 4 is the simulation model system block diagram

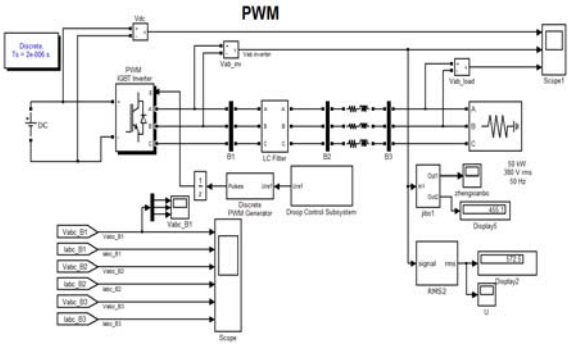

Fig.4. Inverter system model diagram

The frequency and amplitude of harmonic component is one of the most important index to measure the performance of PWM inverter circuit, so it is necessary to us for the PWM and harmonic analysis. By using FFT spectrum analyzer in the powergui module, we on the output line voltage waveform and sine wave output waveform harmonic analysis, set the basic frequency is 50 hz, this time to analyze the output waveform from the zero point, the results of the simulation analysis is shown in figure 5.

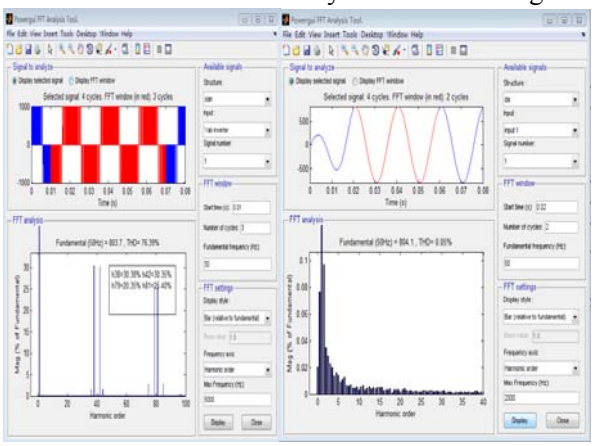

Fig.5 Inverter output ac line voltage waveform and sine waveform

We can see the output line voltage waveform does not contain low harmonics in figure 5, the harmonic amplitude of the larger is 38, 42 times, 79 times and 81 times harmonic.By adding a low-pass filter, we can filter out the harmonic. The output sine wave contains a low harmonic, does not contain higher harmonic.

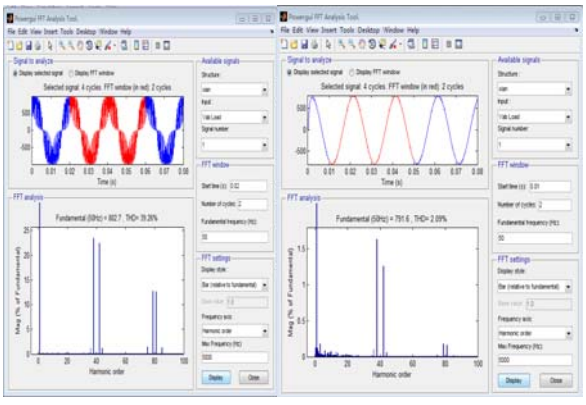

Fig.6 Load waveform and harmonic analysis

The figure 6 is the load voltage waveform by the inverter output. We can see from figure 6 (1) the load voltage waveform contains 38, 42 harmonics, and among them 79 times, 81 times a second harmonic amplitude is smaller. We can make more load voltage waveform sine, through a series LC filter in the circuit. Figure 6 (2) is usually under control inverter work in unit power factor in the doubly-fed wind.

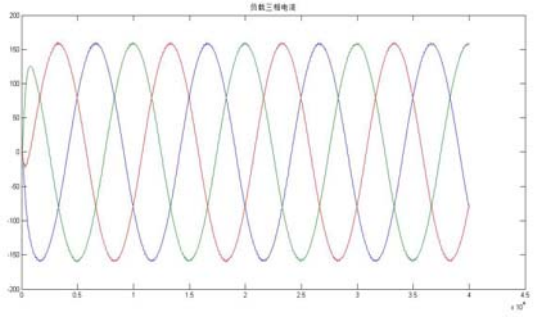

Fig.7 Inverter output line voltage

We can see the output voltage of inverter with good waveform in figure 7, and its power factor is 1, the phase voltage and current on the ac side, the energy flow in the circuit. The waveform of the current is close to sine wave, the PWM rectifier has the function of energy bi-directional flow it satisfy the requirement of ac excitation variable speed constant frequency wind

power generator. Each node voltage must be within the range required voltage quality in the working process of the inverter, thus to ensure the normal operation of power grid and reduce the harmonics and waveform distortion rate. As shown in figure 8 is the rotor side converter on the right side of each node voltage waveform.

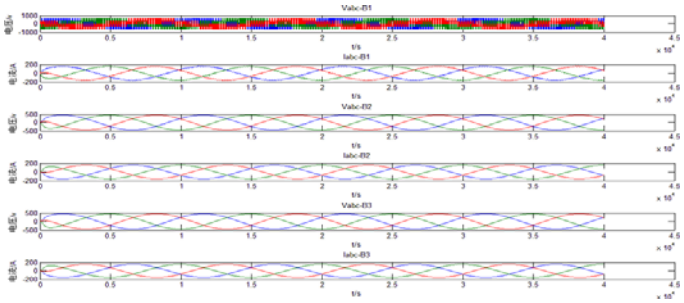

Figure .8 Each node circuit line voltage and line current

We can see the line current of various nodes and each node of the line voltage waveform is close to sine in the circuit in figure 8. And the frequency is stability, the voltage and current are the same phase synchronization. It can conclude that the droop control inverter power in the circuit works well, and each node voltage quality is higher.

VI.CONCLUSION:

IN the wind power system we usually adopt SPWM inverter control technology, which can reduce the harmonic of voltage and current, thereby reduce harmonic pollution and have extensive application prospect. Uncontrolled inverter is simple and reliable, has mature technology, in the range of the linear modulation, its dc voltage utilization rate is low, so sometimes inverter output cannot meet the requirements of the load voltage. And in this paper, the voltage vector droop control PWM converter has the advantages of low output waveform harmonic, does not contain higher harmonic, get the sine input current with unit power factor, realize the advantages of two-way flow of energy; And compared with the traditional A-D-A inverter, it does not contain harmonic related to carrier frequency, of which the voltage utilization rate is higher. Modling the whole system by matlab/simulink, simulating and analyzing the waveform , we have confirmed the validity and feasibility of the control scheme, and we can see that two level voltage type double PWM converter has a potential development prospect in the future.

References

[1] Yikang He, Jiabing Hu ,Lie Xu. Grid double-fed induction wind generator operation control [M]. China electric power press, 2012.

[2] Chengxu Wang , Yuan Zhang. Wind power [M]. China electric power press, 2003.

[3] Yanlei Zhao,Xitong Hu,Yang Song. Modeling and double loop control strategy of PWM inverter. [C]. 2008214-2008214.

[4] Zhijiang Yang ,Pinggang Song. Based on the Matlab single cycle grid inverter control three phase high power factor of the modeling and simulation [J] power converter technology, 2009-02:18-21.

[5] Jiu Wang ,Yang Wei ,Huade Li. Power feedforward voltage type PWM rectifier direct power decoupling control [J] journal of liaoning engineering technology university, the 2007-04, 26 (2) : 238-241.

[6] Cuijuan Wang,Qiaoe Zhao,Qiang Zhang. Research on inverter of grid-connected wind farms is [J] journal of electric power, 2010, 25 (5) : 388-390.

[7] Chunjiang Zhang , Xiaohuan Wang, Haifen Xue. Net class power droop control and parallel three-phase inverter system small signal modeling and analysis [J] journal of electrotechnics, 2012-1, 27 (1) : 32-39.

[8] Mingjuan Li, Fei Lin. Micro power grid inverter control research [D]. Beijing jiaotong university, 2009.

[9] Yingjian Xu. A-D-A wind power system modeling and simulation study [J] electric switch, 2011 - man - 29.

[10] Xiliang Zhang. Wind energy development and utilization [M]. Chemical industry press, 2005.

[11] Gang Shi,Dong Hu,Xu Cai. Permanent magnet direct-drive wind power harmonic analysis of data flow system [J]. Journal of electrical and control applications, 2012-4, 4 (5) : 32 to 38.

[12] Zhaoyan Zhang, Yongguang Ma. Doubly-fed induction wind generator modeling and simulation study [J]. Electric power science and engineering, 2010-01, 26 (1) : 5-9.

[13] Zhaoan Wang,Jinjun Liu. Power electronic technology [M]. 5 edition. Beijing: mechanical industry publishing house, 2010.

[14] A, Kawamura Chuarayapratip R, Haneyoshi t. Deadbeat controlof PWM makes with modified pulse patterns for uninterruptiblepower supply [J]. IEEE the Transactions on Industrial Electronics, 1988, 35 (2) : 295-300.

[15] NaiGang Hong, power electronic and electric drive control system of the MATLAB simulation [M]. Beijing: mechanical industry publishing house, 2006

[16] Qiuyue Xie,Shoudao Huang, Jian Gao. Wind power rectifier control strategy research [J]. Microcomputer information, 2009, (7).

[17] Tao Qiu,Linkang Chen. Inverter PWM rectifier in the design and simulation [J]. Journal of taiyuan university of technology, 2008-05 33 (5) : 6, 311-314.

[18] Zhaoyan Zhang,Yongguang Ma. Doubly-fed induction wind generator modeling and simulation study [J]. Electric power science and engineering, 2010-01, 26 (1) : 5-8.

[19] Linlang Dong,Yong Wang. 1 mw direct-drive wind power system modeling and simulation research. 2011.6

The test of response character of static reactive power compensator SVC

Li Xiang; Cui Jianlei; and Lv Han
（jilin university instrument science and engineering institute,changchun,130021）

Abstract—Because of the national vigorously promoting clean energy, clean energy is becoming more and more necessary. because of the uncertainty of clean energy, it will cause a lot of problems; One of the most serious is a lack of reactive power and unstable of the voltage . the solution is to reactive power compensation. Farm is equipped with a dynamic reactive power compensation device of a certain capacity. In order to select an appropriate reactive power compensation device, it need to test response characteristics .This paper introduces a technology based on virtual instrument, using the LabVIEW software in the PC to create a dynamic reactive power compensation device response characteristic test system, realizing the test of reactive power compensation device SVC response time ,obtaining the response time characteristic.

0.INTRODUCTION

THIS topic is on the basis of the virtual instrument technology and the LABVIEW programming, according to collect the actual voltage current signal source, choose an appropriate calculation method,. according to the design objective programming for the correct operation, get to the response time of the reactive power compensation device features. This topic research design completed the signal conditioning circuit PCB design and production, through the PXI data acquisition platform, has realized the data processing in LabVIEW development environment, calculation, analysis and real-time display of voltage and current waveforms, obtained the expected by the reactive power and reactive current curve, also has realized the response time of the test..

1. INTRODUCTION OF THE RESPONSE CHARACTERISTICS OF THE STATIC REACTIVE COMPENSATION DEVICE

The response characteristics of reactive power compensation device, mainly for the dynamic. In normal power grid of reactive power compensation device and the current curve to approximate straight line, generally when the curve is steep decline or slowly down to normal, we can conclude that the grid has been in a state of flux, and lack of reactive power or current. Now need to run the dynamic reactive power compensation device, injected into power grid reactive power, at the time of injection of reactive power, reactive power current curve will slowly back to normal levels. In the process, we can get the dynamic reactive power compensation device's response time. Among them, the compensation to join points and reach the normal dynamic response time is 90% of the time[1].

2.REACTIVE POWER COMPENSATION

2.1The principle and significance of reactive power compensation

2.1.1 The principle of reactive power compensation

During normal operation of the power supply system, every node voltage amplitude will change with the change of operation mode, deviating from the system voltage rating. Power system reactive power imbalance means that there are a large number of reactive power flows through power lines and transformers. Due to the impedance exist in the line and transformer ,this result to terminal voltage appeared difference. It is the root cause of the system voltage deviation caused by nominal value. Experiments show that the reactive power comp -ensation voltage fluctuation decreases, improve the level of the voltage of the system as a whole.Electric power system, therefore, should have enough reactive power supply to meet the requirements of power grid and the voltage of the load level and economic operation[2].

2.1.2The significance of reactive power compensation

In the operation of the power system, reactive power flows through the circuit and node voltage is a pair of is closely related to the amount of real-time, reactive power shortage and excess will affect the voltage stability of power grid node and the safety of the

power system operation. The benefits of compensating reactive power is mainly composed of the following:

(1) Improve power quality, guarantee the stability of power grid.

(2) To reduce the system reactive power flow in the circuit, when the total apparent power must be active power system transmission ratio will increase relatively.

(3) System circuit of the reactive power flow in the lower can refer to the power factor of system, in the design, power supply device, its design capacity will decrease relatively, and reduce investment, reduce the cost.

(4) Can reduce the loss of line[3].

2.2 Principle of static reactive power compensation device.

Compensation device is named mainly according to its automatic control means of implementation. Because each kind of automatic compensation device control implementation method is different,the principle of compensating reactive power is different too. Due to this project is MCR type SVC, so only introduce the work principle of the compensation device.

MCR type SVC by MCR ontology and each capacitor reactive real-time power adjustment, its electrical structure as shown in figure 2-1. The MCR ontology control dc excitation by controlling the conduction Angle of silicon controlled rectifier , Then control core saturation degree. The higher of the core saturation degree , the smaller inductance of MCR. Conversely, the greater inductance of the MCR. By changing the saturation degree of the core can achieve the purpose of smooth regulating the inductive reactive power output. Main controller calculate the real-time reactive power according to system voltage current, and to implement the reactive power compensation on the system according to the principle of "small reactive power adjustment point of view, a wide range of reactive power for capacitance"[4]

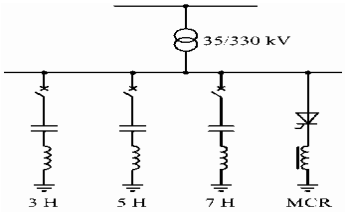

Figure 2-1 MCR electrical diagram

2.3 Introduction to the platform and the data acquisition card

PXI is a platform that is solid and based on PC, which is suitable for measurement and automation systems. Controller has Microsoft's Windows operating system or real-time operating system (NI LabVIEW real-time), high-performance embedded controller, as well as desktops, workstations, servers, or notebook computer control of the remote controller; Module contains more than 450 kinds of function, maximum convenience needs of users for various programming. This topic chose 2 pieces of eight channels of PXIe - 4300 data acquisition card, on PXI platform completed 12 channel synchronous data acquisition. PXIe - 4300 data acquisition card is 8 channal synchronous sampling of analog input channel, the highest sampling rate reached 250 ks/s, is a 24-bit resolution. This system through the DAQ assistant will sampling rate as 2000 hz, for continuous sampling, the sampling points to 2000, maximum input voltage amplitude for 10 v.

3.THE SYSTEM TOTAL DESIGN AND HARDWARE CIRCUIT DESIGN

3.1The system total design thinking

This topic studies the work principle of reactive power compensation device and its response characteristics, the grid signal by reactive power compensation device,then by transformer get input small signal , the small signal after filtering, blocking and amplification processing, after a protection device by PXI data acquisition system into the collection and processing computer system.Finally, by LABVIEW software to get the response characteristics of reactive power compensation device, mainly for the dynamic reactive power compensation device's response time characteristics. The objective of the virtual instrument is refers to the measurement and control platform based on computer, it can replace the traditional measurement and control instruments, such as oscilloscope, signal generator, can be integrated in the automatic control, industrial control system; Free to build into a proprietary instrument system[5].

The total research frame as below 3-1

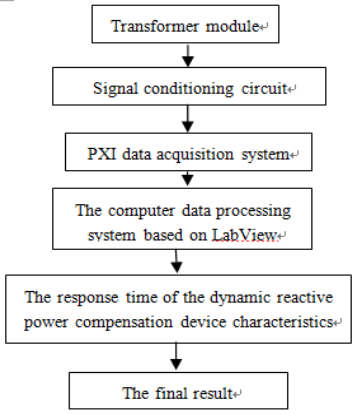

Figure 3-1 Total block diagram of system research

A：Reactive power compensation device secondary side to collect real-time data:reactive power compensation device is not limited to one, should be universal, this project is to MCR for the analysis of the typical test device.

B ： Transformer module: converts power grid voltage current safe low voltage current test available.

C: signal conditioning circuit：The input voltage current signal filtering and amplification of protection, blocking process, make it more close to the theory of using signal.

D: PXI data acquisition system: acquisition part, using PXI platform provides interfaces, signal acquisition.

E: LabVIEW computer analysis control module: by Labview software implementation, to adopt the computing formula of basic signal according to the theory of corresponding curve, parameter analysis and generate the required table.

3.2The selection of the transformer

As stated earlier, the input voltage transformer rated voltage is 100 V, rated current of the input current transformer for 5 A / 1 , so according to the parameters, selects the CHG - 100 VA voltage transformer and CHG - 500M and CHG - 1000M current transformer. Basic electrical parameters of chosen transformer in the following table 3-1 and table 3-2 and table 3-3. By its electrical parameters, the fixed working frequency and the type of transformer for power frequency 50 Hz, high accuracy reached 0.2%, linearity is also very good. In addition, the measurement range of transformer is its rated voltage up to a certain value, thus can meet the requirements of power grid volatility normal work. The type of transformer insulation voltage is very high, at KV level, has the very good electrical isolation performance, thus eliminating isolating circuit design, directly to the output of the transformer input terminal connected to a circuit for signal disposal. Figure 3-2 for the wiring diagram of voltage transformer, figure 3-3 for current transformer wiring diagram.

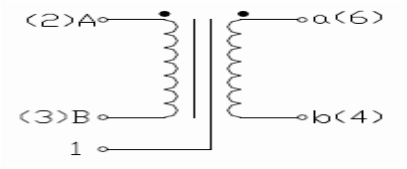

Terminal instructions

1 side： shield 2 side：The primary input(A) 3 side：The primary input(B) 4 side：The secondary output(a) 6 side：The secondary output(b)

Figure 3-2 current transformer wiring diagram and the terminal

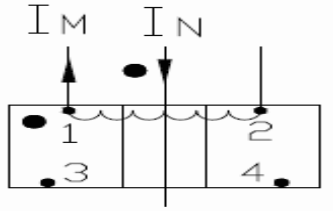

Figure 3-3 voltage transformer wiring diagram

model	The rated voltage	frequency	The output voltage	precision	Insulation voltage	linearity	Measuring range
CHG-100VA	100V	50Hz	5V	0.2%	2.5KV	0.2%	120V

Table 3-1 voltage transformer basic electrical parameters

model	Rated current	Frequency	The output current	Precision	Insulation voltage	Linearity	Measuring range
CHG-500M	1A	50Hz	2mA	0.2%	2KV	0.3%	2A

Table 3-2 current transformer CHG - 500M basic electrical parameters

model	Rated current	Frequency	The output current	Precision	Insulation voltage	Linearity	Measuring range
CHG-100M	5A	50Hz	5mV	0.2%	2KV	0.2%	10A

Table 3-3 current transformer CHG - 1000 - m basic electrical parameters

3.3The signal conditioning circuit design

3.3.1 A voltage signal filter module

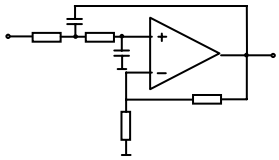

Figure 3-4 The second order type voltage-controlled voltage source LPF

The parameters of all components as shown in table 3-4

Table 3-4 Voltage signal filter parameters

R1	R2	R3	R4	C1	C2
7.5K	15.0K	47.0K	47.0K	10nf	10nF

3.3.2 Current signal filter module

Current signal filter adopted infinite gain multiple feedback low-pass filter, the schematic is shown in Figure 3-5.

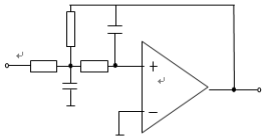

Fig.3-5 Infinite gain multiple feedback low-pass filter

3.3.3 Blocking circuit module

In the actual output signal of power grid , Usually there is a dc component , Therefore dc should be included to dc signal conditioning circuit . According to the previous experience , This topic adopted a simple and reasonable , high applicability to removing straight offset circuit , the schematic is shown in Figure 3-6.

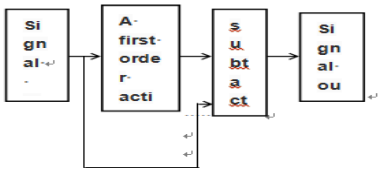

Fig.3-6 Dc isolation principle

3.3.4 Amplifying circuit module

After blocking circuit of the alternating current signal is small ， Needs to be enlarged ， In order to input the PXI for data collection . The amplifying circuit choose LF353 op-amp chip, used two stage amplifier applications, Adjustable magnification can be realized . the schematic is shown in Figure 3-6.

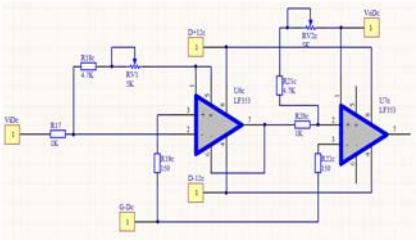

Fig.3-7 Amplifier circuit principle diagram

4.THE SYSTEM SOFTWARE DESIGN

This chapter will introduce this topic at the core of the software design part , The software programming are realized in the LabVIEW2011 development environment .

4.1 the software design

4.1.1 The overall process design of software

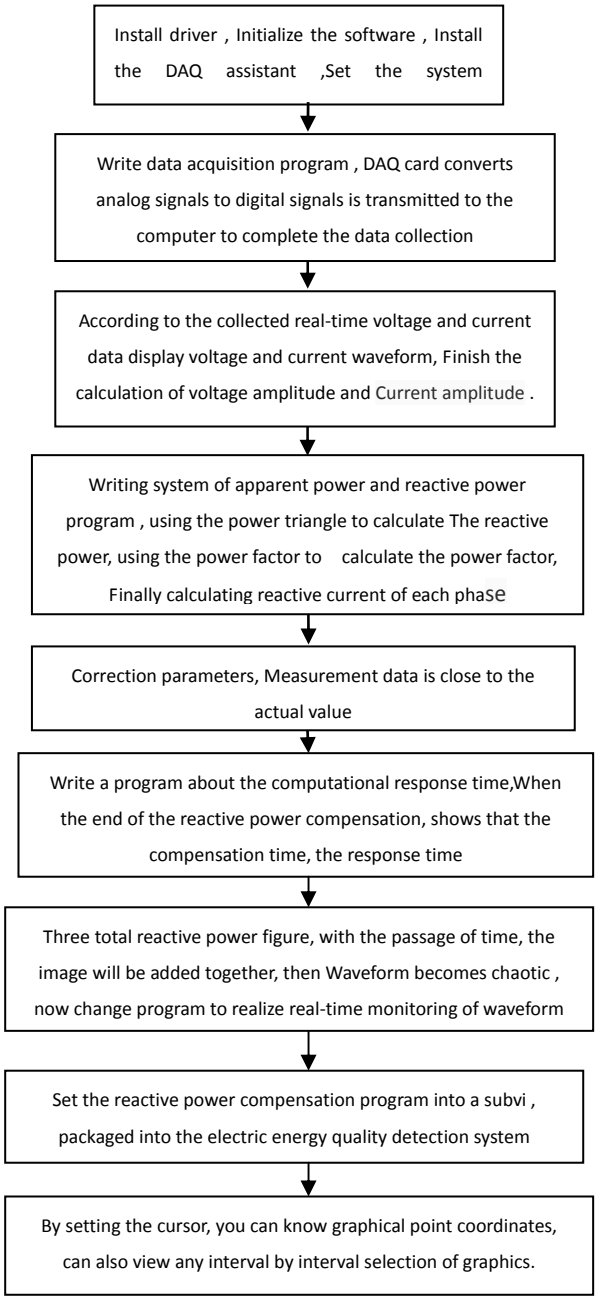

Fig.4-1 Software process design

4.1.2 Signal acquisition module

When using the LabVIEW program analysis processing PC external input signal, Signals by external be collected into the program through the DAQ assistant module ,Signal acquisition module program are shown in figure 4-2.

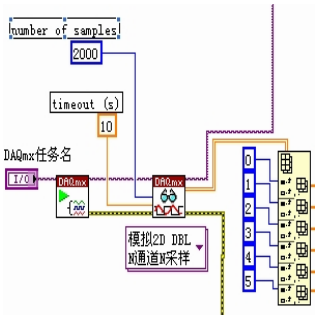

Fig.4-2 Signal acquisition part program chart

DAQ read acquisition of data , the output data is a n d array , The array is the voltage current signal in real time .

4.1.3 The calculation of amplitude and Valid values

According to Acquisition of voltage and current signals , writing the calculating amplitude and Valid values program .The program block diagram are shown in figure 4-3 and figure 4-4.

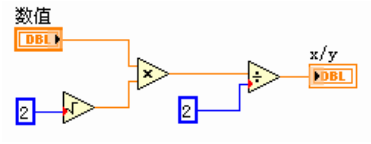

Fig.4-3 RS subvi program

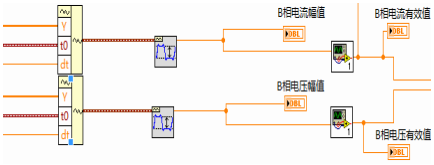

Fig 4-4 Amplitude RMS calculation part of the program

4.1.4 Active power calculation module

Using two FOR loop ， Through multiple sets of data averaging method to calculate active power , The program block diagram are shown in figure 4-5.

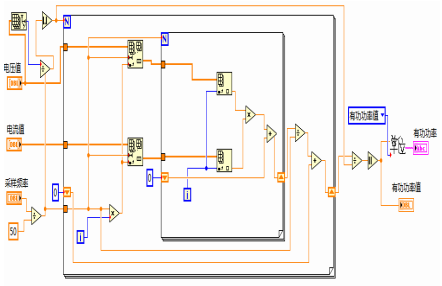

Fig.4-5 Active power calculation part of the program

4.2 parameter calculation method

The calculation formula of apparent power is $S = UI$,

The calculation formula of reactive power is $Q = \sqrt{S^2 - P^2}$, The calculation formula of the power factor is $\cos \varphi = P/S$, The calculation formula of reactive current is $I_Q = I \sin \varphi$.

Through the apparent power and reactive power of the basic method to calculate active power can get accurate data

5.SYSTEM TESTING RESULTS AND INSTRUCTIONS

5.1 Reactive power and response time

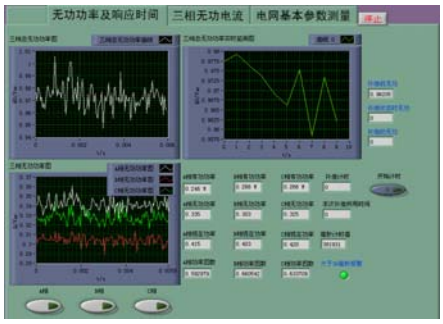

Fig.5-1 Reactive power and response time

At left is a three phase diagram and the total power three-phase reactive power ,At right is real-time monitoring diagram.When power grid normal, reactive power curve fluctuations are small; When the grid is not normal, curve will be lower than under normal circumstances, through the dynamic reactive power compensation, reactive power curve will once again reached the normal level .

5.2 three-phase reactive current

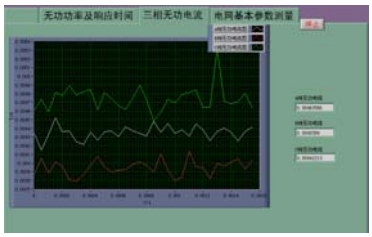

Fig.5-2 Three reactive current figure

When the curve declined precipitously or slowly down to the abnormal, can be concluded that the power grid has been in a state of flux, and reactive power is insufficient, Now need to run the dynamic reactive power compensation device, injected into power grid reactive power, at the time of injection of reactive power, reactive power current curve will slowly back to normal levels.

5.3 measuring basic parameters of the power grid

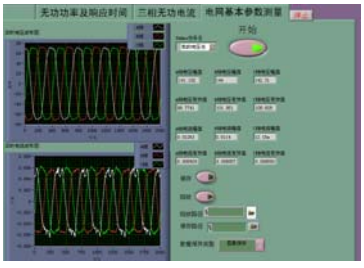

Fig.5-3 Basic parameter measurement figure of power grid

In the program, can be set through the coefficient to calibration, the accuracy can be guaranteed.

5.4 Response time of the display

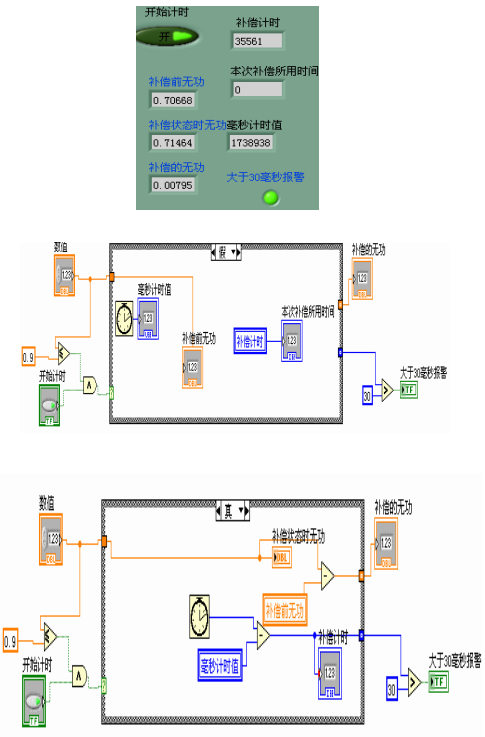

Fig.5-4 Response time figure

A stopwatch timing starts ,To compensate the time is Compensation time is the end Compensation time minus the not compensation time.

6.CONCLUSION

This subject is in the master certain LABVIEW programming method and the reactive power calculation method on the basis , After a month of study and research , realizing the real-time detection of reactive power; Response time of the display; Parameter calibration . The project realize reactive power compensation response time test, which can detect the time of the compensation extent of compensation device and is in line with the requirements, has great practical value in the power plant.

References

[1] Bai runqing,Qin rui,Zhi yong. Dynamic reactive power compensation device parameter measurement and analysis in wind power base[J]. China power.2012,45(2).pp.54-57

[2] Fang xiang,Wang chengduo,Tu yong, The principle and application of dynamic reactive power automatic compensation device. Electrician electrical,2010(4),pp.33-36.

[3] Dai chengmei Zhou qilong ,Yang lin. Dynamic reactive power compensation device based on virtual instrument technology in the design[J] Instrumentation and testing technology , 2009,28(8).pp.87-89.

[4] Ruan qizhen,I and LABVIEW .Beijing,Beijing university press .2009.9

[5] Zhang liuchun,Han rucheng,Zhang shouyu. Instrumentation and testing technology present situation and development trend of reactive power compensation device[J], Journal of taiyuan heavy machinery institute,2004,25(1).pp.30-33

Design and realization of precise oil weight measuring system model based on HTG

Meng Qingchao; Li Jiping; Zuo Chengjun

(College of Instrumentation & Electrical Engineering， Jilin University， Changchun ， 130012，china)

***Abstract*—To tackle the problems of the oil metering ，such as large masses， low precision and sensitivity to temperature，the method of oil tank measurement based on HTG is put forward ，and a precise oil weight measuring system model is designed accordingly. The system model is based on HTG， and the hardware part consists of the modules of data acquisition and display， which is realized by temperature and pressure sensors. The data have been calculated precisely and the error of the model is also analyzed accurately. Experiments show that the model has provided valuable reference for the actual oil metering systems.**

***Keywords*—HTG; MAX1457; data processing**

0 INTRODUCTION

WITH the increasingly higher requirement of the oil metering, the metering methods become more and more diverse, changing from the manual inspection in the past to contemporary digital precision measurement. Metering methods are becoming increasingly advanced and complex. In the field of oil production, due to the universal adoption of oil cans, the mass of oil is so large that it can't be measured in most cases. Although the hand gauging can be used to measure the seized oil volume to calculate the actual mass, the result can be very imprecise due to inevitable manual measurement errors. [1] The oil mass can be measured by tank gauge, however, this method can't exclude the effect of temperature on the oil volume. In order to solve this problem , a new system model based on HTG is designed ,which can meet the measurement requirements with its relative accuracy.

1 OVERALL DESIGN OF THE SYSTEM

The system consists of three main modules: Saving tank model design modules, data acquisition and compensation module , data processing and display module. The overall scheme of the system is shown in Figure 1 .

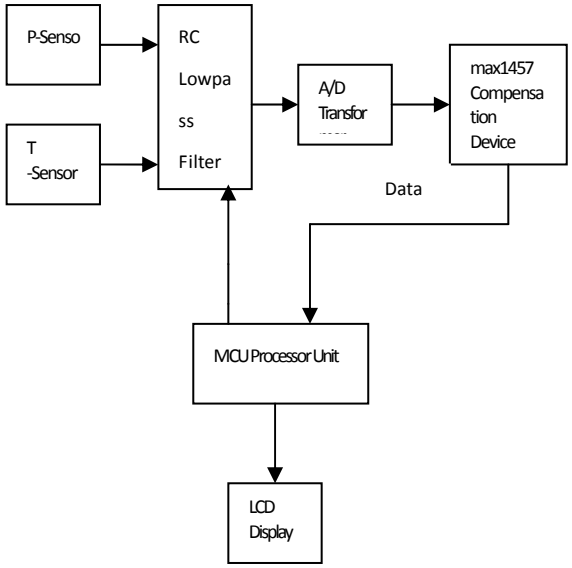

Figure 1 System architecture

To meet the precision requirements, a special container is designed, which is a regular cylinder . The sensor mounting height acts as a standard of the parameters calculation, and hence, mounting height is crucial to the measurement of the sensor and system errors, in these theoretical estimates of the height of the container.

The theoretical calculation is as follows: provided that the system accuracy is 0.3%, the measuring accuracy of the static pressure sensor is 0.2% , the measuring range is 0-10kpa, without considering the influence of temperature, the measurement absolute error is : $10 \times 10^3 \times 0.2\% = 20$pa. The error of the

liquid level: h= $\frac{P}{r \cdot g}$; the liquid mass of the cylindrical container volume per mm: $M_{hm}=\rho R^2 \square r \square 0.001$; fluid mass to be measured is at least : $M=(M_{hm} \times h)/0.3\%$. The liquid level in the container is at least : M/Mhm=h/0.3%≈666.7mm.

Thus, the height of the contained liquid can be at least 67cm. In order to ensure the measurement of the pressure sensor, the height of the container is set 70cm. However, in no case can the dead zone resulted by the lower sensor installed below be avoided. Therefore, only artificial gauging or liquid level gauge can be taken to avoid errors caused by the dead zone. In this case, the installation location of the pressure transmitter should be set as low as possible. The positions of the two sensors are selected at 5cm deep and 30cm deep. The physical map of the tank model is shown in Figure 2.

Figure 2 Physical map of the tank model

2 DATA ACQUISITION AND COMPENSATION

2.1 Design of temperature acquisition circuit

Pt100 is chosen as a temperature sensor, which is a platinum resistance temperature sensor. The sensor has good linearity , high accuracy, wide measurement range , operational ease[9]. Its resistance changing with temperature changes leads to the voltage difference between the Huygens bridge, amplified by the amplifier circuit and converted by AD into msp430 acquisition systems. After data processing, temperature will be displayed on the LCD screen.

The reference voltage of msp430 ADC is 2.5V, so the reference voltage of the bridge is chosen as 2.5V, choosing AD580 chip as the reference voltage source. Advantages of AD580 are listed as follows: initial tolerance reaches ± 0.4%, excellent temperature stability of 10ppm / ° C, long term stability is better than 250 μV[10]. INA114 produced by TI is selected as the instrumentation amplifier, which is integrated into a chip. Having advantages of low noise, high common mode rejection ratio, high input impedance , magnification adjustable, the chip is quite easy to use. To achieve the goal of precision measuring, all resistors are precision resistors with low temperature drift[2] .

Generally, the actual temperature of the oil ranges from 0 ℃ to 100 ℃. The resolution of Msp430 AD converter with 12-bit accuracy reaches 1/4096 .Thus, the actual temperature resolution reaches up to 100/4096 = 0.024414 ℃.At the temperature of 100 ℃, the resistance of pt100 is 138.51Ω,and the corresponding AD input voltage is 2.5V. The actual bridge voltage differential pressure is much smaller than this. In order to reduce the amplification of the noise of internal amplifiers, reducing the amplification to improve accuracy can increase the bridge pressure[5]. Bridge road side resistance is selected as 500Ω and sliding rheostat with 200Ωis chosen as the lower side resistance, consistent with pt100 resistance , so that the balanced output of the bridge at 0 ℃ reaches 0V. Sliding rheostat resistance should be set about 100Ω, the voltage of which is 2.5V at 100℃. In the case, the bridge voltage difference is (138.51/638.51-100/600) * 2.5V ≈ 0.125V, magnification is 2.5/0.125 = 20 , and the resistor R_g= 25 * 2 / (20 -1) = 2.631kΩ, so sliding rheostat with 5KΩ meet the requirement. The simulation of temperature acquisition circuit is shown in Figure 3.

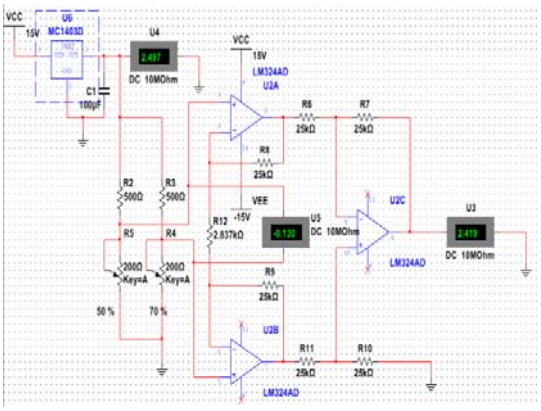

Figure 3 Simulation of temperature acquisition circuit

2.2 Design of the low pass filter

The design set 100kHz as the cutoff frequency of the low-pass filter, using second-order double quadratic filter circuit. Because the cutoff frequency of the low-pass filter is 100kHz, op27 is used as the operational amplifier. The specific value of each resistor capacitor can be calculated by biquadratic equation of low pass filter. The circuit diagram of a low pass filter is shown in Fig.4.

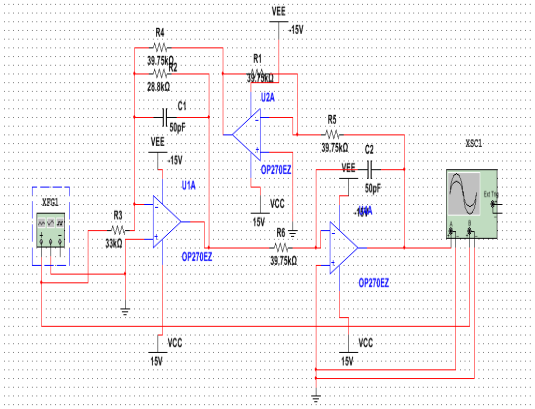

Figure 4 Low -pass filter circuit simulation

With the above circuit diagram simulation, the simulation results are shown in Figure 5 . The red waveform is the input, the green waveform is output ,and the gain is 0.707 .

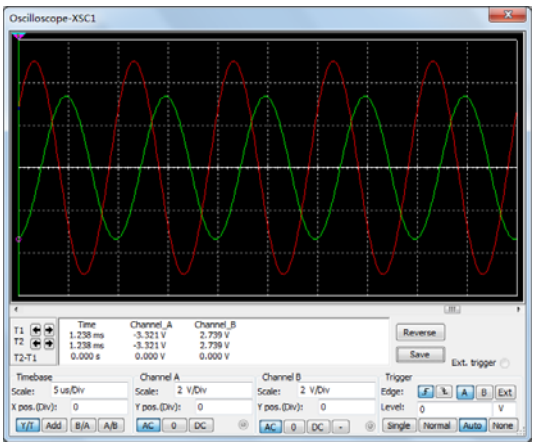

Figure 5 Simulation results of the lowpass filter

2.3 Design of data compensation circuit

MAX1457 is a chip controlled by dedicated sensor signals. This chip is highly integrated, able to compensate for the temperature error of silicon piezoresistive pressure sensors and nonlinear errors [3]. The data compensation circuit based on this chip is shown in Figure 6.

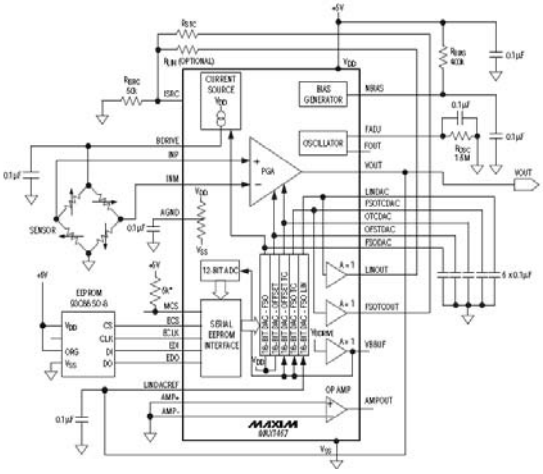

Figure 6 data compensation circuit

Compensation Principle: a programmable current source is used to power the sensor bridge. According to the relationship between bridge the terminal voltage and temperature, take the temperature signal V(T) as the bridge terminal voltage , and use a 12-bit ADC to convert V(T) into digital values and address them in EEPROM, so compensated coefficient D(T) in different linear sections can be obtained [8]. FSO compensation coefficients are written respectively from the EEPROM into two 16-bit DACs (OFFSETTC and FSOTC). Since the bridge terminal voltage is the reference voltage V(T), DAC output voltage can be expressed as:

$$V_{DAC} = \frac{D(T)}{2^{16}} V(T) \qquad (1)$$

For two-way DACs, selecting the appropriate D (T) respectively, the compensation effect can be reached .

The output of compensation circuit is 5V, a voltage follower and divider circuit is set up as shown in Figure 7 ,and the output voltage is 2.5V. The input is on the left side and the output on the right.

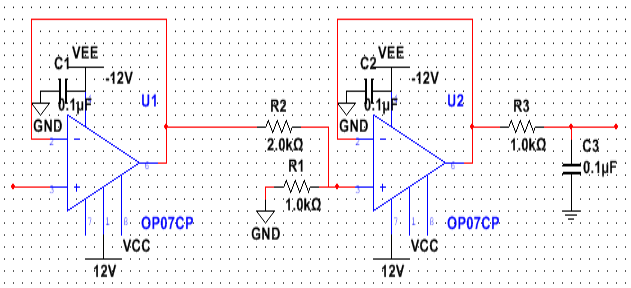

Figure 7 Voltage follower and divider circuit

3 DATA PROCESSING AND DISPLAY

3.1 Pressure sensor testing and acquisition of calibration parameters

Acquisition data of output pressure are shown in Table 1, and data image are drawn in Figure 8. As it shows, output data curves of the sensor are in good agreement with the results of the linear relationship .

Liquid height	5	10	15	20	25	30	35
Output 1	0.037	0.445	0.907	1.348	1．811	2.235	2.697
Output 2	0	0	0	0	0	0．057	0.031
Theoretical output 1	0	0．407	0.815	1.221	1.628	2.035	2.442
Theoretical output 2	0	0	0	0	0	0	0.245

Table 1 Pressure output value

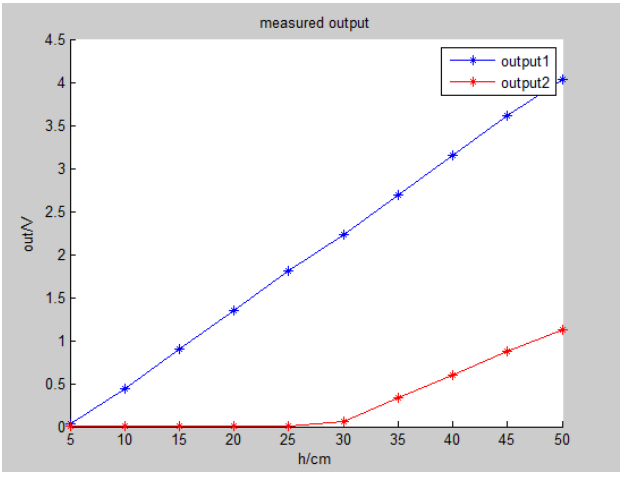

Figure 8 output data curves

Diffused silicon piezoresistive temperature sensors will cause zero drift and temperature drift, which need to be compensated and corrected by MAX1457, but its zero drift and temperature drift must be measured at different temperatures[7]. Specific practices are as follows: perform the zero test without any water in the model, add pre-adjusted water about 40 ℃, and record the output of the sensor, then wait for the water temperature to decrease gradually. Monitoring the temperature changes of the previous step in water through the circuit, record the output of the sensor every time the temperature drops a degrees Celsius. Due to limited laboratory conditions, so only about 15 sets of output data are recorded ranging from 40 ℃ to 25 ℃.

Analysis of the data shows no significant temperature sensor drift with only 2.2mm height of error(When 40 ℃).

Because the MAX1457 addresses EEPROM under different temperatures , using digital-analog conversion to deal with the correction parameter from the inside and adding the output of the sensor to compensate for the effect of the correction[4] . Since the internal DA converters of MAX1457 are 16-bit, the experiment makes compensation at the temperature ranging from 40 ℃ to 25 ℃ and interpolate for 15 times.

Zero calibration can be solved directly by msp430. temperature drift at 0℃ can still occur, however, only temperature correction for zero calibration will be enough due to the inaccurate set of temperature limited by laboratory conditions . Zero output is 0.016V, just substracting 131 in on the AD conversion result.

3.2 Data processing

Since there are totally 4 parameters in the measurement, namely the density , temperature, mass , a total height of the liquid. In order to obtain more accurate parameter value, the density is chosen as the reference calibration for other parameters . Because the temperature sensor can be accurate to two decimals, temperature parameters will be more precise. however, the relationship between density and temperature of the water (water as the experimental subject) is not linear, and there is no precise formula for reference , therefore , liquid density can only be acquired by look-up table.

Formulas of specific parameters are listed as follows [6] (AD reference voltage : 2.5V):

Temperature**:**

$$T = \frac{V_{in}}{2.5} \cdot 100 \qquad (2)$$

Pressure：

$$P = \frac{V_{in}}{2.5} \cdot 6000 \qquad (3)$$

Height：

$$H = \frac{P}{r \cdot g} \qquad (4)$$

Mass：

$$m = \rho R^2 H \pi r \qquad (5)$$

In formula (2), V_{in} is the temperature sensor input , V_{in} in the equation (3) is the pressure sensor input . ρ is the density of water. g is the gravitational constant , R (radius of the container) = 15cm.

Program flow chart is as follows:

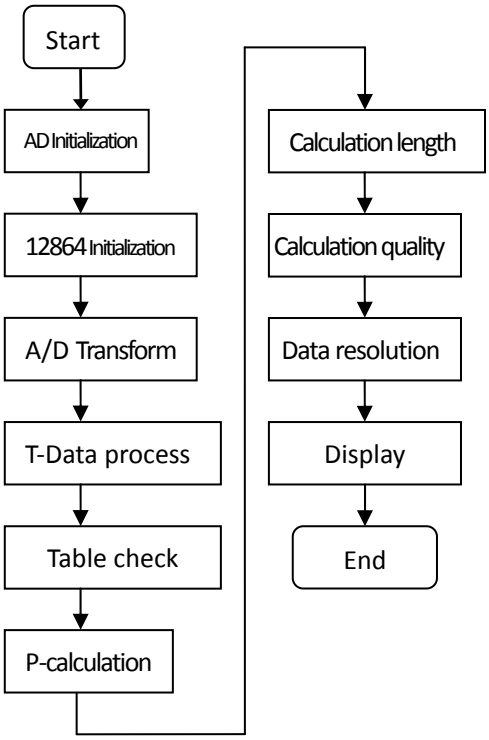

Figure 9 System program flowchart

4 RESULTS AND ERROR ANALYSIS

4.1 Results analysis

Density resolution reaches two decimals. Only the integer part of the temperature is displayed. The liquid resolution can reach millimeters , mass resolution can reach grams. The errors of display and the actual measurement still exist. Height error is about 1.5cm or so. The mass error is about 0.7kg. The range of the sensor at the bottom is 6Kpa, in the case, height error is 2 %, mass error is 1.5 %, which meets the error requirement of 3% .

4.2 Sources of Error

1) Size model is calibrated by hand , so the measurement error is inevitable.

2) All resistors have resistance error and temperature drift , which is one of the reasons for causing 1% errors and 5ppm temperature coefficient.

3) AD converter resolution is limited , and there is a quantization error , the error is 0.0245% .

4) msp430 can only retain its integer parts when doing integer division, greatly reducing the accuracy of the data. Due to the limited time at this stage, the algorithm is not perfect, remaining to more accurate in the future.

5) Measurement accuracy is limited, which is also one of the causes of error. Figure 10 is a pictorial diagram of data processing .

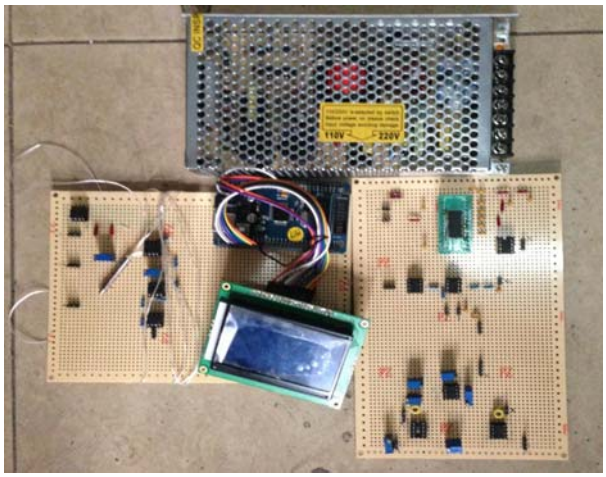

Figure 10 pictorial diagram of data processing

5 CONCLUSIONS

Using msp430 to obtain and process experimental data has the advantages of fast response and high processing accuracy. Making compensation for the data acquired by Max1457 can improve the accuracy of the system. Now the system has met the requirements with measurement error less than 3%. Large numbers of experimental data show that the accuracy of the system model in terms of mass has fully met the requirements, which solve the problem of weighing oil accurately. In addition, the cost is

relatively low. In general, the system provides a reference for the actual measurement .

Reference

[1] Liu Hongwei. HTG law Tank Measurement System in oil blending [J]. 2012. 27 (4).

[2] Dong Haifeng, Huang Cenyue. Automatic tank gauging system and pressure sensor [J]. Oilman Technology , 2003 (3)

[3] Dai Yan. Application of HTG system in the tank farm management [R]. Technological Innovation Herald .2009.10 .

[4] Cao Weiwei. Automatic tank metering system [J]. Petrochemical Automation .2012.48（2）.

[5] Zhang Chunxiao , Liu Qin , Liu Yan . Diffusion silicon pressure transducer precision temperature compensation [J]. Sensor technology .2011 .

[6] Zhou Shaoqi. Reserve tank measurement Study [J]. Gas Storage and Transportation , 1993 (03) :29 -33 .

[7] Li Lin, Shui Aishe, Han Fei. Analysis and improvement of accuracy of tank gauging system [J]. Logistical Engineering University ,2007.33 -37

[8] Jiang Xiaoyan. Application research on intelligent compensation and calibration system based on MAX1457 silicon piezoresistive sensors [D]. Thesis , Lanzhou University , 2000.4 .

[9] Li Yunting , Wan Zhenkai . Pt100 temperature sensor real-time data acquisition system [J]. Instrumentation users. 2007 (05) .

[10] Jiang Jinguang, Wang Yaonan. Realization of precise voltage source with bandgap reference [R]. Semiconductors .2004.7.

Research of asynchronous motor fault diagnosis based on Matlab simulation platform

Yu Tongguo; Zhang Hang; Meng Fanchao

（Jilin university instrument science and engineering institute,changchun,130021）

***Abstract*—To do the common fault simulation like locked rotor, broken bar, power grounding etc of the three-phase AC asynchronous motor by MATLAB and analyze the result using fft method. Take several power ground signals as the training sample of the BP nerve net. Then get the data processing and normalization. Take these parameters as the inputs of the nerve net. To judge the state of the system and recognize the fault after study train.**

***Key words*—Neural network Fault simulation Asynchronous motor Matlab**

I. PREFACE

INDUCTION motor is widely used in industry and agriculture, According to statistics, at present, the number of motor in the whole country Accounts for over 70% of the total of the grid, About more than 3 million units are burnt down every year.

At present, there are two ways, Offline maintenance and online maintenance, to maintain the motor. Online maintenance has a good result of Real-time monitoring. It can avoid or reduce the damage of Motor fault.

In the actual operation, locked rotor, Section bar, power grounding etc are most common. So, in this paper, we used MATLAB to simulate those three faults and focus on the Three-phase power supply grounding. analysis The stator current by FFT. Dealing with and normalizing the data we got ,and put them as the input of The neural network to train the neural network. Realizing that diagnosing the motor fault by the neural network.

II. THE NEURAL NETWORK AND THE PRINCIPLE OF DIAGNOSIS OF MOTOR FAULT

A. The neural network.

The neural network (figure.1) is constituted by lots of neurons In accordance with the topology. Every neurons is the basic unit of the neural network. Generally, it's nonlinear unit with multiple input and only one output. In the figure.1, Y_i is the input of the neurons, Hi is the threshold, Xi is the input signal, W_{ji} is the weight of neurons from U_j to U_i. S_i is the input signal from Exterior. The above model can be described by

$$e_i = \sum W_{ji} X_i + S_i \qquad (1\text{-}1)$$

$$Y_i = f(R_i - H_i) \qquad (1\text{-}2)$$

f is the activation function. Artificial neural manages the information Through three steps. First, completing the operation of input signal and neurons' connection strength, then Trading the result by Activation function (such as sigmoid function) and Threshold function. If the output value is greater than the threshold, Then this neuron is activated, Or in a inhibiting State. Neurons are connected into a network according to a certain mode. The size of the connection weights between the neurons reflect that Signal strength is weak or strong.

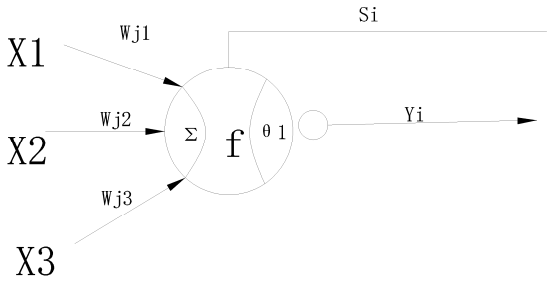

Fig. 1. The neural network

B. BP Network model locked rotor

BP network is a multilayer feed forward network by back propagation neural networks .is The most representative and one of the most widely used network model in Artificial neural network. It consists of input layer, hidden layer, and output layer. In the network, The signal passes on by the input to the output By one direction. And Identical level neuron Does not transmit the signal mutually. Each neuron is connected to adjacent layers of the neurons. The output of A layer of neurons Transport to the next layer of neurons By enhancing or inhibiting the connection weights. Besides input level, Each neuron's input is The output's Weighted value of all neurons in the previous layer.

C. The principle of fault diagnosis

Based on powerful learning features of the neural network, training it by peak-to-peak value of current special electric frequency of motor's different running status, and the network after training can judge the motor runs under the same conditions. Its fundamental principle is diagnosing motor fault by the features of frequency spectrum. Frequency spectrum analysis of Stator current is an Effective method of diagnosis and monitoring of AC motor fault. It can Diagnosis AC motor's section bar, voltage lacks, voltage phase, Power grounding. Cage fracture and Air gap eccentricity etc. can be manifested in Stator current by air-gap magnetic field. By examining the stator current and Frequency spectrum analysis, we can Diagnosis these faults. But, frequency spectrum characteristic analysis is unstable also is complex, using neural network will Judge fault type fast. The normal and fault data of neural network's Fault diagnosis come from Simulation model on MATLAB.

III. SIMULATION OF MOTOR FAULTS AND FREQUENCY SPECTRUM ANALYSIS

A. Rotor broken bar

1. Principle of using detection of stator current to diagnose broken bar

In ideal situation, The frequency of the stator current of motor is single. But If there is a fault of the time, on the Frequency spectra, there will be a Side band that appears on the frequency which Differs two times with Power frequency, This phenomenon is confirmed by Hargis etc. We can Inference The number of broken cage by Sideband amplitude and size of Difference between it and amplitude of Fundamental frequency current. This is the principle of Fault diagnosis by analyzing the frequency of Stator current of Asynchronous motor.

2. Building the model of broken bars fault.

When the actual structure of rotor is not taken into account, Wire-wound motor and Squirrel-cage motors are Exactly the same. And According to the theory of loop, When the broken bar fault happens, In fact only The size and distribution of the loop flux are changed, so, Absolutely we can change the resistance of one Winding to Replace it. Simulation parameters of motor are:

Stator resistance: R_s=0.435Ω;

Rotor resistance: R_r = 0.816Ω;

Self-induction: $L_s = 20e^{-3}$ H;

Mutual inductance: $L = 69.31e^{-3}$ H;

Rotor self inductance: $L_r = 2.0e^{-3}$ H;

The moment of inertia: $J = 0.089kg.m^2$;

Rotor resistance (External), R_a, R_b, R_c (are all 0.1Ω at Normal time, one will change to 0.5Ω-2.0Ω); Rated load is 11.9Nm. Rotor broken bars is simulated as figure2.

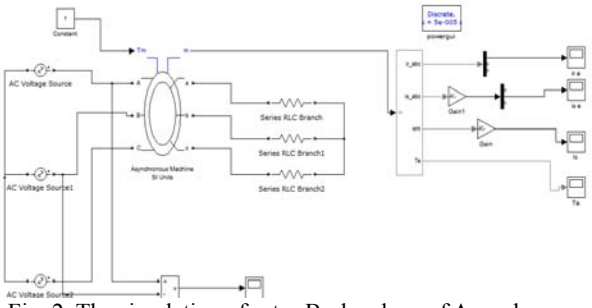

Fig. 2. The simulation of rotor Broken bars of Asynchronous motor

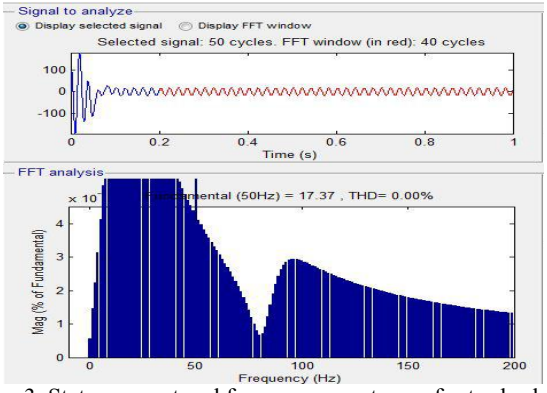

Fig. 3. Stator current and frequency spectrum of rotor broken bars of Asynchronous motor

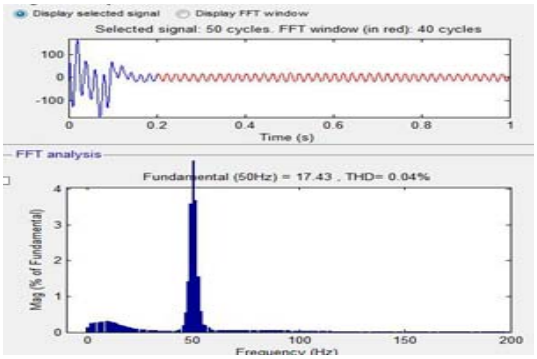

Fig.4.Normal Stator current and frequency spectrum of Asynchronous motor

From the above that Normal and defective frequency spectrum we know, When the normal operation of asynchronous motor, harmonic value of frequency spectrum is 5*10^-4% of the center frequency. But when broken bar happens, this data turns to about 0.5%, differing by three orders of magnitude.

B. Locked rotor

1. Principle of locked rotor

Locked rotor means that the motor rotor does not working Due to a malfunction. The performance is that the Slip s=1 in T equivalent circuit, That is, Additional

resistance is zero. In such a case, s=1, speed n=0, motor is in no running state. When simulating the fault of motor, by modifying the inside of the motor, we can get this simulation. There is no feedback of speed when locked rotor happens, so changing the input to 0.The simulation of locked rotor shows as figure5.

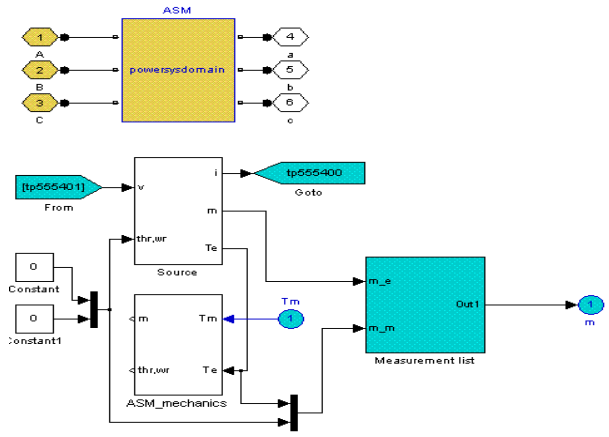

Fig.5. Simulation of locked rotor

2. Principle of fault diagnosis

When locked rotor happens, motor equals to an Electricity Inductance, so the current will be A lot more than it Under normal circumstances, about 12-50times.By analyzing The amplitude of stator current we can Infer the locked rotor. Current of normal circumstance or fault is shown as figure6 and figure7.

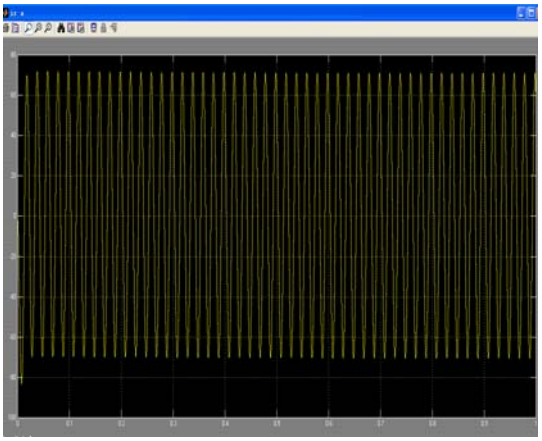

Fig.6. Current of locked rotor

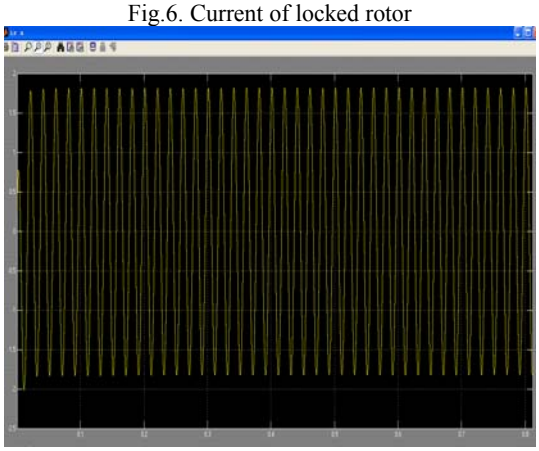

Fig.7. Current of Normal circumstance

According to the Waveform above, the Amplitude of fault is 75A, Normal circumstance's is 2A, It's consistent with the theoretical results.

IV. MOTOR FAULT DIAGNOSIS BY NEURAL NETWORK.

A. Principle of determining neurons of input level.

Because of that most of the scene can't provide operating parameters of motor detailedly, we should choose widely used Characteristic parameters to be input neurons. So, Selection of The characteristic parameters of fault must Follow the guidelines below: Non dimensional quantization. It is Not affected by motor' Capacity. and It is not necessarily associated with the motor structure, types and dimensions. It has the characteristics of variables. and Can respond the change of Degree of fault; Distinguish fault easily, and Easy to extract In engineering.

B. Selection of training samples

Neural network has better Fault-tolerant force than Logical identification. It Cannot make the mistake as a result of a fault of one characteristic quantity. This reduces the risk of miscalculation. But this method need a rich sample. So we built the model that is Suitable for Fault analysis, and get lots of data by the simulation.

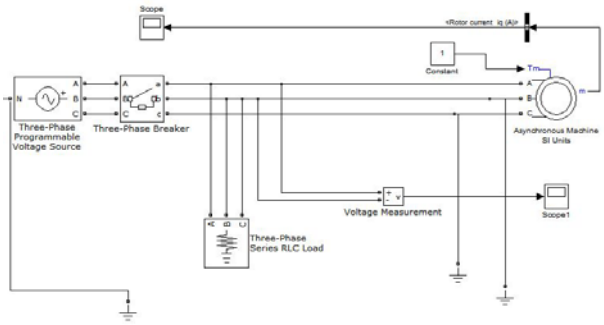

Fig.8. Simulation of loss of phase

This network has 3 layer BP network structure, node of input is 7, node of hidden layer is 2*7-1=13, node of output is 3.In the spectrogram of stator current, after Normalization of characteristic frequency of fault, X= $[X_1,X_2,\ldots,X_n]$, take it as the input, and output （0.0.0） means normal;（1.0.0）means a phase circuit breaker;（0.1.0） means B phase circuit breaker; (0.0.1) means C phase circuit breaker;（1.1.0） means AB phase circuit breaker;（0.1.1） means BC phase circuit breaker;（1.0.1） means AC phase circuit breaker; Characteristic frequency is shown in table 1.Data as follow ：

Table I, stator current of characteristic frequency Normalization is shown in Table II.

TABLE I. CHARACTERISTIC FREQUENCY

Time	0.0067	0.008	0.013	0.02	0.05	0.1	0.2	1
Normal	-326.84	-249.36	163.58	277.42	-11.75	-1.91	1.28	0.70
a	-98.52	-98.52	70.64	129.86	-262.93	120.11	201.26	-186.17
b	-302.21	-269.98	83.35	221.96	-32.08	-85.57	88.75	-0.85
c	-188.70	-188.70	265.16	23.66	-192.98	106.47	-92.82	79.24
ab	-96.31	-117.00	-34.57	121.15	-111.91	99.34	31.57	183.59
ac	-26.24	2.92	126.37	-85.66	83.23	-95.36	-163.77	171.09
bc	-201.84	-179.63	175.01	68.43	-84.49	15.37	34.36	-1.19

TABLE II. NORMALIZATION DATA

Time	0.0067	0.008	0.013	0.02	0.05	0.1	0.2	1
Normal	0.00	0.08	0.66	1.00	0.73	0.43	0.45	0.51
a	0.76	0.63	0.35	0.59	0.00	1.00	1.00	0.00
b	0.08	0.00	0.39	0.85	0.67	0.05	0.69	0.50
c	0.46	0.30	1.00	0.30	0.20	0.94	0.19	0.72
ab	0.77	0.56	0.00	0.57	0.44	0.90	0.54	1.00
ac	1.00	1.00	0.54	0.00	1.00	0.00	0.00	0.97
bc	0.42	0.33	0.70	0.42	0.52	0.51	0.54	0.50

C. Training and Test of Neural network

The following is the program of the training:

```
net=newff(minmax(X1),[17
3],{'tansig','logsig'},'trainlm');
net=init(net);
net.trainparam.epochs=1000;
net.trainparam.goal=0.00001;
LP.lr=0.1;
net=train(net,X1,T1);
y1=sim(net,X1);
save bpnetwork_1.mat net
X_test=x(:,1);
y_test=sim(net,X_test);
for i=1:3;
Y_test(i,:)=y_test(i,:)*(max(t(i,:))-min(t(i,:)))+mi
n(t(i,:));
End;  Y_test
```

Access the max of the number of the repetition is 1000,precision is 0.00001,the speed of study is 0.1 to train the net.The following is the result:

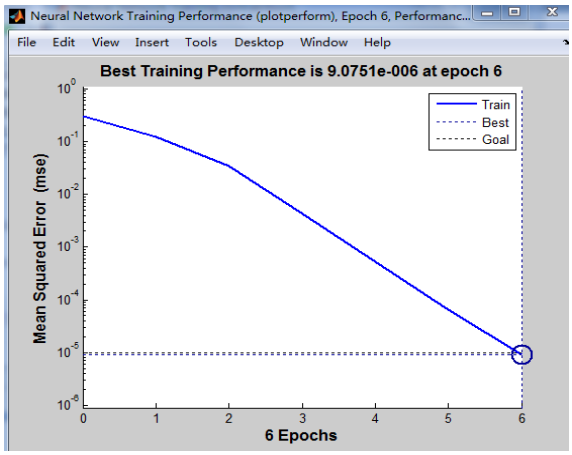

Fig.9. Solution of training of neural network

TABLE III. TEST SAMPLE

Phase A short circuit	0.76	0.63	0.35	0.59	0.00	1.00	1.00	0.00
Phase B short circuit	1.00	1.00	0.54	0.00	1.00	0.00	0.00	0.97
Phase AC short circuit	0.08	0.00	0.39	0.85	0.67	0.05	0.69	0.50

TABLE IV. TEST RESULT

sample	Reason of fault	Ideal output	Actual output
1	A short circuit	1.0.0	0.9998，0，0
2	B short circuit	0.1.0	0，0.854,0
3	AC are short circuit	1.0.1	0.914,0,0.793

It follows that, actual output is close to ideal output in neural network, in order to meet the requirements of training, it can be used diagnosing fault of quarantine mode.

V. Conclusion

Take advantage of utilization make use of matlab to emulate the 3-Phase AC asynchronous motors can responds the breakdown of motors effectively and fast, course the motors' internal structures are extremely complex, one breakdown may caused by multi-parts in most cases, therefore, the use is limited to the certain degree. However, making use of neural network conducting go ahead have on asynchronous motor which diagnosis on line has become a tendency. On account of classifications of the model of artificial neural network, it must have a mass of training samples in the first place, promptly required to be rich in knowledge and experience in the field. Therefore in consequence hence, with the further strengthen study on the motor fault, this is the key to solve the fault diagnosis problem of motor. Based on the method of the diagnosis of BP net, which reduce the error rate to the certain degree. Nonetheless, speed of BP algorithm weaken slowly, regarding a specific question, regardless of increasing the number of the hidden layers or more neuron, it may not give a hand to solve the problem. Therefore, adopt disperse training, select connection weights of the net coefficient initial value and other parameters opportunely at the same time appears to be more vital.

References

[9] Zhang Jianwen , "Electrical equipment fault diagnosis technology" [J]China Water Power Press, 2006，pp.123~152

[10] Wang Hongli, Hou Qingjian,, "Fault diagnosis method and prospect" ,[J]Sensors and Micro systems, 2008，27（5）

[11] Zhang Lijuan, "Online diagnosis system for asynchronous motor",[J]Master's degree thesis, Lanzhou University of Science & Technology 2009

[12] Sun Li,Zhao Xi "Study on fault diagnosis of motor Based on neural network", [J]Technology news 2008，12

[13] Yang Xiaohua, Fu Zhifeng, "Study on the fault causes and treatment of three phase asynchronous motor", [J]Modern commerce industry 2009.8

[14] Liu Jun, "Study of fault diagnosis method and software development" ,[C]Master's degree thesis, Dalian University of Technology 2000

[15] Shen Biaozheng, "Motor fault diagnosis technology", [N]Machinery Industry Press 1996,367~375

[16] Guo Jing, Sun Weijuan, "Neural network theory and MATLAB7", [N]Electronic Industry Press 2005,99~104

[17] Yang Zhi,Zhang Xinwu,He Xin, "The current spectrum analysis and its application in fault diagnosis of motor" [N]Inner Mongolia oil chemical industry 2007,8

[18] He Lizhu, "Fault diagnosis of three-phase asynchronous motor and Solutions",[J] Silicon Valley 2009,2

Portable Inductance Meter

Meng Zelin; Li Yongbin

(College of Instrumentation & Electrical Engineering， Jilin University， Changchun ， 130012，china)

***Abstract*—**This design is a portable inductance meter，which consists of the inductance test module, frequency dividing circuit and data choice circuit. STC89C52 SCM is used to measure frequency and calculate, realize inductance measurement by controlling the system. The final result is displayed on the LCD1602 screen. The system is based on the energy-storage principle of the inductance, along with multivibrator circuit composed of TLC555 timing. Corresponding inductance values can be calculated by measuring the frequency of oscillating circuit. This system design is simple, low cost and wide measurement range. In addition, measurement error is less than or equal to %3.

***Keywords*—**frequency dividing circuit ; multivibrator circuit ; TLC555 timer ; inductor measuring

1、INTRODUCTION

WITH the development of the electronics industry, electronic components increase dramatically, and adaptive range of electronic components has been widened gradually. In applications we often need to measure some components' values. Also, inductive elements are widely used in the circuits, therefore, it is extremely important to measure the inductive element inductor value accurately. However, inductance testers on the market are generally more expensiv, relatively large in size, and inconvenient to carry around. Thus, the design of a reliable, secure, convenient and inexpensive inductance meter has great practical necessity.

2、OVERALL DESIGN

The square wave signals of different frequencies, generated by inductance measurement modules, are shaped and processed by divider circuit , then are sent to the channel selection modules respectively. With the testing inductance elements, the SCM selects inductance test circuits with the key input and automatically detects the corresponding frequency range of the device under test. Controlling channel selection module to select corresponding input channels and the frequency division multiples, automatic shift of measurements can be realized. In addition, after some calculation the SCM will send measurement results to LCD and display the frequency and the values of the components on the LCD.

3、SELECTION OF EACH MODULE

3.1 Inductance test module circuit

Program One: The balanced bridge method to measure inductance. The balanced bridge consists of inductances to measure and a known standard resistance-capacitance, adjusted the parameters by the SCM to balance the bridge. Thus, the values of inductances can be determined by the resistance and the eigenfrequency of the bridge. The program provides precise measurement, obtaining accurate capacitance and resistance. However, duo to the complexity, it Is difficult to implement .

Program Two: LC and transistor oscillator circuit constitute the three-point oscillating circuit, and the inductance value can be determined by measuring the output frequency. This program costs little, but its output waveform is a sine wave, which need to be sent back to the waveform shaping processor. The output frequency is up to several megabytes, difficult to measure for SCMs.

Program Three: TLC555 timer and inductances to be measured constitutes multivibrator based on inductive energy storage inductor and charge-discharge principle, determining the inductor value by measuring the frequency value. The circuit is simple, and its output waveform is TTL level square wave signal. After simple frequency division, ideal range for frequency can be obtained, providing convenience for the accurate measuring of SCMs.

In summar, the design adopts program 3, constituting multivibrator circuit by TLC555 with a good frequency characteristics.

3.2 Frequency Measurement

Program One: direct frequency measurement. During certain gate time, the frequency of the signal under test can be calculated by recording the clock cycles of the test signal. This solution has a low accuracy on frequency signal measurement, suitable for high frequency signals.

Program Two: circle measurement. Choosing the measured signal as the threshold, the frequency of the signal under test can be calculated by recording the number of high-frequency standard clocks in the threshold. However, when the signal frequency is too high, problems of insufficient time and low accuracy can't be avoided. Thus, this program is suitable for measuring the low-frequency signal.

Program Three: equal precision measurement. Its exact threshold is jointly controlled by the signal and the pre-control door. Measurement accuracy is irrelevant to the frequency of measured signal, only associated with the frequency and stability of the reference signal. Thus, the constant accuracy throughout the measurement band can be guaranteed. However, implementation of this program needs FPGA and other special chips to cooperate with the SCM to achieve accurate measurements, which is more complicated and costly .

In summary, the design combines the former programs. Using frequency measurement in the high frequency band and cycle measurement in the low frequency, it can greatly improve the measurement range and accuracy. And the system is simple and easy to realize.

3.3 Theoretical analysis and demonstration program

The schematic diagram of inductance measurement is shown in Figure 1 (a). With a 555 timer and inductors constituting multivibrator, Inductance can be determined by measuring the frequency value. R1, L1, D1 are the timing components of the circuit. 3-pin output is TTL level, the frequency of which changes with the square-wave signal. After energization, the current of L1 can not be mutated. The current of R1 and L1 starts from zero, and the flux of L1 also changes, resulting in changes in the electromotive force. The voltage of pin 2 and 6 V(2,6) = VCC, and the voltage of pin 3 is low. The discharge tube in 555 Timer breakovers. Pin 7 is connected with ground, and loop current of L1 and R1 increases exponentiall . the voltage of R1 decreases and the voltage of VR increases , V (2,6) decreases. When V (2,6) = VCC / 3 , the circuit reverses. The output of Pin 3 is high , and pin 7 disconnects with the ground, the counter electromotive force of inductor L1 decreases exponentially. VR also decreases, and V (2,6) starts to rise. when V (2,6) = 2VCC / 3, the circuit reverses again. The voltage of pin 3 becomes low, with pin 7 connected with the ground again and L1 charging again, and so on. In order to achieve self- oscillation. The waveform of VR and final output waveform are shown in Figure 1 (b). The time of Circuit output high and low waveform is as follows:

$$T_{PL} = t \ln \frac{\frac{2}{3}VCC}{\frac{1}{3}VCC} = t \ln 2 \qquad (1)$$

$$T_{PH} = t \ln \frac{VCC - \frac{1}{3}VCC}{VCC - \frac{2}{3}VCC} = t \ln 2 \qquad (2)$$

Thereinto, $t = L_1 / R_3$ .The output frequency is:

$$f = \frac{1}{T} = \frac{1}{T_{PH} + T_{PL}} = \frac{R_3}{2 \ln 2 L_1} \qquad (3)$$

The value of inductance is:

$$L_1 = \frac{R_1}{2 \ln 2 \cdot f} \qquad (4)$$

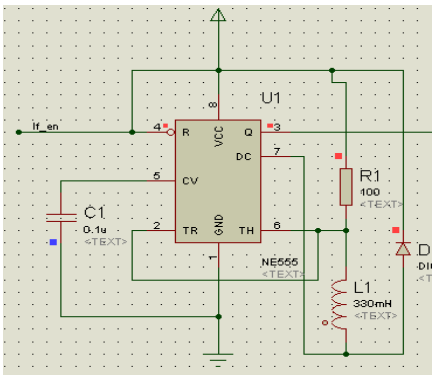

（a）circuit diagram of inductance measurement

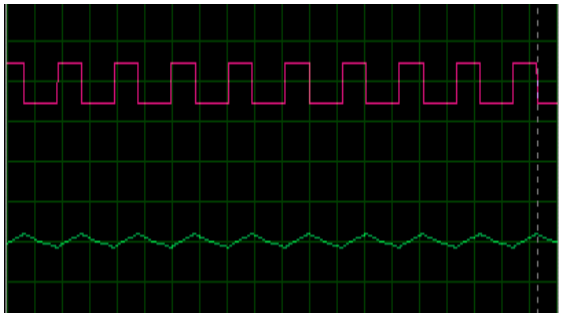

（b）simulation waveforms

Figure 1 Schematic diagram of inductance measurement

4 UNIT CIRCUIT DESIGN

4.1 Hardware Design

4.1.1 Inductance measurement circuit

Given the range of measuring inductance, theoretical analysis shows that the output frequency of the circuit is very high, and hence, the output signal must be divided , which can be completed by SCM. In the design, high-speed timer TLC555 and two counter 74LS196, as the inductance measurement module, make 10 and 100 frequency division processing on the signal respectively, expanding the inductance measurement range. Its original waveform of voltage, the output waveform of the timer and the waveform after frequency division processing are shown in Figure 2. Choosing high-speed Schottky diodes 1N4148 as discharge diode in the circuit can improve the step response. Figure 3 shows the specific parameters of the circuit.

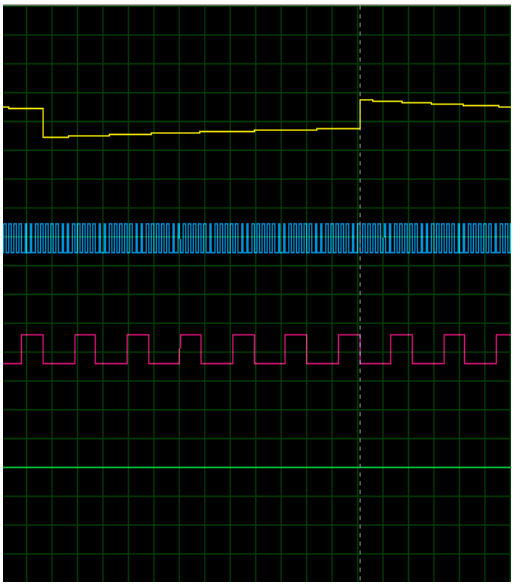

Figure 2. contrast of simulation waveforms

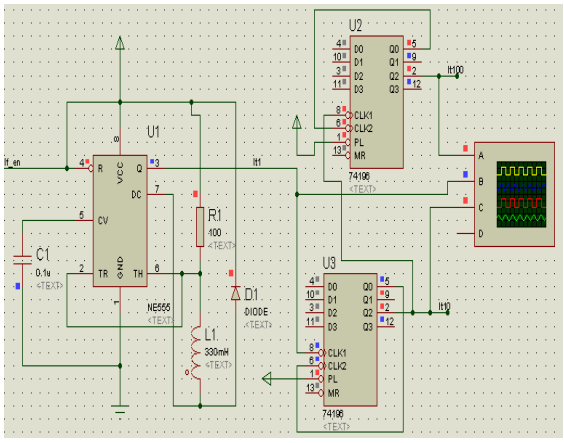

Figure 3. inductance measurement circuit

4.1.2 Channel selection circuit

The design needs to select the signals from three ways, and finally only one signal is sent to SCM for frequency measurement. In this design, 6 channels are controlled by analog 8 -to-1 multi-channel switch CD4052.

4.1.3 Power circuit

The design requires that frequency of each module generates waveform must be stable, thus, less power fluctuations are needed. Ripple linear regulator LM7805 directly decreases supply voltage 15V to the system supply voltage 5V.

4.2 Software design

The main task of STC89C52 is to measure the circuit. control relays and analogue switches realized automatic shift. Meanwhile, the frequency must be measured to calculate from the values of corresponding elements , and control LCD1602 displaying the types and values of measures elements. Software flow chart is shown in Figure 4.

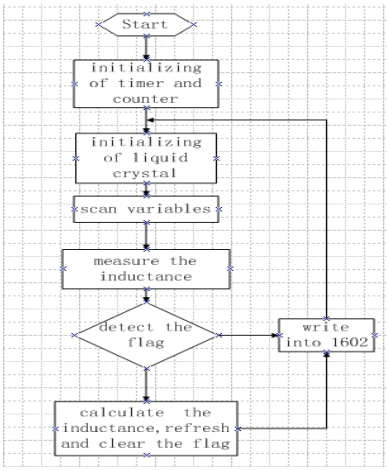

Figure 4. System flowchart

5、SYSTEM TESTING AND RESULTS ANALYSIS

5.1 Final results

The real values of the standard inductors are 330uH, 680uH, 2200uH, 4700uH, the testing results of present system are shown in Table 1.

Real value (uH)	330	680	2200	4700
Measured value (uH)	318.4	682.1	2202.1	4536.3
error (%)	-3.5	0.3	0.1	-3.5

Table 1 inductance measurements

5.2 Analysis of test results

After testing, the inductance measuring-testing instrument can measure the inductance range between 300uH and 10mH. The measurement error between 500uH ~ 5mH is less than 3%, other ranges less than 5%; system can automatically shift. In addition, the design uses inductance and diode to replace multi-resonant oscillator made up with capacitors and TLC555 timers, thereby simplifying the circuit and further reducing the cost of the system, which makes the system innovative.

System measurement interface are shown in Figure 5, Figure 6.

Figure 5 Initial measurement interface

Figure 6 Result of 330uH

5.3 System Error Analysis

According to the table, measurement errors will increase when the value of measuring elements is too large or too small. After analysis, the design adopts resonance frequency method to measure elements. The resonant frequency is small when component parameter is too large. On the contrary, its resonant frequency becomes large. Limited by the performance of SCM , the measurement accuracy decreases when the frequency is too low or too high, in addition, the accuracy of each component will also affect the accuracy of the system . These factors have formed a device measuring error and limits the measurement range.

6、SUMMARIZES

The system can measure the inductance values ranging between 300uH and 10mH, and has a higher measurement accuracy between 500uH ~ 5mH, but there are still some design flaws. As for measurement error, more sophisticated components for the measurement modules can improve the accuracy,and increasing the frequency division will also help. In addition, increasing tap positions for the frequency measurement modules can limit the output frequency, or using a better SCM can also achieve the same effect. In general, all the methods mentioned above can enlarge the measuring range and improve the accuracy of the system.

References

[1] Zhang Yongrui, Liu Zhenqi, Yang Linyao. Basic electronic measurement technology [M] , Xi'an: Xi'an University of Electronic Science and Technology Press ,1994:82 -88.

[2] Sun Xiaozi, Zhang Qimin. Analog Electronics Enterprise [M] , Xi'an: Xi'an University of Electronic Science and Technology Press , 2001:22-72 .

[3] Yu Mengchang. Concise Guide to Digital Electronic Technology [M] Beijing : Higher Education Press, 1999:245-362 .

[4] Hao Qiang , Zhang Wen.Basic C language programming tutorial [M] Beijing : Higher Education Press, 2006:306-307 .

[5] Kang Huaguang. Electronic technology infrastructure

(analog part) Fifth Edition [M] Beijing : Higher Education Press, 2005.

[6] Gao Jixiang. Basic experimental electronic technology and curriculum design [M] Beijing : Electronic Industry Press, 2002:283-288 .

[7] He Jianguo, Liu Lixin, Dang Jianhua . Frequency meter MCU [J]. Based Xi'an Institute of Posts and Telecommunications , 2003 (3) :31 -35.

[8] Liu Nanping. Modern electronic design and production technology [M] Beijing : Electronic Industry Press, 2004:230-232 .

[9] Chen Jianghua. A practical capacitors, inductors and resistors automatic measuring instrument [J] Measurement and Testing Technology, 2002 (1) :21222 . 2005

The Detection Technology of Grid-connected PV Islanding

Zhen Geng;Facong Zhang;Huixuan Wang
（Jilin university Instrument institute jilin changchun）

***Abstract*—Islanding effect is one of the important problems affecting the photovoltaic (pv) grid system and stable operation.With the emergence of distributed photovoltaic power generation,the monitoring of a lonely island becomes even more important. On the basis of commonly used detection methods (AFD, HD, etc.),the method of AFDPF combined with HD island detection is adopted, and aided by the simulation analysis, the effectiveness of this method is verified.**

***Key Words*—Photovoltaic power generation; AFD; HD; the islanding of simulation**

0. INTRODUCTION

ISLANDING is a fundamental issue of photovoltaic system that is the pv system of failing to detect situntion of tripping power grid that continues to supply power to load,which leads to a completely independent system[1].It is vital for system to detect the islanding.Nowdays,we can make sure islanding by the standards of national electric systems,which contains frequency,voltage,phase etc.If the notions change,the pv will stop to work.With the economic development,we have to improve the way of checking islanding.In order to get efficient scheme ,in general,people take posive measures which contain active interference and passive ways[2]。

1. THE REVERSE ISLANDING STRATEGY ON INVERTER

As we all known,there are two kinds of the reverse islanding strategy on inverter.On the one hand,it can be able to be monitored by the load end abnormal voltage and frequency ,phase ,harmonic.but sometimes which will lose their effect in certain circumstances called as passive.On the other hand,the means is active.we take the disturbance variable into the working inverter.Only inislanding circumanc -es,will the disturbance be amplified and will details sxceed the threshold in a short period of time.That will help inverter rapidly to detect islanding.

The active method is also called active method，which is relying on the inverter itself to detect whether an islanding，at the same time,it do not need additional measurement equipment and transformers to save the cost of power system.According to the inverter output current formula: in the meantime, I_m、f、θ_1 were added in the control signal terminal of the inverter, three variables can influence the voltage at the output, when island effect did not occur, owing to the clamping effect of balancing the grid, PCC point signal perturbation is small, difficult to detect. However, the amplitude and frequency can be detected through the output terminal voltage to detect island effect[3]. Each country has different testing standards, so when understanding the principle, first understand islanding detection standards.

1.1 The detection standards of islanding

Due to the structure and operation of grid technology and distribution network system requires a strong relationship, so there is not a unified international standard, every country has its own standard, the main reference in considering islanding detection time I this paper is IEEE Std.1547[4],It requires:after a sudden emergence of distributed island ,power continues to be supplied through a common connection point of the island to the power system, the distributed power supply should be detected within 2s island and stop the power supply to the area.

The test conditions requires an adjustable RLC load, connected in parallel between the PV inverter and the grid .Adjusting the resonant LC circuit, so that oscillation occurs at the nominal frequency $f$of the grid, while the quality factor of the circuit $Q_f = 1$, that is: the reactive power absorbed by the inductor

should be equal to the reactive power produced by capacitance, and is equal to rated power and resistance consumption at rated grid voltage V. The load value of RLC is calculated as follows:

$$L = \frac{V^2}{2\pi f F Q_f} \quad (1)$$

$$C = \frac{F Q_f}{2\pi f V^2} \quad (2)$$

1.2 HD

HD is theoretically avoid detection blind from a passive detection method[5], is independent of the load-side power mismatch influence, in the case of island phenomenon does not occur, the inverter side of the harmonic voltage change weakly, when the grid is disconnected from power instantaneously, the voltage harmonic variation is large, it can be judged by monitoring the harmonic, but in some cases due the excessive load more sensitive ,it may leads to false positive or false negative judgements . As passive detection,the method can be combined used between passive and active detection.

1.3. AFD

AFD is the most commonly used active detection method [6], if the current waveform of the inverter output have a slight distortion, then the current will produce a zero current component causes the frequency offset [7], AFD is in the current frequency of the inverter output , small periodic changes I_f is added to the grid, during normal operation, since the operation of the PLL, the current frequency of output will be synchronized with the grid voltage, thus the frequency of the output current fluctuates in a standard range, but does not exceed the fluctuation range, when the power grid is off power for some reason, in order to make the load circuit resonance frequency and phase angle remains unchanged, the output frequency of the inverter side will change, change will continue to increase or decrease until beyond the standard range, and the island state is detected . AFD is easy to achieve in practice, but would supply system current waveform distortion caused by unstable increases while reducing the NDZ, for inductive load, there is a NDZ. When applied to multi-grid inverter circuit, if the frequency of the frequency shift direction is not uniform, it may cause offset each other, the detection efficiency will reduce a lot. However, the model can then improved and enhanced based on AFD.

Given the premise of passive and active anti-islanding can combine successfully, I will upgrade the HD version AFDPF law and AFD method combining simulation modeling performed islands.

2 ISLANDING DETECTION PRINCIPLE AND METHODS BASED ON AFDPF COMBINING WITH HD

2.1 Simulation principle

AFDPF method is to avoid the load testing to impact the quality of island, based on the original model of AFD, in the inverter side, adding a periodic continuous frequency disturbance, accelerates the speed of the frequency offset, the power grid is in the normal state, and frequency Interference amount of current network side will not have a greater impact on the output side of the inverter voltage frequency, however, in the island state, owing to lossing the influence of the grid side, the current disturbance causes the inverter side (a point) voltage generating large frequency changes ,by changing the speed.

Accelerating the disturbance, after comparison of several disturbances, changes in the frequency direction is determined, and then changes the direction of the applied perturbation continued until the output frequency of the voltage exceeds the normal limits . Judgment island. While relying on real-time monitoring module measuring voltage frequency based on PLL, by writing S function to process frequency, while the voltage harmonics can function as an input preparation, the two nested relations, is a passive detection and active detection combination to reduce the pollution index, and improve efficiency. After processing through the PI regulator, the output control PWM regulator, indirectly controlled inverter, to achieve Anti-islanding local side slightly, with a strong application.

2.2.Simulation Model

Rely on Matlab simulation software to build a photovoltaic power generation and network model to simulate the island phenomenon, and simulation analysis, the simulation model built by Simulink[8,9]is shown in Figure 2-1.

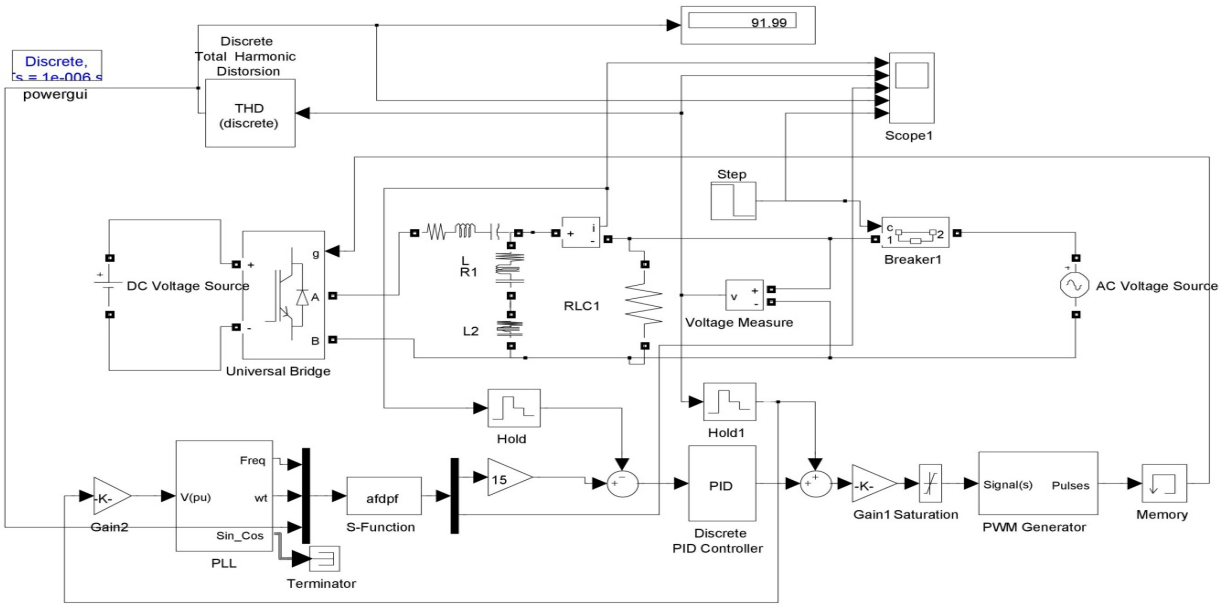

Fig 2-1 Simulink Simulation Model

2.3 Simulation results and analysis

In order to verify the effectiveness of islanding detection method proposed in this paper, so the two cases be verified, one case is not to match up with the load (inductance, capacitance, resistance), and the other one is in the case of load matching, when the load is RLC parallel load, islanding is the hardest to detected, so when choosing RLC load as a local load, while the parallel resonant frequency is equal to the grid frequency, forming the most serious island status, according to the People's Republic's network requirements, load frequency is set to 50 Hz.

Simulated in Matlab software, and add the control switch in the grid side, artificial set-up time, control the generation of the island, in the simulation, island occurs at 0.1s, through the inverter side current, through the voltage waveform to determine whether Anti-islanding is realized effectively. the simulation results from the oscilloscope display, each image contains five small figures, followed by representatives of the current value of the output terminal of the inverter, v, f, voltage harmonics, and curve of the relationship between time of producing island and time, according to the People's Republicof China's frequency limit ,setting standard frequency range of islands detection :49.5-50.5HZ; harmonic is less than 0.5, anti-islanding is on this basis.When the load does not match the type of the load ,simulation results are shown in Figure 2-2, Figure 2-3, Figure 2-4.

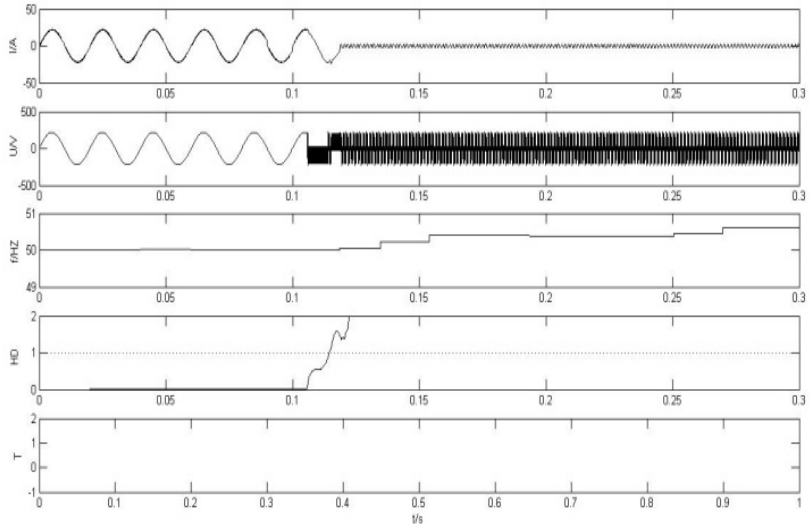

Fig2-2 Inductive load

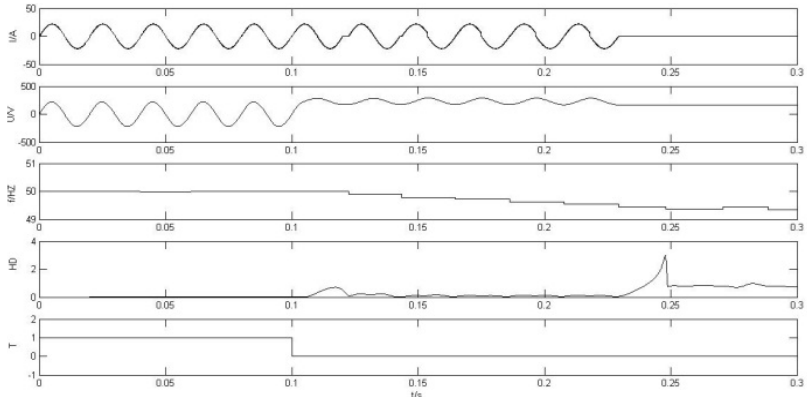

Fig 2-3 Capacitive load

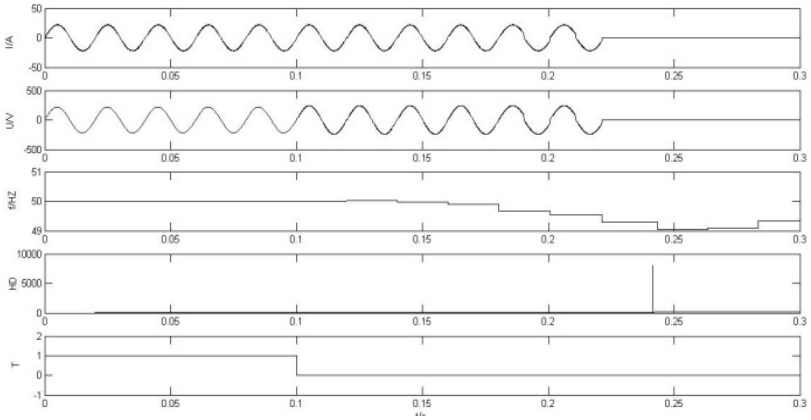

Fig2-4 Resistive load

2.4 Load mismatch simulation analysis

AFDPF + HD model can be in different loads condition, without exceeding international standards, to achieve a rapid anti-islanding strategy, for inductive load, HD changes the fastest and the most effective, when the frequency change is just beginning, it achieved islanding detection, capacitive load, HD lose their effect, changes are weak, but AFDPF compensate up for it, to achieve detection function, for capacitive load, HD and AFDPF can detect changes at the same time, achieve off power, it can be said that HD + AFDPF can achieve islanding detection, and quickly, is a novel detection method. Easy to determine the island phenomenon, and anti-islanding.

When the load match (RLC parallel and $R = \frac{U}{I}, \omega C = \frac{1}{\omega L}$),because the grid voltage amplitude is set to 220V, current is 20A, and therefore the resistance value of R is to select 11, the grid voltage frequency is 50 Hz, therefore, the capacitance C is 1300e-6F, the inductance of L is 7.65 -3H, in standard testing standards, the simulation results are shown in Figure 2-5.

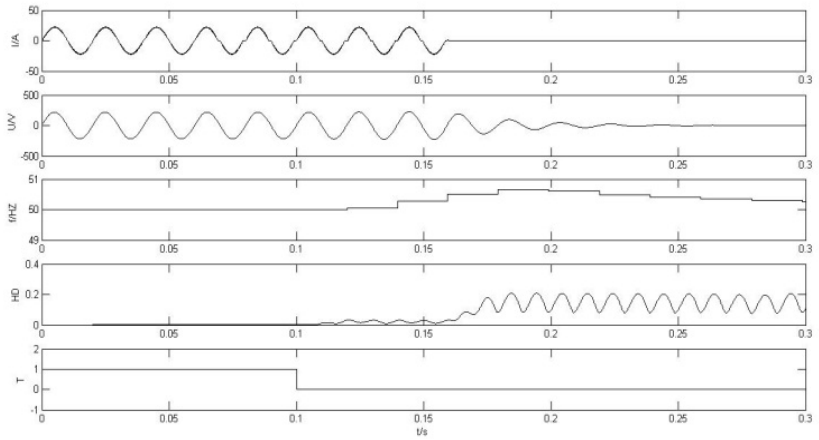

Fig 2-5 Load matching simulation diagram

2.5 Load matching simulation analysis

In the case of load matching, when the PV system occurs islanding phenomenon, the magnitude of the load voltage and current point does not change, the traditional passive approach is not detectable formation of dead zones, but applied with the AFDPF + HD method, it can not only detect the island and can be detected in the standard time, realizing anti-islanding, implementing the anti-islanding control strategy effectively.

3. EFFECTIVE ASSESSMENT STRATEGIES BETWEEN NDZ AND ANTI-ISLANDING

We know that islanding protection is an important part in DG, but in practice there is no one model can be applied under all conditions, therefore, existing the case failed to detect phenomenon-NDZ, these cases have failed to match the power and special load cases, therefore, it is necessary to summarize, as the standard model is applicable to evaluate different scope, but also improves the effectiveness of islanding detection. Because they do not match the size and power of the DNZ specific load can be described quantitatively, while the size of DNZ of the anti-islanding schemes reflects the effectiveness of the program to detect the island state.

Therefore, it can be used as indicators of DNZ measure anti-islanding schemes. Understanding the principles of derivation of various programs[10], which found that $\Delta P \times \Delta Q$ the coordinates of the upper and lower boundaries are DNZ frequency operating range from the lower limit of the decision, and the left and right borders of DNZ voltage operating range from the lower limit of the respective decision. For the phase-frequency-based anti-islanding scheme as the criterion can be found island effect occurs, the system reaches steady state parameters of frequency has a direct relationship with the load, there are a lot of L and C can be the same ΔQ, matched power may draw on the same point, many points may result in failure detection, AFDPF relative effect will be better

4. CONCLUSION

Islanding detection is the core issue in DG normal operation, resolved better, will promote the development of the DG industry. This paper fully aware of the deficiencies of the original model, proposed a combination of passive and active combining simulation model, through simulation and analysis of AFDPF + HD anti-islanding strategy can better solve practical problems, reduce energy pollution, the detection efficiency is also improved to some extent. And because of its limited capacity, the model can be further improved, can be combined with more impact factors, when you build a function, you can analyze the data processing beforehand, which can improve the detection efficiency and reduce the impact on electricity.

Reference

[1] Keliang Zhou,Zheng Wang,Qingshan Xu.Translate.Grid converter of photovoltaic (pv) and wind power system. Mechanical industry press.Beijing.2011.

[2] Juan Gu,Mingyao Lin,Zhujie Shan,Yiran Zhang. Control strategy features analysis of photovoltaic (pv) grid inverter against islanding . Electrician electrical,2009,10(10):23-26.

[3] Qiming Cheng,Yingfei Wang,Yiman Cheng,Mingmei Wang. Distributed grid-connected system in the islands of the review of test method of research. Power system protection and control. 2011,16（3）：148-154.

[4] IEEE Std.1547-2003,IEEE Standard for Interconnecting Distributed Resources With Electric Power Systems.

[5] DeMango,F.,Lisere,M.,Dell'Aquila,A.and Pigazo,A.,'Overview of Anti-islanding Algorithms for PV Systems.Part I:Passive Methods'.In Proceeding of the 12th International Power Electronics and Motion Conference,August

2006,pp.1878-1883.

[6] Ling Yuan,Jianyong Zheng,Xianfei,Zhang. Grid-connected pv system island detection method of analysis and improvement[J]. Automation of electric power systems,2007,31(21):72-75.

[7] Ropp,M.E.,Begovic,M. and Rohatgi,A.,'Analysis and Performance Assessment of the Active Frequency Drift Method of Islanding Prevention'.IEEE Transaction on Energy Conversion,14(3),September 1999,810-816.

[8] Jing Wang,Guoqing Weng,Youbing Zhang. The MATLAB/SIMULINK simulation and application of power system. Xian university of electronic science and technology press.2008.11.

[9] Qun Yu,Na Cao. MATLAB/SIMULINK modeling and simulation of power system. Mechanical industry press.Beijing.2011.5.

[10]Xing Zhang,Renxian Cao,etc. Solar photovoltaic (pv) grid power generation and its control inverter. Machinery industry press.Beijing.2010.9.

A Modified Variable Step Size Perturb and Observe Maximum Power Point Tracking Method

Shuqin Sun, Huixuan Wang, Zhen Geng, Facong Zhang

（Jilin University Instrument Science and Engineering Institute,Changchun,130021）

***Abstract*--Maximum power point tracking (MPPT) is used in photovoltaic (PV) systems to maximum the photovoltaic array output power by tracking continuously the maximum power point (MPP), which is in nonlinear correlation with temperature, irradiation conditions and load electrical characteristics. Perturb and observe maximum power point method is the most common used method due to its ease of implementation. However, the system oscillates around the MPP at steady state and P&O may fail under rapidly changing atmosphere conditions. In this paper it is shown that, an improved method based on P&O can limit the negative effects caused by the drawbacks above. Simulation results using MATLAB are in agreement with the theoretical analysis.**

***Index Terms*--Maximum power point (MPP), maximum power point tracking (MPPT), perturb and observe (P&O), photovoltaic (PV)**

I.INTRODUCTION

AS people are much concerned with the fossil fuel exhaustion and the environment problems caused by the conventional power generation, renewable energy have been widely used. Photovoltaic sources are used in many applications today due to their advantages. In photovoltaic system, the output power of photovoltaic battery is affected not only by the internal characteristics but also by the environmental factors such as temperature, irradiation conditions and load electrical characteristics. A photovoltaic (PV) array under uniform irradiance and temperature exhibits a current-voltage characteristic with a unique point, called the maximum power point (MPP), where the array produces maximum output power. It is necessary to track continuously the MPP in order to maximum the power output from a PV system, for a given set of operating conditions.

Traditional maximum power point tracking (MPPT) method can be divided into open-loop and closed-loop control methods, according to different judging methods [1], [2]. Open-loop control methods, which based on the output characteristics of PV arrays, is easy to be implemented, but the control precision cannot be guaranteed [3]. With high precision, closed-loop control methods track the MPP by measuring the output voltage and current of PV arrays and feeding them back to the control system, and the most common used self-optimizing method belongs to them [4], [5].

Perturb and observe maximum power point method is the most common used method due to its ease of implementation [5]. It perturbs the output voltage in a small step periodically and then makes a measurement of the power and uses it as the feedback variable to control the direction of subsequent perturbation. Increasing the voltage increases the power when operating on the left of the MPP and decreases the power when on the right of the MPP. Therefore, if there is an increase in power, the subsequent perturbation should be kept the same to reach the MPP and if there is a decrease in power, the perturbation should be reversed. The process is repeated periodically until the MPP is reached.

However, ordinary P&O has two main disadvantages. First, the step size for P&O method is generally fixed. The power drawn from the PV battery with a lager step size contributes to faster dynamics but excessive steady state oscillations, resulting in a comparatively low efficiency. This situation is reversed while the MPPT is running with a smaller step size. Thus, the MPPT with fixed step size should make a satisfactory trade-off between the dynamics and oscillations. Such design dilemma can be solved with variable step size iteration. Another disadvantage of P&O method is that this simple tracking method can fail under rapidly changing atmospheric conditions, because during such time intervals, the operating point can move away from the MPP instead of keeping close to it. This drawback is shown in Fig. 3.

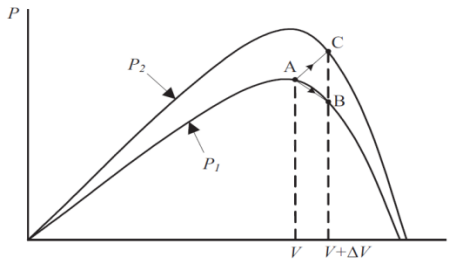

Fig. 1. Divergence of P&O from MPP as shown in [6]

This paper will propose an improved method to enhance the speed and accuracy of tracking. The MATLAB simulation results confirm the theoretical analysis and show the superiority of the method.

II.PV PANEL MODELING

A. Mathematical model

The equivalent circuit of a PV cell is shown in Fig. 2, in which the simplest model can be represented by a one-diode model [7].

The relation between the output current I_L and voltage U_L is the following:

$$I_L = I_{SC} - I_{D0}\left(e^{\frac{q(U_L + I_L R_s)}{AKT}} - 1\right) - \frac{U_L + I_L R_s}{R_{sh}}$$

where I_{SC} is the light induced current, I_{D0} is the saturation current, A is the diode ideality factor, K is the Boltzmann constant, and T is the cell temperature.

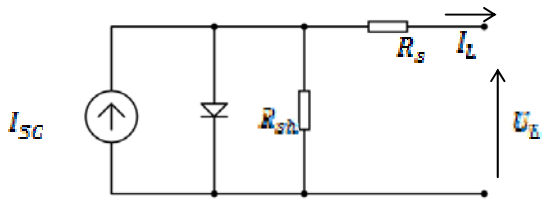

Fig. 2. Equivalent circuit of a PV cell

B. PV panel characteristics

STP295-24/Ve PV battery of SUNTECH is used and its electrical parameters are shown in Table I [8].

TABLE I

Electrical parameters of STP295-24/Ve

Maximum Power	$P_m = 295W$
Optimum Operating Voltage	$U_m = 35.7V$
Optimum Operating Current	$I_m = 8.27A$
Open Circuit Voltage	$U_{oc} = 45.1V$
Short Circuit Current	$I_{sc} = 8.57A$
Temperature Coefficient of I_{sc}	$\alpha = 0.055\%/°C$

The characteristic power curve at Standard Test Condition for this PV battery is shown in Fig. 3.

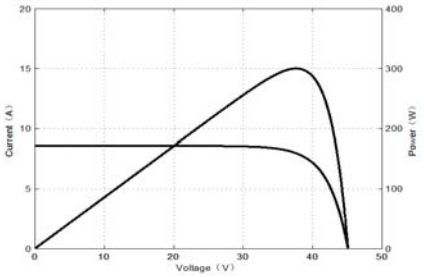

Fig. 3. P-V characteristic and I-V characteristic at Standard Test Condition

III.MODIFIED VARIABLE STEP SIZE P&O METHOD

A modified variable step size P&O method is introduced based on the previous research and detailed analysis of the characteristics of PV power systems. The modifications to the traditional P&O method include variable step size and power prediction.

The flow chart of the Modified variable step size P&O method is shown in Fig. 4.

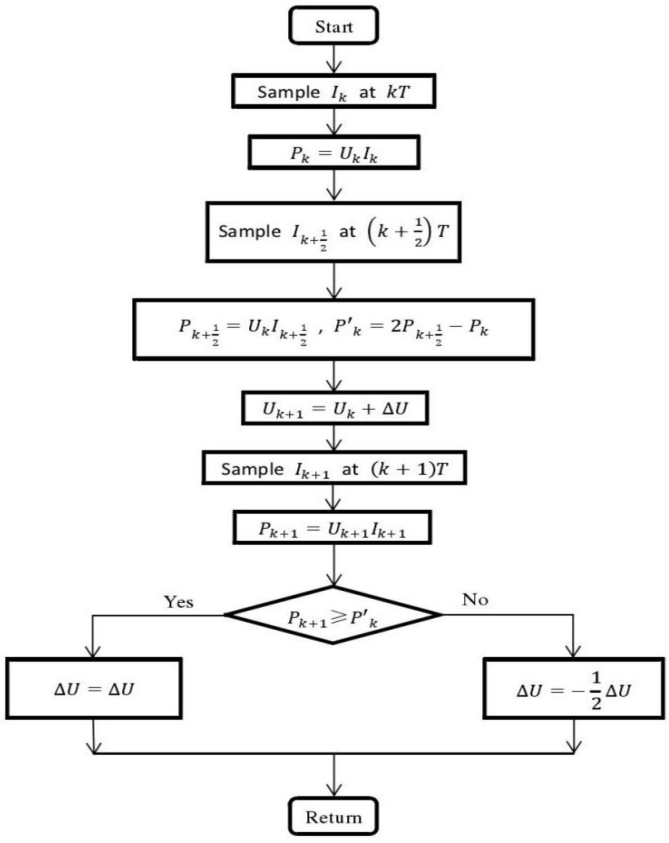

Fig. 4. Flow chart of the modified variable step size P&O method

A. Variable step size

As discussed above, there is a trade-off between dynamic response and steady state performance due to the selection of step size. It is ideal to make step size large during transient stage and step size small in steady

state. In the proposed P&O method, this problem is solved by the automatic tuning of the step size on-line [9].

Assume that the initial operating point is on the right of the MPP and is far away from it, the step size keeps a large value until operating point crosses MPP. Then the step size becomes half of its origin value and the perturbation is reversed. Repeat the process above when operating point crosses MPP again until the step size is smaller than a set value. Generally, we consider the MPP has already been reached when the step size is small enough. With this tuning mechanism, both dynamic and steady-state requirements can be considered in the controller design, because the critical parameter is updated and adjusted adaptively.

B. Power prediction

Traditional P&O method is based on static power curve, but the power curve is always changing actually. Deviation from MPP may never happen if the output power before and after perturbation can be measured at the same time. Obviously it is impossible. However, if a high sampling rate is used, the power curve will change at a constant rate in one sampling period.

Note that U_k, I_k and P_k are the PV battery output voltage, current and power at time kT. In addition, $P_{k+1/2}$ is the power at time $(k+1/2)T$. Thus, the power that PV battery produces before perturbation at time $(k+1)T$ is shown as follows:

$$P'_k = 2P_{k+1/2} - P_k$$

Perturb the voltage by ΔU at time $(k+1)T$, and then measure the power P_{k+1} when PV battery works at U_{k+1}, which is the output voltage after perturbation. The perturbation direction can be determined using P'_k and P_{k+1}.

IV. SIMULATION RESULTS

To verify the performance of the modified variable step size P&O method, a MATLAB model of the PV system is developed. STP295-24/Ve PV battery of SUNTECH is used for the PV array model in simulation.

To compare the performance of the modified variable step size P&O method with the ordinary fixed step size P&O method, the simulations are configured under exactly the same conditions to compare the performances. The PV array in simulation is composed of one PV module, and the sampling period used for MPPT method is chosen as 0.025 s. The voltage command is therefore updated every 0.05 s. The output power performance of P&O with variable step size and fixed step size of 0.5 under irradiation step change conditions are both shown in Fig. 5. The irradiation was suddenly changed from 1100 to 750 W/m^2 at 2.5 s.

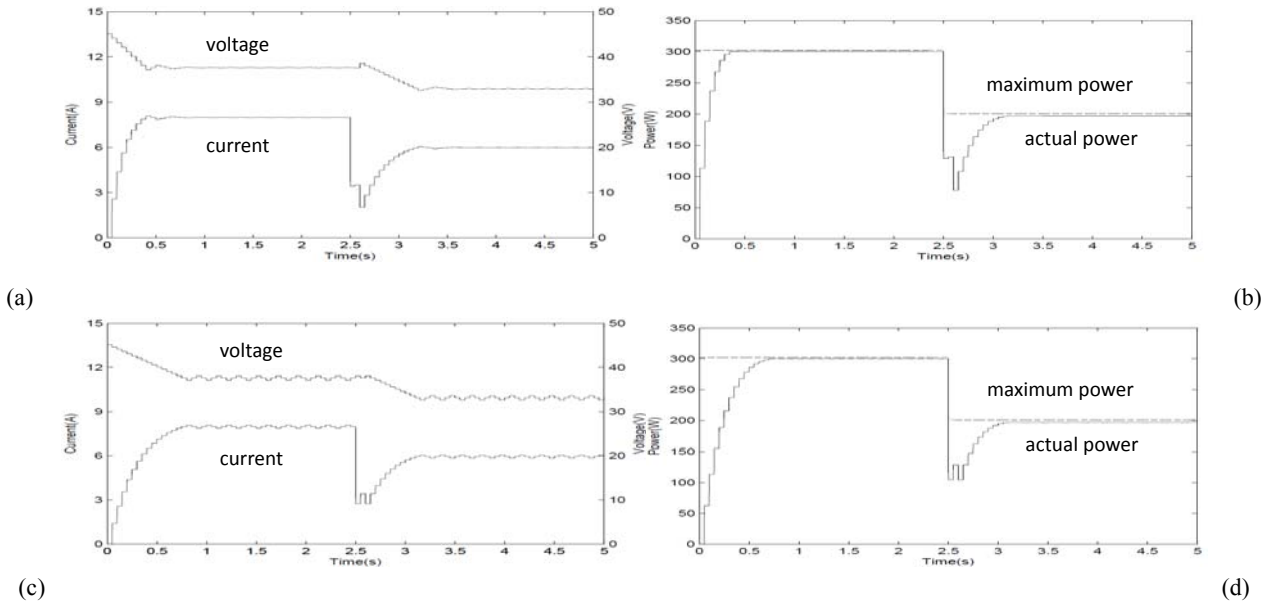

Fig. 5. Simulation results of sudden irradiation change with the two method

(a) PV ouput current and voltage with modified P&O. (b) PV ouput power with modified P&O.

(c) PV ouput current and voltage with ordinary P&O. (d) PV ouput power with ordinary P&O.

Table II
Tracking performance comparison

MPPT Methods	Tracking Time(seconds)		Average Power at Steady State(watt)	
	Initialization	Irradiation change	Irradiation $G=1100W/m^2$	Irradiation $G=750W/m^2$
Ordinary P&O (step size=0.5)	0.70	0.55	299.91	196.50
Modified P&O	0.36	0.65	300.00	196.88

The results illustrate that each maximum power point was determined quickly and tracked accurately by this proposed tracking method. The improved performance of this method over ordinary P&O tracking method can be demonstrated in Table II. The modified P&O shows better overall performance than ordinary fixed step size P&O on both dynamic response and steady state.

V.CONCLUSION

A modified variable step size P&O method was presented in this paper. At the start process of the MPPT, the PV system may exhibit comparable large step change in the output voltage and current due to the large step size. The automatic parameter tuning was implemented to satisfy the requirements of good dynamic and steady-state performances. The power prediction was designed to avoid the tracking deviation. The improved tracking performance of this suggested method was verified through computer simulations.

References

[19]Pallavee Bhatnagar and R.K.Nema, "Maximum power point tracking control techniques: State-of-the-art in photovoltaic applications, " *Renewable and Sustainable Energy Reviews*, vol. 23, pp. 224-241, Jul. 2013.

[20]E. Trishan and P. L. Chapman, "Comparison of Photovoltaic Array Maximum Power Point Tracking Techniques, " *IEEE Trans. on Energy Conversion*, vol. 22, no. 2, pp. 439-449. June 2007.

[21]M. A. S. Masoum, H. Dehbonei, and E. F. Fuchs, "Theoretical and experimental analyses of photovoltaic systems with voltage- and current-based maximum power-point tracking," *IEEE Trans. on Energy Conversion*, vol. 17, no. 4, pp. 517-522, Dec. 2002.

[22]Li Jiyong and Wang Honghua, "A novel stand-alone PV generation system based on variable step size INC MPPT and SVPWM control," in *2009 IEEE 6th International Power Electronics and Motion Control Conf.*, pp. 2155-2160.

[23]H. S. –H. Chung, K. K. Tse, S. Y. R. Ron Hui, C. M. Mok., and M. T. Ho, "A novel maximum power point tracking technique for solar panels using a SEPIC or Cuk converter," *IEEE Trans. on Power Electronics*, vol. 18, no. 3, pp. 717-724, May. 2003.

[24]O. Wasynezuk, "Dynamic behavior of a class of photovoltaic power systems," *IEEE Trans. on Power Apparatus and Systems*," vol. 102, no. 9, pp. 3031-3037, Sept. 1983.

[25]M. G. Villalva, J. R. Gazoli, and E. R. Filho, "Comprehensive approach to modelling and simulating photovoltaic arrays," *IEEE Trans. on Power Electronics*, vol. 25, no. 5, pp. 1198-1208, May 2009.

[26]STP295_Ve Datasheet. [Online]. Available: http://ap.suntech-power.com/images/stories/pdf/datasheets_ Q3_2012/STP295_Ve(H4_295_290_285)v2.pdf

[27]A. K. Abdelsalam, A. M. Massoud, S. Ahmed, and P. Enjeti, "High-Performance Adaptive Perturb and Observe MPPT Technique for Photovoltaic-Based Microgrids, " *IEEE Trans. on Power Electronics*, vol. 26, no. 4, pp. 1010 -1021, April. 2011.

The development of the near infrared spectrum brain function analyzer

Yang Yu ; Huang Linfeng; Li Yuchao

(College of instrumentation and electrical engineering,Jilin University,Changchun 130061,)

***Abstract*—With the continuous development of information era of science and technology level and the further exploration and research of brain science, higher and higher demands for brain function testing technology are proposed. Near infrared brain analyzer uses near infrared spectroscopy (NIRS) for nondestructive testing brain function. It mainly use the good penetrability of near-infrared light to external layer organization, and make it through the outer skin into the cerebral cortex, and use some of its information which is about diffuse light to calculate the blood oxygen parameter .As a consequence, we can further infer the change of blood oxygen and blood volum in the area of the brain so as to analyze the functions of the cerebral cortex. This set of brain function near infrared spectrum analysis instrument includes driven by light - coupling fiber - detector, light control circuit, data acquisition circuit, amplifier and filter circuit, under a machine composed of hardware circuit and the PC software. The hardware circuits of MPU system are used in order to realize the photoelectric signal acquisition and hardware filter, by double machine communication and sending data to machine firstlly, we can calculate the collected signal processing and the cerebral hemodynamic parameters, finally PC, record and storage will be achived.**

***Key words*—NIRS; Cerebral hemodynamic parameters; Optoelectronic signal; Filter circuit**

I.INTRODUCTION

NOWADAYS various of brain detection technology is developing rapidly.The existing technology mainly includes the electro encephalograph (EEG), Event-related-potential(ERP), Magneto encephalography (MEG), Positron emission tomography (PET), Functional magnetic resonance imagine (FMRI), Near Infrared Spectroscopy(NIRS), etc.

Compared with electro encephalography (RRG), magneto encephalography (MEG), near infrared spectroscopy (NIRS) is not only a kind of noninvasive measurement technique, but a kind of technique which has accurate millisecond time resolution. The brain function analyzer uses near infrared spectroscopy analysis system in the field of brain function test which has very broad application prospect, it has many advantages such as inexpensive, light weight, small volume and low energy consumption[1].

In 1977, Jobsis used the near infrared light to test on animal blood oxygen levels in the cerebral cortex for the first time, and became a forerunner of imaging technology research of near infrared spectroscopy .At present, the use of near-infrared light,together with the measurement of blood oxygen parameters, has a very wide range of subjects, including skin, skeletal muscle, liver, breast and brain, etc. As the highest and the most complex organs among them, the brain participates in the activities of all the complex psychological, thus occupies an important position in the field of life science research. Therefore, brain tissue optical parameters measurement is not only the difficulties of the current research topic, but aiso a hot topic about research.

II. THE PRINCIPLE AND THE SCHEME DESIGN

A. The principle of near infrared spectrum brain function detection

The main components of the blood (water,oxyhemoglobin and deaeration hemoglobin) scatter well in the near infrared light of 600-900nm, but in near infrared wave band ,their absorption coefficients of the blood components are different.

Oxy-genated hemoglobin(HbO_2), reduction of hemoglobin concentration(RHb) are two basic parameters of the blood oxygen parameters[3].Using near infrared spectroscopy (NIRS) for brain function test, the basic principle is: The biological tissue has a strong ability of scattering but weak ability of

absorbing in the near infrared, which makes it possible that the photon can penetrate into the deep tissue. HbO_2 and RHb are the main absorbing chromophores in near infrared field, and they have different absorption spectral characteristics, so we can identify the change of concentration of different absorptions[4], which are shown in figure 1 as follows.

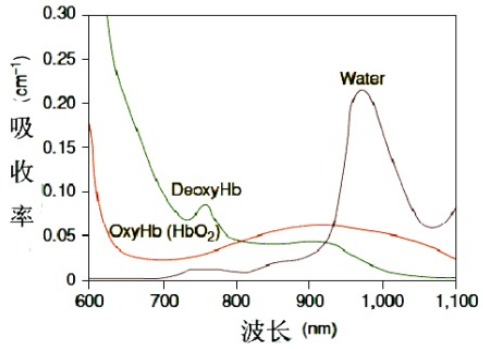

Fig.1. The absorption coefficient of HbO2 and RHb under the near infrared spectroscopy

In this figure, there is a near 805nm absorption point in the two hemoglobins, so the light in wavelength of 805nm can express the organization changes of the blood volume. On both sides of 805nm, the two kinds of hemoglobin show respective comparative advantage of absorption properties, so the near-infrared light of 780nm and 830nm wavelength were used respectively for detecting[5].In this way, the change of blood oxygen concentration can be realized by using near infrared spectroscopy for brain activity according to the analysis of these parameters on brain function.

B. The design scheme of the near infrared spectrum analyzer

The whole brain analyzer includes two parts :software and hardware, hardware part consists of sensor module, control module and serial interface, using single chip microcomputer as main control chip to realize functions such as implement the light source drive control, sampling, data storage, and so on. At the same time, the gathered result of the signal after amplification will be sent into PC software for further processing.

The low photoelectric sensor is made up of LD semiconductor laser source, optical fiber and detector, diagram is shown in figure 2:

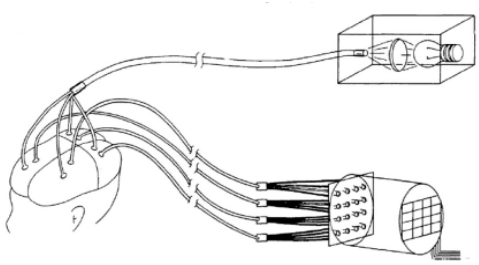

Fig2. The helmet-shaped sensor

All the parts of the whole brain analyzer module are shown in figure 3:

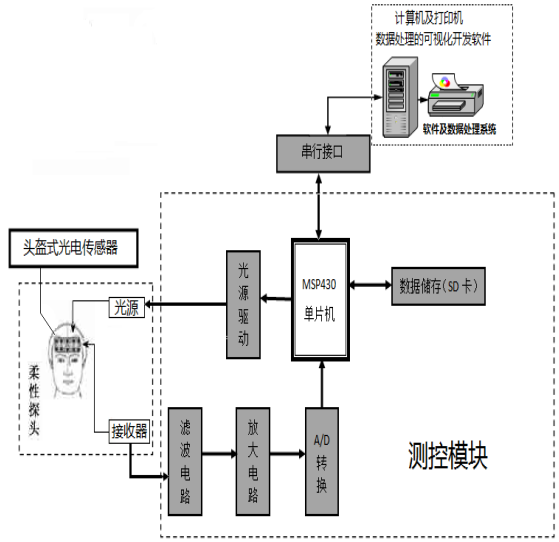

Fig3. The major module of the instrument

Software part is include two parts:the hardware interface module and data processing module.Through the communication with lower machine controls, the beginning and end of the data acquisition data were collected, read and complete the data processing.

Overall instrument work process is shown in figure 4:

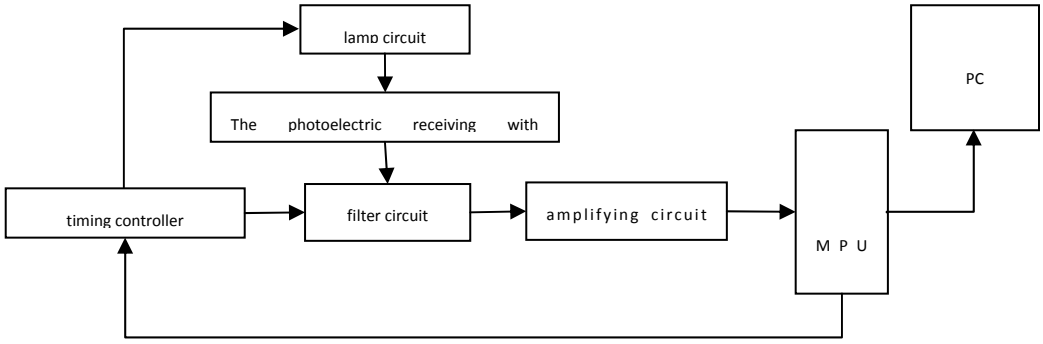

Fig4. Overall instrument work process

III . THE HARDWARE DESIGN

A. Hardware amplification and filter circuit design

Hardware amplifying circuit used OP07.This is a kind of integrated operational amplifier circuit with low noise and the chopper stabilizing zero bipolar.As the OP07 has very low input offset voltage, the noise is low. Preamplifier circuit design is shown in figure 5:

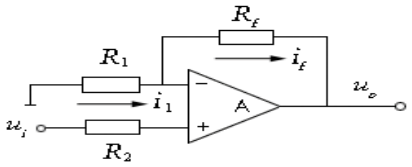

Fig.5 the pre-amplification electric

Choose low pass filter , secondary passive type, and cutoff frequency is 2000 Hz.Circuit diagram is shown in figure 6:

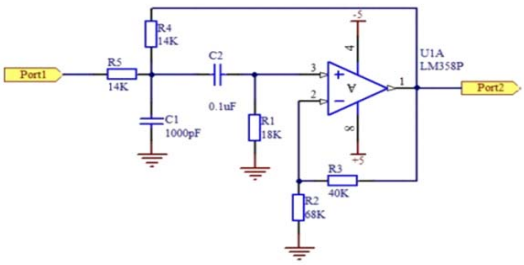

Fig.6 the filter circuit

B. Module design under a machine drive control

The drive control circuit of single chip processor system selects MSP430F249 micro-controller at the core of the controller. The single chip microcomputer have advantages of low power supply voltage, low power consumption and the hardware serial port[6].MCU time-sharing drive laser source drive sequence diagram is shown in figure 7.

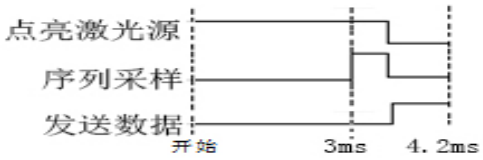

Fig.7 One of the LD driver sequence chart

Program design, please light the 780nm laser source firstly, and wait for 3ms for stability, trigger a sequence of sampling as well as wait for the end of the sampling, turn off the LD laser of 780nm, 780nm laser logo, transformation, and send the first wavelength (780nm), during which, 4.2ms execution time of the acquisition will be needed for the collection of data along the way. And the LD driver circuit diagram is shown in figure 8.

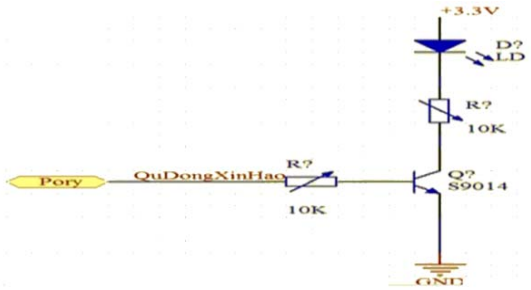

Fig.8 One of the LD driver circuit

C.Hardware design of double machine communication

The single chip microcomputer system and computer system are connected by MAX232 communication level interface circuit. Firstly, connect two DB9 connector J1, J2 In the MAX3222 chip level connection, and it will produce level need for the serial communication interface, which can enter through the DB9 connector J1, J2 directly and connect to the PC serial interface[7]. Through the micro controller programming, double machine can get protocol communications, PC is under control of a single chip microcomputer, and in this way

collected data can be sent to the PC. MAX232 level of communication interface circuit is shown in figure 9:

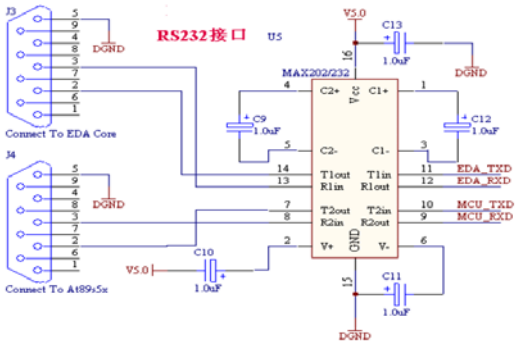

Fig.9 The MAX232 Communication level circuit

IV. DATA PROCESSING OF UPPER COMPUTER SOFTWARE

A. The data processing

The near infrared can be attributed to the essence of the study of the optical properties of biological tissue[8], it mainly includes two aspects of content[9]: the light transmission rule in the brain tissue and brain tissue signal extraction technology .

Scattering photons will pass through thousands of random until it leave sthe organization after entering into the organization, during which, its path cannot be recorded exactly, but we can get the possible paths distribution[10] through the calculation of probability ,it is shown in figure 10.

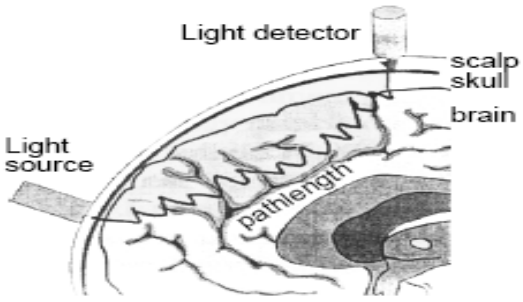

Fig.10 The photon propagation path in the organization

Brain tissue is a strong scatterer[11], through multiple scattering ,the light can transport from the light source to the detector[12] in the organization.In biomedical photonics research, when dealing with interaction between light and matter, we are mainly considering the particle nature of light and ignoring the volatility of light and the polarization effect, etc.[13].Because of unique optical properties are contained in HbO_2 and RHb in near-infrared light wave. In the measurement method which is on the basis of the absorption of light , the concentration of molecular changes can be detected[14].

The basic principle of near infrared spectrum for brain function testing is to regard the biological tissue as uniform and semi-infinite medium, and describe light propagation with application of Lambert - Beer's law (Lambert Beer) in biological tissue[15]. As a consequence, corrected lambert beer's law can be revised according to the characteristics of human tissue.

When the light enters through the flat and free scattering medium, we ought to only consider the medium for the absorption of photons, the relationship between the emergent light intensity and the incident light intensity can be described with lambert - bill[16]equation as:

$$OD = \log(I_0/I) = eCL \quad (1)$$

OD is the optical density in this course, which means the reduce of emergent light intensity compared with the incident light intensity.L is the distance from the light source to the detector, and C is the absorption of concentration, I0 represents incident light while I is the light intensity.E is called extinction coefficient, it is a constant number related to the types of absorber and wavelength.

Human biological tissue is highly scattering medium, so the basic of Lambert Beer's law is no longer suitable.Because transmission path length increases due to multiple scattering effection, the probability of photon is greatly increased.In order to reflect the influence of the scattering light loss, Delpy etc.[17] put forward correction about Lambert Beer's law in 1988, namely Type G represents the background caused by the loss,

$$OD=\ln=e\cdot C\cdot DPF+G \quad (2)$$

DPF is called path difference factor, which is used to describe the increased length that are caused by the scattering of light propagation,and some related literatures also show the different organizations in the scope of DPF[18]. We can calculate the concentration of the material by the application of multiple wavelength absorption spectrum,if G values and DPF

can be gathered under test[19].

B. PC software design

During the design process,besides the ability of interface communication between software and hardware , it still should be able to deal with the data accurately, and used conveniently . So the entire software development system shall have operability, friendly interface, wide application, and real-time, etc.

The complete set of PC software can be divided into two parts: one part is the interface unit which is connected with the hardware module, and it is responsible for a serial port parameters set and the control hardware acquisition signal, namely, the serial communication with the machine;and the other part is responsible for the signal process, calculation, real-time apperence and storage.

I will introduce them respectively as follows:

Hardware interface module:PC connects with the hardware via a serial port connection, the upper machine and lower machine can get specified protocol communication. By sending signals and commands to control the start and stop of acquisition , it can receive and store data.

The data processing module:Due to the hardware part of the data is collected by a mixture of two wavelengths of data, we should separate the data firstly. The received data can be divided into two groups respectively, and then filte.

Near infrared spectrum data process as aforesaid.In this part ,the software can complete the implementation of the computer language of the algorithm, through the computer platform management and real-time Apperence.Software can drawcurve of change over time about HbO_2 and RHb variation, and the results are stored and used for subsequent analysis.

The main function of this set of computer processing system is real-time control, data processing, display and storage. Now it can realize the function of computer software development, such as Matlab and Visual C++6.0, the Labview and Visual Stadio 2010 etc. We chose to use the Matlab software, its powerful data is used to calculate the ability to complete the computer language implementation of the proposed algorithm[20], and through its GUI platform realizes the visual interface design.

Matlab is a numerical calculation software introduced by the American Mathworks company.In this experiment, as the data processing and computer management software, the Matlab platform reflects its advantages about powerful data process and visualization platform development.The PC software design flow chart is shown in figure 11.

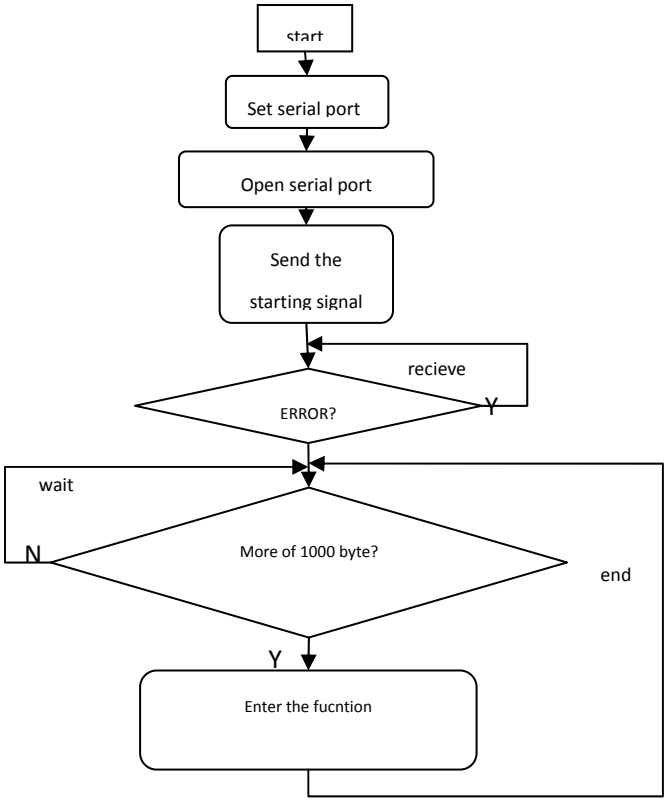

Fig.11 The software flow char

V. THE EXPERIMENTAL RESULTS

After completing the hardware part encapsulation, it is connected to PC through a serial port.Upper machine which is based on Matlab GUI tool design of interface is shown in figure 12.

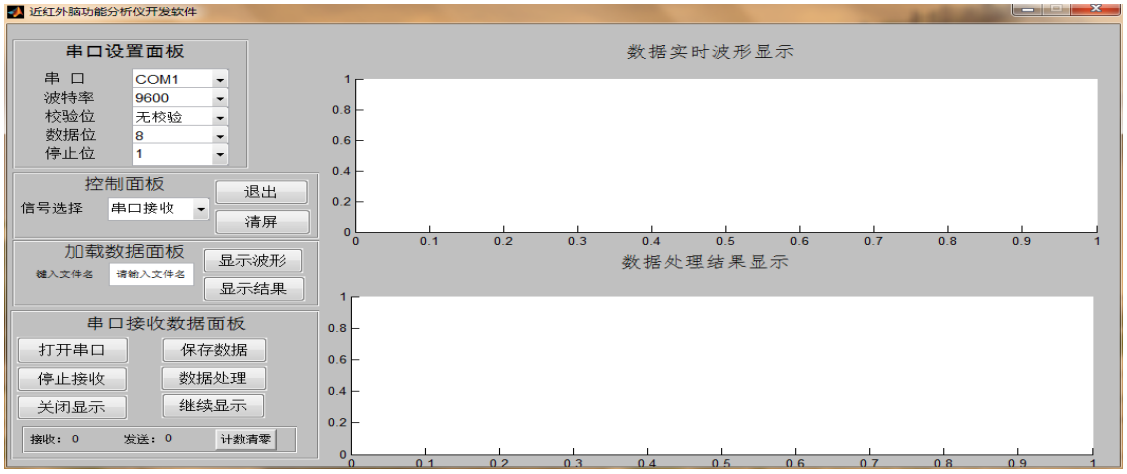

Fig.12 The software operation interface

After the completion of the test, we ought to choose a volunteer as experimental object, and draw variation curve changes over time about the oxidation of hemoglobin concentration variation and reduction of hemoglobin concentration, curve is shown in figure 13.

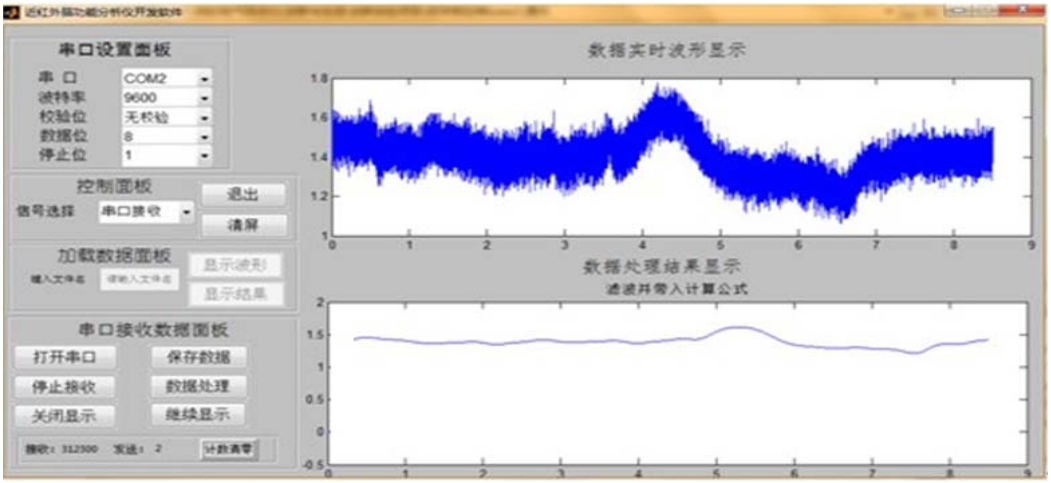

Fig 13 Curve of cerebral hemodynamic parameters variation

VI .CONCLUSION

As a means of non-invasive optical monitoring with real-time, Near infrared spectrum technique can be continuous used, etc. and application scope is more and more widely in the biomedical field.On the basic of near infrared spectroscopy is real-time with brain function monitoring system c, non-intrusive to measure a region of oxygenated hemoglobin in the cerebral cortex and reduction of hemoglobin concentration relative variation, and the function of the cerebral cortex activity monitoring.Brain function analysis system is convenient to carry and easy to operate.

On the analysis of the development of near infrared spectrum technology and the application status quo, moreover,on the basis of study of the detection principle for cerebral hemodynamic parameters, the technical design has developed a set of brain function analyzers.In this article, we introduce the design prosess about the instrument of hardware and software in two aspects respectively, as well as the design scheme of the analyzer, device selection and implementation function.Finally, the experiment results are given, that is,by using the instrument about cerebral hemodynamic parameters,we draw variation curve changes over time and completed the analysis of brain functions.

References

[1] Villringer A, Chance B. Non-invasiveoptical spectroscopy and imaging of human brain function[J].Trends Neurosci.1997, 20:435- 442.

[2] Zheng Yi, Elwell C E, Delpy D T. Estimation of Cerebral Oxy- and Deoxy-haemoglobin Concentration Changes in a Layered Adult Head Model Using Near-infrared Spectroscopy and Multivariate Statistical Analysis[J]. Physics in edicineand Biology, 2005, 50(24):5783–5798.174

[3] Ding Haishu, Hoshi Y, Tamura M, et al. Quantitative Evaluation of the Relative Contri-bution Ratio of Cerebral Tissue to Near-infrared Signals in the Adult Human Head:A Preliminary Study[J]. Physiological Measurement, 2002, 23(2):301–312.175

[4] Zhang Yan. Near-infrared Light Propagation in an Adult Head Model.I. Modeling of Low-level Scattering in the Cerebrospinal Fluid Layer[J]. AppliedOptics, 2003, 42(16):2906–2914.176

[5] Cohen M S. Real-time Functional Magnetic Resonance Imaging[J]. Methods,2001, 25:201–220.177

[6] Hiraoka M, Firbank M, Essenpreis M, et al. A Monte Carlo Investigation of Opti-cal Pathlength in Inhomogeneous Tissue and its Application to Near-infrared Spec-troscopy[J]. Physics in Medicine and Biology, 1993, 38:1859–1876.

[7] Wang Hai. Newborn Infant Using Phase Resolved Optical Spectroscopy [D].Dong Bei University.2008,03

[8] Zhang Qi,Zhang Ying,ect. Adult Head,Calf and Forearm and the Head of the Newborn Infan [J]. Advances In Experimental Medicine and Biology.2007,Vol.5,No.1

[9] Gan Zhuo,. Deriving the Respiratory SinusArrhythmia from the Heartbeat Time Series Using Empirical Mode Decomposi-tion[J]. Chaos, Solitons and Fractals, 2004, 20:171–177.179

[10] Durduran T, Yu G Q, Burnett M G. Diffuse Optical Measurement of Blood Flow,Blood Oxygenation, and Metabolism in a Human Brain During Sensorimotor Cor-tex Activation[J]. Optics Letters, 2004, 29(15):1766–1768.180

[11] Kocsis L, Herman P, Eke A. The Modified Beer-lambert Law Revisited[J]. Physicsin Medicine and Biology, 2006, 51:N91–N98.181

[12] Wang Hai: A Review of Time-series Analysis Methods for Near-infrared Spectroscopy of the Brain[J]. AppliedOptics, 2009, 48(10):D280–D298.182

[13] Uludag K, Kohl M, Steinbrink J, et al. Cross Talk in the Lambert-beer Calculationfor Near-infrared Wavelengths Estimated by Monte Carlo Simulations[J]. Journalof Biomedical Optics, 2002, 7(1):51–59. [9]

[14] Wanatabe E.Nagahori Y.Mayanagi Y.Focus diagnosis of epilepsy using near-infrared spectroscopy. Epilepsia[J], 2002,43:50-55

[15] Delpy DT,Cope M,Vander Zee P,et al. Estimation of Optical Pathlength Through Tissue from Direct Time of Flight Measurements[J]. Physics in medicine and biology,1988,33(12):1433-1442.

[16] Toronov V, Webb A, Choi J H, et al. Study of Local Cerebral Hemodynamicsby Frequency-domain Near-infrared Spectroscopy and Correlation with Simultane-ously Acquired Functional Magnetic Resonance Imaging[J]. Optics Express, 2001,9(8):417–427.

[17] Liang H, Lin Z, McCallum R W. Articfact Reduction in Electrogastrogram Basedon Empirical Mode Decomposition Method[J]. Medical & Biological Engineering& Computing,

2000, 38:35–41.

[18] Duncan A, Meek J H,Clemence M,et al. Optical Pathlength Measurements on Adult Head, Calf and Forearm and the Head of the Newborn Infant Using Phase Resolved Optical Spectroscopy[J]. Physics in Medicine and Biology,1995,40(2):295-304.

[19] Van der Zee P,Cope M,Arridge S R,et al. Experimentally Measured Optical Pathlengths for the Adult Head,Calf and Forearm and the Head of the Newborn Infant as a Function of Inter Optode Spacing [J]. Advances In Experimental Medicine and Biology,1992,316:143-153.

[20] Qin S R, Zhong Y M. A New Envelope Algorithm of Hilbert-huang Transform[J].Mechanical Systems and Signal Processing, 2006, 20:1941–1952.185

Design of DDS signal generator based on FPGA

ZHANG Lin-hang, ZHAO Mei-cong, SHANG Xiao-hu, LIU Yang
（Jilin University Instrument Science and Engineering Institute,Changchun,130021）

***Abstract*—A method based on FPGA was presented for DDS signal generator. The DDS signal generator can provide sine wave, triangle wave and square wave. Meanwhile, the frequency and amplitude of the signal are adjustable. PLL is used to make the output signal frequency stability. This design has the advantages over the traditional signal generator of lower cost, smaller volume and easier to implement.**

I. INTRODUCTION

DIRECT Digital Synthesis technology is based on sampling technique and calculation. Waveform signals were generated based on Digital Synthesis. Frequency and phase of the signal with fixed reference frequency is adjustable. The DDS signal source has high frequency resolution, rapid frequency switching speed. The output phase noise is low and it can easily be integrated. DDS has a wide range of applications in modern electronics, communications, medical imaging, wireless PCS/PCN system, radar and satellite communications.

FPGA has been widely used in the design of special digital integrated circuits based on high integration, high speed and the use to realize the characteristics of large capacity storage function. Phase-locked loop is a kind of technology to make sure the synchronization of the frequency and phase based on feedback control principle. Its role is to make the output clock circuit and its external reference clock in sync. Based on FPGA of Altera Cyclone series design PLL and DDS signal source, the FPGA design can effectively realize DDS technology, greatly improve the performance of waveform generator and reduce the production cost.

II. THE PRINCIPLE SCHEME OF DDS SIGNAL SOURCE

Write programming through the VHDL language, using Quartus2 software based on FPGA. Design phase-locked loop to control the different working clock, to ensure that the inside and outside work in the synchronous frequency. Design frequency generation and control part, by addressing waveform ROM to generate sine wave, triangular wave and square wave, and to frequency and phase meanwhile. Rectangular wave and sawtooth wave can be generated through phase adjustment. Again after D/A conversion, output the waveform signal. By controlling the D \ A reference voltage to adjust the amplitude of the output signal.

III. THE PRINCIPLE SCHEME OF DDS SIGNAL SOURCE

Select CycloneII EP2C5T144C8N chip of Altera corporation as the control system. Provide 50M system clock input the FPGA chip built-in phase-locked loop. Using VHDL language design a phase-locked loop to output a 50M clock as a clock for frequency generation and frequency adjustment. The system clock after 16 frequency division supplies serial interface module. Frequency control word PFSK and PASK/PSK are generated by frequency control module. They are sent to NCOFSK and NCOASK/PSK module respectively to generate control signal as ASKOUT, PSKOUT, FSKOUT. Return the control signal back to the PC via a serial port way to verify analysis. At last, through D/A conversion, convert digital signals into analog signals, as the output signal of the DDS signal source.

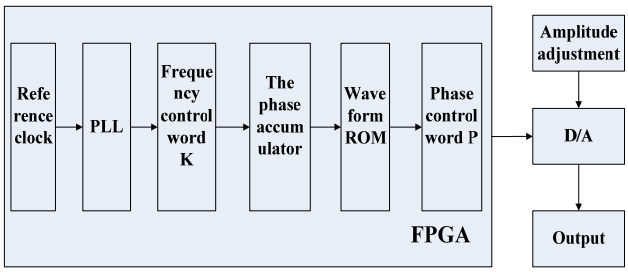

Fig. 1. Block diagram of the total design

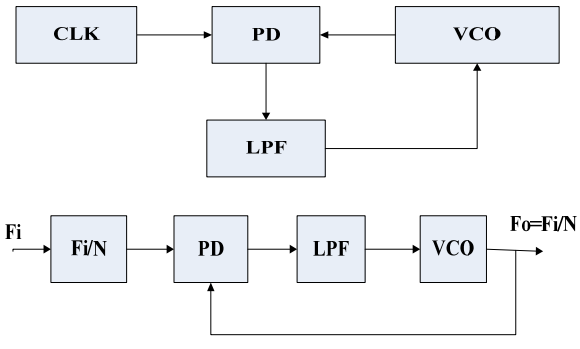

Fig. 2. Block diagram of PLL

1. The design of the frequency control module

Design frequency step is 100 Hz, due to the frequency range is very wide, changing the frequency span larger requires a long time by frequency step to change the output frequency. So in the actual frequency control module, increase the frequency adjustment of the two additional step buttons, the minimum step 10 times 100Hz which is 1KHz and 100 times 100Hz which is 10KHz. Use the frequency buttons can change the signal frequency quickly.

To realize this design, by the formula (1) it can be seen that when $f_c / 2^N$ is determined, f_0 is proportional to the K. Calculate the value of K when the output frequency $f_0 = 100HZ$, then the K is the increment of the K when the frequency step is 100 Hz, and write it as DK. To multiply the step frequency, simply increase in DK multiples of the same value.

$$f_0 = k \quad f_c / 2^N \qquad (1)$$

$$f = 2MHz \bullet 40\% = 800KHz \ddagger 100KHz \qquad (2)$$

$$f_{\min} = \frac{f_{clk}}{2^N} = \frac{30MHz}{2^{24}} \gg 1.788Hz \pounds 100Hz \qquad (3)$$

2. The design of the phase accumulator

The phase accumulator consists of a full adder and a register. When the system clock is a positive edge, the phase and the frequency words of the lase clock cycle are added, and the sum is set to a register. Then output W higher bits to the address line of the waveform memory, at the same time phase values will be sent back to the full adder for phase accumulation.

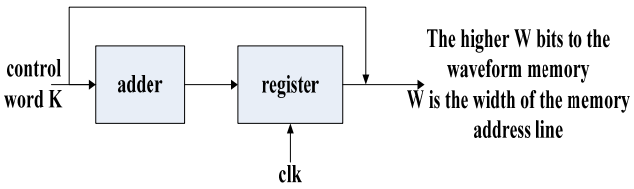

Fig. 3. Block diagram of the phase accumulator

Due to the frequency resolution is equal to or less than the frequency step value, and accumulator word length is eight commonly integer times. According to the formula (2) and (3) design accumulator word length as N = 24.

3. The design of the waveform ROM

According to the noise power perspective waveform ROM address line digits should be equal to or slightly greater than the word length. Due to the selection of DAC figures of 8, so choose the ROM word length and DAC word appearance is consistent, select the address line as eight bits. The higher eight bits of the output waveform storage form the phase accumulator are used as address line. Waveform ROM outputs the corresponding binary phase sine amplitude according to the address line. Edite the program to generate sine data based on MATLAB:

```
>> clear tic;
t=2*pi/256
t=[0:t:2*pi];
y=128*sin(t)+128;
round(y);
t =0.0245
ans
```

Convert the results into eight binary data, amplitude corresponding to the 00000000-11111111 range. Finally use the binary data written in VHDL program to design the sine ROM.

4. The design of the amplitude adjustment

With two pieces of DAC chip cascade, of which the first piece of DAC as D/A conversion chip, its voltage as a reference voltage for the generation of the signal source. The second piece of DAC is used for amplitude adjustment. Input the adjusted voltage to the first piece of DAC as its reference voltage, so as to realize amplitude adjustment.

IV. RESULT

Through software simulation and actual test, the signal source can generate sine wave, triangle wave, square wave, square wave and sawtooth wave. The signal frequency, phase and amplitude can be flexibly adjusted by keys, the frequency of the output signal is stable. In conclusion, the purpose of the design was achieved.

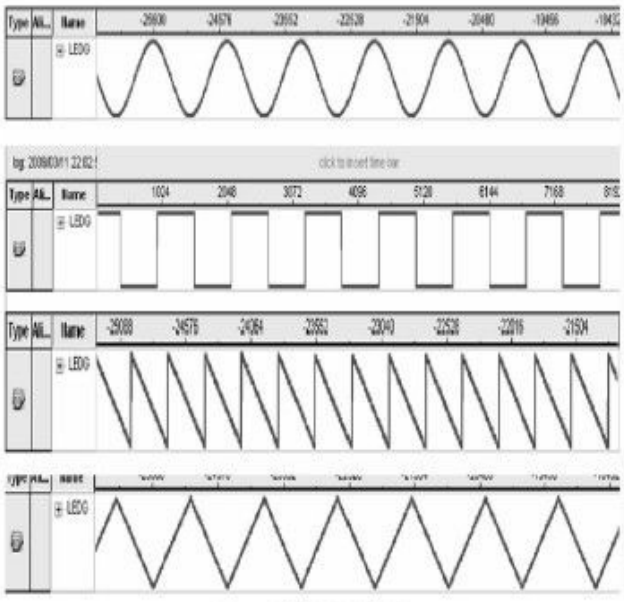

Fig. 4. Simulation diagram of the signal source

References

[22]JIANG Tao，TANG Zong-xi，ZHANG Biao. Design of frequency synthesizer based on DDS+PLL[J]. Journal of Electronic Measurement and Instrument，2009,23（10）：91-95.

[23]YANG Ping，WU Dan-hui，YANG Liang-yu. Application of DDS Technology in Sine Wave Function Generator[J]. Computer Measurement & Control，2008,16（11）：1738-1740.

[24]HUANG Zhi-wei. Phase-locked Loop and Frequency Synthesizer Circuit Design [M]. Xian：Xian University of Electronic Science and Technology Press，2008.

[25]YANG Xiu-zeng. Design of a signal generator based on FPGA and DDS[J] . Electronic Design Engineering, 2009 (11) : 7-8, 11.

[26]HU Sheng-ping，SONG Yue，LEI Rui-ting，YU Chi-ye. Study on Generation and Realization of DD S-AM Wave Based on FPGA [J]. Instrumentation Technology，2007（4）:7-8.

[27]ZHENG Huang-ting，LAI Wan-chang，MAO Wei. Design of DDS signal generator based on FPGA[J]. Electronic Design Engineering，2012，20（24）:153-154,158.

[28]ZHANG Kai-lin，SU Shu-jing，LIU Li-sheng，YI Chun-li，ZHENG Wen-qiang. Design of Multi－channel DDS Signal Generator Based on FPGA [J]. Electirical Measurement & Instrumentation，2011,48（543）:63-65.

[29]WANG Qing-dong，XIE Chang-sheng，WANG Hai-wei. An High Integrated Direct Digital Frequency Synthesis System Design on FPGA[J]. Computer Science，2007,34（10）：299-300.

[30]Wang Wei，Zhao Ji-xiang. Control design based on FPGA+DDS [J]. Measurement & Control Technology，2008（06）：13-15,19.

[31]Wang A Y, Ling Z H. Dynamical analysis and circuit simulation of a new three-dimensional chaotic system[J]. Chinese Physics B, 2010, 19(7):070506.

[32]SHEN Hui，WANG Shi-kui，WEI Fu-ya. Design of the Digital Control Signal Source Based on FPGA and DDS Technology[J]. Electronic Science and Technology，2012,25（3）：82-84,89.

An intelligent and safer design of multi-function temperature adjustable water dispenser

Duan Qing-ming，Peng Xing-xing，Yang Kai-qi ，Lin jie

(College of instrumentation and Electrical Engineering, Jilin University, Changchun 130022, China)

***Abstract*—In view of the shortcomings in the traditional water dispenser, this paper provides a smarter and more energy-efficient design. In this design the controller of water dispenser was MCU, the sensor of water temperature was DS18B20, and the keyboard and six-interlock switch were used as human interface device to set water temperature and choose operation modes. All of this information was showed by LCD. Two cans were needed to store the raw water and boiled water. The volume of the water in the cans that is determined by sensor was used to choose operating modes, automatic power off mode for shortage of water and automatically mode switch for unattended time. The experimental results show that this design can meet the demands of friendly operation interface, energy-saving and intelligence.**

***Keywords*—Temperature setting; Multilevel model; Energy saving and safety; Automatic control**

I. INTRODUCTION

IN our country, water dispenser has become indispensable to family and office space, with huge potential in domestic and international market. However, when picking the hot water from the traditional dispenser, cold water is directly into the heating can, making a substantial increase in heating frequency. So as to consume a lot of power and form yin-yang water for the mixture of hot and cold water. When the room has no one regardless of day or night after turning on the power, water dispenser has been still in heat insulation state.Water will be harm for healthy when been heating repeatedly or a long time. Thirdly, packing water generally relies on manual valves which are easily leading to cross infection of viruses. Fourthly, heating temperature in our life can not be selected generally and there is no real-time temperature display. However, in life, the water temperature is different for various purposes such as instant cup noodles, coffee, etc, which causes inconvenience to daily life. At last, when water dispenser is in the state of insulation or heating for a long time, it will cause air burning. There are huge amount of household water dispenser in our country, air burning easily will cause fire failure and waste a lot of energy .When water dispenser is access to power and it will be in work condition, then if children touch, it may cause burns and other unsafe incidents.

To achieve intelligent, energy saving, healthy design of water dispenser, the project uses single-chip for controlling water dispenser work, DS18B20 digital temperature sensor for temperature acquisition, Nixie tube for display. The raw water and boiled water were stored in two cans for prevent yin-yang water. The pressure sensor is placed in the tank below to measure the amount of water in order to prevent air burning. If there is no person to operate within the set time, it automatically jumps to low energy-saving mode. This brings convenience to people's daily drinking.

II. SYSTEM DESIGN

The water dispenser we design is a product with temperature control, level control, real-time display, security, intelligence and other technical integration. System has two parts with automatic control and artificial control, which can complete the tasks of setting temperature, testing, displaying and water level detecting, displaying, specific response to a particular water level system, gear setting and intelligent jump. Dispenser main portion have sound monitoring system, display system, automatic control and reliable enforcement agencies. The system block diagram is shown in Figure 1.

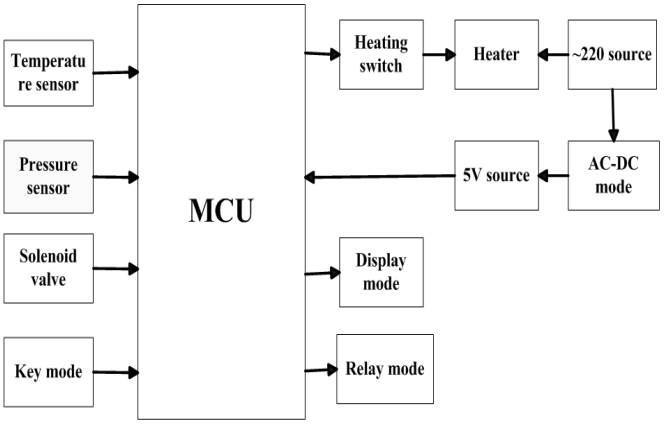

Fig.1 Water machine system block diagram

III. WATER DISPENSER HARDWARE DESIGN

A.Anti-dry device design

Strain type pressure sensor is put under the can. We use the sensor to measure the weight of the can when it has no water and has full water. It sends a dry signal to MCU when the weight is less than 5% and sends a full water signal to MCU to close the water inlet when the weight is more than 95%.When it is short of water, MCU will send a signal to the solenoid valves and then the solenoid valves opens the water inlet to fill the can with water. If water is less than 5% for a setting time, it means devices has no water and will be power off automatically.Gravity measurement circuit is showed in Figure 2.

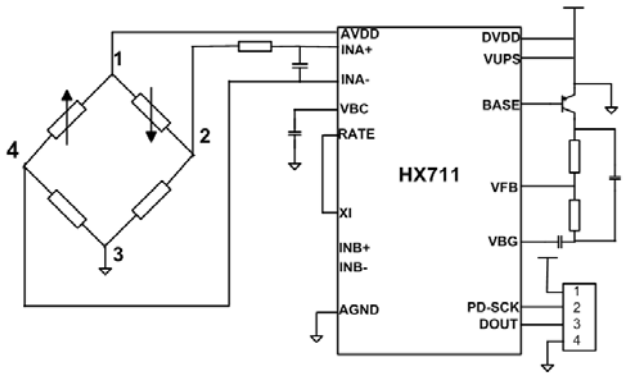

Fig.2 Gravity measurements schematic

B.Temperature gathering and multiple temperature mode settings

Temperature sensor is integrated digital temperature sensor DSl8B20 which works in bus mode. There are three pins in DSl8B20,including ground pin, power pin, data pin.DSl8B20 power can be provided by the data lines rather than external power supply and Communicate with the MCU only by one data line so as to save MCU pins.DSl8B20 measurement temperature ranges from -55 ℃ to +125 ℃ and Incremental value is 0.5 ℃.It can transform the temperature analogue value to digital value within one second .Accuracy and speed meets the design requirements.

Temperature keys are independent buttons so as to set a specific temperature. Six-interlock switch were used to set multiple temperature modes. The Water dispenser has intelligent temperature control system that it can automatically jump to the low temperature mode when no one operates the system for a long time. For example, when there is no one in or the power without being turned off at night, it can save energy because water is not heating for a long time. Specific conditions are as follows in Table 1.

Table1.Temperature modes

name	APO	drink	honey	milk	coffee	tea
temperature	off	45℃	55℃	65℃	85℃	95℃

C.Dual can design and running water automatically

The design uses two cans to store cold and hot water separately. Heating device is only in the hot water tank. When water level in the hot water can is below the setting level, cold water can supplies automatically until the can is full. Its characteristic is to prevent people picking hot water from mixing with cold water.

Picking water is controlled by manual button or induction system designed with photoelectric sensor.The cup will block photoelectric sensor when put on the corresponding position, which the sensor will sense the signal and then send signals to MCU.MCU will open relay to pour the water. When time set before is up, water valve is back and relay is close. And then warning device works.The water sensing circuit is showed as follows figure 4.

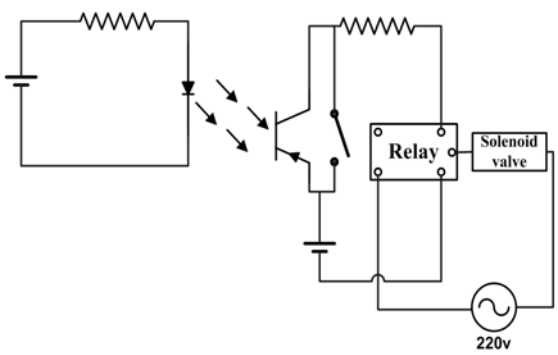

Fig 4 Water flow Control circuit Schematics

D.Display mode

The real-time temperature is displayed by nixie tube. 74LS48 used as latch is selecting nixie tube to display dynamically. Use the LCD screen to display the calendar, set temperature, time and work modes.LCD is driven by a 74LS164 and transformed from serial to parallel to saving pins.

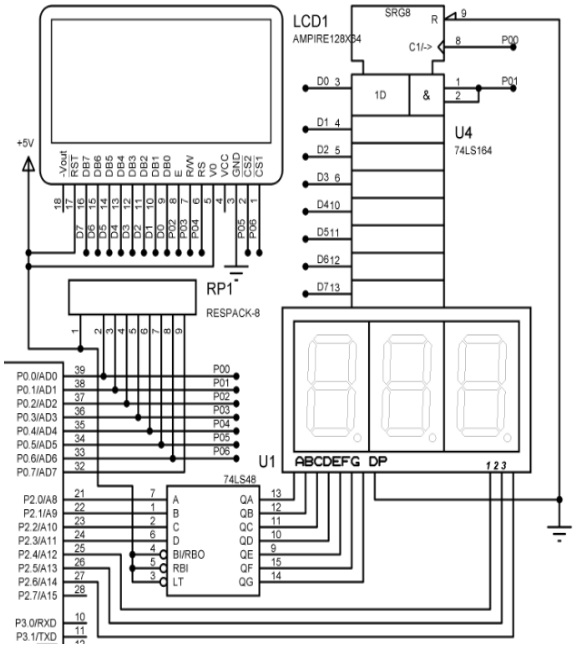

Fig.4 The circuit of display part

Ⅳ.SOFTWARE DESIGN

Master controller program flowchart is shown in Figure 3

The flowchart mainly includes Module initialization，temperature and water level test，the cup detection ，signal processing and display。The main task is processing the signals from sensors to miss setting mode.

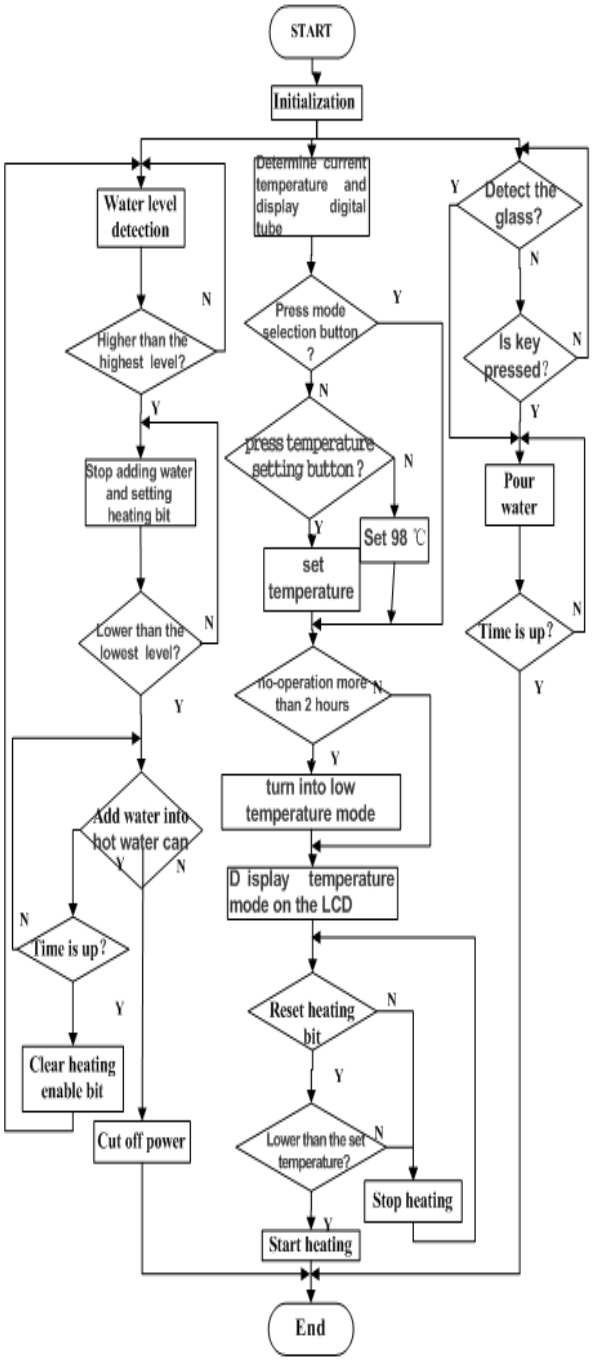

Fig.3 Software flow chart

Ⅴ. ANALYSIS OF EXPERIMENTAL RESULTS

In order to test performance merits of the design, we measure and record some data about pouring water time, water level test deviation, heating time and heating-stop temperature. Every glass of water is measured with balance and the quality is 160 g. Use a stopwatch to measure time and graduation ruler to measure water level. The measure data is showed as table2.

Table 2 Measurement data sheet

Water-short level	Response time	Setting time	Response temperature	Water outflow
5%	1.0s	95℃	95.0℃	200ml
6%	1.2s	95℃	94.5℃	198ml
5%	1.1s	95℃	95.3℃	199ml
5%	1.8s	95℃	95.2℃	202ml
5%	1.0s	95℃	95.3℃	200ml
5%	1.1s	95℃	95.3℃	205ml
3%	1.5s	95℃	95.2℃	198ml

From the experimental data, deviation is in the normal range including testing water level by pressure sensor ,solenoid valve opening and closing, response time and temperature .

Ⅵ. CONCLUSION

In this design,the controller of water dispenser was STC89C52 and the sensor of water temperature was DS18B20.When the temperature of the water reaches the temperature that was setted, buzzer alarms. When timeout, the water dispenser turn into low temperature mode, it will automatically cut off the power when no one operates the system for a long time. In order to reduce power consumption to achieve the purpose of energy saving. Temperature setting is not only has five gear concise model, but also can be set arbitrary temperature, bringing great convenience to people.

This water dispenser adopts double tanks to placed hot and cold water respectively. It controls solid state relay SSR – IOA to heat the heating pipe and cold water tank is not connected to the hot water tank when heating. So cold-water will not flow into the heating-water tank, which is different from the traditional water dispenser. It improves the efficiency of the heating and saves electricity. The pressure sensor as a means of water level collection, when the water level is lower than 5% for a period of time and it still no response, it will automatically cut off the power to prevent empty fire. LCD displays the model of temperature that was setted by button and the heating mode. The digital tube displays tank temperature in real time. The design of this water dispenser is safe, intelligent and more humanized.

References

[1] Wang Qingyuan. The principle and application of new type of sensor [M]. Beijing: China Machine Press, 2003.

[2] Zhang Fuxue. Sensor application and circuit selection [volume one][M].Beijing: Publishing House of Electronics Industry,1990.

[3] Tan Haoqiang. Program Designing C Language [M]. The fourth edition. Beijing: Tsinghua University Press, 2010.

[4] Yuan Xiaoping. Intelligent energy-saving water dispenser can be achieved [J].Modern Household Appliances, 2008(19):63.

[5] Liu Huadong, Zhang Yahua. The principle and the application of single chip microcomputer (the second edition) [M]. Beijing: Publishing House of Electronics Industry, 2006.

[6] Lin Qisheng, Xiong Qi, Peng Weiqiang .The design of the water dispenser temperature control system based on single chip microcomputer [J].E-World,2012(3):39-42+45

[7] Guo Tianxiang. C language program of 51 single chip tutorial [M]. Beijing: Publishing House of Electronics Industry, 2010.

[8] Qiu Shi science and technology. 8051 series microcontroller C language programming [M].Beijing:Posts & Telecom Press,2006.

[9] Zhao Jianling, Xue Yuanyuan explanation of 51 MCU development and application technology [M].Beijing: Publishing House of Electronics Industry, 2009.

[10]Zhen Feng, Wang Qiaozhi, Cheng Liping.

The typical application examples of 51 single-chip microcomputer[M] Beijing: China railway industry press,2011

[11]Fan Honggang, Wei Xuehai, Ren Sijing 51 microcontroller self-study notes [M].Beijing: Beijing university of aeronautics and astronautics press, 2010.

[12]Zhang Yigang, Peng Xiyuan, Peng Yu. The principle and the application of single chip microcomputer [M].Beijing: Higher Education Press, 2010.

[13]Xue Xiaoling, Liu Zhiqun, Jia Junrong. Single chip microcomputer interface module application and development of example explanation [M].Beijing: Beijing university of aeronautics and astronautics press, 2010.